IASJ
المجلات الاكاديمية العراقية
KJPS
AL-Kitab Journal For Pure Sciences

AL-Kitab Journal For Pure Sciences

Volume : 9 (2025)

Issue: 1

ISSN: 2617-1260 (print)

ISSN: 2617-8141 (online)

DOI: http://10.32441/kjps

Deposit number at the Notional House of Books and Archives, Iraq, 2271 in 2017

Al-Kitab Journal for Pure Science

KJPS

ISSN: 2617-1260 (print), 2617-8141(online)
DOI: http://10.32441/kjps
https://isnra.net/index.php/kjps

An Academic Semi-Annual Journal

Volume: 09 Issue: 01 Dec. 2025

Iraqi Academic Scientific Journals IASJ: **https://iasj.rdd.edu.iq/journals/journal/view/103**
Journal Website: **https://isnra.net/index.php/kjps**
E-mail: **kjps@uoalkitab.edu.iq**

Editorial Board for Al-Kitab Journal for Pure Sciences

Aims and Scope

The Al-Kitab Journal for Pure Sciences aims to provide an international forum for the publication and dissemination of original work that contributes to the understanding of the principal and related disciplines of science. Al-Kitab Journal for Pure Sciences publishes two peer-reviewed issues per year, an online and print journal, which publishes innovative research papers, literature reviews, and technical notes on the fields of Biology, Computer Sciences, Chemistry, Physics, and Mathematics.

Authors Guidelines

Rules and Instructions for Publication in Al-Kitab Journal for Pure Sciences

First: General requirements

1. The paper is submitted to the Editorial Secretariat directly in four copies with CD-ROM or E-mail of the magazine in MS Word and PDF files.
2. Research before being sent to scientific evaluators is subject to the quotation Turnitin program.
3. Research shall be accepted for publication after being judged by scientific evaluators and according to the rules.
4. The publication fee is (100,000 ID) for researchers from Iraqi Universities and (free of charge) for foreign researchers.

Second: To prepare research for publication, authors must follow the following procedures.

1. **The article:**

   The article needs to be typed on one side of A4 paper (Right margin =2.5 cm, left margin =2.5 cm, and 2cm for the top and bottom) with 1.5 space, and the pages must be numbered.

2. **The content organization:**

   MS Word is to be used as follows: "Simplified Arabic" font for the Arabic articles, and "Times New Roman" for the English articles. The Size of the title is 18 bold. The names of the authors will be typed in 11 bold in Arabic and 11 bold in English. Abbreviations, keywords, the main headings, the reference, and the acknowledgment will be typed in 14. Subheadings will be in 12 bold. The abstract will be size 12. The body of the article/paper is in size 12. The order of the paper's content will be as follows:

The article heading, the names of authors and their addresses, and the abstract (Both in Arabic and English).

3. **Research paper title:**

The title must be as short as possible and indicate the contents of the subject together with the name (names) of the authors. The names of the authors to whom correspondence is to be made should be indicated with (*) and show his / her email.

4. **The size:**

The paper should contain no more than 25 pages of journal pages including charts and diagrams.

5. **Abstract:**

The abstract should include the purpose and the means of the founding results and the conclusions. It should also contain the knowledge values of the subject of research. It is meant to be no more than 250 words. It should also emphasize the content of the subject and include the keywords used throughout the paper.

6. **Diagrams:**

Figures and diagrams must be given following the explanation referring to the diagram. Each diagram must contain its title below the diagram at the first size of 12. The diagram should be editable in terms of enlargement or reduction within the margins of the paper size. The parts of each diagram must be grouped into drawing parts.

7. **Tables:**

The tables should follow the parts of the main body and should be located below the indicated part of the text. Tables must have titles with a text size of 12. The text used inside the tables should be of size 12 and kept within the cells of the table.

8. **References:**

The references used in the paper must be given in order and their numbers given inside the square bracket **[ ]**. The following instructions are to be followed:

If the reference is a book, the First name of the reference must be given first followed by the other names. Then the title (bold and Italic) of the book, edition, year of publication, the publisher, and place of publication (year of publication).

Example: **[1]** P. Ring and P. Schuck, "**The Nuclear Many-Body Problem**", First Edition, Springer-Verlag, New York (1980).

(b) If the reference is a research paper or an article in a journal: The name of the author must be given first, the title of the article, the name of the journal, the volume (issue), page (Year). **Example:** **[1]** Ali H. Taqi, R. A. Radhi, and Adil M. Hussein,

"Electroexcitation of Low-lying Particle-Hole RPA States of ^{16}O with WBP Interaction", Communication Theoretical Physics, 62(6), 839 (2014).

c) If the reference is an M.Sc. or Ph.D. thesis, the name of the anther must be written with the first name first followed by the surname, title of the thesis, the name of the university, and Country (Year).

Example: [1] R. A. Radhi, **"Calculations of Elastic and Inelastic Electron Scattering in Light Nuclei with Shell-Model Wave Functions**", Ph.D. Thesis, Michigan State University, USA (1983).

(d) If the reference is from the conference. Authors Name, "**Paper Title**", Conference, Country, Publisher, volume, page (Year).

Example: [1] Ali H. Taqi and Sarah S. Darwesh, **"Charge-Changing Particle-Hole Excitation of ^{16}N and ^{16}F Nuclei"**, 3rdInternational Advances in Applied Physics and Materials Science Congress, Turkey, AIP Conf. Proc., 1569, 27 (2013)

Third: Privacy Statement

1. The names and e-mail addresses entered into the journal's website will be used exclusively for the purposes stated in this journal and will not be provided for any other purpose or to any other party.
2. The editor of the journal has the right to change any statement or phrase of the research content he may find necessary to express the work suitable to the general style of the journal.
3. After publishing the paper and its presentation on the journal page, the editors' team will destroy all the scrap papers. The author has no right to ask for them in any case.

Fourth: Modernity of sources:

The percentage of modern references used in the research should not be less than 50% of the total references used in the research. Modernity is measured within the last ten years of the year of submission of the research. For example, when submitting the research in 2018, the references should be from 2008 upwards and not less than 50%. The journal prefers to have at least one of the reference types of research published in the previous journal issues.

Note: For more information, visit:

Iraqi Academic Scientific Journals IASJ: **https://iasj.rdd.edu.iq/journals/journal/view/103**
Or Journal Website: https://isnra.net/index.php/kjps
The Journal can also be e-mailed to kjps@uoalkitab.edu.iq

Table of Contents

Volume: 09 Issue: 01 Dec. 2025

Al-Kitab Journal for Pure Sciences (2025); 9(1):1-13.
https://doi.org/10.32441/kjps.09.01.p1

Al-Kitab Journal for Pure Sciences
ISSN: 2617-1260 (print), 2617-8141(online)
https://isnra.net/index.php/kjps

Soft Voting Classifier of Machine Learning Algorithms to Predict Earthquake

Oqbah Salim Atiyah

Department of Computer Science, College of Computer Science and Mathematics, University of Tikrit, Iraq.

*Corresponding Author: oqbah_salim@tu.edu.iq

Citation: Atiyah OS. Soft Voting Classifier of Machine Learning Algorithms to Predict Earthquake. Al-Kitab J. Pure Sci. [Internet]. 2024 Dec. 28;9(01):1-13.DOI: https://doi.org/10.32441/kjps.09.01.p1

Keywords: Earthquakes, Machine Learning, Soft Voting Classifier.

Article History

Received	16 Aug.	2024
Accepted	22 Oct.	2024
Available online	28 Dec.	2024

Abstract:

Earthquakes are among the most dangerous natural disasters that can cause major losses to buildings and threaten human lives. The research community is very interested in the topic of earthquakes because they occur suddenly and predicting them is very important for human safety. Creating accurate earthquake prediction techniques by applying machine learning (ML) approaches will help save people's lives and prevent damage. To identify important features and analyze the correlation between these features before submitting them to classification models, we proposed a new feature selection approach in this paper which combines two filtering ways: Normalization which is based on the Chi-square approach and analysis of variance, and the correlation approach based on the logistic regression technique (CLR-AVCH). Accordingly, three algorithms are applied. Then a facilitated voting classifier is created that combines the two best models with the highest prediction accuracy (histogram-based gradient boosting, adaptive boosting) to create a single technique that includes the strengths of the techniques that were combined to help find important patterns in the acquired data to obtain a model capable of early prediction of earthquakes. The proposed work achieved higher accuracy, F1_score, recall, and precision (0.94, 0.92, 0.94, 0.92), respectively.

Keywords: Earthquakes, Machine Learning, Soft Voting Classifier.

مصنف التصويت الناعم من خوارزميات التعلم الآلي للتنبؤ بالزلازل

عقبه سالم عطية
قسم علوم الحاسوب، كلية علوم الحاسوب والرياضيات، جامعة تكريت، العراق
oqbah_salim@tu.edu.iq

الخلاصة:

تعتبر الزلازل من أخطر الكوارث الطبيعية التي يمكن أن تسبب خسائر كبيرة في المباني وتهدد حياة الإنسان. يهتم المجتمع البحثي كثيراً بموضوع الزلازل لأنها تحدث بشكل مفاجئ والتنبؤ بها مهم جداً لسلامة الإنسان. إن إنشاء تقنيات دقيقة للتنبؤ بالزلازل من خلال تطبيق أساليب التعلم الآلي *(ML)* سيساعد في إنقاذ حياة الناس ومنع الضرر. لتحديد الميزات المهمة وتحليل الارتباط بين هذه الميزات قبل تقديمها إلى نماذج التصنيف، لقد اقترحنا نهجًا جديدًا لاختيار الميزات في هذا البحث والذي يجمع بين طريقتين للتصفية: التطبيع الذي يعتمد على نهج مربع كاي (*Chi-square*) وتحليل التباين، ونهج الارتباط المعتمد على تقنية الانحدار اللوجستي *(CLR-AVCH)*. وبناءً على ذلك، تم تطبيق ثلاث خوارزميات. وتم إنشاء مصنف التصويت الميسر الذي يجمع بين أفضل نموذجين يتمتعان بأعلى دقة للتنبؤ (*AdaBoost , HGBoost*) ، لتكوين تقنية واحدة تضم نقاط قوة التقنيات التي تم دمجها للمساعدة في العثور على الأنماط المهمة في البيانات المكتسبة للحصول على نموذج قادر على التنبؤ المبكر بالزلازل. حقق العمل المقترح اعلى النتائج بدقة ٠,٩٤ و *F1_score* ٠,٩ و*recall* ٠,٩٤ و*precision* ٠,٩٢.

الكلمات المفتاحية: الزلازل ، التعلم الآلي ، مصنف التصويت الناعم.

1. Introduction:

An earthquake is a mild to severe tremor caused by the sudden movement of underground rocks. There are four types of earthquakes: tectonic, collapse, explosive, and volcanic. Earthquakes occur at tectonic fault boundaries. A tectonic earthquake occurs due to the breaking of the Earth's crust due to geological forces affecting adjacent plates, causing a change in the chemical and physical structure. Often tectonic blocks move slowly, so they are trapped at their edges due to friction. Thus, when the pressure on the edge of friction increases, an earthquake occurs, and there are energy waves that are transmitted to the Earth’s crust and cause the vibration that forms the earthquake **[1]**, many losses and injuries due to earthquakes. Every day, there are natural disasters in all countries of the world. The countries most vulnerable to earthquakes are Taiwan, Southern California, Iran, Indonesia, Turkey, and Japan.

People feel an earthquake if its magnitude is greater than 2.5, and people do not feel it if its magnitude is less than 2.5. Destructive earthquakes have a magnitude greater than 4.5 **[2]**. Sometimes earthquakes cause serious deaths and great material damage, so researchers make a great effort to predict earthquakes to stop such negative events. To notify people of the danger promptly. Humans cannot prevent earthquakes, but preventive measures can be taken to reduce negative events, using machine learning approaches, the strength and danger of earthquakes

can be predicted [3]. Many technologies can be used, such as sensors, magnetic and electrical waves, and other devices that can estimate the size of an earthquake based on seismic indicators by analyzing available data on previous earthquakes [1]. Until now, there is no optimal model that gives results with 100% accuracy, but there are still attempts to increase the accuracy of the results provided [4]. Many factors affect the machine learning prediction process, such as the amount of features, the number of constraints in the data set, and the nature of the classification or regression problem. Therefore, we will use several algorithms in ML and compare their results to discover the most suitable one for the specific situation [5]. The main goal of earthquake forecasting is to determine three important things: the future earthquake, where it will occur, when, and its size, to reduce losses resulting from earthquakes. Predicting earthquakes can significantly reduce seismic damage, and this is the primary goal. Accordingly, there is a great interest in conducting research studies on earthquake prediction [6].

2. Related Work:

- Koehler, J., Li, W., Faber, etc. (2023). This study was conducted to predict earthquakes by using deep learning (DL) to discover whether a time series lasting more than two years generates an earthquake larger than five magnitudes or not. The trained technique was evaluated, and the accuracy was approximately 72.3%. Therefore, it should be developed by using more available data [7].

- Sajan, K. C., Bhusal, A., (2023). The paper applies four techniques of decision tree, random forest, logistic regression, and eXtreme gradient boosting (XGBoost) in machine learning to predict the degree of damage and rehabilitation. By comparison with other techniques, XGBoost predicts the collapse of institutions and buildings with better accuracy. However, prediction techniques must be developed to achieve better accuracy [8].

- Researchers Yang, F., and Kefalas, M., (2022), presented a regression model in machine learning. They developed an automated regression model based on laboratory seismic data, which helps predict earthquakes. This automated model included modeling, optimization, feature extraction, and selection techniques. The Bayesian approach is used to develop hyper-parameters. The results achieved for the model on test and training data mean square error (MSE) 1.48, 1.51, and mean absolute error (MAE) 1.52, 1.59. However, this model needs to be developed to achieve the best results for predicting laboratory earthquakes [9].

- Another study by (Berhich, A., Belouadha, F. Z., & Kabbaj, M. I), applied recurrent neural network technology to predict earthquakes based on location. K-Means is used to aggregate data based on geographical parameters to provide a prediction depending on location. The data set was divided into two groups. The first group includes seismic events whose

magnitude is between 2 and 5, while the second group includes events whose magnitude is greater than 5. The model needs to be developed to provide accuracy in performance [10].

- An, Z., et al. (2023), presented a model that combines the multilayer perception (MLP) and deep interest network (DIN) models and simulated data tests to predict earthquakes. In this study, the data were processed, and the DIN model was used to predict earthquakes. The results achieved by the proposed approach are 0.69, and this indicates an improvement rate of about 11% over the original DIN technology. With this improvement, there is still a need to develop the models used to enhance the monitoring accuracy and model efficiency [11].

3. Methodology:

This stage introduces some classification techniques in ML in this study:

3.1 Hist Gradient Boosting (HGBOOST): Histogram-based gradient boosting, or Hist Gradient Boosting (HGBoost) [12], is a boosting ensemble that utilizes the histograms of features for accurate selection and fast for best splits. It is characterized by fast processing. It reduces the number of features by pooling with graphs to increase the speed of the algorithm.

3.2 ADABOOST: Adaboost (Ada) or adaptive boosting, is a popular technique that fits into the basic series of algorithm classifiers to update the weight of samples by giving the misclassified samples more weight and then adapting the learner with the newly updated weights. By combining the results utilizing the majority voting technique in the classifier base, the final prediction is reached, and by reaching a higher weight, the highest performance of the basic classifier is determined [13].

3.3 K-nearest Neighbour (KNN): It is one of the common techniques used in classifying data, as it works to create another case that is added to the sample that currently exists in a specific space, and the nearest neighbor is found by calculating features similar to the sample. Where k is a constant value, through which features similar to the new case are calculated, this leads to selecting new samples and classifying them into similar categories [12] [14].

In this paper, the researcher proposes using a classification voting technique, which combines multiple methods to provide the best prediction accuracy for earthquake detection.

4. Proposed method:

The proposed work consists of three steps: pre-processing, feature selection step, and prediction models. A dataset of earthquakes was downloaded from Kaggle. Which includes two possibilities: tsunami (1) and other (0). It contains categorical data as well as numerical data and is stored in CSV format. The 782 samples consist of 2001–2023 [15]. **Figure 1** depicts a system workflow.

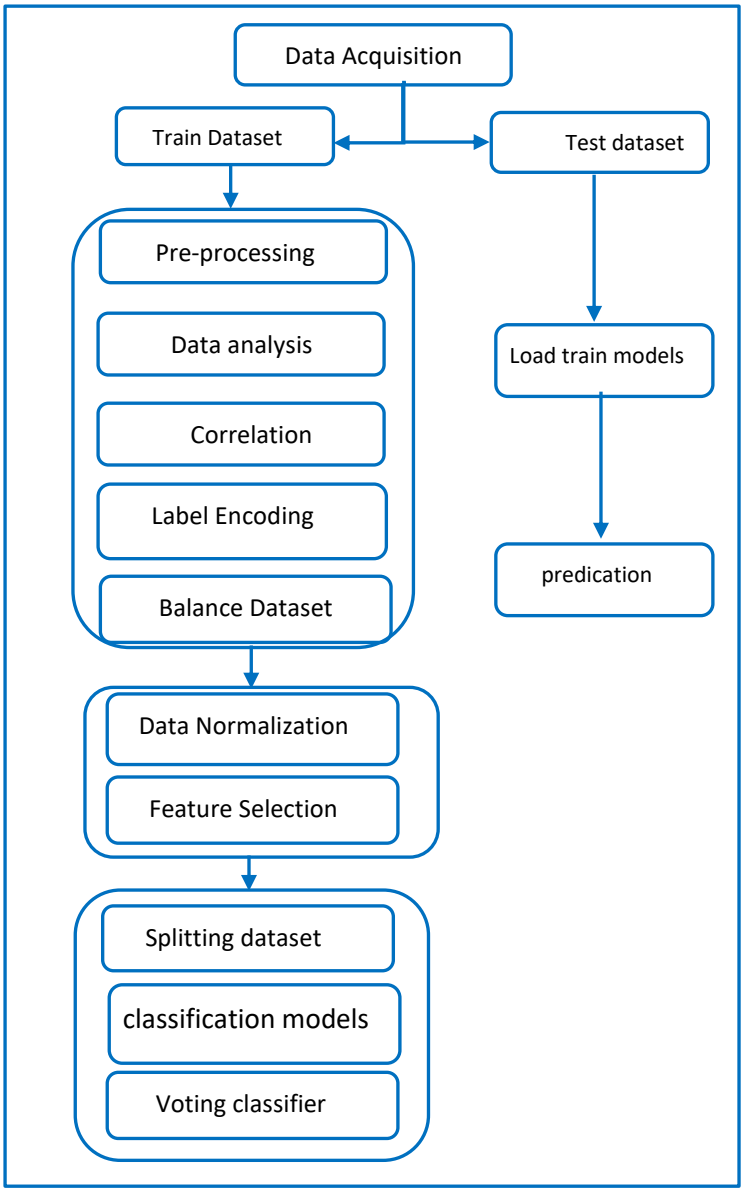

Figure 1: System workflow

4.1 Pre-processing Phase: We apply a series of preliminary operations on the data to improve its efficiency so that the classification techniques work optimally. The basic operations in this step are cleaning, and processing missing values. If the missing value is numeric, the column average will be calculated and replaced with the missing value, and if the missing values are nominal, it will be replaced with neighborhood values **[16]**. Now, to produce the dataset free of missing values, ready for later use, and encoding the data in the data set, as **Table 1**. And identify useful features for developing the model **[17]**.

Table 1: Summary of the analyzing dataset.

Seq.	features	Missing data	After handling	types
0	title	0	0	object
1	magnitude	0	0	float64

2	date time	0	0	object
3	cdi	0	0	int64
4	mmi	0	0	int64
5	alert	367	0	object
6	tsunami	0	0	int64
7	sig	0	0	int64
8	net	0	0	object
9	nst	0	0	int64
10	dmin	0	0	float64
11	gap	0	0	float64
12	magType	0	0	object
13	depth	0	0	float64
14	latitude	0	0	float64
15	longitude	0	0	float64
16	location	0	0	object
17	continent	0	0	object
18	country	0	0	object

4.2 Correlation: Correlation indicates the relationship between changes with other pairs. So, correlations are displayed to illustrate low and high correlations between variables **[18]**. The correlation technique is widely used in datasets to identify relationships that help to understand the importance of attributes with respect to the target group to be predicted, as in **Figure 2**. Thermal correlations measure the degree of correlation between features, where the values are [-1,1]. Value (1): represents the presence of correlation between the two features. And (0): represents the absence of correlation between the two features. The value (−1): represents the inverse correlation between the two features, the equation below is used to calculate correlation **[19]**. n is a sample size, x_i , y_i are data points in dataset, and the $\bar{x}$ is mean of x-values, $\bar{y}$ is mean of y-values.

$$r_{xy} = \frac{\sum_{i=1}^{n} (x_i - \bar{x})(y_i - \bar{y})}{\sum_{i=1}^{n} \sqrt{(x_i - \bar{x})^2 \sum_{i=1}^{n} (y_i - \bar{y})^2}} \quad (1)$$

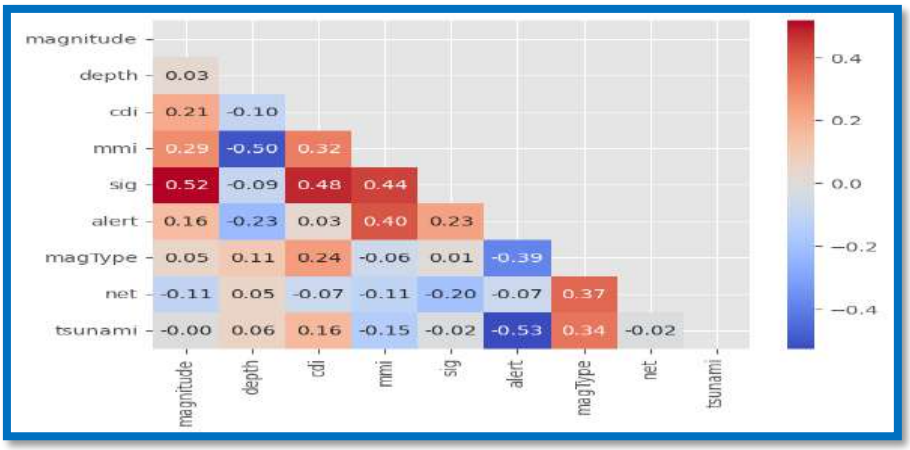

Figure 2: The correlations.

4.3 Data Encoding: Variables are affected by the scale of qualitative factors. Therefore, these variables must be converted into numerical values through encryption techniques, as some machine learning algorithms only deal with numerical variables **[20]**. Therefore, categorical

data must be converted to numerical values (**Table 2**). In this paper, the label coding approach was used, the labels of categorical data were converted into numerical values to be used in modeling and analysis. This approach is effective and simple. The working principle of the label encoding approach into each class value in the class variable a unique integer is assigned. The three categorical variables in the data set were coded to improve the functioning of the model.

Table 2: depicts the data encoding.

a. data before labeling

	magnitude	date_ time	cdi	mini	alert	tsunami	sig	net	nst	dmi	gap	Mag Type	depth	latitude	longitude
0	7.0	22-11-2022 02:03	8	7	green	1	768	us	117	0.5	17.0	mww	14	-10	159.6
1	6.9	18-11-2022 13:37	4	4	green	0	735	us	99	2.2	34.0	mww	25	-5.0	100.8
2	7.0	12-11-2022 07:09	3	3	green	1	755	us	147	3.1	18.0	mww	579	-20.1	-178.3
3	7.3	11-11-2022 10:48	5	5	green	1	833	us	149	1.8	21.0	mww	37	-19.3	-172.1
4	6.6	09-11-2022 10:14	0	2	green	1	670	us	131	5.0	27.0	mww	624	-25.6	178.3
...	...	...	...	...	...	...	...	...	...	...	...	...	...	...	...
777	7.7	13-01-2001 17:33	0	8	red	0	912	us	427	0	0.0	mwc	60	13	-88.7
778	6.9	10-01-2001 16:02	5	7	red	0	745	ak	0	0	0.0	mw	36.4	56.8	-153.3
779	7.1	09-01-2001 16:49	0	7	red	0	776	us	372	0	0.0	mwb	103	-15.0	167.2
780	6.8	01-01-2001 08:54	0	5	red	0	711	us	64	0	0.0	mwc	33	6.6	126.9
781	7.5	01-01-2001 06:57	0	7	red	0	865	us	324	0.	0.0	mwc	33	6.9	126.6

782 rows x 15 columns

data after labeling

	magnitude	date_ time	cdi	mini	alert	tsunami	sig	net	nst	dmi	gap	Mag Type	depth	latitude	longitude
0	7.0	22-11-2022 02:03	8	7	0	1	768	9	117	0.5	17.0	8	14	-10	159.6
1	6.9	18-11-2022 13:37	4	4	0	0	735	9	99	2.2	34.0	8	25	-5.0	100.8
2	7.0	12-11-2022 07:09	3	3	0	1	755	9	147	3.1	18.0	8	579	-20.1	-178.3
3	7.3	11-11-2022 10:48	5	5	0	1	833	9	149	1.8	21.0	8	37	-19.3	-172.1
4	6.6	09-11-2022 10:14	0	2	0	1	670	9	131	5.0	27.0	8	624	-25.6	178.3
…	…	…	…	…		…	…		…	…	…		…	…	…
777	7.7	13-01-2001 17:33	0	8	2	0	912	9	427	0	0.0	7	60	13	-88.7
778	6.9	10-01-2001 16:02	5	7	2	0	745	0	0	0	0.0	5	36.4	56.8	-153.3
779	7.1	09-01-2001 16:49	0	7	2	0	776	9	372	0	0.0	6	103	-15.0	167.2
780	6.8	01-01-2001 08:54	0	5	2	0	711	9	64	0	0.0	7	33	6.6	126.9
781	7.5	01-01-2001 06:57	0	7	2	0	865	9	324	0.	0.0	7	33	6.9	126.6

782 rows x 15 columns

4.4 Data Normalization: Normalization is the process of preparing data for machine learning. Normalization aims to reduce the number of features to a similar extent. Which stabilizes the training, improves its function, leads to more data, and increases its safety **[21]**. The MinMaxScaler function was used, it a function converts data to a specified range and

rescales the data to set the minimum value to 0, and the maximum value to 1, which scales each feature individually and has a maximum and minimum value, with values of 1 and 0.

4.5 Feature Selection Phase: In this step, appropriate features are selected to obtain the best results. Less important data gives fewer opportunities to make decisions due to noise. Less frequent data gives greater accuracy, and this speeds up the work of the algorithms **[22]**. Which reduces training time **[23]**. The proposed method combines the filtering approach, and their association through logistic regression with the normalization process, works on analysis of variance (ANOVA), and uses the chi-square technique (CL-ANCH), as in **Figure 3** which shows the proposed method for our study. Correlation analysis uses the logistic regression function (logis. coef) to determine the target value and measure the correlation between features. Where these values are treated as a set of correlation values. Highly related features are grouped into a single group that includes similar elements. The common features that have the best values are kept in a group and the rest of the features are neglected. The correlation of numerical variables is measured using the logistic regression model, the normalization technique, and ANOVA, which compare the differences through the average values of the variables. The P value represents the result of ANOVA. These values represent the difference between the variance within the group, which produces values that show that the null hypothesis is supported or rejected. The null hypothesis is rejected if the difference between variables is large. The Chi-squared technique performs a statistical test to examine the variance between categorical features that were randomly selected. The candidate variable for the feature is neglected and is not related to the problem. This approach shows that all categorical variables are important values, as the P value for the Chi-squared technique is <0.05. As in **Table 3**. This approach searches for variables that have correlation values less than 1 by analyzing the thermal correlations of the variables identified in **Figure 2**. It combines the existing set of correlated variables into a single group. AVONA and Chi-squared are applied to find variances through the mean values of the groups and find the P value for variables whose values are less than 0.05 as in (**Table 3**). While the remaining variables in each group are neglected. **Figure 3** shows the proposed method for our study. Unimportant variables were removed, and variables were kept that enabled the model to be trained correctly to give better results.

Table 3: display the feature selection phase.

Features	With feature selection	With proposed method
magnitude	1.44	0.022
depth	3.02	0.002
mmi	-0.25	-0.003

sig	3.08	-0.01
alert	-0.078	-0.03
magType	-3.40	-0.04
net	-5.8	-0.07
tsunami	0.457333	-0.074

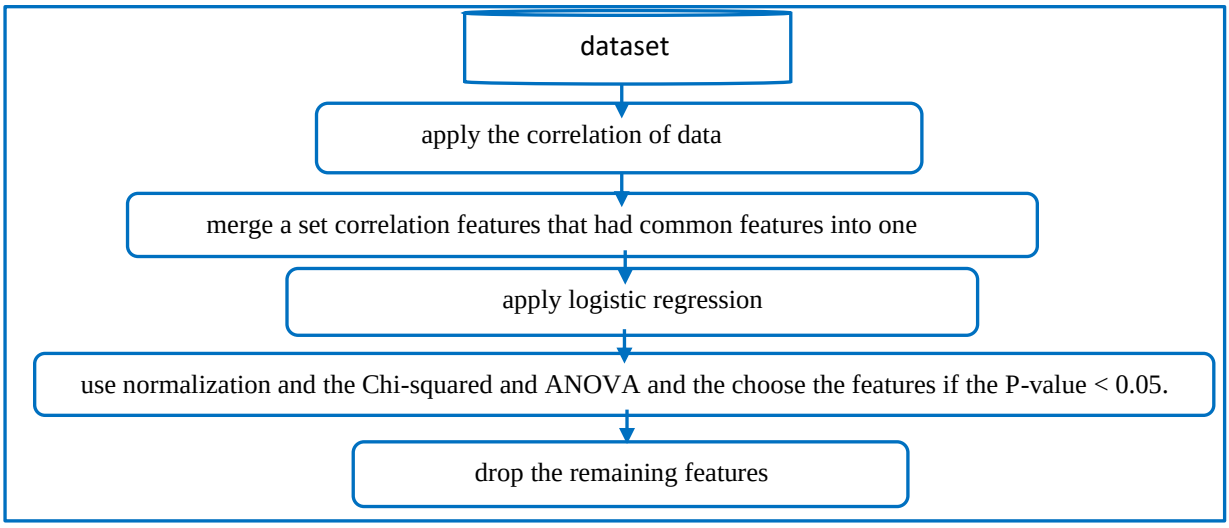

Figure 3: shows the proposed method

4.6 Split the Dataset: After performing the previous operations, the data becomes ready for training. At this stage, the data set is divided into two parts (training data = 0.8 and testing data = 0.2) (k=5). The K-Fold (k=5) class is used. It is given as arguments to the number of splits.

5. Applying Models and Results:

Data collection was implemented in Jupyter Notebook using Python code after pre-processing. Missing values and outliers were handled. The data set used in the study includes two tsunami cases (1) and (0) otherwise. Categorical data was digitized because some algorithms only deal with numerical values. The data set was segmented, and the machine learning algorithms were trained, identifying which ones were highly accurate.

5.1 Voting Classifier: It is one of the types of classification techniques known as group classifiers that rely on machine learning approaches as it works by combining some techniques to create a single technique that carries the power of the collected techniques, which gives a better prediction result **[24]**. A simplified voting technique was used by introducing two machine learning classifiers (HGBoost, and AdaBoost), which gave the best results in our study based on experiments. This new classifier works on a cumulative probability basis, as it uses the highest probability rate for the input models, which produces a probability value for class 0 or 1, as shown in **Figure 4**. The proposed method implements some processing steps to develop

the data set, after which the best features are identified, and the soft voting classifier technique is used to provide the best results in classifying earthquake types with the best results.

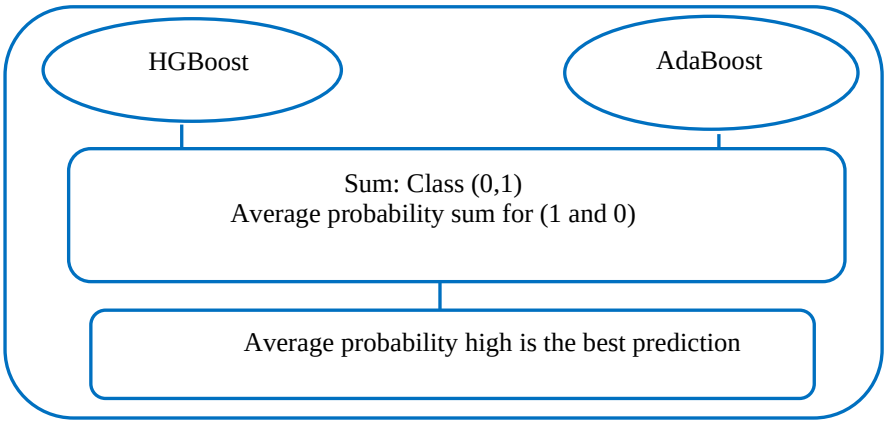

Figure 4: Display the proposed model (Soft Voting classifier).

5.2 Evaluation: Three popular algorithms in this stage are used to help identify data patterns resulting from the testing process. At this stage, the results will be verified by algorithms and their presentation. To identify classification errors specific to each algorithm to test its accuracy, relying on the confusion matrix. The new model (soft voting classifier) is built by selecting the two best algorithms in terms of results. Where the performance of the techniques used (HGBoost, AdaBoost, and KNN) was compared and the model (soft voting classifier) was built, the features gained from the proposed feature selection approach (CLR-ANCH) were passed to the data set segmentation process to be divided into a training part and a test part for the classifiers to be used. The performance of the new classifier was compared with other techniques used. **Table 4** represents the comparison results for these models. The soft voting classifier gave the best classification accuracy. **Table 4** displays the soft voting classifier gave the highest degree of accuracy (.094), F1 score (0.92), recall (0.94), and precision (0.92) because the voting classifier depends on integrating the two models into one model that carries the strength of these combined models, which leads to the best prediction accuracy. **Figure 5** displays the receiver operating characteristic (ROC) curves for HGBoost, AdaBoost, KNN, and the soft voting classifier.

Table 4: displays the result of models.

Models	confusion matrix		accuracy	F1_score	recall	precision
	TP	FP				
	FN	TN				
KNN	57	6	0.91	0.89	0.89	0.90
	7	87				
AdaBoost	59	7	0.92	0.90	0.92	0.89
	5	86				
HGBoost	61	8	0.92	0.91	0.95	0.88
	3	85				
Voting model	60	5	0.94	0.92	0.94	0.92
	4	88				

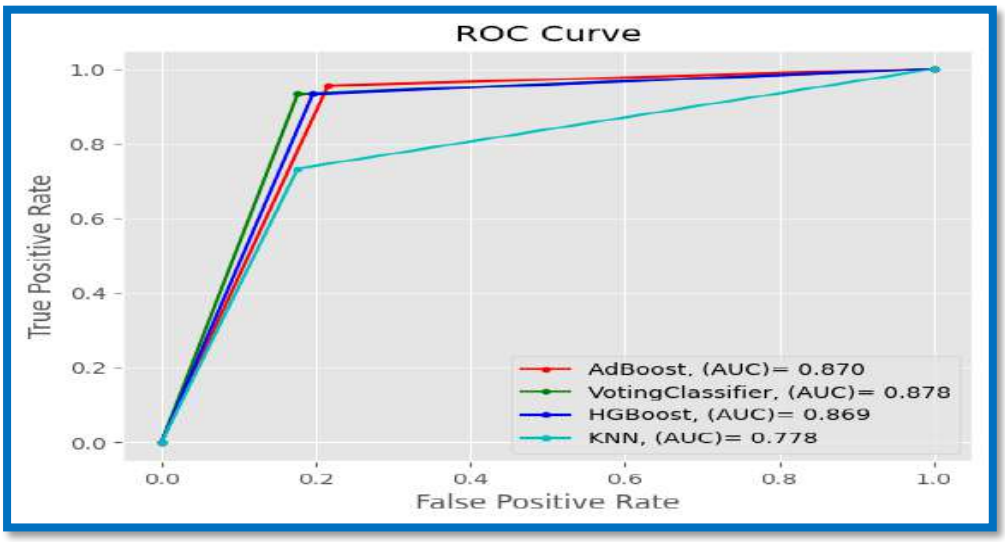

Figure 5: Display the ROC curves

6. Conclusion:

The proposed method consists of data pre-processing, normalization, and feature selection process through a correlation based on logistic regression as well as a normalization process with an analysis of variance (ANOVA) and chi-square (CL-ANCH), to select the best features to improve samples in the data set. The models proposed for earthquake prediction are (KNN, AdaBoost, HGBoost, and soft voting). The new model (Soft Voting) includes two techniques (HGBoost, and AdaBoost). The models are based on seismic indices calculated statistically and mathematically from the data set and later used as input for the proposed algorithms. Several metrics were utilized to evaluate the power of each algorithm. When comparing the performance of the techniques used and the new model, the highest performance and most power in the prediction process was for the proposed new model. It achieved an accuracy of 0.94, a recall of 0.94, precision of 0.92. and F1 score of 0.92. My future work for the study is to apply more feature selection models to a large dataset to improve diagnosis. In addition, using deep learning models.

7. References

[1] Acula, D. D. Detection of Earthquake Damages from Satellite Images using Gradient Boosting Algorithm with Decision Trees as Base Estimator. Acta Manilana, 2022; 70, 13-28.

[2] Chittora, P., Chakrabarti, T., Debnath, P., Gupta, A., Chakrabarti, P., Praveen, S. P., ... & Elngar, A. A. Experimental analysis of earthquake prediction using machine learning classifiers, curve fitting, and neural modeling. 2022; . doi.org/10.21203/rs.3.rs-1896823/v2

[3] Al Banna, M. H., Taher, K. A., Kaiser, M. S., Mahmud, M., Rahman, M. S., Hosen, A. S., & Cho, G. H. Application of artificial intelligence in predicting earthquakes: state-of-the-art and future challenges. IEEE Access, 2020; 8, 192880-192923.

[4] Salam, M. A., Ibrahim, L., & Abdelminaam, D. S. Earthquake prediction using hybrid machine learning techniques. International Journal of Advanced Computer Science and Applications, 2021; 12(5), 654-6652021. DOI: 10.1109/ICEEE.2019.8884562

[5] Atiyah, O. S., & Thalij, S. H. A comparison of Coivd-19 cases classification based on machine learning approaches. Iraqi Journal for Electrical and Electronic Engineering, (2022). 18(1), 139-143.

[6] Li, J., Zhang, C., Chen, X., Cao, Y., & Jia, R. Improving abstractive summarization with iterative representation. In 2020 International Joint Conference on Neural Networks (IJCNN), 2020; (pp. 1-8). IEEE. DOI: 10.1109/IJCNN48605.2020.9206950.

[7] Koehler, J., Li, W., Faber, J., Ruempker, G., & Srivastava, N. Testing the Potential of Deep Learning in Earthquake Forecasting. arXiv preprint arXiv, 2023; 2307.01812. doi.org/10.48550/arXiv.2307.01812

[8] Sajan, K. C., Bhusal, A., Gautam, D., & Rupakhety, R. Earthquake damage and rehabilitation intervention prediction using machine learning. Engineering Failure Analysis, 2023;144, 106949.

[9] Yang, F., Kefalas, M., Koch, M., Kononova, A. V., Qiao, Y., & Bäck, T. Auto-rep: an automated regression pipeline approach for high-efficiency earthquake prediction using lanl data. In 2022 14th International Conference on Computer and Automation Engineering (ICCAE), 2022; (pp. 127-134). IEEE.

[10] Berhich, A., Belouadha, F. Z., & Kabbaj, M. I. A location-dependent earthquake prediction using recurrent neural network algorithms. Soil Dynamics and Earthquake Engineering, 2022; 161, 107389.

[11] An, Z., Si, G., Tian, P., Li, J., Liang, X., Zhou, F., & Wang, X. Research on Earthquake Data Prediction Method Based on DIN–MLP Algorithm. Electronics, 2023; 12(16), 3519.

[12] Cho, S. B., & Won, H. H. Machine learning in DNA microarray analysis for cancer classification. In Proceedings of the First Asia-Pacific Bioinformatics Conference on Bioinformatics 2003; 19 (pp. 189-198).

[13] Freund, Y. Boosting a weak learning algorithm by majority. Information and Computation, 1995; 121(2), 256-285.

[14] Abd, N. S., Atiyah, O. S., Ahmed, M. T., & Bakhit, A. Digital Marketing Data Classification by Using Machine Learning Algorithms. Iraqi Journal for Electrical And Electronic Engineering, 2024; 20(1).

[15] C. Chauhan. Earthquake dataset, Kaggle Dataset, 2023. Available: https://www.kaggle.com/datasets/warcoder/earthquake-dataset.

[16] Atiyah, O. S., & Thalij, S. H. (2022). Evaluation of COVID-19 Cases based on Classification Algorithms in Machine Learning. Webology, 19(1), 4878-4887.

[17] Mangalathu, S., Sun, H., Nweke, C. C., Yi, Z., & Burton, H. V. Classifying earthquake damage to buildings using machine learning. Earthquake Spectra, 2020; 36(1), 183-208.

[18] Seeram, E. An overview of correlational research. Radiologic Technology, 2019; 91(2), 176-179.

[19] Real Statistics Using Excel, "Basic Concepts of Correlation", retrieved 22 February 2015. https://en.wikipedia.org/wiki/Pearson_correlation_coefficient#cite_note-RealCorBasic-13 .

[20] Lopez-Arevalo, I., Aldana-Bobadilla, E., Molina-Villegas, A., Galeana-Zapién, H., Muñiz-Sanchez, V., & Gausin-Valle, S. A memory-efficient encoding method for processing mixed-type data on machine learning. Entropy, 2020; 22(12), 1391.

[21] Ali, P. J. M., Faraj, R. H., Koya, E., Ali, P. J. M., & Faraj, R. H. Data normalization and standardization: a technical report. Mach Learn Tech Rep, 2014; 1(1), 1-6.

[22] Yu, L., Liu, H., Efficient Feature Selection via Analysis of Relevance and Redundancy, Journal of Machine Learning Research, 2004; 5, 1205-1224,

[23] Büyükkeçeci, M., & Okur, M. C. A comprehensive review of feature selection and feature selection stability in machine learning. Gazi University Journal of Science, 2022, 36(4), 1506-1520.

[24] Wang. H., H. Moayedi, and L. Kok Foong, Genetic algorithm hybridized with multilayer perceptron to have an economical slope stability design. Engineering with Computers, 2021; (37), 3067-3078.

Al-Kitab Journal for Pure Sciences (2025); 9(1):14-33.
https://doi.org/10.32441/kjps.09.01.p2

Al-Kitab Journal for Pure Sciences
ISSN: 2617-1260 (print), 2617-8141(online)
https://isnra.net/index.php/kjps

Review On Systematic Mapping Study For Synthesis Of Polymers Containing 1,3,4 Thiadiazole

Hiba Shihab Ahmed[1]*, Mostefe Khalid Mohammed[2], Noor Hatem Khorsheed[3], Eman Mudher Esmail[4]

[1]Presidency University of Diyala, Iraq, [2]Education for Pure Science College, University of Diyala, Iraq, [3]Agriculture College, University of Diyala, Iraq, [4]General Directorate of Education, Diyala, Iraq.

*Corresponding Author: hiba.s.ahmed@uodiyala.edu.iq

Citation: Ahmed HS, Mohammed MK, Khorsheed NH, Esmail EM. Review on Systematic Mapping study for synthesis of polymers containing 1,3,4 Thiadiazole. Al-Kitab J. Pure Sci. [Internet]. 2024 Dec. 29;9(01):14-33. DOI: https://doi.org/10.32441/kjps.09.01.p2

Keywords: Systematic Mapping, Co-Polymers, 1,3,4- Thiaidiazole, Polymerization Method, Energy Storage.

Article History

Received	11 Apr.	2024
Accepted	09 Jun.	2024
Available online	29 Dec.	2024

Abstract:

Due to the unique properties of a heterocyclic compound, it gained attention in the field of materials science. This study aims to provide a comprehensive synthesis of new co-polymers containing 1,3,4-thiadiazole. For this, a thorough search of electronic databases was conducted to identify relevant articles published from 2010 to 2021, using appropriate keywords and inclusion criteria. The selected studies were critically evaluated, and data was extracted and synthesized. The review includes a discussion of the various approaches used to prepare copolymers containing 1,3,4-thiadiazole, such as oxidative polymerization, electrochemical polymerization, and other methods. The properties and applications of the synthesized copolymers were also analyzed, including their thermal stability, electrical conductivity, and optical properties. The review concludes with an outlook on the prospects of co-polymers containing 1,3,4-thiadiazole and their potential applications in various fields, such as optoelectronics, sensors, and energy storage devices. The findings provide a valuable resource for researchers and engineers interested in the synthesis and properties of co-polymers containing 1,3,4-Thiadiazole.

Keywords: Systematic Mapping, Co-Polymers, 1,3,4- Thiaidiazole, Polymerization Method, Energy Storage.

مراجعة لدراسة رسم خرائط منهجية لتخليق البوليمرات المشتركة يحتوي على ١،٣،٤ ثيادايازول

هبة شهاب احمد*[١]، مصطفى خالد محمد[٢]، نور حاتم خورشيد[٣]، إيمان مظهر إسماعيل[٤]

[١]رئاسة جامعة ديالى–العراق، [٢]كلية التربية للعلوم الصرفة–جامعة ديالى–العراق، [٣]كلية الزراعة–جامعة ديالى–العراق [٤]المديرية العامة لتربية ديالى–العراق.

eman.mudher1991@gmail.com hiba.s.ahmed@uodiyala.edu.iq , mostafa.khalid.mohammed@uodiyala.edu.iq , Nour_Hatem_enge@uodiyala.edu.iq ,

الخلاصة:

بسبب الخصائص الفريدة للمركب الحلقي غير المتجانس، فقد اكتسب الاهتمام في مجال علم المواد. تهدف هذه الدراسة إلى توفير توليفة شاملة من البوليمرات المشتركة الجديدة التي تحتوي على ١،٣،٤-ثياديازول. ولهذا السبب، تم إجراء بحث شامل في قواعد البيانات الإلكترونية لتحديد المقالات ذات الصلة المنشورة في الفترة من ٢٠١٠ إلى ٢٠٢١، باستخدام الكلمات الرئيسية ومعايير الإدراج المناسبة. تم تقييم الدراسات المختارة بشكل نقدي، وتم استخراج البيانات وتوليفها. تتضمن المراجعة مناقشة للطرق المختلفة المستخدمة لتحضير البوليمرات المشتركة التي تحتوي على ١،٣،٤-ثياديازول، مثل البلمرة التأكسدية، والبلمرة الكهروكيميائية، وطرق أخرى. كما تم تحليل خصائص وتطبيقات البوليمرات المشتركة المصنعة، بما في ذلك ثباتها الحراري، وموصليتها الكهربائية، وخصائصها البصرية. وتختتم المراجعة بنظرة عامة على آفاق البوليمرات المشتركة التي تحتوي على ١،٣،٤-ثياديازول وتطبيقاتها المحتملة في مجالات مختلفة، مثل الإلكترونيات الضوئية وأجهزة الاستشعار وأجهزة تخزين الطاقة. توفر النتائج موردا قيما للباحثين والمهندسين المهتمين بتخليق وخصائص البوليمرات المشتركة التي تحتوي على ١،٣،٤-ثياديازول.

الكلمات المفتاحية: رسم خرائط منهجية، البوليمرات المشتركة، ١،٣،٤- الثياديازول، طريقة البلمرة، تخزين الطاقة.

1. Introduction:

1,3,4-Thiadiazole is a heterocyclic compound that has received noteworthy consideration within the field of materials science due to its particular properties, such as its high electron affinity [1], good thermal stability, and strong electron-accepting ability. Co-polymers containing 1,3,4-thiadiazole have emerged as promising materials for various applications, such as optoelectronics, sensors, and energy storage devices, due to their tunable electronic and optical properties. The synthesis of co-polymers containing 1,3,4-thiadiazole involves the polymerization of 1,3,4-thiadiazole-based monomers with other monomers, such as carbazole, thiophene, and benzothiadiazole, to form a polymer with a copolymer structure [2]. The selection of the appropriate monomers and polymerization method plays a crucial role in controlling the properties of the resulting co-polymer. In recent years, there has been a significant increase in the research on co-polymers containing 1,3,4-thiadiazole, and many new synthetic approaches have been developed to prepare these materials. The synthesis of co-polymers containing 1,3,4-thiadiazole has become an active area of research due to the

potential applications of these materials in various fields [3]. A literature search identified a significant number of studies published between 2015 and 2023 that focused on the synthesis of co-polymers containing 1,3,4-thiadiazole. Various synthetic approaches were employed in the studies, including oxidative polymerization, electrochemical polymerization, and other methods. The studies reported the properties and applications of the synthesized co-polymers, such as their thermal stability, electrical conductivity, and optical properties. In this systematic mapping, we provide a comprehensive overview of the synthesis of new co-polymers containing 1,3,4-thiadiazole, including the various synthetic approaches and the properties and applications of the synthesized materials [4]. Systematic mapping aims to provide a comprehensive overview of the research in this field and identify the recent advancements made in the synthesis and characterization of co-polymers containing 1,3,4-thiadiazole.

2. Previous Related Work:

Several studies on the synthesis of co-polymers containing 1,3,4-thiadiazole are vast and have been extensively studied in recent years. Khudhair, et al. (2018) studied the optical and electronic characteristics of eight compounds, which are samples based on the acceptor benzothiophene and the four 1,3,4-thiadiazole. All of the quarter 1,3,4-thiadiazole and benzothiophene structures outlined in this work have giver gather substituents (COH and CP) and acceptor gather substituents (Br, OH, Cl, F, and CN). Using the DFT B3LYP/6-31G(d) approach, the optimization's geometric, electronic, and optical properties were considered and computed. The results showed that all of the structures under ponder have the same shape (packer and shape), demonstrating that the substituent does not influence the auxiliary geometries of the particles. When the particles included substituents from the giver and acceptor bunches, the whole energies expanded, demonstrating that the structures changed over more stability[5].

Shad, et al (2014) indicated that synthesized Using the microwave induction heating approach, new functional poly(amide-thioester-imide)s were created by a one-step poly condensation reaction of a diamine with a 2-amino-5-mercapto-1,3,4-thiadiazol substituent and several diacids that had flexible amino acid links in molten TBAB salt. The polymers exhibited a higher degree of solubility than the traditional fully aromatic polyimides. The thin films made from these polymers have a smooth, pinhole-free surface. Consequently, in the UV-vis light region, all of the polymeric low-colored thin films showed great optical transparency and were noticeably flexible [6].

Alberto, et al (2020) mentioned that Synthesis Lactosyl-lysine and lactosyl-octapeptide derivatives are synthesized via the SuFEx process. Given the experimental characteristics, it's probably reasonable to say that SuFEx has the added benefit of having a bio-orthogonal click reaction in addition to being bio-orthogonal. Consequently, there is a ready supply of fluoro-based reagents. According to Marra, (2020), the benefits of integrating the click chemistry qualities with the bio-orthogonal feature in SuFEx open up new avenues for biological chemistry applications that are not possible with the more established CuAAC. Because of this, numerous attempts have been made to get around this restriction by substituting other metals for the copper catalyst, but it doesn't seem like any positive outcomes have been achieved thus far **[7]**.

Artesian, et al (2020) tested various benzotriazole-based coating recipes on copper and bronze specimens with varying corrosion patinas using chemicals that are green and brown. Conducting preventive corrosion experiments on bare bronze in the absence of any coating revealed that, as anticipated, the green patinated bronze had a greater corrosion current density (36.3 µA cm^{-2}). The current density of the naked bronze was 3.16 µA cm^{-2}, but the brown patina-covered bronze had a density of 16.1 µA cm^{-2}. The fact that bare and brown bronze have low current densities suggests that these kinds of compounds restrict current flow, shielding the metal substrate. Conversely, a high current (found for the green patina) indicates that the material flows through the sample with ease, indicating rapid corrosion of the metal **[8]**.

Overall, the previously mentioned studies highlight the importance of co-polymers containing 1,3,4-thiadiazole in the development of novel materials for various applications, identify the recent advancements made in the synthesis and characterization of these materials, and provide insights into the prospects of co-polymers containing 1,3,4-thiadiazole.

3. Research Questions:

The following are research questions that could guide a Systematic review study for the synthesis of new co-polymers containing 1,3,4 Thiadiazole.

Q1 /What are the different synthetic approaches used for the preparation of co-polymers containing 1,3,4-thiadiazole?

Q2/What are the properties of co-polymers containing 1,3,4-thiadiazole, such as their thermal stability, electrical conductivity, and optical properties?

Q3/What are the potential applications of co-polymers containing 1,3,4-thiadiazole in various fields, such as optoelectronics, sensors, and energy storage devices?

Q4/What are the challenges in the synthesis of co-polymers containing 1,3,4-thiadiazole, and how have they been addressed in recent studies?

4. Research Statement :

The following is a search statement for the systematic review study on the synthesis of new co-polymers containing 1,3,4-thiadiazole:

("1,3,4-Thiadiazole" OR "thiadiazole-based monomers" AND ("copolymer* OR "co-polymer*") AND ("synthesis" OR "preparation" OR "fabrication" OR "construction") AND ("properties" OR "characterization" OR "performance") AND ("applications" OR "devices" OR "optoelectronics" OR "sensors" OR "energy storage")

The data has been collected from various scientific databases, including Web of Science, Scopus, Google Scholar, springer, and PubMed, and will include articles published between 2010 and 2021. They are limited to articles published in English.

5. Screening Of Papers :

In a systematic mapping review, the screening process typically involves several stages to identify relevant papers that will be included in the review. The following are the general steps involved in the screening process. **Figure 1** below explains these steps:

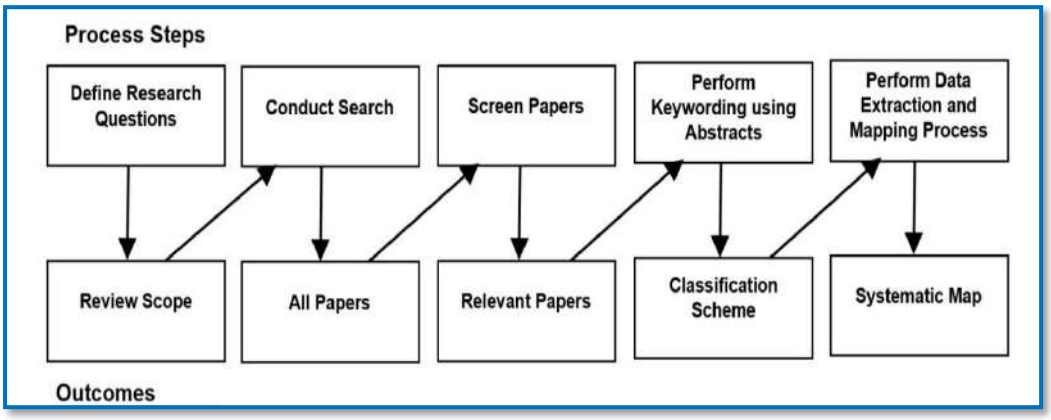

Figure 1: shows the systematic review process.

6. Use Various Models to Build Different Perspectives:

We can explain any schema or description of any topic by constructing schemas. Define an overall vision for the article on each topic and approach it with some options. In this article, we show how to use these scenarios as explained below:

A. Distribution of studies according to years:

This graph shows the distribution of the number of studies per year and the percentage of publications per year, it focuses on which papers have full pages or short pages **Figure 2** shows the distribution of studies in each year.

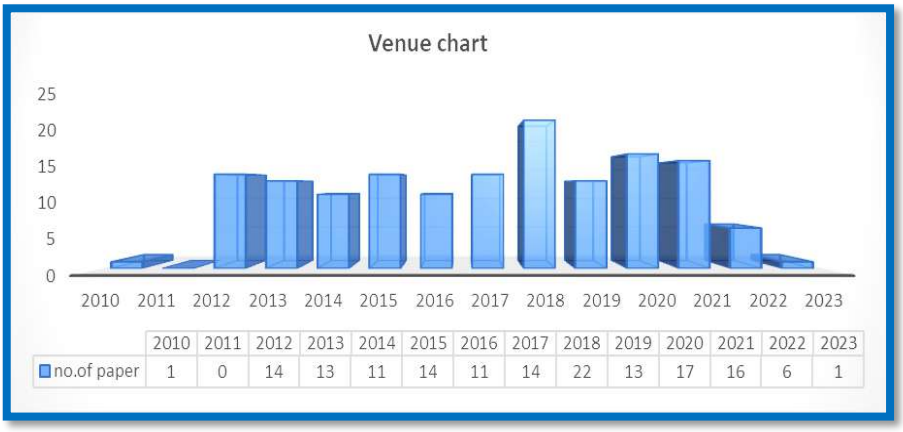

Figure 2: shows the distribution of studies in each year

B. Venue Chart:

The chart offers researchers a different perspective. Distribute papers by year, number of short or full-page papers, and paper type for conferences and journals **Figure 3** shows the Venue Chart).

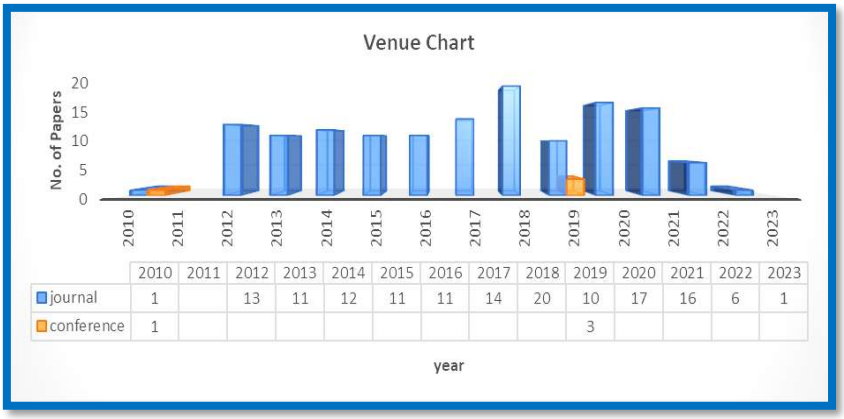

Figure 3: shows the Venue Chart

7. Classification Schemes:

To conduct a systematic review of studies on co-polymers containing 1,3,4- thiadiazol, a classification scheme can be developed based on several key criteria. These criteria include:

A. Polymerization method: The first classification scheme could be based on the method of polymerization used to synthesize the co-polymers. For example, co-polymers can be synthesized using various methods such as solution polymerization, emulsion polymerization, suspension polymerization, and others.

This classification can help to identify the differences in the properties of the resulting copolymers based on the polymerization method used [9].

1. solution polymerization
2. emulsion polymerization
3. suspension polymerization
4. bulk polymerization

B. Chemical structure: Another classification scheme could be based on the chemical structure of the co-polymers. This scheme could focus on the variations in the chemical structure of the 1,3,4 thiadiazol monomer [10], the other monomers used in the co-polymerization, and their distribution in the polymer chain **Figure 4** polymerization method with chemical structure), **Table 1**. This can help to understand the relationship between the chemical structure of the co-polymers and their properties [11].

1. co-polymers
2. homo polymer

C. Application: A classification scheme based on the application of the co-polymers can also be developed. This could include different applications such as energy storage devices, organic electronics, and sensors, among others. This can help to understand the specific properties required for different applications and how the chemical structure and polymerization method can affect these properties [12].

1. Energy storage
2. Organic electronics

D. Properties: Another classification scheme could be based on the properties of the co-polymers, such as their thermal stability, solubility, conductivity, and mechanical properties **Figure 5** shows Properties with Chemical structure scheme), **Table 2**. This can help to identify the different factors that can affect the properties of the co-polymers and how these factors can be optimized to obtain desired properties [13].

1. Thermal stability
2. Solubility
3. Conductivity

These classification schemes can be used to categorize and synthesize the information obtained from different studies on co-polymers containing 1,3,4 thiadiazol, allowing for a comprehensive understanding of the field.

Table 1: shows The Polymerization method with Chemical structure schema

Polymerization Method	Chemical structure	
	homo polymer	CO-polymer
Bulk Polymerization	[16]	[14][15][16][17][18][19] [20[[21][22]
Emulsion Polymerization	[23] [25] [26] [27][28] [18]	[23] [24] [25] [26] [27][28] [29] [30]
Solution Polymerization	[31] [34] [36] [37] [38] [39] [40] [41] [43]	[32] [33] [34][35] [36] [37] [38] [39] [40] [41] [42] [43]
Suspension Polymerization	[44] [50] [74] [75] [76] [77] [78] [79] [80] [81] [82] [83] [84] [85] [86] [87] [88] [89] [90] [91] [92] [93] [94] [95] [96] [97] [98] [99]	[44] [45] [46] [47] [48] [49] [50] [51] [52] [53] [54] [55] [56] [57] [58] [59] [60] [61] [62] [63] [64] [65] [66] [67] [68] [69] [70] [71] [72] [73]

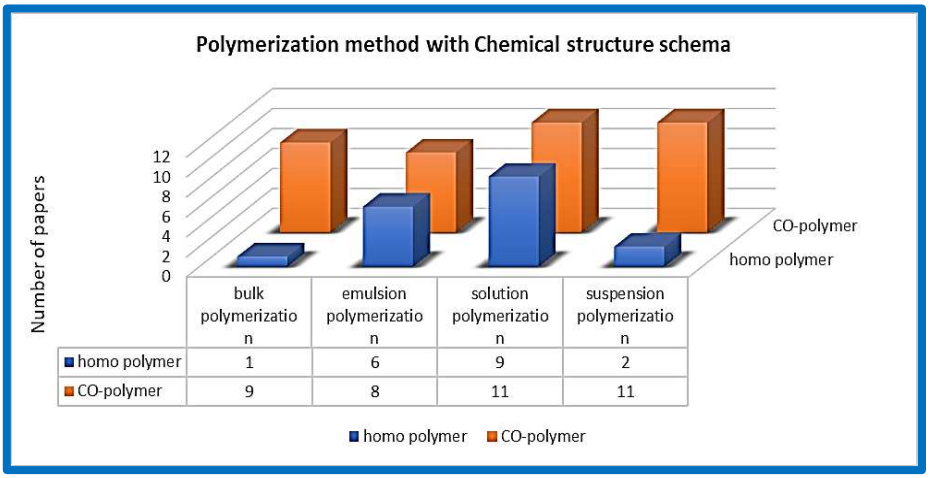

Figure 4: Polymerization method with Chemical structure scheme

Table 2: Shows The Properties With Chemical Structure Schem

Properties	Chemical structure	
	homo polymer	CO-polymer
Thermal Stability	[100][107]	[100][101] [102] [103] [104[[105][106][107][108][109]
Solubility	[111] [112] [113] [114][1115] [116] [118]	[110][111][112[[112] [113] [114] [115] [116][117][118]
Conductivity	[123] [124] [125] [126] [130]	[119][120][121][122] [123][124[[125] [126] [127][128][129][130]

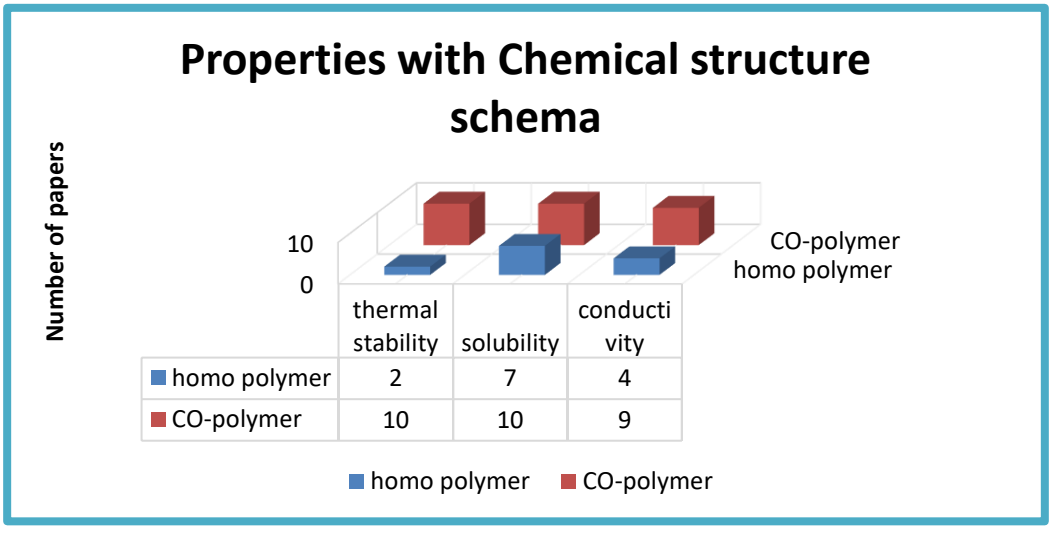

Figure 5: shows Properties with Chemical structure schema.

4. Conclusions

The synthesis of new co-polymers containing 1,3,4-thiadiazole has distinctive properties of 1,3,4-thiadiazole including high thermal stability, chemical resistance, and optical transparency. The most common method is the polycondensation of 1,3,4-thiadiazole

monomers with other monomers, such as aromatic diamines and dicarboxylic acids. Other methods include the ring-opening polymerization of 1,3,4-thiadiazole-containing cyclic monomers and the copolymerization of 1,3,4-thiadiazole monomers with other monomers using transition metal catalysts. The properties of 1,3,4-thiadiazole-containing co-polymers can be tailored by varying the type of monomers used in the synthesis. For example, co-polymers with high thermal stability can be synthesized using monomers with high glass transition temperatures. Co-polymers with high chemical resistance can be synthesized using monomers with electron-withdrawing substituents. Co-polymers with high optical transparency can be synthesized using monomers with low refractive indices. 1,3,4-Thiadiazole-containing co-polymers have been shown to have a wide range of applications. Future research on the synthesis of 1,3,4-thiadiazole-containing co-polymers should focus on developing new methods that are more efficient and environmentally friendly.

5. References

[1] Hu Y, Li CY, Wang XM, Yang YH, Zhu HL. 1, 3, 4-Thiadiazole: synthesis, reactions, and applications in medicinal, agricultural, and materials chemistry. Chemical reviews. 2014 May 28;114(10):5572-610.

[2] Hacıefendioğlu T, Yildirim E. Design principles for the acceptor units in donor–acceptor conjugated polymers. ACS omega. 2022 Oct 18;7(43):38969-78.

[3] Shadike Z, Tan S, Wang QC, Lin R, Hu E, Qu D, Yang XQ. Review on organosulfur materials for rechargeable lithium batteries. Materials Horizons. 2021;8(2):471-500.

[4] Abbas AK, Fleh SQ, Safi HH. Systematic Mapping Study On Managing Variability In Software Product Line Engineering: Communication. Diyala Journal of Engineering Sciences. 2015 Dec 1:511-20.

[5] Fleh SQ, Abbas AK, Saffer KM. A systematic mapping study on runtime monitoring of services. InThe Iraqi Journal For Mechanical And Material Engineering, Special for Babylon First International Engineering Conference, Issue (A) 2015 Dec.

[6] Khudhair AM, Ajeel FN, Mohammed MH. Engineering and design of simple models from dye-sensitive of solar cells and photovoltaic cells applications: Theoretical study. Chemical Physics Letters. 2018 Dec 1;713:166-71.

[7] Mallakpour S, Zadehnazari A. Chiral poly (amide-thioester-imide) s having thiadiazol group: microwave-assisted synthesis and study of thermo-optical behavior. Chemical Engineering Communications. 2016 May 4;201(5):635-49.

[8] Marra A, Nativi C, Dondoni A. On the scope of SuFEx as a bioorthogonal click process. New Journal of Chemistry. 2020;44(12):4678-80 .

[9] Semsarilar M, Abetz V. Polymerizations by RAFT: Developments of the Technique and Its Application in the Synthesis of Tailored (Co) polymers. Macromolecular Chemistry and Physics. 2021 Jan;222(1):2000311.

[10] Nieswandt K, Georgopanos P, Abetz V. Well-defined polyvinylpyridine-block-polystyrene diblock copolymers via RAFT aqueous-alcoholic dispersion polymerization: Synthesis and isoporous thin film morphology. Polymer Chemistry. 2021;12(15):2210-21.

[11] Ye H, Wang Z, Yang Z, Zhang S, Gong X, Hua J. Bandgap engineering of novel peryleno [1, 12-bcd] thiophene sulfone-based conjugated co-polymers for significantly enhanced hydrogen evolution without co-catalyst. Journal of Materials Chemistry A. 2020;8(38):20062-71.

[12] Sarı A, Alkan C, Bicer A. Synthesis and thermal properties of polystyrene-graft-PEG copolymers as new kinds of solid–solid phase change materials for thermal energy storage. Materials Chemistry and Physics. 2012 Mar 15;133(1):87-94.

[13] Sana B, Unnikrishnan G, Jana T, KS SK. Polybenzimidazole co-polymers: their synthesis, morphology and high temperature fuel cell membrane properties. Polymer Chemistry. 2020;11(5):1043-54.

References for Table

[14] Zhukova O, Bulgakova S. Preparation of a Doxorubicin Conjugate with (Co) Polymers of Methacrylic acid for Targeted Tumor Therapy. Journal of Applied Pharmaceutical Science. 2016 Jul 28;6(7):020-6.

[15] Ji C, Wang W, Sheng Y, Yin P, Zhang B, Du L, Yang S. New Perfluorocyclobutyl Ether-Based Polymers with High Thermostability and Adjustable Mechanical Properties Derived from Biorenewable Eugenol. Available at 22 Mar 2023 SSRN4397096: https://ssrn.com/abstract=4397096 or http://dx.doi.org/10.2139/ssrn.4397096.

[16] Wiacek M, Jurczyk S, Kurcok M, Janeczek H, Schab-Balcerzak E. Synthesis of polystyrene modified with fluorine atoms: Monomer reactivity ratios and thermal behavior. Polymer Engineering & Science. 2016 May;54(5):1170-81.

[17] Grignard B, De Winter J, Gerbaux P, Gilbert B, Jerome C, Detrembleur C. Merging supercritical carbon dioxide and organocatalysis for the precision and green synthesis of poly (lactide)-based (co) polymers. European Polymer Journal. 2017 Oct 1;95:635-49.

[18] Ding H, Tang H, Wang F, Zhang H, Guo Y. The molecular structure control of butyl methacrylate/acrylamide (co) polymers. Materials & Design. 2015 Dec 25;88:820-6.

[19] Hanifpour A, Bahri-Laleh N, Nekoomanesh-Haghighi M, Karimi M. Study on unsaturated structure and tacticity of poly1-hexene and new copolymer of 1-hexene/5-hexene-1-ol prepared by metallocene catalyst. Journal of Organometallic Chemistry. 2016 Sep 15;819:103-8.

[20] Hanifpour A, Bahri-Laleh N, Nekoomanesh-Haghighi M, Karimi M. Study on unsaturated structure and tacticity of poly1-hexene and new copolymer of 1-hexene/5-hexene-1-ol prepared by metallocene catalyst. Journal of Organometallic Chemistry. 2016 Sep 15;819:103-8.

[21] Mehnath S, Rajan M, Sathishkumar G, Praphakar RA, Jeyaraj M. Thermoresponsive and pH triggered drug release of cholate functionalized poly (organophosphazene)–polylactic acid co-polymeric nanostructure integrated with ICG. Polymer. 2017 Dec 20;133:119-28.

[22] Levina YV, Plutalova AV, Zaitsev SD, Toms RV, Serkhacheva NS, Lysenko EA, Chernikova EV. Amphiphilic Copolymers of Acrylic Acid and n-Butyl Acrylate with the Predetermined Microstructure: Synthesis and Properties. Polymer Science, Series B. 2020 May;62:225-37.

[23] Sofyane A, Ayed EB, Lahcini M, Khouloud M, Kaddami H, Ameduri B, Boufi S, Raihane M. Waterborne butyl methacrylate (co) polymers prepared by pickering emulsion polymerization: Insight of their use as coating materials for slow release-fertilizers. European Polymer Journal. 2021 Aug 5;156:110598.

[24] Abandansari HS, Nabid MR, Rezaei SJ, Niknejad H. pH-sensitive nanogels based on Boltorn® H40 and poly (vinylpyridine) using mini-emulsion polymerization for delivery of hydrophobic anticancer drugs. Polymer. 2015 Aug 5;55(16):3579-90.

[25] Zahran MK, Hamed AI, Ali AE. Synthesis and characterization of polymerizable surfactants based on ethoxylate alcohol cinnamate for emulsion polymerization. Journal of Radiation Research and Applied Sciences. 2022 Jun 1;15(2):59-66.

[26] Fang J, Wang S, Luo Y. Onepot synthesis of octablock copolymers of high-molecular weight via RAFT emulsion polymerization. AIChE Journal. 2020 Jan;66(1):e16781.

[27] Cao Y, Mohamed AM, Mousavi M, Akinay Y. Poly (pyrrole-co-styrene sulfonate)-encapsulated MWCNT/Fe–Ni alloy/NiFe2O4 nanocomposites for microwave absorption. Materials Chemistry and Physics. 2021 Feb 1;259:124169.

[28] Wu Y, Zhang D, Ma P, Zhou R, Hua L, Liu R. Lithium hexamethyldisilazide initiated superfast ring opening polymerization of alpha-amino acid N-carboxyanhydrides. Nature communications. 2018 Dec 13;9(1):5297.

[29] Maciejewska M, Bolbukh YM. Study on synthesis and characterization of porous microspheres with pendant amine groups. Adsorption Science & Technology. 2015 Aug;33(6-8):617-23.

[30] Ahmed MI, Ismail AS. Synthesis and Characterization of Sustainable Co-polymers Using a Series of Methacrylate Monomers and β-myrcene.

[31] Cao Y, Mohamed AM, Mousavi M, Akinay Y. Poly (pyrrole-co-styrene sulfonate)-encapsulated MWCNT/Fe–Ni alloy/NiFe2O4 nanocomposites for microwave absorption. Materials Chemistry and Physics. 2021 Feb 1;259:124169.

[32] Semsarilar M, Abetz V. Polymerizations by RAFT: Developments of the Technique and Its Application in the Synthesis of Tailored (Co) polymers. Macromolecular Chemistry and Physics. 2021 Jan;222(1):2000311.

[33] Scheerder J, Langermans H. The synthesis, interfacial, and colloidal properties of waterborne cationic methacrylic co-polymers. Colloid and Polymer Science. 2016 Apr;292(4):991-1001.

[34] Xiong XB, Binkhathlan Z, Molavi O, Lavasanifar A. Amphiphilic block co-polymers: preparation and application in nanodrug and gene delivery. Acta biomaterialia. 2015 Jul 1;8(6):2017-33.

[35] Xiong XB, Binkhathlan Z, Molavi O, Lavasanifar A. Amphiphilic block co-polymers: preparation and application in nanodrug and gene delivery. Acta biomaterialia. 2012 Jul 1;8(6):2017-33.

[36] Techie-Menson R, Rono CK, Etale A, Mehlana G, Darkwa J, Makhubela BC. New bio-based sustainable polymers and polymer composites based on methacrylate derivatives of furfural, solketal and lactic acid. Materials Today Communications. 2021 Sep 1;28:102721.

[37] Girard E, Marty JD, Ameduri B, Destarac M. Direct synthesis of vinylidene fluoride-based amphiphilic diblock copolymers by RAFT/MADIX polymerization. ACS Macro Letters. 2012 Feb 21;1(2):270-4.

[38] Patel MR, Chitte PS, Bharambe DP. Oleic acid based polymeric flow improvers for Langhnaj (North Gujarat, India) crude oil. Egyptian Journal of Petroleum. 2017 Dec 1;26(4):895-903.

[39] Ghorpade RV, Cho DW, Hong SC. Effect of controlled tacticity of polyacrylonitrile (co) polymers on their thermal oxidative stabilization behaviors and the properties of resulting carbon films. Carbon. 2017 Sep 1;121:502-11.

[40] Toktabayeva AK, Alikulov AZ, Rakhmetullayeva RK, Mun GA, Tumabayeva AM, Urkimbayeva PI, Yu VK, Seilkhanov TM. Synthesis and study of physico-chemical characteristics of novel cationic (Co) polymers based on n-isopropylacrylamide and N-(2-vinyloxyethyl)-n-(2-cyanoethyl) amine. Journal of Chemical Technology and Metallurgy. 2019 May 1;54(3):467-74.

[41] Ansari I, Singh P, Mittal A, Mahato RI, Chitkara D. 2, 2-Bis (hydroxymethyl) propionic acid based cyclic carbonate monomers and their (co) polymers as advanced materials for biomedical applications. Biomaterials. 2021 Aug 1;275:120953.

[42] Ghorpade RV, Cho DW, Hong SC. Effect of controlled tacticity of polyacrylonitrile (co) polymers on their thermal oxidative stabilization behaviors and the properties of resulting carbon films. Carbon. 2017 Sep 1;121:502-11.

[43] Ascencio Carvente P, Maldonado Textle H, Soriano Moro G, Rivera Vallejo CC, González Coronel V, Jiménez Regalado EJ, St Thomas C. Synthesis of linear and branched hydrophobically associating multiblock copolymers via a one-pot process. Journal of Polymer Research. 2020 Aug;27:1-1.

[44] Mayer EA, Pestryakov AN, Klimov IG, Dudchenko VK. Development of technology of suspension polymerization of propylene at "Tomskneftekhim" Company. Advanced Materials Research. 2017 Oct 10;560:510-5.

[45] Wawrzkiewicz M, Podkościelna B. Innovative polymer microspheres with chloride groups synthesis, characterization and application for dye removal. Processes. 2022 Aug 10;10(8):1568.

[46] Podkościelna B, Lutomski M. Study of porous structures and thermal properties of luminescent polymeric microspheres derivatives of naphthalene-2, 7-diol. Adsorption Science & Technology. 2015 Aug;33(6-8):531-7.

[47] Rios LA, Ocampo D, Franco A, Cardona JF, Cardeño F. Efecto de surfactantes polimerizables en la distribución de tamaño de partícula, pH, viscosidad, contenidos de sólidos y de monómero residual de una resina estireno-butilacrilato. Polímeros. 2018;23:352-7.

[48] Ganaie NB, Peerzada GM, Gull U. In vitro synthesis of nearly ultra high molecular weight (NUHMW) polymers using solvent-water suspension method. Colloid and Polymer Science. 2017 Jan;295:89-97.

[49] Nunes RD, Pires RV, Lucas EF, Vianna A, Lomba R. New filtrate loss controller based on poly (methyl methacrylatecovinyl acetate). Journal of Applied Polymer Science. 2015 Aug 15;131(16).

[50] Lei D, Zhao Y, Cheng T, Zeng S, Luo Q. Self-encoding resin beads of combinatorial library screeningg screening. InMicroarrays and Combinatorial Technologies for Biomedical Applications: Design, Fabrication, and Analysis 2015 Jul 18 (Vol. 4966, pp. 146-153). SPIE.

[51] Panahi HA, Mehramizi A, Hosseinifard Z, Moniri E. Synthesis and characterization of new molecular imprinting poly [1-(N, N-bis-carboxymethyl) amino-3-allylglycerol-co-dimethylacrylamide] for selective sorption and determination of cefuroxime sodium in biological and pharmaceutical samples. Reactive and Functional Polymers. 2018 Jan 1;73(1):132-40.

[52] Ganaie NB, Peerzada GM, Gull U. In vitro synthesis of nearly ultra high molecular weight (NUHMW) polymers using solvent-water suspension method. Colloid and Polymer Science. 2017 Jan;295:89-97.

[53] Karki I, Li P, Vik EC, Manzewitsch A, Divirgilio E, Brewer WE, Shimizu KD. Absorption properties of monolithic poly (divinylbenzene-co-N-vinylpyrrolidone) over a wide range of monomer ratios. Reactive and Functional Polymers. 2021 Jun 1;163:104888.

[54] Lashgari S, Arabi H, Mahdavian AR, Ambrogi V. Thermal and morphological studies on novel PCM microcapsules containing n-hexadecane as the core in a flexible shell. Applied energy. 2017 Mar 15;190:612-22.

[55] Ye H, Wang Z, Yang Z, Zhang S, Gong X, Hua J. Bandgap engineering of novel peryleno [1, 12-bcd] thiophene sulfone-based conjugated co-polymers for significantly enhanced hydrogen evolution without co-catalyst. Journal of Materials Chemistry A. 2020;8(38):20062-71.

[56] Shukla G, Ferrier Jr RC. The versatile, functional polyether, polyepichlorohydrin: History, synthesis, and applications. Journal of Polymer Science. 2021 Nov 15;59(22):2704-18.

[57] Stockmann PN, Van Opdenbosch D, Poethig A, Pastoetter DL, Hoehenberger M, Lessig S, Raab J, Woelbing M, Falcke C, Winnacker M, Zollfrank C. Biobased chiral semi-crystalline or amorphous high-performance polyamides and their scalable stereoselective synthesis. Nature communications. 2020 Jan 24;11(1):509.

[58] Zheng M, Wang C, Xu Y, Li K, Liu D. A water-soluble binary conductive binder for Si anode lithium ion battery. Electrochimica Acta. 2019 May 10;305:555-62.

[59] Yao L, Liao H, Ravva MK, Guo Y, Duan J, Wang Y, Yu Y, Li Z, McCulloch I, Yue W. Metal-free polymerization: synthesis and properties of fused benzo [1, 2-b: 4, 5-b′] bis [b] benzothiophene (BBBT) polymers. Polymer Chemistry. 2020;11(22):3695-700.

[60] Tan S, Campi EM, Boysen RI, Saito K, Hearn MT. Batch binding studies with thermo-responsive polymer grafted sepharose 6 fast flow sorbents under different temperature and protein loading conditions. Journal of Chromatography A. 2020 Aug 16;1625:461298.

[61] Li M, Berritt S, Wang C, Yang X, Liu Y, Sha SC, Wang B, Wang R, Gao X, Li Z, Fan X. Sulfenate anions as organocatalysts for benzylic chloromethyl coupling polymerization via C= C bond formation. Nature Communications. 2018 May 1;9(1):1754.

[62] Faingol'd, I. I., Lozhkin, A. D., Smolina, A. V., Soldatova, Y. V., Obraztsova, N. A., Kurmaz, S. V., & Kotel'nikova, R. A . Membranotropic properties of fullerene-containing amphiphilic (co) polymers of N-vinylpyrrolidone. Russian Chemical Bulletin. 2018. 67; 800-805.

[63] Dunlap JH, Loszko AF, Flake RA, Huang Y, Benicewicz BC, Greytak AB. Multiply-binding polymeric imidazole ligands: Influence of molecular weight and monomer sequence on colloidal quantum dot stability. The Journal of Physical Chemistry C. 2018 Nov 1;122(46):26756-63.

[64] Messina MS, Messina KM, Bhattacharya A, Montgomery HR, Maynard HD. Preparation of biomolecule-polymer conjugates by grafting-from using ATRP, RAFT, or ROMP. Progress in polymer science. 2020 Jan 1;100:101186.

[65] Bhebhe MN, De Eulate EA, Pei Y, Arrigan DW, Roth PJ, Lowe AB. Reactive Conjugated Polymers: Synthesis, Modification, and Electrochemical Properties of Polypentafluorophenylacetylene (Co) Polymers. Macromolecular Rapid Communications. 2017 Jan;38(2):1600450.

[66] Faingol'd II, Lozhkin AD, Smolina AV, Soldatova YV, Obraztsova NA, Kurmaz SV, Romanova VS, Shtol'ko VN, Kotel'nikova RA. Membranotropic properties of fullerene-containing amphiphilic (co) polymers of N-vinylpyrrolidone. Russian Chemical Bulletin. 2018 May;67:800-5.

[67] Dunlap JH, Loszko AF, Flake RA, Huang Y, Benicewicz BC, Greytak AB. Multiply-binding polymeric imidazole ligands: Influence of molecular weight and monomer sequence on colloidal quantum dot stability. The Journal of Physical Chemistry C. 2018 Nov 1;122(46):26756-63.

[68] Abaci U, Ustalar A, Yilmaz M, Guney HY. Synthesis of new 2, 5-di (thiophen-2-yl) furan-3-carbonitrile derivatives and investigation of the electrochromic properties of homopolymers and co-polymers with EDOT. RSC advances. 2016;6(33):27836-45.

[69] Bhebhe MN, De Eulate EA, Pei Y, Arrigan DW, Roth PJ, Lowe AB. Reactive Conjugated Polymers: Synthesis, Modification, and Electrochemical Properties of Polypentafluorophenylacetylene (Co) Polymers. Macromolecular Rapid Communications. 2017 Jan;38(2):1600450.

[70] Fila K, Grochowicz M, Podkościelna B. Thermal and spectral analysis of copolymers with sulphur groups. Journal of Thermal Analysis and Calorimetry. 2018 Jul;133:489-97.

[71] Aldosari MA, Othman AA, Alsharaeh EH. Synthesis and characterization of the in situ bulk polymerization of PMMA containing graphene sheets using microwave irradiation. Molecules. 2016 Mar 11;18(3):3152-67.

[72] Abaci U, Ustalar A, Yilmaz M, Guney HY. Synthesis of new 2, 5-di (thiophen-2-yl) furan-3-carbonitrile derivatives and investigation of the electrochromic properties of homopolymers and co-polymers with EDOT. RSC advances. 2016;6(33):27836-45.

[73] Siddiqui MN, Redhwi HH, Gkinis K, Achilias DS. Synthesis and characterization of novel nanocomposite materials based on poly (styrene-co-butyl methacrylate) copolymers and organomodified clay. European polymer journal. 2013 Feb 1;49(2):353-65.

[74] Fila K, Grochowicz M, Podkościelna B. Thermal and spectral analysis of copolymers with sulphur groups. Journal of Thermal Analysis and Calorimetry. 2018 Jul;133:489-97.

[75] Nieswandt K, Georgopanos P, Abetz V. Well-defined polyvinylpyridine-block-polystyrene diblock copolymers via RAFT aqueous-alcoholic dispersion polymerization: Synthesis and isoporous thin film morphology. Polymer Chemistry. 2021;12(15):2210-21.

[76] Strehmel V, Wetzel H, Laschewsky A. Ionic liquids as advantageous reaction media for free radical polymerization. InMacromolecular Symposia 2014 Aug (Vol. 342, No. 1, pp. 78-85).

[77] Ray P, Hughes T, Smith C, Simon GP, Saito K. Synthesis of bioacrylic polymers from dihydro-5-hydroxyl furan-2-one (2H-HBO) by free and controlled radical polymerization. ACS omega. 2018 Feb 20;3(2):2040-8.

[78] Areephong J, Mattson KM, Treat NJ, Poelma SO, Kramer JW, Sprafke HA, Latimer AA, De Alaniz JR, Hawker CJ. Triazine-mediated controlled radical polymerization: new unimolecular initiators. Polymer Chemistry. 2016;7(2):370-4.

[79] Mandal M, Chakraborty D, Ramkumar V. Zr (iv) complexes containing salan-type ligands: synthesis, structural characterization and role as catalysts towards the polymerization

of ε-caprolactone, rac-lactide, ethylene, homopolymerization and copolymerization of epoxides with CO 2. RSC advances. 2015;5(36):28536-53.

[80] Sarkar P, Bhowmick AK. Terpene based sustainable methacrylate copolymer series by emulsion polymerization: Synthesis and structure-property relationship. Journal of Polymer Science Part A: Polymer Chemistry. 2017 Aug 15;55(16):2639-49.

[81] Sahu P, Bhowmick AK. Sustainable self-healing elastomers with thermoreversible network derived from biomass via emulsion polymerization. Journal of Polymer Science Part A: Polymer Chemistry. 2019 Mar 15;57(6):738-51.

[82] Kohut A, Voronov S, Demchuk Z, Kirianchuk V, Kingsley K, Shevchuk O, Caillol S, Voronov A. Non-conventional features of plant oil-based acrylic monomers in emulsion polymerization. Molecules. 2020 Jun 30;25(13):2990.

[83] Deane OJ, Musa OM, Fernyhough A, Armes SP. Synthesis and characterization of waterborne pyrrolidone-functional diblock copolymer nanoparticles prepared via surfactant-free RAFT emulsion polymerization. Macromolecules. 2020 Feb 5;53(4):1422-34.

[84] Ma J, Lu M, Zhang H. Poly (methyl methacrylate)-b-poly (butyl acrylate) block copolymers synthesized via RAFT emulsion polymerization. Journal of Macromolecular Science, Part A. 2014 Apr 3;51(4):279-85.

[85] Engelis NG, Anastasaki A, Nurumbetov G, Truong NP, Nikolaou V, Shegiwal A, Whittaker MR, Davis TP, Haddleton DM. Sequence-controlled methacrylic multiblock copolymers via sulfur-free RAFT emulsion polymerization. Nature chemistry. 2017 Feb;9(2):171-8.

[86] Chardon F, Denis M, Negrell C, Caillol S. Hybrid alkyds, the glowing route to reach cutting-edge properties?. Progress in Organic Coatings. 2021 Feb 1;151:106025.

[87] Deane OJ, Musa OM, Fernyhough A, Armes SP. Synthesis and characterization of waterborne pyrrolidone-functional diblock copolymer nanoparticles prepared via surfactant-free RAFT emulsion polymerization. Macromolecules. 2020 Feb 5;53(4):1422-34.

[88] Xu L, Xu L, Dai WS, Tsuboi T. Preparation and characterization of a novel fluoro-silicone acrylate copolymer by semi-continuous emulsion polymerization. Journal of Fluorine Chemistry. 2013 Sep 1;153:68-73.

[89] Engelis NG, Anastasaki A, Nurumbetov G, Truong NP, Nikolaou V, Shegiwal A, Whittaker MR, Davis TP, Haddleton DM. Sequence-controlled methacrylic multiblock copolymers via sulfur-free RAFT emulsion polymerization. Nature chemistry. 2017 Feb;9(2):171-8.

[90] Schiavo SL, Mineo P, Cardiano P, Piraino P. Novel propylmethacrylate-monofunctionalized polyhedral oligomeric silsesquioxanes homopolymers prepared via radical bulk free polymerization. European Polymer Journal. 2017 Dec 1;43(12):4898-904.

[91] Guimarães TR, Khan M, Kuchel RP, Morrow IC, Minami H, Moad G, Perrier S, Zetterlund PB. Nano-engineered multiblock copolymer nanoparticles via reversible addition–fragmentation chain transfer emulsion polymerization. Macromolecules. 2019 Apr 3;52(8):2965-74.

[92] Li K, Qin Y, Zhao Y, Wang D, Dong JY. Industrial adaptability of the Ziegler–Natta catalyst-friendly synthesis of long-chain-branched polypropylene based on ω-alkenylmethyldichlorosilane-assisted propylene polymerization. Industrial & Engineering Chemistry Research. 2021 Mar 16;60(12):4589-601.

[93] Ferreira GR, Braquehais JR, da Silva WN, Machado F. Synthesis of soybean oil-based polymer lattices via emulsion polymerization process. Industrial Crops and Products. 2015 Mar 1;65:14-20.

[94] Atta AM, Brostow W, Lobland HE, Hasan AR, Perez JM. Porous polymer oil sorbents based on PET fibers with crosslinked copolymer coatings. RSC advances. 2015;3(48):25849-57.

[95] Engelis NG, Anastasaki A, Nurumbetov G, Truong NP, Nikolaou V, Shegiwal A, Whittaker MR, Davis TP, Haddleton DM. Sequence-controlled methacrylic multiblock copolymers via sulfur-free RAFT emulsion polymerization. Nature chemistry. 2017 Feb;9(2):171-8.

[96] Soller BS, Zhang N, Rieger B. Catalytic Precision Polymerization: Rare Earth MetalMediated Synthesis of Homopolymers, Block Copolymers, and Polymer Brushes. Macromolecular Chemistry and Physics. 2015 Oct;215(20):1946-62.

[97] Brotherton EE, Jesson CP, Warren NJ, Smallridge MJ, Armes SP. New AldehydeFunctional Methacrylic Water-Soluble Polymers. Angewandte Chemie. 2021 May 17;133(21):12139-44.

[98] Jesson CP, Cunningham VJ, Smallridge MJ, Armes SP. Synthesis of high molecular weight poly (glycerol monomethacrylate) via RAFT emulsion polymerization of isopropylideneglycerol methacrylate. Macromolecules. 2018 Apr 16;51(9):3221-32.

[99] Deane OJ, Lovett JR, Musa OM, Fernyhough A, Armes SP. Synthesis of well-defined pyrrolidone-based homopolymers and stimulus-responsive diblock copolymers via RAFT aqueous solution polymerization of 2-(N-Acryloyloxy) ethylpyrrolidone. Macromolecules. 2018 Sep 25;51(19):7756-66.

[100] Cekingen SK, Saltan F, Yildirim Y, Akat H. A novel HEMA-derived monomer and copolymers containing side-chain thiophene units: Synthesis, characterization and thermal degradation kinetics. Thermochimica acta. 2015 Oct 20;546:87-93.

[101] Sana B, Unnikrishnan G, Jana T, KS SK. Polybenzimidazole co-polymers: their synthesis, morphology and high temperature fuel cell membrane properties. Polymer Chemistry. 2020;11(5):1043-54.

[102] Xu X, Wu Y, Fang J, Li Z, Wang Z, Li Y, Peng Q. Side Chain engineering of Benzodithiophene-fluorinated Quinoxaline low bandgap co polymers for high performance polymer solar cells. Chemistry–A European Journal. 2017 Oct 6;20(41):13259-71.

[103] Diao L, Su K, Li Z, Ding C. Furan-based co-polyesters with enhanced thermal properties: poly (1, 4-butylene-co-1, 4-cyclohexanedimethylene-2, 5-furandicarboxylic acid). RSC advances. 2016;6(33):27632-9.

[104] Sivasankarapillai G, McDonald AG, Li H. Lignin valorization by forming toughened lignin-co-polymers: Development of hyperbranched prepolymers for cross-linking. biomass and bioenergy. 2015 Dec 1;47:99-108.

[105] Liu Q, Moghe D, Sardar G, Manzhos S, Bottle SE, Kyaw AK, Kabra D, Sonar P. Structural geometry variation of 1, 4-naphthalene-based co-polymers to tune the device performance of PVK-host-based OLEDs. Polymers. 2021 Aug 30;13(17):2914.

[106] Meo PL, Lazzara G, Liotta L, Riela S, Noto R. Cyclodextrin–calixarene co-polymers as a new class of nanosponges. Polymer Chemistry. 2018;5(15):4499-510.

[107] Matos M, Sousa AF, Mendonça PV, Silvestre AJ. Co-Polymers based on Poly (1, 4-butylene 2, 5-furandicarboxylate) and Poly (propylene oxide) with Tuneable Thermal Properties: Synthesis and Characterization. Materials. 2019 Jan 21;12(2):328.

[108] Diao L, Su K, Li Z, Ding C. Furan-based co-polyesters with enhanced thermal properties: poly (1, 4-butylene-co-1, 4-cyclohexanedimethylene-2, 5-furandicarboxylic acid). RSC advances. 2016;6(33):27632-9.

[109] Dircio J, Gelover-Santiago A, Caicedo C, Carreón-Castro MD, Valdez-Hernández Y, Rivera E. Synthesis and characterization of novel polythiophenes containing azobenzene units and well-defined oligo (ethylene glycol) spacers: thermal and optical properties, and preparation of langmuir films. Designed Monomers and Polymers. 2012 Jan 1;15(2):175-95.

[110] Amna B, Isci R, Siddiqi HM, Majewski LA, Faraji S, Ozturk T. High-performance, low-voltage organic field-effect transistors using thieno [3, 2-b] thiophene and benzothiadiazole co-polymers. Journal of Materials Chemistry C. 2022;10(21):8254-65.

[111] Schmied FP, Bernhardt A, Moers C, Meier C, Endres T, Klein S. A novel aminomethacrylate-based copolymer for solubility enhancement—From radical polymer synthesis to manufacture and characterization of amorphous solid dispersions. Polymers. 2022 Mar 22;14(7):1281.

[112] van Hensbergen JA, Ganda S, Roth PJ, Burford RP, Lowe AB. ROMP synthesis of novel thermo-, p H-, and salt-responsive (co) polymers containing the morpholino functional group. Journal of Polymer Science Part A: Polymer Chemistry. 2015 Jan 1;53(1):50-8.

[113] Schmied FP, Bernhardt A, Klein S. Preparation of solid self-nanoemulsifying drug delivery systems (S-SNEDDS) by co-extrusion of liquid SNEDDS and polymeric carriers—A new and promising formulation approach to improve the solubility of poorly water-soluble drugs. Pharmaceuticals. 2022 Sep 11;15(9):1135.

[114] Quek JY, Zhu Y, Roth PJ, Davis TP, Lowe AB. RAFT Synthesis and aqueous solution behavior of novel pH-and thermo-responsive (co) polymers derived from reactive

poly (2-vinyl-4, 4-dimethylazlactone) scaffolds. Macromolecules. 2017 Sep 24;46(18):7290-302.

[115] Quek JY, Roth PJ, Evans RA, Davis TP, Lowe AB. Reversible addition–fragmentation chain transfer synthesis of amidine-based, CO2-responsive homo and AB diblock (Co) polymers comprised of histamine and their gas-triggered self-assembly in water. Journal of Polymer Science Part A: Polymer Chemistry. 2015 Jan 15;51(2):394-404.

[116] Bhebhe MN, De Eulate EA, Pei Y, Arrigan DW, Roth PJ, Lowe AB. Reactive Conjugated Polymers: Synthesis, Modification, and Electrochemical Properties of Polypentafluorophenylacetylene (Co) Polymers. Macromolecular Rapid Communications. 2017 Jan;38(2):1600450.

[117] Zhu Y, Noy JM, Lowe AB, Roth PJ. The synthesis and aqueous solution properties of sulfobutylbetaine (co) polymers: comparison of synthetic routes and tuneable upper critical solution temperatures. Polymer Chemistry. 2015;6(31):5705-18.

[118] Sun W, Sun B, Li Y, Huang X, Fan H, Zhao X, Sun H, Sun W. Thickening supercritical CO2 with π-stacked Co-polymers: molecular insights into the role of intermolecular interaction. Polymers. 2018 Mar 6;10(3):268.

[119] Sulaiman TN, Larasati D, Nugroho AK, Choiri S. Assessment of the Effect of PLGA Co-polymers and PEG on the Formation and Characteristics of PLGA-PEG-PLGA Co-block Polymer Using Statistical Approach. Advanced Pharmaceutical Bulletin. 2019 Aug;9(3):382.

[120] Bier F, Six JL, Durand A. DOPO-Based Phosphorus-Containing Methacrylic (Co) Polymers: Glass Transition Temperature Investigation. Macromolecular Materials and Engineering. 2019 Apr;304(4):1800645.

[121] Tiwari R, Sonker E, Kumar D, Kumar K, Adhikary P, Krishnamoorthi S. Preparation, Characterization and electrical properties of alkali metal ions doped co-polymers based on TBF. Materials Science and Engineering: B. 2020 Dec 1;262:114687.

[122] Grytsenko O, Spišák E, Dulebová Ľ, Moravskii V, Suberlyak O. Sorption capable film coatings with variable conductivity. InMaterials Science Forum 2015 Jun 1 (Vol. 818, pp. 97-100). Trans Tech Publications Ltd.

[123] Iliescu S, Augusti MG, Fagadar-Cosma E, Plesu N, Fagadar-Cosma G, Macarie L, Popa A, Ilia G. Synthesis of new phosphorus-containing (co) polyesters using solid-liquid phase transfer catalysis and product characterization. Molecules. 2016 Jul 31;17(8):9090-103.

[124] Ghosh NG, Sarkar A, Zade SS. The type-II nn inorganic/organic nano-heterojunction of Ti3+ self-doped TiO2 nanorods and conjugated co-polymers for photoelectrochemical water splitting and photocatalytic dye degradation. Chemical Engineering Journal. 2021 Mar 1;407:127227.

[125] Michálek J, Abbrent S, Musil M, Kovářová J, Hodan J, Dybal J. New type of gel polymer electrolytes based on selected methacrylates and their characteristics. Part II. Fluorinated Co-polymers. Electrochimica Acta. 2016 Aug 1;208:211-24.

[126] Gomez I, Mantione D, Leonet O, Blazquez JA, Mecerreyes D. Hybrid sulfur− selenium co-polymers as cathodic materials for lithium batteries. ChemElectroChem. 2018 Jan 12;5(2):260-5.

[127] Lebedeva OV, Pozhidaev YN, Sipkina EI. The synthesis and properties of copolymers based on N-vinylpyrazole. International Polymer Science and Technology. 2015 Apr;42(4):27-32.

[128] Salikhov RB, Biglova YN, Mullagaliev IN, Salikhov TR, Mustafin AG. Functionalized polyanilines: influence of the surface morphology on the electrophysical and sensory properties of thin films based on them. Letters on Materials. 2021 May 1;11(2):140-5.

[129] Venkatesan S, Obadja N, Chang TW, Chen LT, Lee YL. Performance improvement of gel-and solid-state dye-sensitized solar cells by utilization the blending effect of poly (vinylidene fluoride-co-hexafluropropylene) and poly (acrylonitrile-co-vinyl acetate) co-polymers. Journal of Power Sources. 2015 Dec 5;268:77-81.

[130] Kumar AG, Bera D, Banerjee S, Veerubhotla R, Das D. Sulfonated poly (ether imide) s with fluorenyl and trifluoromethyl groups: Application in microbial fuel cell (MFC). European Polymer Journal. 2016 Oct 1;83:114-28.

Al-Kitab Journal for Pure Sciences (2025); 9(1):34-50.
https://doi.org/10.32441/kjps.09.01.p3

Al-Kitab Journal for Pure Sciences
ISSN: 2617-1260 (print), 2617-8141(online)

https://isnra.net/index.php/kjps

Investigation Of the Effects of Three COVID-19 Vaccines

Ali Farhan Hashoosh[1*], Hmood Madhi Hasan[2]

[1]Department of Mathematics, College Basic Education, University of Misan University, the Country Iraq.
[2]Department of Medicine, College Medicine, University of Misan, the Country Iraq

[*]Corresponding Author: ali_fr@uomisan.edu.iq

Citation: Hashoosh AF, Hasan HM. Investigation Of The Effects Of Three COVID-19 Vaccines. Al-Kitab J. Pure Sci. [Internet]. 2024 Dec. 31;9(01):34-50. DOI: https://doi.org/10.32441/kjps.09.01.p3

Keywords: Applied Statistics, AstraZeneca, Sinopharm, Pfizer-Biontec, SPSS Program.

Article History
Received 16 Mar. 2024
Accepted 13 Jun. 2024
Available online 31 Dec. 2024

Abstract:

This research deals with the three types of COVID-19 vaccines (AstraZeneca vaccine, Sinopharma, and Pfizer-Biontech) in terms of manufacturing, producing companies, and the countries in which the tests were conducted, in addition to the teams that provided the researchers with these vaccines. In this research, a statistical study about the effectiveness of these vaccines is presented and the extent of their impact on the vaccinator if he was healthy or carrying some other diseases. After that, a statistical study is presented, comparing it between the types of vaccines and which one is the most used, by taking a sample from the State of Iraq, Maysan Governorate, consisting of 60 individuals who took the vaccine. a special questionnaire was used for this purpose and the results were, another questionnaire about the acceptance of the local community results were analyzed using an SPSS program (**Table 5**, **6** and **7**). Another questionnaire about the acceptance of the local community representing Maysan Governorate to obtain the vaccine for the emerging coronavirus, COVID-19. The questionnaire was also delivered to statistical specialists before submitting the questionnaire. Important results were obtained, including the most received vaccine Pfizer-BioNTech and Sinopharm, by 40% and all those who received the vaccine were not infected after taking the vaccine.

Keywords: Applied Statistics, AstraZeneca, Sinopharm, Pfizer-Biontec, SPSS Program.

دراسة تأثيرات اللقاحات الثلاث لكوفيد-١٩

علي فرحان حاشوش*[١]، حمود ماضي حسن[٢]

قسم الرياضيات، كلية التربية الأساسية، جامعة ميسان، العراق
كلية الطب، جامعة ميسان، العراق

ali_fr@uomisan.edu.iq , Hmood.mcm@uomisan.edu.iq

الخلاصة:

تعرفنا في هذا البحث على الأنواع الثلاث للقاحات كوفيد-١٩ (لقاح أسترازينيكا، وسينوفارما، وفايزر-بيونتك) من حيث التصنيع والشركات المنتجة والدول التي أجريت فيها الاختبارات، بالإضافة إلى الفرق التي قدمت لنا هذه اللقاحات. وقد قدمنا في هذا البحث دراسة إحصائية عن فعالية هذه اللقاحات ومدى تأثيرها على الملقّح إذا كان سليماً أو حاملاً لبعض الأمراض الأخرى. بعد ذلك قمنا بعرض دراسة إحصائية، ومقارنتها بين أنواع اللقاحات وأيها الأكثر استخداما، وذلك من خلال أخذ عينة من دولة العراق محافظة ميسان، مكونة من ٦٠ فردا ممن أخذوا اللقاح. وزودناهم باستبيان خاص بنتائج الاستبيانات، وتم تحليل نتائج الاستبيان باستخدام برنامج SPSS، وقدمنا استبياناً آخر حول مدى قبول المجتمع المحلي ممثلاً في محافظة ميسان للحصول على اللقاح المضاد لفيروس كورونا المستجد، كوفيد-١٩، كما تم عرض الاستبيان على المختصين الإحصائيين قبل تقديم الاستبيان. وتم الحصول على نتائج مهمة، من بينها اللقاح الأكثر تلقيا هو فايزر-بيونتك وسينوفارم بنسبة ٤٠٪ وجميع من تلقوا اللقاح لم يصابوا بالعدوى بعد أخذ اللقاح COVID-19.

الكلمات المفتاحية: إحصاء تطبيقي، لقاح استرازينيكا، لقاح سينوفارم، لقاح فايزر- بايونتك، برنامج SPSS.

1. Introduction

Following the disease's initial appearance in Wuhan, China, in early December 2019, and its subsequent spread to other Chinese cities before rapidly expanding to the rest of the world, the World Health Organization formally declared on January 30 that the virus outbreak represents a public health emergency of global concern and verified On March 11, the outbreak developed into a pandemic, resulting in an unprecedented occurrence that could necessitate a concerted international response and threaten the public health of other nations due to the disease's international spread. As of May 26, 2021, there have been over 167 million cases of Covid-19 infections across more than 188 countries and regions. which includes over 3,480,000 deaths and over a million infected individuals who have recovered. With over 25% of the confirmed infections worldwide, the United States is the nation most impacted by the pandemic **[1][2]**. The primary method of virus transmission is close contact between people, frequently through respiratory droplets from talking, sneezing, or coughing. Droplets typically don't travel very far

through the air before landing on the ground or other surfaces. In an uncommon scenario, people can contract the virus by touching their mouth, nose, or eyes after coming into contact with a contaminated surface [1][3][4][5].

In patients who are asymptomatic, the disease may spread prior to the onset of symptoms, with the highest transmissibility occurring in the first three days following the onset of symptoms.

Significant global social and economic harm was caused by the pandemic, including the greatest recession since the Great Depression, as well as the postponement or cancellation of athletic, religious, political, and cultural events, a severe shortage of supplies and equipment made worse by panic buying, and a decrease in greenhouse gas and pollutant emissions. Online misinformation about the virus has proliferated, and there have been instances of racial discrimination and xenophobia directed towards Chinese individuals and those who are thought to be Chinese or to originate from regions with elevated infection rates. Approximately 73.5% of students worldwide were impacted by the national or local closure of schools, universities, and colleges in 190 different countries. After that, most universities and schools resorted to electronic study, and their level of success varied from one country to another and from one city to another, where students whose financial condition is not Good. They are suffering from the costs of using educational aids, because they require the availability of the Internet and continuous electric power, which has caused many students to leave their schools and universities [6][7].

All of this required the developed countries to conduct tests and take samples to find a vaccine that would help end this pandemic. Therefore, many teams in companies, universities, and research centers (Oxford University, Edward Jenner Institute, ...) conducted many tests and took samples to reach a suitable vaccine. We all know the importance of mathematics, as many diseases are studied based on mathematical models [8] Sometimes the stability of these diseases or the extent of their control is studied [9][10].

2. Research Importance

The following are just a few of the statements that highlight the significance of the research:

1. Educating others about the significance of receiving the vaccination.
2. Providing enough details about every kind of vaccination, including its composition, effectiveness, level of safety, and adverse effects.
3. Outlining the community sample's views on vaccination acceptance and the degree to which it is accepted.

4. Knowing the most used types of vaccines through the statistics mentioned in the research.

3. Questions

• The most important questions about taking the vaccine are as follows:

• What does the AstraZeneca vaccine mean?

• What does the Sinopharm vaccine mean?

• What does the Pfizer-BioNTech vaccine entail?

• What are the most used vaccines?

• What are the side effects after taking the vaccine?

• Is the person infected after taking the vaccine?

•How many doses should the vaccinator take?

4. Target Groups

There are targeted groups to take this vaccine because they are more likely to be exposed to Covid-19 compared to the rest of their peers, so the priority was for them to take the vaccine dose, and these groups are:

1- Employees of the Ministry of Health (with all their job titles) (high risk, medium risk, low risk).

2- The elderly ($50-59$ years old, $60-69$ years old, over 70 years old)

3- People with chronic diseases.

4- Personnel from security forces (all kinds).

5- Displaced persons and refugees in camps.

6- People with cancer, immune disorders, and hereditary blood diseases.

7- Those with high-risk professions: (teaching staff, media professionals, employees at railroad and border crossings, eateries, and convicts residing in state houses and prisons.

5. Methods

For the purpose of this review, English-language articles published between January 15, 2020, and January 1, 2022 were searched using international databases such as PubMed, Web of Science, and Scopus. There were articles of every kind: OVID-19, new coronavirus, 2019-nCoV, coronavirus disease 2019, vaccination, Sputnik V, Gamaleya, Gam-COVID-Vac, Sinopharm, BBIBP-CorV, Oxford, ChAdOx1 nCoV-19, AstraZeneca, and AZD1222 were the keywords used. References were imported into Endnote software and duplicate titles were eliminated after collecting articles of interest. In the chosen research there are a total of 13 vaccines that have been approved by the emergency use listing (EUL), have national licenses,

or have conditional use, according to the UNICEF website (**Table 1**). Three vaccines are available in Iran: FAKHRAVAC (MIVAC), which has one trial, Razi Vaccine and Serum Research Institute (Razi Cov Pars), which has two trials, and Shifa Pharmed Industrial Co., which has four trials [15].

Table 1: Number of vaccine approvals reported by UNICEF [11][12][13][14]

Vaccine developer	WHO EUL	Licensure	Emergency/conditional use
Anhui Zhifei Longcom Biopharmaceutical	-	1	1
AstraZeneca	2	4	65
Beijing Institute of Biological Products (CNBG)	1	2	16
Bharat Biotech	-	-	6
CanSino Biologicals	-	-	5
Chumalov	-	1	-
Gamaleya Research Institute	-	8	54
Janssen	1	1	37
Moderna	1	1	33
Pfizer/BioNTech	1	6	58
Sinovac	-	-	23
Vector State Research Center	-	1	-
Wuhan Institute of Biological Products	-	1	1

6- COVID-19 Vaccines

After a lot of time has passed, the World Health Organization approved some types of vaccines after they proved their effectiveness. In this research, three types of these vaccines are explained that are more effective and accepted in most countries of the world.

6.1. AstraZeneca vaccine (AZD1222)

Oxford-AstraZeneca OZD1222 Vaccine (in English: AZD1222) It is also known as: ChAdOx1 nCoV-19 and is referred to in the media as: AstraZeneca vaccine, Oxford vaccine, or the newly formed Vacciferia vaccine. It is a vaccine against Coronavirus disease. It was developed and produced by Oxford University in collaboration with the British-Swedish company AstraZeneca. It is meant to be injected intramuscularly. A group led by Sarah Gilbert, Adrienne Hill, Andrew Pollard, Theresa Lambie, Sandy Douglas, and Catherine Green from the Oxford Vaccine Group and the Edward Jenner Institute for Vaccine Research is conducting the vaccine research. Phase III clinical trials for the vaccine were started in November 2020 [16].

Based on a regimen that involves administering half the dose and then the full dose after a minimum of one month, the vaccine proved to be 90% effective. These findings were derived from multiple trials involving participants who were all under the age of fifty-five. When two complete doses were administered at least one month apart, another dosage schedule demonstrated 62% efficacy [17]. Working with the Italian vaccine manufacturer Advent SRI in Pomezia, on the IRPM campus, the Edward Jenner Institute and the Vaccine Research Group

at the University of Oxford conducted the study. The first batch of the COVID-19 vaccine for use in clinical trials was made at this facility [18]. Leading the research team were Sandy Douglas, Catherine Green, Teresa Lambie, Andrew Pollard, Adrienne Hill, and Sarah Gilbert. On December 30, 2020, the vaccine was approved for use in the UK immunization program, and on January 4, 2021, the first dose was given. In March 2021, some countries stopped Among them, Germany, France, Italy, Spain, the Netherlands, Norway, Denmark and Sweden have used the vaccine temporarily for fear of its connection to rare cases of blood clotting that have been observed in a small number of vaccine recipients. After the European Medicines Agency's statement, European countries resumed AstraZeneca vaccinations [19][20]. However, the controversy over the vaccine's relationship to rare blood clotting cases continued after doubts about the vaccine's effectiveness, which were later corrected, in addition to the death of seven people in Britain who received the AstraZeneca vaccine, Table 2 shows the characteristics of the vaccine [21].

Table 2: Characteristics Of The AstraZeneca Vaccine (AZD1222)

Property	the details
Vaccine Making Technology	Non-Replicating Viral Vector
Number Of Doses	2
The Interval Between Doses	٤weeks
Target Groups	+١٨ years old
Method Of Administration	Deltoid glaucoma
Storage Temperature	$(+2\ to\ +8)$degrees Celsius
Packing Type	Multi-dose vial
The Amount Of Vaccine In One Vial	(١٠)potions
Dose	0.5 ml
Pharmaceutical Form	Liquid
Vaccine Vial Monitor Vvm	Nothing
Open Bottle Policy	The vial is damaged 6 hours after opening it or at the end of the vaccination session
Effectiveness	70.4 %
Expiry	٦months
Light Sensitivity	Photosensitive
Side Effects	•Very common symptoms: pain, swelling and slight redness at the injection site, headache, joint and muscle pain, fever and feeling tired. •Common symptoms: flu-like symptoms (high temperature, pharyngitis, runny nose, cough and chills), fever, vomiting. •Uncommon symptoms: loss of appetite, abdominal pain, excessive sweating, itchy skin or rash, swollen lymph nodes.

6.2. Sinopharm vaccine (BBIBP-CorV)

It is one of the two candidate vaccines against coronavirus disease, which the China National Pharmaceutical Industries Group is developing and producing, and it is intended for intramuscular injection. As of December 2020, the vaccine has entered phase III clinical trials in: Among those with more than 60,000 subjects were Argentina, Bahrain, Egypt, Morocco, Pakistan, Peru, and the United Arab Emirates. Through China's emergency use program, almost one million people had received the vaccine as of November 2020. Nearly 100,000 UAE residents had gotten the vaccination by December 2020 as part of a voluntary program **[22][23]**. The Sinopharm vaccine was formally registered by the UAE on December 9, 2020, following an interim analysis of Phase III trials that revealed the vaccine's 86% efficacy against COVID-19 infection. It was given permission to use the vaccine along with Bahrain, but the UAE did not specify how it would be used **[24]**. On December 12, 2020, Peru halted trials of the Sinopharm vaccine to investigate an adverse event in a volunteer before restarting trials on December 16. The vaccine uses similar, more traditional technology as CoronaVac and other vaccines being developed in phase III trials **[25]**. Such technology has been successfully applied to many well-known vaccines such as the rabies vaccine, but the lack of public data could limit the vaccine's distribution in a variety of other countries, **Table 3**. shows the characteristics of the vaccine.

Table 3: characteristics of the Sinopharm vaccine (BBIBP-CorV) 6.3. Pfizer–BioNTech

Property	the details
Vaccine making technology	Inactivated virus (IV)
number of doses	2
The interval between doses	21 days
Target groups	60-18 years old
method of administration	Deltoid glaucoma
storage temperature	$(+2\ to\ +8)$degrees Celsius
packing type	Various fillings
The amount of vaccine in one vial	single and multiple
Dose	0.5 ml
Pharmaceutical form	Liquid
Vaccine Vial Monitor VVM	Nothing
Open bottle policy	The vial is damaged 6 hours after opening it or at the end of the vaccination session
Effectiveness	79.34 %
Expiry	9 months
light sensitivity	Photosensitive
side effects	Common symptoms (10%): such as pain, swelling and stiffness at the injection site, fatigue, body aches, mild diarrhea and fever that disappears within 4 days after taking the vaccine. Note: No other serious side effects have been reported with this vaccine, although people who are allergic to other vaccines or to the first dose of this vaccine may be at risk of an allergic reaction.

The WHO Strategic Advisory Group of Experts on Immunization released policy recommendations regarding the launch of Pfizer-BioNTech's COVID-19 vaccine, which was the first to be approved by the WHO under the Emergency Use Protocol. The Pfizer-BioNTech COVID-19 vaccine with mRNA technology is a safe and effective vaccination, according to the Strategic Expert Group. On the other hand, immunization is not advised for a few specific groups due to contraindications, a lack of supplies, or insufficient information. Currently, these groups include individuals who have experienced severe allergic reactions in the past, the majority of pregnant women, non-priority international travelers, and children under the age of sixteen. Currently, immunizing health workers who are at high risk of infection comes first, then the elderly, and then the general public. People with allergies The vaccine shouldn't be administered to anyone who has experienced severe allergic reactions to any of its ingredients in the past. expectant and nursing mothers COVID-19 is linked to an increased risk of accessible delivery and puts pregnant women at higher risk of serious complications. However, because there is not enough information at this time, the organization does not advise pregnant women to get vaccinated. A pregnant woman may be advised to consider vaccination in consultation with her healthcare provider if there is an unavoidable risk of exposure (such as working in healthcare). The nursing mother can get the vaccination if she belongs to a group that is advised to get it (like health professionals). The WHO advises against quitting breastfeeding following immunization. Children younger than 16 have not been subjected to vaccination trials. Therefore, even though they belong to one of the groups most at risk of infection, the WHO does not currently recommend immunizing children under the age of sixteen. Individuals with Recognized Health Issues It has been demonstrated that the vaccine is both safe and effective in individuals with a range of illnesses linked to a higher risk of developing serious illnesses. This covers stable and managed chronic conditions as well as diabetes, asthma, pulmonary disease, liver, and kidney disease. Further research on how the vaccine affects individuals with compromised immune systems is required. According to the initial recommendation, immunocompromised individuals who belong to a group that is advised to be vaccinated may get the recommended vaccination, but only after receiving information and counseling, if available. COVID-19 can cause serious complications for people living with HIV. Little information about the safety of vaccines in HIV-positive individuals under close observation has been obtained from clinical trials. As much as possible, those getting immunizations should be advised and made aware of the data that is currently available. People who have had COVID-19 in the past can be vaccinated. However, due to limited vaccine supplies, these people may

wish to defer vaccination for up to 6 months after they have been infected with SARS-CoV-2. As more information on the length of acquired immunity following infection becomes available, this time frame may be adjusted. It is not advised to test for prior infections when making vaccination decisions. Visitors At this time, the World Health Organization opposes requiring proof of COVID-19 vaccination from foreign visitors in order to grant them permission to enter or exit a nation or to travel abroad. View the WHO's preliminary travel advice while visiting other countries during the Covid-19 pandemic. The first dose of the vaccine has a protective effect that lasts for 12 days. However, in order to obtain complete protection, two doses must be administered; the recommended interval between the two doses is 21 to 28 days. More research is needed to understand the longer-lasting protection that may occur after receiving just one dose of the virus, **Table 4**. shows the characteristics of the vaccine **[26]**.

Table 4: characteristics of the vaccine Pfizer–BioNTech

Property	the details
Vaccine making technology	Transfer RNA (mRNA) technology
number of doses	2
The interval between doses	21 to 28 days
Target groups	$+١٨$ years old
method of administration	Deltoid glaucoma
storage temperature	$(-60)\ to\ (-80)\ degrees\ Celsius$
packing type	Multi-dose vial
The amount of vaccine in one vial	(6) potions
Dose	0.3 ml
Single dose packing size	$1.8cm^3$
Pharmaceutical form	frozen liquid
Solvent type	The vial is damaged 6 hours after opening it or at the end of the vaccination session
Solvent type	9% Sodium Chloride solution
The amount of solvent required for each dose	$1.8ml$
Vaccine Vial Monitor VVM	Nothing
Open bottle policy	The vial is damaged 6 hours after opening it or at the end of the vaccination session
Effectiveness	95 %
Expiry	a- 6 months from 60 to 80 degrees Celsius b- Five days at $+2\ to\ +8$ degrees Celsius c- 6 hours after thawing at the time of the vaccination session
light sensitivity	Photosensitive
side effects	• Very common side effects include headaches, joint and muscle pain, mild pain and swelling at the injection site, fever (especially after the second dose), and so on. All of these symptoms usually go away in a few hours or with the help of basic analgesics. • Common signs and symptoms include injection site redness and nausea. • Uncommon symptoms include enlarged lymph nodes, sleeplessness, limb pain, overall weakness, and injection site itching. • Bell's palsy is a rare condition characterized by numbness

	and weakness in one side of the face's muscles. • Severe allergy symptoms that go undiagnosed; • Anaphylactic shock.

Table 5: The (Approximate) Number Of Targets In Maysan Governorate

Target group (approximate)					population	Governorate name
The total	Elderly people	risk groups	security forces	Health personnel		
271935	175635	35000	50000	11300	1171802	Maysan

7. The Questionnaire

A questionnaire about the emerging coronavirus (COVID-19) vaccine in Iraq, Maysan Governorate was conducted. It included two surveys, as follows:

7.1. A sample survey of people who had taken the COVID-19 vaccine

A sample survey of people who had taken the COVID-19 vaccine is presented in this section. The questionnaire included 60 people (**Figure1**), and the questionnaire appeared as follows:

1-What type of vaccine did you receive?

a) AstraZeneca 20% b) Sinopharm 40% c) Pfizer-BioNTech 40%

2- Were you afraid when you took the vaccine?

a) Yes 10% b) No 70% c) Some what 20%

3- Do you have the social media to get the vaccine?

a) Yes 100% b) No 0% c) somewhat 0%

4- Were you forced by virtue of your work to take the vaccine?

a) Yes, 5% b) No, 80% c) Somewhat 15%

5-What were the reasons that prompted you to take the vaccine (if you were not forced to take it)?

a) In response to the recommendations of the World Health Organization 10%

b) to the severity of your workplace 30% c) Self-desire 60%

6- Do you advise others to take the vaccine?

a) Yes, 95% b) No 0% c) Somewhat 5%

7- Are you satisfied with how the health staff dealt with you while you were vaccinated?

a) Yes, 95% b) No 0% c) Somewhat 5%

8- Do you have chronic diseases?

a) Yes, 25% b) No, 75%

9- Are you already infected?

a) Yes, 60% b) No, 30% c) Contact 10%

10- Did you contract the virus (Corona) after taking the vaccine?

a) Yes 0% b) No 100%

11- Have you made sure to educate others about the need to receive the vaccine?

a) Yes, 95% b) No 0% c) Kind of 5%

12- After you took the vaccine, did you return to your daily life as before?

a) Yes, 80% b) No 5% c) Somewhat 15%

13- What kind of vaccines would you advise others to choose when vaccinating?

a) AstraZeneca 20% b) Sinopharm 25% c) Pfizer-BioNTech 55%

14- Did you have any side effects after taking the vaccine?

a) Yes, 30% b) No 45% c) Somewhat 25%

15- Did you take the second dose of the vaccine?

a) Yes, 75% b) No 25%

By using the SPSS program, the possible measurements of central tendency and measures of dispersion for this questionnaire were found and explained:

Table 6: SPSS program

a

Statistics

		1-What type of vaccine did you receive?	2- Do you fear when you take the vaccine?	3- Do you have social contact with to do what?	4- Were you forced by virtue of your work to take the vaccine?	5-What were the reasons that prompted you to take the vaccine (if you were not forced to take it)	6-Do you advise others to take the vaccine	7- Are you satisfied with how the health staff dealt with you while you were vaccinated?	8-Do you have chronic diseases?
N	Valid	60	60	60	60	60	60	60	60
	Missing	0	0	0	0	0	0	0	0
Mean		2.20	2.10	1.00	2.10	2.50	1.10	1.10	1.75
Std. Error of Mean		.097	.070	.000	.057	.087	.057	.057	.056
Median		2.00	2.00	1.00	2.00	3.00	1.00	1.00	2.00
Mode		2[a]	2	1	2	3	1	1	2
Std. Deviation		.755	.543	.000	.440	.676	.440	.440	.437
Variance		.569	.295	.000	.193	.458	.193	.193	.191
Skewness		-.352	.079		.520	-1.019	4.236	4.236	-1.185
Std. Error of Skewness		.309	.309	.309	.309	.309	.309	.309	.309
Kurtosis		-1.148	.436		2.019	-.135	16.494	16.494	-.619
Std. Error of Kurtosis		.608	.608	.608	.608	.608	.608	.608	.608
Range		2	2	0	2	2	2	2	1
Minimum		1	1	1	1	1	1	1	1
Maximum		3	3	1	3	3	3	3	2
Sum		132	126	60	126	150	66	66	105
Percentiles	10	1.00	1.10	1.00	2.00	1.10	1.00	1.00	1.00
	20	1.20	2.00	1.00	2.00	2.00	1.00	1.00	1.00
	25	2.00	2.00	1.00	2.00	2.00	1.00	1.00	1.25
	30	2.00	2.00	1.00	2.00	2.00	1.00	1.00	2.00
	40	2.00	2.00	1.00	2.00	2.40	1.00	1.00	2.00
	50	2.00	2.00	1.00	2.00	3.00	1.00	1.00	2.00
	60	2.60	2.00	1.00	2.00	3.00	1.00	1.00	2.00
	70	3.00	2.00	1.00	2.00	3.00	1.00	1.00	2.00
	75	3.00	2.00	1.00	2.00	3.00	1.00	1.00	2.00
	80	3.00	2.80	1.00	2.00	3.00	1.00	1.00	2.00
	90	3.00	3.00	1.00	3.00	3.00	1.00	1.00	2.00

a. Multiple modes exist. The smallest value is shown

b

Statistics

		9-Are you already infected	10-Did you contract the virus (Corona) after taking the vaccine	11-Have you made sure to educate others about the need to receive the vaccine	12-After you took the vaccine, did you return to your daily life as before	13-What kind of vaccines would you advise others to choose when vaccinating	14-Did you have any side effects after taking the vaccine?	15-Did you take the second dose of the vaccine
N	Valid	60	60	60	60	60	60	60
	Missing	0	0	0	0	0	0	0
Mean		1.50	2.00	1.10	1.35	2.35	1.95	1.25
Std. Error of Mean		.087	.000	.057	.095	.103	.096	.056
Median		1.00	2.00	1.00	1.00	3.00	2.00	1.00
Mode		1	2	1	1	3	2	1
Std. Deviation		.676	.000	.440	.732	.799	.746	.437
Variance		.458	.000	.193	.536	.638	.557	.191
Skewness		1.019		4.236	1.749	-.726	.082	1.185
Std. Error of Skewness		.309	.309	.309	.309	.309	.309	.309
Kurtosis		-.135		16.494	1.273	-1.040	-1.168	-.619
Std. Error of Kurtosis		.608	.608	.608	.608	.608	.608	.608
Range		2	0	2	2	2	2	1
Minimum		1	2	1	1	1	1	1
Maximum		3	2	3	3	3	3	2
Sum		90	120	66	81	141	117	75
Percentiles	10	1.00	2.00	1.00	1.00	1.00	1.00	1.00

Table 7:Questionnaire About Vaccines For The Emerging Coronavirus (COVID-19) In Iraq, Maysan Governorate,the possible measurements of central tendency and measures of dispersion for this questionnaire

Question1		Frequency	Percent	Valid Percent	Cumulative Percent
Valid	AstraZeneca	12	20.0	20.0	20.0
	Sinopharm	24	40.0	40.0	60.0
	Pfizer-BioNTech	24	40.0	40.0	100.0
	Total	60	100.0	100.0	
Question2		Frequency	Percent	Valid Percent	Cumulative Percent
Valid	Yes	6	10.0	10.0	10.0
	No	42	70.0	70.0	80.0
	Somewhat	12	20.0	20.0	100.0
	Total	60	100.0	100.0	
Question3		Frequency	Percent	Valid Percent	Cumulative Percent
Val	Yes	60	100.0	100.0	100.0
Question4		Frequency	Percent	Valid Percent	Cumulative Percent
Valid	Yes	3	5.0	5.0	5.0
	No	48	80.0	80.0	85.0
	Somewhat	9	15.0	15.0	100.0
	Total	60	100.0	100.0	
Question5		Frequency	Percent	Valid Percent	Cumulative Percent
Valid	In response to the recommendations of the World Health Organization	6	10.0	10.0	10.0
	to the severity of your workplace	18	30.0	30.0	40.0
	Self-desire	36	60.0	60.0	100.0
	Total	60	100.0	100.0	
Question6		Frequency	Percent	Valid Percent	Cumulative Percent
Valid	Yes	57	95.0	95.0	95.0
	Somewhat	3	5.0	5.0	100.0
	Total	60	100.0	100.0	
Question7		Frequency	Percent	Valid Percent	Cumulative Percent
Valid	Yes	57	95.0	95.0	95.0
	No	3	5.0	5.0	100.0
	Total	60	100.0	100.0	
Question8		Frequency	Percent	Valid Percent	Cumulative Percent
Valid	Yes	15	25.0	25.0	25.0
	No	45	75.0	75.0	100.0
	Total	60	100.0	100.0	
Question9		Frequency	Percent	Valid Percent	Cumulative Percent
Valid	Yes	36	60.0	60.0	60.0
	No	18	30.0	30.0	90.0
	Contact	6	10.0	10.0	100.0
	Total	60	100.0	100.0	
Question10		Frequency	Percent	Valid Percent	Cumulative Percent
Va	No	60	100.0	100.0	100.0
Question11		Frequency	Percent	Valid Percent	Cumulative Percent
Valid	yes	57	95.0	95.0	95.0
	Kind of	3	5.0	5.0	100.0
	Total	60	100.0	100.0	

Question12		Frequency	Percent	Valid Percent	Cumulative Percent
Valid	Yes	48	80.0	80.0	80.0
	No	3	5.0	5.0	85.0
	Somewhat	9	15.0	15.0	100.0
	Total	60	100.0	100.0	
Question13		Frequency	Percent	Valid Percent	Cumulative Percent
Valid	AstraZeneca	12	20.0	20.0	20.0
	Sinopharm	15	25.0	25.0	45.0
	Pfizer-BioNTech	33	55.0	55.0	100.0
	Total	60	100.0	100.0	
Question14		Frequency	Percent	Valid Percent	Cumulative Percent
Valid	Yes	18	30.0	30.0	30.0
	No	27	45.0	45.0	75.0
	Somewhat	15	25.0	25.0	100.0
	Total	60	100.0	100.0	
Question15		Frequency	Percent	Valid Percent	Cumulative Percent
Valid	Yes	45	75.0	75.0	75.0
	No	15	25.0	25.0	100.0
	Total	60	100.0	100.0	

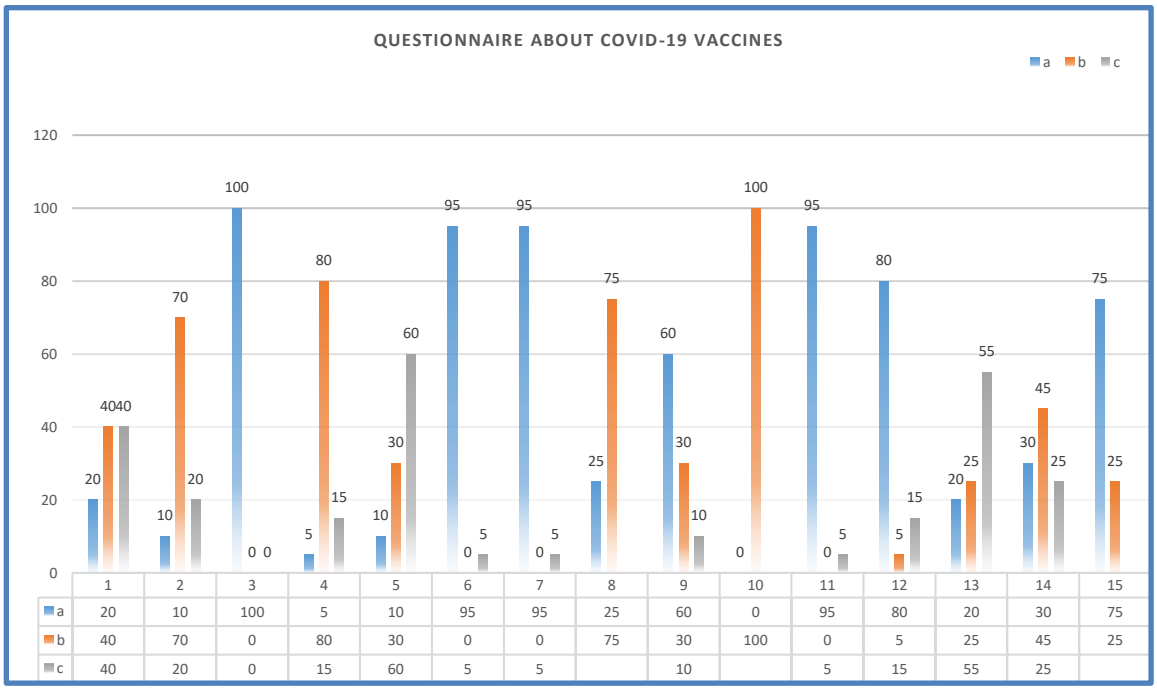

Figure 1: A Questionnaire About Vaccines For The Emerging Coronavirus (COVID-19) In Iraq, Maysan Governorate

7.2 A survey about the acceptance of the local community

A survey about the acceptance of the local community represented in Maysan Governorate was conducted to obtain the emerging coronavirus (COVID-19) vaccine in the event that the vaccine spreads more widely in the coming months. The questionnaire included 1666 people divided into three age groups

- The first is between 20 – 35 years old
- The second is between 36 – 60 years old

• The third is over 60 years old

The results of the questionnaire **Figure 2** were as follows:

1) If a vaccine against the emerging coronavirus (COVID-19) was available, would you take it?

a) Yes, 27% b) No 41% c) I don't know 32%

2) Do you think taking the vaccine is necessary?

a) Yes,2% b) No, 31% c) Somewhat 37%

3) Does taking the vaccine help you practice your daily life as before?

a) Yes, 26% b) No 39% c) Somewhat 35%

4) Are there any members of your family who received the vaccine?

a) Yes, 17% b) No 83%

5) Do you have concerns about receiving the vaccine?

a. Yes, 71% b) No 13% c) Somewhat 16%

6) Many vaccines are currently being circulated around the world. Do you find that the quality of the vaccine will be a reason to obtain it?

a) Yes, 42% b) No 21% c) Somewhat 37%

7) Do you agree or disagree with the following statement: "I will get the vaccine if I have enough information about its effectiveness, composition, safety, and side effects"?

a. Yes, 71% b) No 14% *b*)Somewhat 15%

8) Do you agree or disagree with the following statement: "I will get the vaccine if the majority of the public takes it"?

a. Yes, 26% b) No 51% c) Somewhat 23%

9) Did you make sure to educate others about the need to receive the vaccine?

a. Yes, 26% b) No, 57% c) Somewhat 17%

10) What are the categories that should be vaccinated as a priority if the COVID-19 vaccine is available?

a) Medical personnel 44%
b) Education cadres (professors, teachers, and educators) 13%

c) The elderly or those with chronic diseases 43%

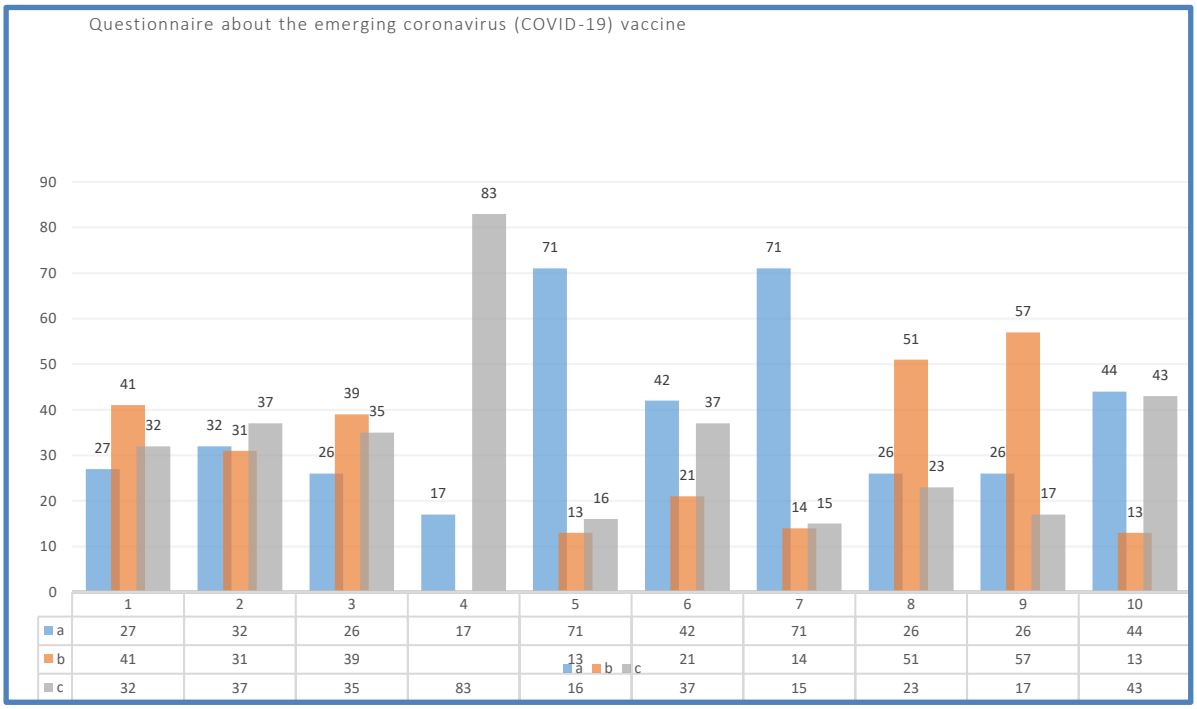

Figure 2: A questionnaire about the emerging coronavirus (Covid-19) vaccine in Iraq, Maysan Governorate

8. Conclusions:

In light of the results of the research, the following can be concluded:

1- The most received vaccine is Pfizer-BioNTech, and Sinopharm by 40%.

2- The largest percentage of those who received the vaccine did not have any fear when they took the vaccine.

3-Most of those who received the vaccine were not forced to do so.

4- 93% of those who took the vaccine advise others to take the vaccine.

5- There is a high level of satisfaction with the performance of the medical staff in the governorate.

6- All those who received the vaccine were not infected after taking the vaccine.

9. Recommendations:

In light of the results and conclusions reached by the researcher, the following recommendations are set:

1- The need to receive one of the vaccines approved by the World Health Organization.

2- Educating the community and disseminating information to ensure that they understand the symptoms and the benefits of receiving the vaccine.

3- Develop counseling programs based on psychological methods that reduce community fears.

10. Future work:

Complementing the findings of the current research, the researchers suggest the following:

1- Conducting broader studies on vaccines (AstraZeneca vaccine, Sinopharm vaccine, Pfizer-BioNTech vaccine) in a way that shows the community more information about these vaccines.

2- Conducting studies that include questionnaires on samples in different countries of those who have taken the vaccine and presenting the results to reliable sources.

11. References

[1] Ndwandwe D, Wiysonge CS. COVID-19 vaccines. Curr Opin Immunol. 2021;71:111-116.

[2] Ndwandwe D. COVID-19 vaccines Duduzile Ndwandwe and Charles S Wiysonge. Curr Opin Immunol. 2021;71:111-116.

[3] Ndwandwe D, Wiysonge CS. COVID-19 vaccines. Curr Opin Immunol. 2021;71:111-116.

[4] Ndwandwe D. COVID-19 vaccines Duduzile Ndwandwe and Charles S Wiysonge. Curr Opin Immunol. 2021;71:111-116.

[5] Ndwandwe D, Wiysonge CS. COVID-19 vaccines. Curr Opin Immunol. 2021;71:111-116.

[6] Ndwandwe D, Wiysonge CS. COVID-19 vaccines. Curr Opin Immunol. 2021;71:111-116.

[7] Yang L, et al. COVID-19: immunopathogenesis and immunotherapeutics. Signal Transduct Target Ther. 2020;5(1):128.

[8] Hashoosh AF, Basirzadeh H. Stability on optimal control problems and multi-population mathematical models. Util Math. 2023;120:500-505.

[9] Farhan Hashosh A, Basirzadeh H. Routh stability criterion and Lyapunov-Routh method in control theory. Int J Nonlinear Anal Appl. 2024;15(5):111-120.

[10] Hashoosh AF. Special methods controllability and observability in optimal control systems. Al-Kitab J Pure Sci. 2024;8(2):78-93.

[11] Daniel SJ. Education and the COVID-19 pandemic. Prospects. 2020;49(1):91-96.

[12] Malik AA, et al. Determinants of COVID-19 vaccine acceptance in the US. EClinicalMedicine. 2020;26:100495.

[13] Graham BS. Rapid COVID-19 vaccine development. Science. 2020;368(6494):945-946.

[14] UNICEF. Number of vaccine approvals. 2021 May 21.

[15] Zahraei SM, et al. Immunization coverage of children aged 24–35 months in the Islamic Republic of Iran: a national cluster coverage survey. East Mediterr Health J. 2022;28(2):121-129.

[16] Sadighpour T, et al. Efficacy and side effects of Sputnik V, Sinopharm, and AstraZeneca vaccines to stop COVID-19: a review and discussion. 2021.

[17] AstraZeneca COVID-19 vaccine authorised for emergency use by the World Health Organization [Internet]. 2021. Available from: https://www.astrazeneca.com/media-centre/press-releases/2021/astrazeneca-covid-19-vaccine-authorised-for-emergency-use-by-the-world-health-organization.html

[18] Interim recommendations for use of the ChAdOx1-S [recombinant] vaccine against COVID-19 (AstraZeneca COVID-19 vaccine AZD1222, SII Covishield, SK Bioscience) [Internet]. 2021. Available from: https://www.who.int/publications/i/item/WHO-2019-nCoV-vaccines-SAGE_recommendation-AZD1222-2021.1

[19] World Health Organization. The Oxford/AstraZeneca COVID-19 vaccine: what you need to know. World Health Organization. 2021.

[20] Zee Business. Coronavirus Vaccine Covishield: Side effects, benefits of Serum Institute-AstraZeneca vaccination. Zee Business. 2021.

[21] AstraZeneca COVID-19 Vaccine (AZD1222) [Internet]. Available from: https://www.precisionvaccinations.com/vaccines/astrazeneca-covid-19-vaccine-azd1222

[22] Logunov DY, et al. Safety and efficacy of an rAd26 and rAd5 vector-based heterologous prime-boost COVID-19 vaccine: an interim analysis of a randomised controlled phase 3 trial in Russia. Lancet. 2021;397(10275):671-681.

[23] Formeister EJ, et al. Preliminary analysis of association between COVID-19 vaccination and sudden hearing loss using US Centers for Disease Control and Prevention Vaccine Adverse Events Reporting System data. JAMA Otolaryngol Head Neck Surg. 2021;147(7):674-676.

[24] Wang H, Zhang Y, Huang B. Development of an inactivated vaccine candidate, BBIBP-CorV, with potent protection against SARS-CoV-2. Cell. 2020;182:713-721. doi: 10.1016/j.cell.2020.06.008.

[25] Faso B, Equatorial Guinea. Sinopharm/BIBP COVID-19 vaccine.

[26] Xia S, et al. Effect of an inactivated vaccine against SARS-CoV-2 on safety and immunogenicity outcomes: interim analysis of 2 randomized clinical trials. JAMA. 2020;324(10):951-960.

Al-Kitab Journal for Pure Sciences (2025); 9(1):51-67.
https://doi.org/10.32441/kjps.09.01.p4

Al-Kitab Journal for Pure Sciences
ISSN: 2617-1260 (print), 2617-8141(online)

https://isnra.net/index.php/kjps

The Use of Technetium-99m Radioactive Isotope in The Diagnosis and Treatment of Thyroid Diseases: A Review

Shlair I. Mohammed[1*]

[1]Department of Physiology, College of Medicine, University of Kirkuk, Iraq.

[*] Shlair I. Mohammed: Shlair-mohammed@uokirkuk.edu.iq
https://orcid.org/0009-0000-3065-015X

Citation: Mohammed SI. The Use of Technetium-99m Radioactive Isotope in The Diagnosis and Treatment of Thyroid Diseases: A Review. Al-Kitab J. Pure Sci. [Internet]. 2025 Jan. 01;9(1):51-67. DOI: https://doi.org/10.32441/kjps.09.01.p4.

Keywords: Technetium-99m, Radioactive Isotope, Thyroid, Radiation Exposure, Scanning Protocols.

Article History

Received	19 Jun.	2024
Accepted	09 Sep.	2024
Available online	07 Jan.	2025

Abstract:

A Tc-99m thyroid scanning is one of the most common diagnostic modalities in nuclear medicine for the evaluation of various thyroid dysfunctions and anomalies. Therefore, this review study will delve into the various dimensions related to patient exposure during Tc-99m thyroid scanning. Various subjects are covered, such as radiation risks from the procedure, methods for reducing patient exposures, imaging technology developments, and the importance of an effective radiation safety program. In this review, some new developments in and possible ways toward better safety for the patient and diagnostic accuracy of the thyroid imaging methods are also discussed.

Keywords: Technetium-99m, Radioactive Isotope, Thyroid, Radiation Exposure, Scanning Protocols.

(Immediately after the abstract, provide 5-7 keywords and arrange them alphabetically, using American spelling and avoiding general and plural terms and multiple concepts (avoid, for example, 'and', 'of'). Be sparing with abbreviations: only abbreviations firmly established in the field may be eligible. These keywords will be used for indexing purposes).

أستخدام النظائر المشعة التكنيتيوم-٩٩ m في تشخيص وعلاج أمراض الغدة الدرقية: مراجعة

شلير إبراهيم محمد

العراق، جامعة كركوك، كلية طب، فرع فسلجه

Shlair-mohammed@uokirkuk.edu.iq

الخلاصة:

في الطب النووي، يعد مسح الغدة الدرقية بالتكنيتيوم-٩٩m (Tc-$99m$) تقنية تشخيصية شائعة الاستخدام لتقييم وظيفة الغدة الدرقية وتحديد الحالات الشاذة. تبحث دراسة المراجعة هذه في المشاكل التي يتعرض المريض أثناء عمليات فحص الغدة الدرقية Tc-99m. وهو يغطي المخاطر الإشعاعية لهذا الإجراء، وطرق تقليل تعرض لهذه المخاطر، والتطورات في تكنولوجيا التصوير، وأهمية بروتوكولات السلامة الإشعاعية القوية. وتناقش المراجعة أيضًا التطورات الجديدة والمسارات المحتملة لطرق تصوير الغدة الدرقية لتحسين سلامة المرضى ودقة التشخيص.

الكلمات المفتاحية: التكنيشيوم-٩٩m، النظائر المشعة، الغدة الدرقية، التعرض للإشعاع، تحسين بروتوكولات المسح.

1. Introduction:

The thyroid is a relatively large endocrine organ in the body that plays a very important role in body growth, metabolism, and maturation **[1, 2],** the thyroid gland regulates numerous biological processes by constantly releasing many thyroid hormones into the bloodstream. When a woman is pregnant, when it's chilly outside, or when her body requires more energy, it releases more hormones **[3].** This organ produces two hormones: triiodothyronine (T3) and thyroxin (T4) **[4, 5, 6].** There are several stages to thyroid disorders, from early to late stages. Individuals suffering from thyroid diseases are classified as having either "hypothyroidism" (low T4 levels) or "hyperthyroidism" (high T4 or T3 and low TSH) based on the function parameters **[7, 8].** Hypothyroidism is regarded as one of the most prevalent illnesses in endocrine therapy **[9],** it refers to a reduction in thyroid hormone **[10, 11].** Hypothyroidism symptoms include weariness, muscle swelling or cramping, loss of balance, weight gain, hair loss, and cold intolerance. Ultrasound, computed tomography (CT), and magnetic resonance imaging (MRI) are three common imaging modalities used to diagnose thyroid problems. Ultrasound is the first-line imaging modality because it is good at evaluating thyroid nodules and determining their features, such as size and content, which can signal malignancy risk **[12].** CT scans are highly effective for determining the severity of thyroid illness, particularly in cases of suspected malignancy or

when evaluating adjacent structures **[13].** While MRI is less widely used than ultrasound and CT, it can produce comprehensive images of the thyroid and adjacent tissues, making it useful in certain clinical settings, such as assessing big goiters or invasive thyroid malignancies **[14].** Besides that, nuclear medicine methods that include thyroid scintigraphy are used to assess thyroid function and detect hyperfunctioning nodules **[15].**

Other than medical applications, radioactive isotopes are used in countless other applications within soil science, wastewater treatment, and industry. In the medical profession, lasers abound in therapeutic procedures as external radiation sources, and injections are performed for hyperthyroidism and malignancies **[16, 17]**. Thyroid scanning by technetium-99m radioactive isotope is now a very common diagnostics technique of nuclear medicine **[18].**

Patient exposure in such scans should be kept in mind for potential risks and precautions **[19].** One major precaution to be taken needs to find the right quantity and potential radio isotopic nature which can be used in a human body safely. It can be calculated by giving an appropriate dose to a particular individual according to their body weight and medical history. The whole-body doses that reach the patient make it necessary to use lead or lead glass shields when performing the procedure. Besides, it is important to inform the patient beforehand and get their consent before proceeding with the thyroid scan. Such a consent form should point at the advantages a given process has on the health of the subject, the potential risk of radiation exposure, and alternative measures. In general, the technetium-99m radioactive isotope scans of the thyroid are of great importance for diagnostic purposes in the field of nuclear medicine. Adequate precautions should be taken and informed consent by the patient is to be ensured for patient safety **[18].** On every occasion during the use of radioisotopes, some precautions should be taken to ensure the safety of the scientist **[20].** Some of the considerations, relative to isotopes used most frequently in biological research, include proper shielding and protective gear, proper safe-handling procedures, and reduction of manual handling procedures of the radioisotopes **[21].** Furthermore, it becomes essential to ensure regular radiation level monitoring within the laboratories alongside very strict procedures on storage and disposal of radioactive materials with a view of reducing the possible risks of exposure to healthcare workers and patients. The last year marked the beginning of a period with computer technology advances in the actual development of imaging techniques without using ionizing radiation. These techniques, applied in the diagnoses, are costly conventional procedures but are also rich sources of functional and morphological information. Informed consent from the patients should be routinely obtained

prior to any radiography procedure, including thyroid scanning with technetium-99m radioactive isotope [18]. Imaging of thyroid nodules remains important in the evaluation of thyroid scintigraphy because it helps in determining benign from malignant lesions [22, 23].

Initial results for the use of 99mTc in thyroid scintigraphy following inconclusive results of the exact-needle biopsy, especially ultrasound EU-TIRADS, are highly promising [24]. Consecutive pertechnetate- and MIBI scans have also been described as useful methods to display hypofunctional thyroid tissue and, therefore, allow the diagnosis of dystopic tissue or metastases [25]. Establishing diagnostic reference levels for thyroid scans with 99mTc is a step required for the optimization of nuclear medicine investigations in connection with the radiation safety requirements [26]. Thyroid scintigraphy can be helpful in providing information in difficult cases. The results show that it makes a significant contribution to the thyroid nodule detection process. Radiation dose rates were recorded at different distances after treatment with Technetium (Tc-99m) for thyroid scintigraphy.

The present article intends to provide an overview of the application of Technetium (Tc-99m) in thyroid scans looking into the risks of radiation exposure methods, for improving scanning processes and new developments, in thyroid imaging technology. Through discussing these points the review aims to support the endeavors to improve the safety and efficiency of Tc 99m related thyroid imaging tests.

2. Material and methods:

2.1. Role of Technetium-99m for thyroid scintigraphy: One of the two elements lacking stable isotopes with an atomic number less than 83 is technetium. 99Tc was found in a sample in 1937 by Perrier and Segré using the Berkeley Radiation Laboratory's 37-inch cyclotron to blast a Mo sample with deuterons [27]. They questioned Lawrence, who in 1929 created the cyclotron [28], to make the bombardment. Segré and Seaborg found the 99Tc metastable state in 1938 [29]. Technetium (Tc-99m) is, due to its concentrating nature in the thyroid, an important isotope for diagnosing thyroid disorders [30, 31]. It has a significant contribution to many diagnostic tests for thyroid diseases with benefits over other imaging modalities [30]. Technetium-99m is unique in nuclear medicine due to the versatility of applications and its most favored properties. This has been recently obtained from a 99Mo/99mTc generator, which offers easy accessibility of the isotope to medical applications [32]. The 99mTc being employed decays by gamma emission and has a physical six-hour half-life, and is thus perfect

for soft tissue imaging like the thyroid and brain and bones **[33].** Its electron configuration makes it apt for the formation of complexes with various ligands, helping materialize the concept of mainly targeting imaging and therapy at different parts of the body through SPECT **[34].** Moreover, 99mTc has been utilized in examinations of pediatric nuclear medicine with a high rate of residual radioactivity; it is hence quite vital in the diagnosis of many ailments in children **[35].** In summary, the ability to produce 99mTc, its property for imaging, and the eventual residual behavior have collectively made the radionuclide an important substance in nuclear medicine applications.

Tc-99m pertechnetate thyroid scintigraphy is very useful in assessing thyroid function and estimating thyroid uptake percentage as well as for the diagnosis of hyperthyroidism and hypothyroidism **[36, 37].** The Tc-99m scan is indicated for the diagnosis of congenital hypothyroidism and the differentiation of agenesis from thyroid versus reduced uptake. The Tc-99m pertechnetate scintigraphy is also useful for the diagnosis of cold nodules of the thyroid, which determines the possibility of malignancy and aids in treatment decisions.

Of the isotopes in use in medicine, technetium-99m occupies a very special niche in nuclear medicine diagnosis, whose metastable isotope is greatly utilized. On the other hand, 99mTc finds wide applications for all types of diagnostic procedures, including SPECT imaging, which it has made a workhorse compared to other isotopes **[32-34].** Also, new ways of implementing nanodiamonds as 99mTc carriers have been investigated, showing the versatility of this radionuclide and an expectation of further development in medical diagnostics **[35].** What has made the isotope 99mTc special for nuclear medicine, compared with other isotopes applied for similar purposes in diagnosis, is the good storage properties of Tc-99m and its use in clinical routines, in addition to the specific features of 99mTc.

Scanning with Tc-99m in nuclear medicine is an important tool that allows for the noninvasive assessment of thyroid morphology, function, and pathology **[38].** Gamma radiation emissions combined with excellent imaging characteristics make Tc-99m thyroid scanning useful in the management and diagnosis of various thyroid disorders **[39].** Common indications for Tc-99m thyroid scanning include assessing thyroid- nodules and evaluating thyroid function in hyperthyroidism and hypothyroidism, other than detecting the relapse of thyroid cancer after treatment **[40].** Techniques like the Tc-99m MIBI scintigraphy can, therefore, clearly discriminate thyroid from parathyroid tissue. This feature makes the diagnosis more accurate

[41]. Secondly, Tc-99m thyroid uptake is a good alternative to radioiodine in thyrotoxicosis, where it provides an accurate diagnosis for many thyroid diseases **[42].**

However, on the downside, despite being diagnostic, Tc-99m thyroid scanning involves radiation exposure and its associated health Hazards. Although the radiation doses for thyroid scans are generally relatively low compared with other nuclear medicine examinations, meticulous concerns for radiation safety principles that directly contribute to the reduction of patient radiation exposure and reduction of risks associated with it become paramount. This paper reviews the dosimetry of Tc-99m thyroid scanning, comparative radiation doses from other imaging modalities for the diagnosis of similar pathologies, and strategies for the optimization of imaging protocols to achieve diagnostic efficacy at the lowest possible radiation exposures, Pertechnetate Tc99m is a radiopharmaceutical that finds utilization in diagnosing thyroid diseases primarily due to its sodium iodide symporter (NIS) facilitated uptake mechanism **[43].** This glycoprotein aids the transportation of iodide ions into the thyroid follicular cells through active means which allows for a concentration of Tc99m within the thyroid gland thus enabling visualization using gamma cameras or single photon emission tomography (SPECT) imaging techniques **[44].** In this process, localization of the radiopharmaceutical as well as biodistribution can be confirmed by demonstrating where NIS-expressing tissues such as salivary glands and thyroid are located **[44].** Additionally, mechanisms underlying the action of thyroid hormones should be understood since they inform the interpretation of imaging findings and clinical implications of thyroid disorders **[45].** By leveraging machine learning models in the classification of thyroid diseases, diagnostic accuracy is further improved especially with challenges related to data imbalance and model interpretability **[43].** Altogether, Tc99m-pertechnetate is an essential tool for the diagnosis of various types of thyroid conditions characterized by efficient imaging obtained from its specific uptake mechanism

2.2. Radiation Exposure Risks: Radiation dangers have become an issue with the growing usage of computed tomography (CT) scans in the medical industry **[46].** Radiation dose levels — even low ones — through ionizing radiation can lead to cancer development risk increase especially in pediatric patients because their developing tissues and organs are increasingly radiation-sensitive. Maximizing diagnostic value while minimizing harm is dependent on a keen consideration of radiation dosimetry, as well as the implementation of strategies for imaging protocol optimization. While the use of Tc-99m for thyroid imaging is an established diagnostic modality, it's important that one knows the associated radiation doses so one can be

able to compare them with alternative imaging techniques: The effective doses typically delivered by Tc-99m thyroid scans range from 1-5 mSv which generally is lower than other nuclear medicine procedures like radioiodine thyroid uptake studies **[47].** However, the amount of radiation from repeat Tc-99m thyroid scans can add up: in cases where multiple scans are done or when other imaging modalities are used along with it, especially in children. Among the Tc-99m thyroid technique, especially with 99mTc-MIBI, it seems to have an edge over the others in risk assessment and diagnostic accuracy. A major multicenter study recorded that 99mTc-MIBI imaging had a high negative predictive value—sensitivity of 96% for excluding malignancy in hyperfunctioning thyroid nodules—but poor specificity, 21%, because of frequent false positives, hence requiring careful pre-test selection of nodules **[48].** In contrast, 99mTc scintigraphy showed better accuracy in diagnosing Graves' disease compared to thyroid ultrasonography with a sensitivity of 96.1% versus 23.5%, respectively, for ultrasound **[49].** Additionally, the gamma camera measurement of 99mTc pertechnetate uptake showed better diagnostic accuracy than that of the gamma probe method with a sensitivity of 93.4% and specificity of 94.8% **[50].** These results indicate that, although the Tc-99m techniques seem to have some limitations in terms of specificity, their high sensitivity and diagnostic accuracy render them, when taken together, good tools for thyroid assessment, particularly for the differential diagnosis among thyroid diseases. Tc-99m thyroid technique provide an advantages many grounds when compared with the traditional techniques, more specifically I-131. First, Tc-99m pertechnetate presents better image quality due to its low radiation dose of about 10,000 times less compared to that of I-131, and at the same time, it emits no beta radiation, reducing exposure to the patient. Besides, Tc-99m has a rather short half-life time and a biological retention time, allowing faster procedures and less discomfort to the patient. This technique is also relatively inexpensive and very accessible, hence its availability for clinical use **[51].** Besides, the Tc-99m scintigraphy can even differentiate between amiodarone-induced thyrotoxicosis types of thyroid disorders, which helps in appropriate diagnosis and treatment planning **[52].** On the whole, these factors create an increasing preference for the use of Tc-99m in thyroid imaging, hence making it a very valuable tool in clinical practice **[51, 52].**

2.3. Optimizing Protocols for Tc-99m Thyroid Scanning: Several techniques can be used to reduce radiation exposure during Tc-99m thyroid scanning. Patient selection and justification for imaging should be Entailed primarily. Where Tc-99m thyroid scanning is indicated, optimization of the scanning protocol by altering parameters such as administered radiotracer

activity, imaging time, collimator selection, etc., should be done. **[47, 53].** In addition, it can be seen that new modalities of imaging, in particular, SPECT and combined SPECT/CT, are capable of providing better diagnostic information while presumably keeping at the lowest level the radiation doses applied compared to conventional planar imaging **[54]**. Patient factors, especially age- and body habitus-dependent variables, are another strong determinant of clinical indications that may also guide protocol optimization. In particular, pediatric patients require special consideration since they are more radiosensitive and could benefit from additional procedures in terms of dose reduction, such as low-dose CT for hybrid imaging modalities' attenuation correction **[47, 53].**

2.4. Emerging Trends in Thyroid Imaging Technology: Investigation, in the domain of nuclear medicine imaging, is currently focused on enhancing the safety and effectiveness of thyroid scans utilizing Tc- 99m. Technetium 99m plays a role in nuclear medicine especially for thyroid imaging **[55].** Scientists are exploring imaging techniques like Computed Tomography (CT) combined with Single-Photon Emission Computed Tomography (SPECT) to improve the accuracy and specificity of thyroid scans **[56, 57].** Additionally, studies are being conducted on radioisotopes and radiopharmaceuticals such as Thallium 199. Gallium 68, for thyroid imaging, shows potential in diagnosing various conditions, including cancer **[58, 59].** These developments aim to not only enhance the capabilities of nuclear medicine but also prioritize patient safety and optimize treatment outcomes for thyroid-related disorders.

3. Results:

According to the literature review, there are a few studies that have looked into the patient radiation exposure in Technetium-99m based thyroid scans. Several techniques were used by these studies including phantom-based measurements, Monte Carlo simulations, and patient-specific dose assessments to quantify radiation exposure to various organs as well as the effective doses of patients.

Reported effective doses ranged between about 1-5 mSv from technetium-99m thyroid scans and varied depending on factors like imaging protocol, patients' characteristics and specific radiopharmaceutical formulation used. In some cases, the organ-specific doses were calculated with the thyroid gland experiencing relatively high radiation compared to other organs examined.

Some factors such as Technetium-99m administered activity, imaging protocol parameters (for example acquisition time or number of views), body habitus of patients, and particular radiopharmaceutical formulation were found during the review to affect patient radiation dose during thyroid scans.

4. Discussion

This review has found that it is important for one to know how much radiation a patient gets during a Technetium-99m based thyroid scan as shown in **Figure 1**, which gives a good and clear image of the thyroid with different doses **[60]**. Although the diagnostic benefits of these scans are well known, health risks associated with radiation exposure cannot be ignored.

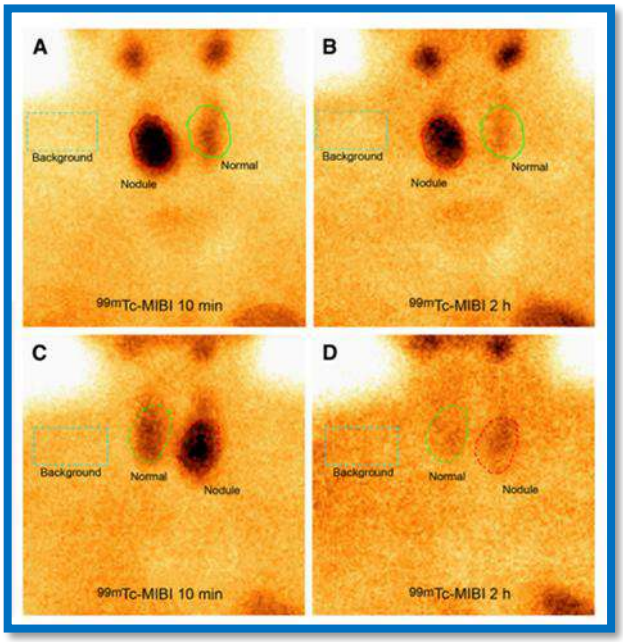

Figure 1: 99mTc-MIBI Thyroid scan. A&B A single chilly thyroid nodule in the right lobe that was histologically identified as non-oncocytic solid/trabecular poorly differentiated carcinoma is a representative positive case (RI, 71.76). (A) An early image shows tracer buildup in a nodule (ER, 2.62). (B) Tracer retention in the lesion with delayed imaging (DR, 4.50). (C & D) Representative nugatory case (RI, 240.64) A solitary chilly thyroid nodule in the left lobe was diagnosed as a micro follicular goiter. (C) early picture with Tracer raised uptake in nodules (ER, 2.81). (D) A delayed picture with a complete tracer fiasco from the nodule (DR = 1.67).

The reported effective dose range of 1-5 mSv is generally within the recommended limits for medical imaging procedures. However, this does not account for cumulative radiation doses from multiple diagnostic tests, especially in patients with chronic thyroid conditions and who may require regular follow-up scans.

Efforts towards optimizing radiation protection should therefore emphasize establishing appropriate imaging protocols, utilizing advanced imaging techniques (e.g., low-dose

protocols), and taking into consideration patient-specific factors (e.g., body habitus) that can minimize unnecessary irradiation.

Also, the review revealed that Technetium-99m administered activity, imaging protocol parameters, patient body habitus, and specific radiopharmaceutical formulation were some of the factors affecting patient's radiation dose in thyroid scans. The present findings also highlight proper dosimetry strategies as well as optimization of imaging protocols to guarantee patients' safety during thyroid scans.

5. Recommendations

This requires health workers to maintain at least one meter's distance from the patient after injection because of radiation safety reasons **[61].** Finally, it was put into consideration that members of the public should keep their distance from proximity to the patient for at least 3 hours after injection to avoid risks associated with radiation exposure **[62].** These precautions are therefore very important, with nuclear radiation being hazardous material in nature, and thus any exposure should be reduced to ensure minimum medical effects on medic workers and public protection from potential harm **[63].** Safety distances and lengths of time should, therefore, be observed both before and after injection to minimize risks related to exposure to radiation of all persons involved or around nuclear medicines procedures.

6. Conclusions

This review explores Technetium-99m thyroid scans; and how much patients are exposed to radiation from the procedure. The results show that nuclear medicine imaging must continue being optimized as far as the protection and safety of patients against radiation are concerned.

The dose received during Tc-99m thyroid scanning should be evaluated carefully and adjusted to achieve appropriate diagnostic efficacy and to minimize radiation exposure, particularly in vulnerable populations like children. By implementing appropriate radiation protection strategies, including justification of imaging, optimization of scanning protocols, and the use of alternative modalities when feasible, healthcare providers can ensure the safe and effective use of Tc-99m thyroid imaging.

It was established that the high sensitivity and diagnostic accuracy of the TC-99 m technique makes it a good tool for thyroid assessment, particularly in the differential diagnosis of thyroid diseases. When compared to traditional methods, including I-131, the Tc-99m thyroid

technique offers several advantages. To begin with, better quality images are produced by Tc-99m pertechnetate because its radiation dose is approximately 10,000 times less than that of I-131 and it does not emit beta radiation; thus reducing patient exposure. Further still, Tc-99m has a relatively short half-life time as well as a biological retention period such that procedures can be done more quickly and comfortably for patients. The other reason why this procedure is advantageous includes its low cost implying that it is affordable to many people and hence used in clinical practice. Additionally, even the Tc-99m scintigraphy can differentiate between amiodarone-induced thyrotoxicosis types of thyroid disorders which helps in appropriate diagnosis and treatment planning. Therefore, an increasing preference towards using Tc-99m for thyroid imaging due to these factors makes it a very important tool in clinical practice.

7. References

[1] Mohammed AK, Abdulmahdi T, Nabat ZN. Estimation of the Serum Concentration Levels of Ferritin and Vitamin D for Hypothyroid Patients. Indian Journal of Forensic Medicine & Toxicology [Internet]. 2020 Mar 1;14(1):956–61. Available from: https://www.i-scholar.in/index.php/ijfmt/article/view/193028.

[2] Sabah Mohammed Salih, Wijdan Abdullameer Kamel, Mohammed Talat Abbas, Kasim Sakran Abass. Prevalence of Hyperthyroidism and Hypothyroidism and Its Correlation with Serum Antithyroglobulin among Patients in Kirkuk-Iraq. Journal of Advanced Pharmacy Education and Research, 2021; 11(2): 57–60, https://doi.org/10.51847/kWVD06AagO.

[3] Kadhim NM, Hussain KS. Estimation of Trace elements and Thyroid Hormones in thyroid disorders patients in Kirkuk –Iraq. BioGecko. 2023;12(3). ISSN NO: 2230-5807.

[4] Kinoshita-Ise M, Martinez-Cabriales SA, Alhusayen R. Chronological association between alopecia areata and autoimmune thyroid diseases: A systematic review and meta-analysis. The Journal of Dermatology [Internet]. 2019 Jun 14;46(8):702–9. Available from: https://doi.org/10.1111/1346-8138.14940.

[5] Alawy Ghamri K, Alawy Ghamri R. Evaluation of Thyroid Dysfunction and Thyroid Antibodies Among Subjects with Gestational and Pre-Gestational Diabetes at King Abdulaziz University Hospital, Jeddah: A Retrospective Analysis (2014-2018). Int J Pharm Res Allied Sci., 2020;9(1):168-175. ISSN: 2277-3657.

[6] Chandra A. The dilemma of subclinical hypothyroidism in chronic kidney disease. J Assoc Physicians India. 2018 Jul 1;66(7): 76-79. PMID: 31325269. Available from: https://pubmed.ncbi.nlm.nih.gov/31325269.

[7] Ruggeri RM, Trimarchi F, Giuffrida G, Certo R, Cama E, Campennì A, Alibrandi A, De Luca F, Wasniewska M. Autoimmune comorbidities in Hashimoto's thyroiditis: different patterns of association in adulthood and childhood/adolescence. Eur J Endocrinol. 2017;176(2):133-141. doi: 10.1530/EJE-16-0737. PMID: 27913607.

[8] Ranjbar R, Aghamohammadzadeh N, Houshyar J, Aliasgarzadeh A, Sadra V, Najafipour M, et al. The comparison of GDM therapeutic methods between positive and negative anti TPO patients. Arch Pharm Pract. 2020;11(2):60-4.

[9] Fallahi P, Ferrari SM, Ruffilli I, Elia G, Miccoli M, Sedie AD, Riente L, Antonelli A. Increased incidence of autoimmune thyroid disorders in patients with psoriatic arthritis: a longitudinal follow-up study. Immunol Res. 2017 Jun;65(3):681-686. doi: 10.1007/s12026-017-8900-8. PMID: 28101810.

[10] Iglesias P, Bajo MA, Selgas R, Díez JJ. Thyroid dysfunction and kidney disease: An update. Rev Endocr Metab Disord. 2017 Mar;18(1):131-144. doi: 10.1007/s11154-016-9395-7. PMID: 27864708.

[11] Mehdizadeh A, Valizadeh N, Azar MA. Comparing the Serum Level of Vitamin D in Patients with Autoimmune Hypothyroidism and Control Group Subjects. J Biochem Tech. 2019;(2):70-74. ISSN: 0974-2328.

[12] Martín-Noguerol T, Santos-Armentia E, Fernandez-Palomino J, López-Úbeda P, Paulano-Godino F, Luna A. Role of advanced MRI sequences for thyroid lesions assessment. A narrative review. Eur J Radiol. 2024 Jul;176:111499. doi: 10.1016/j.ejrad.2024.111499. Epub 2024 May 8. PMID: 38735157.

[13] Drakshaveni, G., Hamsavath, P.N. Comparative Analysis of Medical Imaging Techniques Used for the Detection of Thyroid Gland with an Emphasis on Thermogram. In: Shetty, N.R., Patnaik, L.M., Prasad, N.H. (eds) Emerging Research in Computing, Information, Communication and Applications. Lecture Notes in Electrical Engineering, 2023, 928: 691-700. Springer, Singapore. https://doi.org/10.1007/978-981-19-5482-5_60.

[14] Zaromytidou E, Notopoulos A. Thyroid Imaging Tests [Internet]. Hypothyroidism - Causes, Screening and Therapeutic Approaches [Working Title]. IntechOpen; 2024. Available from: http://dx.doi.org/10.5772/intechopen.1004702.

[15] Jeremy Ross M.D., Hemant A. Parmar M.D., Anca Avram M.D., Mohannad Ibrahim M.D., Suresh K. Mukherji M.D. Chapter 36 - Imaging in Thyroid Cancer. Oncologic Imaging: a Multidisciplinary Approach (Second Edition), 2023, 616-629. https://doi.org/10.1016/B978-0-323-69538-1.00036-7.

[16] Siyal AL, Hossain A, Siyal FK, Jatt T, Iram S. Use of Radioisotopes to Produce High Yielding Crops in Order to Increase Agricultural Production. Chemistry Proceedings. 2022; 10(1):86. https://doi.org/10.3390/IOCAG2022-12267.

[17] Wan Q. Application Prospect of Radionuclide Tracer Technology in Clinical Imaging Therapy and Drug Development. Highlights in Science, Engineering and Technology. 2022 Sep 29; 14: 177-182. https://doi.org/10.54097/hset.v14i.1608.

[18] Minhas AS, Frush DP. Compendium of resources for radiation safety in medical imaging using ionizing radiation. J Am Coll Radiol. 2013;10(5):354-360.e3602. https://doi.org/10.1016/j.jacr.2012.10.005.

[19] Villoing D, Yoder RC, Passmore C, et al. 0216 Occupational radiation doses in nuclear medicine: a us multi-centre study. Occupational and Environmental Medicine. 2017; 74(1): A65. https://doi.org/10.1136/oemed-2017-104636.172.

[20] Meisenhelder, J., & Bursik, S. Safe Use of Radioisotopes. Current Protocols in Molecular Biology, 2007; 79(1), A.1F.1-A.1F.18. https://doi.org/10.1002/0471142727.mba01fs79.

[21] Chruscielewski W, Olszewski J, Jankowski J, Cygan M. Hand exposure in nuclear medicine workers. Radiat Prot Dosimetry. 2002;101(1-4):229-232. DOI: 10.1093/oxfordjournals.rpd.a005973.

[22] Laçi I, Spahiu A, Bodeci A, Shpuza A. The Role of Ultrasound, Scintigraphy, and Cytology in Evaluating Thyroid Nodules. Open Access Maced J Med Sci [Internet]. 2022 Sep. 23 [cited 2024 Aug. 13];10(B):2382-6. Available from: https://doi.org/10.3889/oamjms.2022.10883.

[23] Schenke SA, Campennì A, Tuncel M, et al. Diagnostic Performance of 99mTc-Methoxy-Isobuty-Isonitrile (MIBI) for Risk Stratification of Hypofunctioning Thyroid Nodules: A European Multicenter Study. Diagnostics (Basel). 2022;12(6):1358. Published 2022 May 31. https://doi.org/10.3390/diagnostics12061358.

[24] Ayesha Ammar; Kahkashan Bashir; Sadaf Batool; Adnan Saeed. Appearance of Thyroid Gland on Bone Scan, Case of Euthyroid Sick Syndrome. Int. J. Diabetes Endocrinol. 2023, 8(2), 28-30. DOI: 10.11648/j.ijde.20230802.11.

[25] Al-Muqbel KM. Utility of 99m Technetium Pertechnetate Thyroid Scan and Uptake in Thyrotoxic Patients: Jordanian Experience. World J Nucl Med. 2022 Sep 2;22(1):7-14. PMID: 36923985; PMCID: PMC10010862. DOI https://doi.org/10.1055/s-0042-1751053.

[26] Ma J, Yang J, Chen C, et al. Use of 99mTc-sestamibi SPECT/CT imaging in predicting the degree of pathological hyperplasia of the parathyroid gland: semi-quantitative analysis. Quant Imaging Med Surg. 2021;11(10):4375-4388. http://dx.doi.org/10.21037/qims-21-66.

[27] Singh, B. K., Kim, J., Pak, D., Kim, K., & Um, W. (2023). Technetium (Tc)/Rhenium (Re) solubility and leaching behavior from waste forms: An overview. Frontiers in Nuclear Engineering, 2023; 1:1112080. DOI: 10.3389/fnuen.2022.1112080.

[28] Volkov MA, Novikov AP, Grigoriev MS, Kuznetsov VV, Sitanskaia AV, Belova EV, Afanasiev AV, Nevolin IM, German KE. New Preparative Approach to Purer Technetium-99 Samples—Tetramethylammonium Pertechnetate: Deep Understanding and Application of Crystal Structure, Solubility, and Its Conversion to Technetium Zero Valent Matrix. International Journal of Molecular Sciences https://doi.org/10.3390/ijms24032015.

[29] Johnstone EV, Mayordomo N, Mausolf EJ. Discovery, nuclear properties, synthesis and applications of technetium-101. Commun Chem. 2022;5(1):131. https://doi.org/10.1038/s42004-022-00746-9 | www.nature.com/commschem.

[30] Abdelhamed HM, Abdo Soliman MS, Mahmoud AA, Mohamed R, Ali IM, Abdelhai SF. The utility of technetium-99m pertechnetate thyroid scintigraphy assessing thyroid/salivary ratio as an alternative to thyroid uptake percentage in evaluation of thyroid function, with establishing normal reference values of both parameters: single Egyptian center study. Nucl Med Commun. 2022;43(12):1181-1187. DOI: 10.1097/MNM.0000000000001620.

[31] N., P. N., Maben, R., Chako, N., & Soans, S. T. Role of technetium scan in diagnosis of congenital hypothyroidism. International Journal of Research in Medical Sciences. 2017; 5(7):3218–3221. https://doi.org/10.18203/2320-6012.ijrms20173016.

[32] Nagai, Y., Igashira, M. 99Tc in stars, reactors, and nuclear medicine. Eur. Phys. J. A 2022; 58:235. https://doi.org/10.1140/epja/s10050-022-00883-8.

[33] Gong J, Zhao L, Yang J, Zhu M, Zhao J. [99mTc]Tc-Labeled Plectin-Targeting Peptide as a Novel SPECT Probe for Tumor Imaging. Pharmaceutics. 2022; 14(5):996. https://doi.org/10.3390/pharmaceutics14050996.

[34] Jan Cleynhens, and Alfons Verbruggen. Technetium-99m radiopharmaceuticals—Radiochemistry and radiolabeling. Nuclear Medicine and Molecular Imaging. 2022; 1:79-94. https://doi.org/10.1016/B978-0-12-822960-6.00006-5.

[35] Shahzad K, Majid A, Khan M, Iqbal M, Ali A. Recent advances in the synthesis of (99mTechnetium) based radio-pharmaceuticals. Reviews in Inorganic Chemistry.2021; 41(3): 151-198. https://doi.org/10.1515/revic-2020-0021.

[36] Mohanty S, Sreenivas, T VR, Devipriya, M V. Technetium scintigraphy as a predictive tool of thyroid malignancy. International Journal of Otorhinolaryngology and Head and Neck Surgery [Internet]. 2017 Mar 25;3(2):308. Available from: https://doi.org/10.18203/issn.2454-5929.ijohns20171183.

[37] Czepczyński R. Nuclear medicine in the diagnosis of benign thyroid diseases. Nucl Med Rev Cent East Eur. 2012;15(2):113-119. Published 2012 Aug 29.DOI:10.5603/NMR.2012.0008.

[38] Giovanella L, Avram A, Clerc J. Molecular Imaging for Thyrotoxicosis and Thyroid Nodules. J Nucl Med. 2021Jul;62(Supplement 2):20S-25S. DOI: https://doi.org/10.2967/jnumed.120.246017.

[39] McGrath N, Hawkes CP, Ryan S, Mayne P, Murphy N. Infants Diagnosed with Athyreosis on Scintigraphy May Have a Gland Present on Ultrasound and Have Transient Congenital Hypothyroidism. Horm Res Paediatr. 2021 Jan 1;94(1-2):36-43.https://doi.org/10.1159/000514989.

[40] Ji Young Kim, Jae Hoon Moon, Kyung Min Kim, Tae Jung Oh, Dong Hwa Lee, So Y, et al. Utility of Quantitative Parameters from Single-Photon Emission Computed Tomography/Computed Tomography in Patients with Destructive Thyroiditis. Korean J Radiol. 2018 May-Jun;19(3):470-480. https://doi.org/10.3348/kjr.2018.19.3.470.

[41] Campennì A, Siracusa M, Ruggeri RM, Laudicella R, Pignata SA, Baldari S, et al. Differentiating malignant from benign thyroid nodules with indeterminate cytology by 99mTc-MIBI scan: a new quantitative method for improving diagnostic accuracy. Scientific Reports. 2017 Jul 21;7(1): 6147. https://doi.org/10.1038/s41598-017-06603-3.

[42] Campennì A, Giovanella L, Siracusa M, Alibrandi A, Pignata SA, Giovinazzo S, et al. 99mTc-Methoxy-Isobutyl-Isonitrile Scintigraphy Is a Useful Tool for Assessing the Risk of Malignancy in Thyroid Nodules with Indeterminate Fine-Needle Cytology. Thyroid. 2016 Aug;26(8):1101–9.https://doi.org/10.1089/thy.2016.0135.

[43] Akter S, Mustafa HA. Analysis and interpretability of machine learning models to classify thyroid disease. PLOS ONE. 2024 May 31;19(5). doi:10.1371/journal.pone.0300670.

[44] Boschi F, Pagliazzi M, Rossi B, Cecchini MP, Gorgoni G, Salgarello M, et al. Small-animal radionuclide luminescence imaging of thyroid and salivary glands with TC99M-pertechnetate. Journal of Biomedical Optics. 2013 Jul 10;18(7):076005. https://doi.org/10.1117/1.JBO.18.7.076005.

[45] Brent GA. Mechanisms of thyroid hormone action. Journal of Clinical Investigation. 2012 Sept 4;122(9):3035–43. doi:10.1172/jci60047.

[46] Kalra MK, Sodickson AD, Mayo-Smith WW. CT Radiation: Key Concepts for Gentle and Wise Use. Radiographic. 2015; 35(6):1706-1721. https://doi.org/10.1148/rg.2015150118.

[47] Khong P-L, Frush D, Ringertz H. Radiological protection in paediatric computed tomography. Annals of the ICRP. 2012 Oct;41(3-4):170–8. https://doi.org/10.1016/j.icrp.2012.06.017.

[48] Simone Agnes Schenke, Campennì A, Murat Tuncel, Bottoni G, Sager S, Tatjana Bogovic Crncic, et al. Diagnostic Performance of 99mTc-Methoxy-Isobuty-Isonitrile (MIBI) for Risk Stratification of Hypofunctioning Thyroid Nodules: A European Multicenter Study. Diagnostics. 2022 May 31;12(6):1358–8. https://doi.org/10.3390/diagnostics12061358.

[49] Mansour S, Noura Almuqbil, Alabsi A, Bodour Alnasser, Assuhebani D, Haya Alsaif, et al. Technetium-99m (99mtc) and Iodine-123 (123i) in Comparison with Thyroid Ultrasonography in Differential Diagnosis of Saudi Patients with Graves' Disease. 2024;19. Available at SSRN: https://ssrn.com/abstract=4711679 or http://dx.doi.org/10.2139/ssrn.4711679.

[50] Jin M, Ahn J, Jo S, Park J, Min Ji Jeon, Tae Yong Kim, et al. Comparison of 99MTC Pertechnetate thyroid uptake rates by gamma probe and gamma camera methods for differentiating graves' disease and thyroiditis. Nuclear Medicine and Molecular Imaging [Internet]. 2022 Jan 7;56(1):42–51. Available from: https://doi.org/10.1007/s13139-021-00734-2.

[51] Ohiduzzaman M, Khatun R, Reza S, Kadir MA, Akter S, Uddin MF, Rahman MA, Mallick R, Samad MA, Billah MM, Ahasan MM. Thyroid Uptake of Tc-99m and Its Agreement with I-131 for Evaluation of Hyperthyroid Function. Universal Journal of Public Health [Internet]. 2019 Sep 1;7(5):201–6. Available from: https://doi.org/10.13189/ujph.2019.070502.

[52] Wang R, Better N, Sivaratnam D, Westcott J, Forehan S, Christie M, Pattison DA, Fourlanos S. 99MTC-Sestamibi Thyroid Scintigraphy in Amiodarone-Induced Thyrotoxicosis. Clinical Nuclear Medicine [Internet]. 2022 Jul 15;47(9):e582–4. Available from: https://doi.org/10.1097/rlu.0000000000004332.

[53] Young C, Owens CM. Pediatric computed tomography imaging guideline. Acta Radiologica [Internet]. 2013 Nov 1;54(9):998–1006. Available from: https://doi.org/10.1177/0284185113476020.

[54] Zapata ÁML, Rodríguez CM. Radioprotection and contrast agent use in pediatrics: what, how, and when. Radiología. 2016 May 1;58:92–103. PMID: 27085511. Available from: https://doi.org/10.1016/j.rx.2016.02.002.

[55] Lepareur N, Ramée B, Mougin-Degraef M, Bourgeois M. Clinical advances and perspectives in targeted radionuclide therapy. Pharmaceutics [Internet]. 2023 Jun 14;15(6):1733. Available from: https://doi.org/10.3390/pharmaceutics15061733

[56] Mushtaq S, Bibi A, Park JE, Jeon J. Recent Progress in Technetium-99m-Labeled Nanoparticles for Molecular Imaging and Cancer Therapy. Nanomaterials (Basel). 2021;11(11):3022. Published 2021 Nov 10;11(11):3022. https://doi.org/10.3390/nano11113022.

[57] Herrero Álvarez N, Bauer D, Hernández-Gil J, Lewis JS. Recent Advances in Radiometals for Combined Imaging and Therapy in Cancer. ChemMedChem. 2021;16(19):2909-2941.doi.org/10.1002/cmdc.202100135.

[58] Ross JC, Hutt DF, Burniston M, et al. The role of serial 99mTc-DPD scintigraphy in monitoring cardiac transthyretin amyloidosis. Amyloid. 2022 Oct 27;29(1):38-49.https://doi.org/10.1080/13506129.2021.1991302.

[59] Galli F, Varani M, Lauri C, Campagna G, Balogh L, Weintraub BD, et al. In Vivo Imaging of Thyroid Cancer with 99mTc-TR1401 and 99mTc-TR1402: A Comparison Study in Dogs. Journal of Clinical Medicine. 2021 Apr 26;10(9):1878. https://doi.org/10.3390/jcm10091878.

[60] Enrico Saggiorato, Tiziana Angusti, Rosas R, Morena Martinese, Finessi M, Arecco F, et al. 99mTc-MIBI Imaging in the Presurgical Characterization of Thyroid Follicular Neoplasms: Relationship to Multidrug Resistance Protein Expression. The Journal of Nuclear Medicine. 2009 Oct 16;50(11):1785–93. https://jnm.snmjournals.org/content/jnumed/50/11/1785.

[61] Namratha B, Apoorva Gupta, Vandana Vasudev, Resham Gupta, Saraswathi P Devi. Thyomental distance is a good difficult airway indicator: Truth or a misconception- A

prospective observational study. Indian Journal of Clinical Anaesthesia. 2023; 10(2):175-181. https://doi.org/10.18231/j.ijca.2023.034.

[62] Nakamura Y, Kangai Y, Sato S, et al. [Impact of Residual Radioactivity Rate of 99mTc-Macro Aggregated Albumin (MAA) in Syringes and Administration Routes with a Focus on Pediatric Nuclear Medicine Examinations]. Japanese Journal of Radiological Technology. 2023; 79(8):802-809. https://doi.org/10.6009/jjrt.2023-1352.

[63] Iori M, Grassi E, Piergallini L, et al. Safety injections of nuclear medicine radiotracers: towards a new modality for a real-time detection of extravasation events and 18F-FDG SUV data correction. EJNMMI Phys. 2023;10(1):31. Published 2023 May 23. https://doi.org/10.1186/s40658-023-00556-5.

See The Author Guidelines (Click Here)

Al-Kitab Journal for Pure Sciences (2025); 9(1):68-90.
https://doi.org/10.32441/kjps.09.01.p5

Al-Kitab Journal for Pure Sciences
ISSN: 2617-1260 (print), 2617-8141(online)

https://isnra.net/index.php/kjps

A Review of Side Effects of Artificial Preservatives on the Human Health

Zahraa A. Hussein Al-Tameemi

Faculty of Medicine, Al-Iraqi University, Iraq

*Corresponding Author: Zahraaa-tameemi@aliraqia.edu.iq

Citation: Al-Tameemi ZAH. A Review of Side Effects of Artificial Preservatives on the Human Health. Al-Kitab J. Pure Sci. [Internet]. 2025 Jan. 9;9(01):68-90. DOI: https://doi.org/10.32441/kjps.09.01.p5.

Keywords: Food Preservation, Natural Preservatives, Chemical Preservatives, Nitrites and Nitrates, Sodium Benzoate, Cosmetics Preservatives, Paraben, Phenoxyethanol.

Article History

Received	03 Jun.	2024
Accepted	09 Aug.	2024
Available online	09 Jan.	2025

Abstract:

Food is necessary for all living humans to survive. Numerous nutrients, including proteins, lipids, carbs, vitamins, and minerals, are found in food. An organism consumes and breaks down these nutrients to create energy needed to support development and preserve regular bodily functions .

Food products can deteriorate due to microbiological, enzymatic, or chemical reactions to their surroundings. Preservatives extend the expiration of food and are also inserted into food goods to preserve quality; however, they may also have adverse side effects. Additionally, safety concerns are increasing as the need for cosmetics for teenagers and adults worldwide rises.

This review article's primary topic is the adverse effects of some specific preservatives commonly used in food and cosmetics, such as [sodium benzoate, parabens, and sulfites], to preserve or enhance their quality.

Keywords: Food preservation, Natural Preservatives, Chemical Preservatives, Nitrites and Nitrates, Sodium Benzoate, Cosmetics preservatives, Paraben, Phenoxyethanol.

الآثار الجانبية للمواد الحافظة الصناعية على صحة الإنسان

زهراء علي حسين التميمي

كلية الطب - الجامعة العراقية - العراق

Zahraaa-tameemi@aliraqia.edu.iq

الخلاصة:

الغذاء ضروري لجميع الكائنات الحية للبقاء على قيد الحياة. توجد العديد من العناصر الغذائية في الطعام، بما في ذلك البروتينات والدهون، والكربوهيدرات، والفيتامينات، والمعادن. يستهلك الكائن الحي هذه العناصر الغذائية ويكسرها لإنتاج الطاقة اللازمة لدعم النمو والحفاظ على وظائف الجسم المنتظمة.

يمكن أن تتدهور المنتجات الغذائية بسبب التفاعلات الميكروبيولوجية أو الأنزيمية أو الكيميائية مع البيئة المحيطة بها. تعمل المواد الحافظة على إطالة مدة صلاحية المواد الغذائية ويتم إدخالها أيضًا في السلع الغذائية للحفاظ على الجودة؛ ومع ذلك، قد يكون لها أيضًا آثار جانبية ضارة. بالإضافة إلى ذلك، مع تزايد الحاجة إلى مستحضرات التجميل للمراهقين والبالغين في جميع أنحاء العالم، تتزايد المخاوف المتعلقة بالسلامة.

الموضوع الرئيسي لمقالة المراجعة هذه هو الآثار الضارة لبعض المواد الحافظة المحددة المستخدمة بشكل شائع في الأغذية ومستحضرات التجميل، مثل [بنزوات الصوديوم، والبارابين، والكبريتات]، للحفاظ على جودتها أو تحسينها.

الكلمات المفتاحية: مواد حافظة غذائية، مواد حافظة طبيعية، مواد حافظة كيميائية، نتريت ونترات، بنزوات الصوديوم، ثاني أكسيد الكبريت، ميتابيسلفيت الصوديوم، مواد حافظة لمستحضرات التجميل، بارابين، فينوكسي إيثانول.

1. Introduction:

The functional use of a broad range of substances that prevent or slow down bacterial and enzymatic development in several products, such as meals, medications, and personal care items, is called "preservatives." These materials may be artificial or natural. Preservatives are essential in many kinds of stuff that people use daily because they help stop the growth of hazardous germs and keep products from spoiling or being contaminated [1]. Preservatives are added to prevent food from rotting due to germs, molds, fungus, and yeast. If preservatives are added, food can have a longer shelf life and stay fresher for longer. Additionally, food preservatives are employed to postpone rancidity and reduce or stop color, taste, or texture changes [2]. Preservatives are often used in medicine and pharmaceuticals to help prevent microbial contamination. Examples of these products include insulin, cough syrup, and acetaminophen. In other words, preservatives play a crucial role in our safety by inhibiting the growth of microorganisms, mainly bacteria, and fungi, that may cause disease or infection.

Preservatives are not just limited to food; they are also present in cosmetics and personal hygiene items. This versatile ingredient prevents contamination and the development of dangerous germs in items like toothpaste, sunscreen, lotions, and shampoos. Moreover, preservative-treated wood can be used in a wide range of construction projects, from raised flower beds to road signs [3].

1- Food Preservatives

Before the creation of preservatives, food was kept fresh and stored in vessels like clay jars. Food drying was a standard method of food preservation since most bacteria and fungi need moisture to thrive. Foods such as meat, fruits, and vegetables were frequently dried to preserve them. Salting is still used to protect various forms of meat, including fish and hams, as well as jams and jellies, which are high-sugar solutions [4-6].

1.2. Classification of Preservatives: Preservatives are classified into:

1.2.1 Natural Preservatives: Food preservatives come from Nature, such as Salt, Sugar, Vinegar, Spices, Honey, Edible Oil, etc. [7].

1.2.2. Chemical Preservatives: These food preservatives include benzoates, sorbates, nitrates and nitrates, potassium sulfate, glutamates, glycerides, and synthetic or semi-synthetic. There are three types of chemical preservatives: antimicrobial, antioxidant, and anti-enzymatic [8].

1.2.2.A: Antimicrobials: For instance, nitrites and nitrates stop food poisoning caused by bacteria in meat products [9]. Additionally, they can eradicate or stop the growth of mold, yeast, and bacteria. Sulfur dioxide prevents the deterioration of wine, beer, and fruits. Antifungal substances like benzoates and sorbates stop the growth of fungi and are used in cheese, pickles, jams, and salad dressings [10].

1.2.2.B: Antioxidants: These inhibit or halt the process of fats and oils in food, breaking down in the presence of air and leading to rancidity. There are three types of antioxidants:

(a) Synthetic Antioxidants: Butylated hydroxyanisole (BHA) and butylated hydroxytoluene (BHT).
(b) Reducing Agents: Ascorbic Acid
(c) Antioxidants Synergists: Sodium Edetate [11].

1.2.2.C: Anti-Enzymatic Preservatives: These inhibit the enzymatic processes that cause food items to ripen even after they are harvested. For example, erythorbic acid and citric acid avert the action of the enzyme phenology and cause the exposed surface of sliced fruits to turn brown [12]. Examples of these preservatives and their allowable quantities are provided in **Table 1**.

Table 1: Maximum Possible Limits of Preservatives and Food Products That Can Be Used [13]

Preservatives	Class	Max Possible Limit	Products Where They Are Found
Sodium And Potassium Benzoate, Benzoic Acid	Antimicrobial	200ppm	Pickles, Margarine, Fruit Juices, Jams, Cheese, Baked Goods, Snacks
Methyl And Propyl Paraben	Antimicrobial	0.1%	Baked Goods, Beverages, Dressings, Relishes
Sorbic Acid, Sodium, Potassium and Calcium Sorbates	Antimicrobial	200ppm	Dairy Products, Bakery Goods, Sweets, Syrups, Fruit Juices, Jams, Jellies, Beverages
Sulfites And Sulfur Dioxide	Antimicrobial	200-300ppm	Dry Fruits and Fruits, Molasses, Fried or Frozen Potatoes, Shrimp and Lobster
Propionates	Antimicrobial	0.32%	Bakery Products, Cheese, Fruits

1.3. The Perfect Preservative Properties:

1. It ought not to cause irritation.
2. It ought not to be poisonous.
3. It must possess both chemical and physical stability.
4. The preservatives and other chemicals in the formulation should work well together.
5. It should have a broad range of action and function well as an antibacterial agent.
6. It must be strong enough to function as a preservative at low concentrations[13].

1.4. Dangers to Health Associated with Artificial Preservatives:

Although most artificial preservatives are thought to be harmless, a few have unfavorable and perhaps fatal adverse effects, like:

1.4.1. Nitrites and Nitrates: Meat and other perishable goods are frequently cured using nitrite and nitrate salts. In addition to helping to preserve food, they also impede the growth of potentially dangerous germs, such as Clostridium botulinum, the bacterium that causes the deadly botulism disease [9].

The component hemoglobin, which delivers oxygen from the blood to the body's tissues, attaches to nitrate and changes chemically to become methemoglobin, which reduces oxygen delivery to tissues and gives the skin its blue hue [14]. In adults, being subjected to greater levels of nitrates or nitrites (Figure 1) has been linked to a more significant risk of cancer; in children, some studies have suggested a rising risk of brain tumors, leukemia, and nasopharyngeal cancers [15-22]. Methemoglobinemia, or decreased hemoglobin oxygenation, has been linked to drinking water polluted with nitrate and nitrite. Because of the cyanotic (low oxygen) symptoms that arise from this reduced oxygenation of the blood, it is often referred to as the "blue baby syndrome [23].

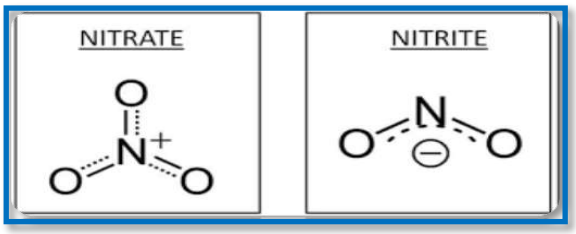

Figure 1: Nitrate and Nitrite structure [24]

Intrauterine development retardation was one of the additional health consequences that resulted from exposing a fetus to high amounts of nitrates in drinking water [25, 26], cardiac defects [27], and increased risk of nervous system defects. Research has also shown that children exposed to nitrates may be at risk for additional health problems, including a higher risk of childhood diabetes [28], recurrent respiratory tract infections, and diarrhea [29]. Brain tumors, leukemia, and nasopharyngeal cancers in children and young people have also been reported [19, 21] [30-34]. Additionally, another study found that drinking water containing nitrates might induce non-Hodgkin's lymphoma (NHL) because nitrate consumption results in the production of N-nitroso compounds, which are known to be carcinogenic after being absorbed in the stomach [35].

1.4.2. Sodium Benzoate: Sodium Benzoate is used in food to stop dangerous bacteria, yeasts, and molds from causing spoiling. Delaying or preventing alterations in food's color, flavor, PH, and texture also contributes to preserving freshness [36].

Sodium benzoate is a common preservative that enhances flavor and lengthens shelf life in various foods and beverages, including salad dressings, pickles, sauces, condiments, fruit juices, wines, and soft drinks. In laboratory animals, it has also been connected to cancer. It has been discovered that bottled tomato paste may be kept for up to 40 weeks without losing its quality, thanks to the widely used sodium benzoate (**Figure 2**). However, when mixed with vitamin C, it can produce the carcinogen benzene [37].

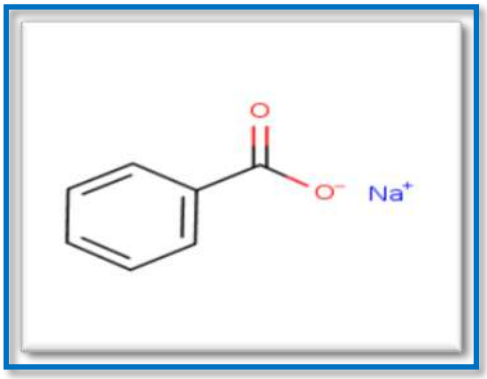

Figure (2): Sodium Benzoate structure[38]

Research has been done on how preservatives containing sodium benzoate affect the induction of micronuclei and chromosomal breakage. The lymphocyte cell line was treated with sodium benzoate at doses of 0.5,1.0,1.5, and 2.0 mg/mL for 24 and 48 hours, respectively. PCR, automated sequencing, conventional chromosome culture, and micronucleus tests were used to find micronucleus and chromosomal breaks. The findings demonstrated that, compared to the control group, micronucleus production was elevated at 24- and 48-hour incubation times at sodium benzoate doses of 1.0, 1.5, and 2.0 mg/mL ($P < 0.05$). Sodium benzoate doses of 2.0 mg/mL at 24- and 48-hour incubation times enhanced chromosomal break compared to the control group ($P < 0.05$). When micronuclei formed, and chromosomes broke in lymphocytes, sodium benzoate exhibited mutagenic and cytotoxic effects [39].

Short-lived exposure to sodium benzoate can disturb the eyes, skin, and respiratory system; however, repeated or sustained exposure can increase skin sensitivity [40]. High dosages can lead to alterations in gastrointestinal mucus production, ulcers, and the release of prostaglandin and histamine [41, 42]. Furthermore, research on soft drinks and fruit juices has shown that the presence of metal catalysts during the reaction between ascorbic acid and benzoic acid produces benzene [43].

Afshar et al. found that mice's fetal absorption rate was statistically significant at 280 and 560 mg sodium benzoate dosages. These doses also resulted in a decrease in the fetus's weight and crown-rump length in contrast to the control group [44, 45]. Sohrabi et al. conducted a study on mice in which they found that progesterone hormone at a dosage of 280 mg was lower than in the control group and that sodium benzoate at a concentration of 560 mg/kg decreased the weight of the ovaries and the hormones FSH and LH [46].

According to different research, mice's weight can be decreased by 200 mg/kg of sodium benzoate; however, the mice's separated serum included greater amounts of urea, uric acid, and creatinine. In a study involving rats and mice, Fujitani et al. located that at a concentration of 2.4%, the average weight of the rats decreased in comparison to the control group; at a concentration of 2.4% weight gain in the liver and kidney occurred in the rats, and at a concentration of 3%, the weight of the liver and kidney increased in comparison to the control group in the mice [47]. Eber Chukwu et al.'s study of sodium benzoate's effects in rats showed that it could reduce hemoglobin levels at all doses and the number of white blood cells at 60 and 120 mg/kg in comparison to the control group. As a result of this decline, the rats' WBCs are more vulnerable to infection [48]. Ibekwe et al.'s study on sodium benzoate's effects on rats showed that the drug might reduce hemoglobin at all doses and the number of white blood cells at 60 and 120 mg/kg in comparison to the control group. The rats' WBCs are more vulnerable

to infection due to this decline [49]. Yilmaz et al. examined how 200 and 500 µg/ml of benzoate sodium affected human cell lymphocytes. At 500µg/mL, benzoic acid lowered the mitotic index and raised the indices of chromosomal aberration (CA), sister chromatid exchanges (SCEs), and micronucleus (MN) [50]. Other studies have observed that sodium benzoate could alter the shape of lymphocytes and cause damage to the cell membrane when they examined lymph node cells taken from mice that were given varying amounts of the chemical compared to control cells. The negative effects of this chemical grow with higher concentrations and longer exposure time [51, 52].

1.4.3. Sulfites, Sulfur Dioxide, and Sodium Metabisulfite: Broad-spectrum antimicrobials that inhibit bacteria, yeasts, and molds include sulfites and sulfating agents, including sulfur dioxide (SO2), sodium and potassium sulfite, metabisulphite, and bisulfites (**Figure 3**). It is specifically used to stop malolactic fermentation during wine production. Sulfites are preservatives for food and drink goods to avoid oxidation and bacterial growth. Sulfites are also applied to keep fruits and vegetables that are canned, dried, frozen, and frozen from browning enzymatically and nonenzymatically [53].

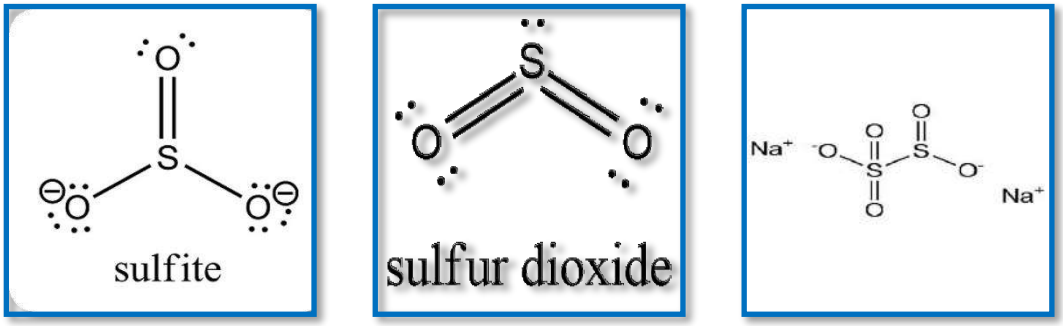

Figure 3: Structures of Sulfite, Sulfur dioxide, and Sodium metabisulfite [54]

The following goods are permitted to include SO2, sulfite, and metabisulfite according to the Codex General Standard for Food Additives: Fruit products, fresh, frozen, fermented, canned, and dried fruit; and dried vegetables; starches; precooked pasta; fish and some shellfish products; sugar products; herbs and spices; vinegar varieties; mustards; sauces; cider, wines; flavored water drinks; distilled spirituous drinks with a minimum 15% alcohol content; and snacks. Depending on the product, the maximum concentration allowed might vary from 15 to 1000 ppm [55].

Although sulfite additions are widely used because they seem harmless, reports of negative responses to sulfite exposure started to surface in the 1970s [56, 57]. Most reports, however, described the induction of bronchoconstriction in asthmatic patients. These comprised inducing anaphylactic responses and various symptoms, including flushing, dermatitis, urticaria,

diarrhea, hypotension, and stomach discomfort [58, 59]. Some people get mild to extremely severe asthmatic symptoms when exposed to sulfite, whereas, for some people, these responses can be fatal [60].

Til et al. investigated the sulfite toxicity in recently weaned Wistar rats. Six groups, each with 20 males and 20 females, were created from the 120 males and 120 females. For up to two years and three generations, the groups were kept on the stock diet that included 0.0 (control), 0.125, 0.25, 0.5, 1.0, or 2.0% sodium metabisulphite. In two generations of rats, a 2% sulfite level somewhat slowed their development, but not significantly. There was blood in the stools for the groups that received 1% or more sulfite. Pathological analysis showed that the three generations had hyperplastic alterations in the epithelial and foregut with 2% and 1% sulfite levels, respectively. A series of brief experiments involving 10 male and 10 female rats were conducted on high sulfite levels (0–8%) for 10–56 days. Growth depression and substantial food intake and efficiency decreases were seen in diets containing 6% sulfite. At 2% and above, anemia was seen. Levels of 4% and above were associated with increased splenic weight. The presence of blood in the stool and alterations in the shape of the stomach were the most sensitive indicators of sulfite injury in the current investigations [59].

The same research group investigated the sub-chronic and chronic oral toxicity of sodium metabisulphite. Twenty pigs, twenty females, and twenty males were fed diets containing 0.0, 0.125, 0.25, 0.5, 1.0, or 2.0% Na2S2O5. Fourteen males and fourteen females from each group were slain after fifteen weeks. For 48 weeks, the six male and six female survivors in each group were fed identical meals. The average amounts of sulfite that remained in the different experimental diets after the pigs ate them were determined to be 0.06, 0.16, 0.35, 0.83, and 1.72%, respectively. The liver, kidneys, heart, and spleen showed a substantial rise in organ-to-body weight ratios when fed at dietary levels of 1.72% after 15 and 48 weeks and only at dietary levels of 0.83% after 48 weeks. The study determined that 0.35% Na2S2O5 in the pigs' diet for 48 weeks was the no-effect threshold [61]. More recently, Kadi et al. assessed the sub-chronic toxicity of sodium metabisulphite on 24 female Wistar rats that were split into four groups and given different amounts of sodium metabisulphite (0.0, 0.25, 1, and 4%) in their drinking water for 90 days. The 1% and 4% Na2S2O5 injections significantly affected body weight, food intake, and water consumption. Biochemical markers such as calcium, urea, creatinine, uric acid, and transaminases increased, but immunoglobulin levels decreased. Hematology showed leukocytosis and a reduction in hemoglobin and red blood cells. They concluded that sub-chronic Na2S2O5 1% and 4% ingestion in Wistar rats appeared to affect the immunological function and biochemical, hematological, and physiological parameters [62].

1.5 Can Food Preservatives Cause Hormone Disturbances in People and Encourage Obesity?

According to a new study published in Nature Communications, Cedars-Sinai researchers developed a unique platform and process for assessing the effects of chemicals known as endocrine disruptors on humans. The preservatives under investigation in this study are commonly accessible in modern society. Some products, such as cookware and carpeting, contain a polymer called perfluorooctanoic acid (PFOA); paints contain a compound called tributyltin (TBT), which can contaminate water and accumulate in seafood; and breakfast cereals and other foods often contain an antioxidant called butylhydroxytoluene (BHT) to preserve nutrients and prevent fats from going rancid. In mice genetically predisposed to the condition, these alterations resulted in aberrant immune systems that led to chronic colitis. It is exceedingly tough to shed weight due to obesity since this process slows down metabolism and depletes the liver of energy. The mice developed weight gain and insulin resistance prediabetes when they were subjected to the same quantity of propionate as humans normally ingest on a long-term basis [63]. The research aimed to design human subject studies to test its hypothesis. The researchers used tissues that generate hormones from human stem cells to reveal how long-term use of these compounds can hinder the signals the digestive system delivers to the brain, signaling when a person feels "full" after eating. People eat more when this signaling system isn't working correctly, which leads to weight gain. It was found that each of these preservatives harmed hormones that connected the gut with the brain. When all three chemicals were evaluated together, there was a significant amount of combined stress, with BHT having some of the most potent negative impacts. While other scientists have appeared, these compounds can hold up hormone systems in laboratory animals. This is the first research to document how preservative-containing compounds may block hormones essential for gut-to-brain transmission and avoid obesity in humans using human pluripotent stem cells and tissues. Used the stem cells to grow human epithelial tissue, which lines the intestines, as well as neuronal tissues of the hypothalamus area of the brain, which controls metabolism and hunger. Then, tissues were exposed to BHT, PFOA, and TBT alone and in combination, and the researchers watched to see how the cells responded. They found that the chemicals disrupt the networks that allow signaling hormones to stay structurally intact and be transported outside of cells, rendering them ineffective. Mitochondria were also damaged by the poisons. Because the "young" cells that suffered the chemical harm were still in the early stages of development, the findings suggest that a hormone system breakdown might affect the unborn child as well as the pregnant woman [64].

2. Cosmetics preservatives

Many people use lotions on their bodies and skin almost every day. The skin creams are sometimes contained in little pots. We apply the cream with our fingers and don't always wash our hands before applying the cream to our skin. As a result, bacteria from the hands enter the cream pots. The creams frequently contain loads of water and are kept in warm bathrooms, which creates ideal circumstances for the bacteria's fast microbial development within the pots. For this reason, extra precautions need to be taken to prevent the cream from being damaged. Nearly all body lotions and skin creams contain preservatives. Without preservatives, bacteria would grow and multiply in the cream, eventually leading to skin issues or even dermatitis [65]. Because makeup products are nutrient-rich environments that promote the growth of microorganisms, this impacts the effectiveness of the preservatives [66].

2.1 Stages of preservation

To supply cosmetic goods with adequate defense against microbiological pollution, the industry offers:

2.1.1. Primary Preservation Strategy: GMPs must be rigorously followed when manufacturing cosmetics. Cosmetics must be prepared in an absolutely aseptic manner to prevent microbiological contamination. Ways to lower the risk of contamination are water handling, microbiological domination of raw materials, tools disinfection, and staff qualification [67, 68].

2.1.2. Secondary Preservation Strategy: In order to maintain the firm of cosmetics throughout storage, transportation, and use, three fundamental methods have been utilized: physical, chemical, and physicochemical preservation [69].

2.1.2.A. Secondary Preservation in Physical Terms: In order to maintain the firmness of cosmetics throughout storage, transportation, and use, three fundamental methods have been utilized: physical, chemical, and physicochemical preservation [69]. Primary packaging is used to accomplish this sort of preservation in situations when a physical barrier is present to avoid microbiological contamination [70]. The packaging can offer two layers of protection: one versus pollution during use and another opposed to contamination building up in the apportionment chain [71].

2.1.2.B. Physicochemical Secondary Preservation

• Water Activity. • Emulsion Form. • pH Control [72].

2.1.2.C. Chemical Secondary Preservation

• Synthetic Chemical Preservatives.

• Natural Chemical Preservatives.

• Multifunctional Ingredients [73].

The following is a list of preservative chemicals and their applications:

Table (2) Preservative cosmetics detected in the previous study [74-85]

Preservative detected	Products
2-phenoxyethanol 4-hydroxybenzoic acid Benzalkonium chloride Benzothiazolinone Benzoic acid Benzyl alcohol Benzyl paraben Bronopol Butylated hydroxy anisole Butylated hydroxy toluene Butyl paraben Cetrimonium chloride Chlorhexidinedigluconate Chlorhexidine dihydrochloride Chloroacetamide Chlorphenesin Dehydroacetic acid Dimethylol dimethyl hydantoin Ethyl benzoate Ethylparaben Formaldehyde Formalin Formic acid Glutaral Imidazolidinyl urea Iodopropynylbutylcarbamate Glutaral Imidazolidinyl urea Iodopropynylbutylcarbamate Isobutylparaben Kathon CG Methamine Methyl chloroisothiazolinone Methyldibromoglutaronitrile Methylisothiazolinone Methyloldimethylhydantoin Methylparaben	Aftershave balms Anti-stretch marks cream Bath gel Body care product Body milk Cosmetics Creams Deodorant Eye drop Face cream Hair conditioners Hand creams / gel Hand soaps Hygiene wash Lanoline cream Lipsticks Liquid formulations Liquid soaps Lotions Makeup Moisturizing creams Multi-purpose cleaners Oil-based lotions Ointments Products for babies Shampoos Shower gel Skin cream Skin milk Sun-related cosmetics Toiletries Washing-up liquids Water-based lotions Wet tissues

2.2 Hazardous Ingredients in Cosmetics:

Cosmetics with a high water content are susceptible to microbiological contamination, which might change the product's composition or pose a health risk to the consumer. Pathogenic bacteria frequently reside in contaminated cosmetics. To avoid contamination in bacteria like (Staphylococcus aureus and Pseudomonas aeruginosa), manufacturers insert preservers into cosmetic products [85]. Colorless, odorless, water-soluble, nonpoisonous, non-allergic, non-irritating, influential across a broad pH range, and able to inhibit the growth of bacteria and fungus—these qualities make the preservatives excellent for cosmetics [86]. As of right now, no preservative meets all these requirements. Among the most widely used cosmetic

preservatives in the last 20 years are parabens (methyl, propyl, butyl, and ethyl paraben), formaldehyde, formaldehyde releasers, and methylchloroisothiazolinone /methylisothiazolinone (MCI/MI) [87, 88]. Numerous recent investigations have determined that preservatives are the most prevalent allergens in cosmetic contact [89, 90].

Three primary categories may be used to classify them: UV light absorbers, antioxidants, and antimicrobials. Additional classifications of antimicrobial agents include formaldehyde-releasers, non-formaldehyde-releasing preservatives, and formaldehyde preservatives. Quaternium-15, 2-bromo-2-nitropropane-diol, imidazolidinyl urea, diazolidinyl urea, and DMDM hydantoin are examples of formaldehyde-releasing preservatives (FRP). Preservatives that don't release formaldehyde include parabens, methyl dibromo glutaronitrile-phenoxyethanol (MDBGN-PE), methyl chloroisothiazolinone-methylisothiazolinone (MCI-MI), and iodopropynyl butylcarbamate. Anyone with a formaldehyde allergy may also have an allergy to any of the FRPs [91].

Human meibomian gland epithelial cells (HMGECs) have recently been found to be particularly sensitive to the cosmetic preservative formaldehyde and benzalkonium chloride. At doses permitted for human consumption, exposure to these substances causes cellular atrophy and death in a matter of hours. We propose that additional cosmetic preservatives may potentially have detrimental effects on HMGECs and that these effects are not exclusive to them. Parabens, phenoxyethanol, and chlorphenesin are among these substances; studies have shown that they irritate the eyes and are harmful to the kidney, liver, and corneal and conjunctival epithelial cells[92]. This hypothesis was investigated to examine the effects of phenoxyethanol, chlorphenesin, and parabens on the morphology, signaling, survival, proliferation, and lipid expression of immortalized (I) HMGECs. These cells were cultured in either proliferating or differentiating conditions for up to five days, with varying concentrations of methylparaben, ethylparaben, phenoxyethanol, and chlorphenesin. The IHMGECs' capacity to transmit signals, their quantity, appearance, neutral lipid content, and lysosome buildup were observed. The results show that after being exposed to these preservatives for 30 minutes, IHMGECs' Akt pathway activity significantly decreased. This dose-dependent activity is seen at concentrations comparable to chlorphenesin and lower than all other doses approved for human use. Furthermore, cellular atrophy and mortality occur when the IHMGECs are exposed for a whole day to concentrations of methylparaben, ethylparaben, phenoxyethanol, and chlorphenesin that are close to or equivalent to the recommended human dose. No preservative did not increase IHMGEC proliferation at any of the tested doses. Of special note, because the cells did not make it through the treatment, it was impossible to assess the impact of these

preservatives, at doses almost equivalent to those permitted for humans, on IHMGEC differentiation. In conclusion, the findings validate the theory and demonstrate the toxicity of methylparaben, ethylparaben, phenoxyethanol, and chlorphenesin [93].

Frequently, cosmetic goods like mascara, eye shadow, eyeliner, and makeup remover usually include preservatives (like Benzalkonium chloride BAK and formaldehyde-releasing preservatives FA) to stop microorganisms from growing [94]. These preservatives were conjectured to harm the ocular surface and adnexal cells at quantities (FA = 0.74 mg/ml; BAK = 1 mg/ml) authorized for consumer usage. Thus, the effects of BAK and FA on the morphology, survival, proliferation, and signaling capacity of corneal (iHCECs), conjunctival (iHConjECs), and meibomian gland (iHMGECs) were investigated. For a maximum of seven days, iHMGECs, iHCECs, and iHConjECs were grown in various BAK (5 µg/ml to 0.005 µg/ml) or FA (1 mg/ml to 1 µg/ml) concentrations under basal, increasing, or differentiating conditions. Was used modest BAK concentrations since was discovered that 0.5 mg/ml and 50 µg/ml BAK eliminated iHMGECs in just one day after a 15-minute treatment. The three cell types were subjected to studies of AKT signaling, lysosome accumulation (LysoTracker), and cell appearance, number, and neutral lipid content (LipidTox) [95]. Results showed that iHMGECs, iHCECs, and iHConjECs undergo dose-dependent alterations in their morphology, survival, proliferation, and AKT signaling. After five days of exposure, several measured doses caused poor adherence, reduced proliferation, and cell death. Furthermore, AKT phosphorylation after 15 (FA) or 30 (BAK) minutes of treatment demonstrated that cellular signaling was decreased in a dose-dependent way in all three cell types, irrespective of whether the cells had been grown in proliferating or differentiating conditions. The findings support the research's hypothesis, demonstrating that cosmetic preservatives BAK and FA have several negative effects on the ocular surface and adnexal cells [96].

2.3 The most prevalent preservatives' adverse effects on cosmetic items:

2.3.1 Paraben: Various cosmetic products use parabens (**Figure 4**) as preservatives, including (deodorants, scrubs, shampoos, eye makeup, and lotions), food items, and pharmaceutical items that the general public is exposed to [97].

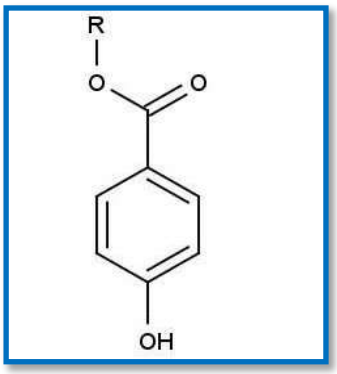

Figure 4: Structure of Paraben [98]

Thin-layer chromatography may be used to extract parabens from human breast tissue and identify them, according to preliminary research. Through more thorough research, the mean amounts of each paraben were found and measured in samples of 20 human breast cancers using tandem mass spectrometry and high-pressure liquid chromatography. The average paraben concentration in 20 human breast tumors was (20.6 ± 4.2 ng g−1) tissue. Upon comparing the different parabens, it was found that methylparaben exhibited the most significant degree of presence (mean value of 12.8 ± 2.2 ng g−1 tissue), accounting for 62% of the total parabens taken back during the extraction processes. Investigations showed that parabens are present in a sound form in the breast of humans, which should theoretically pave the way for the acquisition of more thorough data regarding paraben body loads and, in particular, whether or not these burdens change between normal tissues and malignancy [99]. The water solubility of parabens diminishes as the ester chain length increases, and they have a high oil/water partition coefficient. Consequently, if any parabens can enter the human body unharmed, they may be able to accumulate in biological tissues' fatty components similarly to other lipophilic [100, 101].

Although the majority of research has shown that parabens do not induce mutations, certain reports have shown that they can cause chromosomal abnormalities, especially when polychlorinated biphenyls are present. Additionally, rats who receive methylparaben subcutaneously have been shown to develop mammary adenocarcinomas [102]. Research has demonstrated that parabens can cause mitochondrial malfunction and impede lysosomal enzyme secretion, hence impairing cellular function [103].

2.3.2 Phenoxyethanol: Cosmetic items include Phenoxyethanol (**Figure 5**) as a preservative (it can be found in makeup products and skin, body, and hair care products for adults, baby wipes, baby lotions, fragrances, hair removal waxes, hand sanitizer, and ultrasound gel) and also as a stabilizer in perfumes and soaps [104].

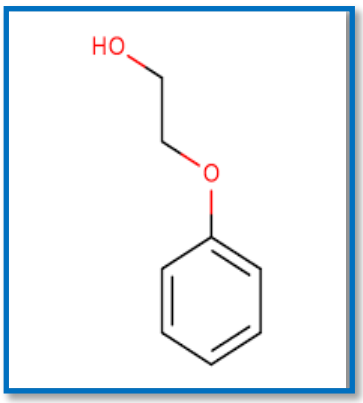

Figure (5): Phenoxyethanol structure [105]

Phenoxyethanol exposure has been connected to a variety of allergic responses, including anaphylaxis, eczema, and hives. Another typical adverse response to products containing one percent or more phenoxyethanol on the skin is eczema. Only the application area reacts, and eczema goes away if the irritating substance is avoided [106]. According to research in 2015, the most common side effect of Doppler ultrasonography gel was skin irritation, yet there were also sporadic instances of potentially fatal responses called anaphylaxis. Doppler ultrasonography gel containing mixtures of phenoxyethanol and parabens may cause more severe allergy responses than phenoxyethanol alone [107]. Effects on the infant's acute nervous system: The FDA warned customers in 2008 not to buy Mommy's Bliss Nipple Cream. Breastfeeding infants had vomiting and diarrhea due to phenoxyethanol, a substance present in the cream that depressed their central nervous system. Reduced hunger, trouble awakening the baby, limp extremities, and skin color changes are all signs of a depressed neurological system [108].

3. Conclusion:

The primary purpose of preservatives in food and cosmetics is their antibacterial effectiveness. However, the food and cosmetics industries must worry about these compounds' toxicity. Therefore, it is essential to keep looking for safe and valuable preservatives. Because of their toxicity, laws restrict or even forbid using the most vital preservatives. They also demand that food and cosmetic items be free of contamination.

Consequently, food and cosmetics producers seek innovative preservation techniques to get around legal restrictions while presenting a safer product regarding toxicological and microbiological aspects. However, a preservative's range of action is limited based on the microorganisms and the target species, which incentivizes producers to combine different preservative forms.

4. References

[1] G. Evans, B. de Challemaison, and D. N. Cox, "Consumers' ratings of the natural and unnatural qualities of foods," Appetite, vol. 54, no. 3, pp. 557-563, 2010.

[2] Z. Ashagrie and D. Abate, "Improvement of injera shelf life through the use of chemical preservatives," African journal of food, agriculture, nutrition and development, vol. 12, no. 5, pp. 6409-6423, 2012.

[3] H. K. HN, A. K. Jha, K. K. Taneja, K. Kabra, and H. M. Sadiq, "A study on consumer awareness, safety perceptions & practices about food preservatives and flavoring agents used in packed/canned foods from South India," National Journal of community medicine, vol. 4, no. 03, pp. 402-406, 2013.

[4] C. Kulkarni, A. Deshpande, and S. More, "Assessment of microbial contamination in commercial herbal oral medicinal liquids," Int J Pharm Res Dev, vol. 2, no. 9, pp. 191-193, 2010.

[5] A. P. Fraise, J.-Y. Maillard, and S. Sattar, Russell, Hugo and Ayliffe's principles and practice of disinfection, preservation and sterilization. John Wiley & Sons, 2012.

[6] P. K. Kumari, S. Akhila, Y. S. Rao, and B. R. Devi, "Alternative to artificial preservatives," Syst. Rev. Pharm, vol. 10, pp. 99-102, 2019.

[7] J. S. Anjali Langeh*, Anju Bhat, Julie D. Bandral, Seerat Gupta and Skarma Choton, " Role of Preservatives in Preservation of Fruits and Vegetables: A review," Chemical Science Review and Letters, vol. Volume 12(48):217-221, 2023.

[8] A. Deshpande and B. Deshpande, "Food additives and preservation: A review," Indian Journal of Sciences and Research, vol. 13, pp. 219-225, 2017.

[9] M. Govari and A. Pexara, "Nitrates and Nitrites in meat products," Journal of the Hellenic veterinary medical society, vol. 66, no. 3, pp. 127-140, 2015.

[10] S. Dey and B. H. Nagababu, "Applications of food color and bio-preservatives in the food and its effect on the human health," Food Chemistry Advances, vol. 1, p. 100019, 2022.

[11] S. Dwivedi, P. Prajapati, N. Vyas, S. Malviya, and A. Kharia, "A review on food preservation: methods, harmful effects and better alternatives," Asian J. Pharm. Pharmacol, vol. 3, no. 6, pp. 193-199, 2017.

[12] Z. M. Sharif, F. Mustapha, J. Jai, and N. Zaki, "Review on methods for preservation and natural preservatives for extending the food longevity," Chemical Engineering Research Bulletin, vol. 19, 2017.

[13] R. Gupta and R. K. Yadav, "Impact of chemical food preservatives on human health," Palarch's Journal Of Archaeology Of Egypt/Egyptology, vol. 18, no. 15, pp. 811-818, 2021.

[14] L. Knobeloch, B. Salna, A. Hogan, J. Postle, and H. Anderson, "Blue babies and nitrate-contaminated well water," Environmental health perspectives, vol. 108, no. 7, pp. 675-678, 2000.

[15] J. Sanchez-Echaniz, J. Benito-Fernández, and S. Mintegui-Raso, "Methemoglobinemia and consumption of vegetables in infants," Pediatrics, vol. 107, no. 5, pp. 1024-1028, 2001.

[16] L. B. Dusdieker, J. P. Getchell, T. M. Liarakos, W. J. Hausler, and C. I. Dungy, "Nitrate in baby foods: adding to the nitrate mosaic," Archives of pediatrics & adolescent medicine, vol. 148, no. 5, pp. 490-494, 1994.

[17] W. S. Fisher, L. E. Jackson, G. W. Suter, and P. Bertram, "Indicators for human and ecological risk assessment: a US Environmental Protection Agency perspective," Human and Ecological Risk Assessment: An International Journal, vol. 7, no. 5, pp. 961-970, 2001.

[18] D. Douer, S. Preston-Martin, E. Chang, P. W. Nichols, K. J. Watkins, and A. M. Levine, "High frequency of acute promyelocytic leukemia among Latinos with acute myeloid leukemia [see comments]," 1996.

[19] M. H. Ward et al., "Dietary exposure to nitrite and nitrosamines and risk of nasopharyngeal carcinoma in Taiwan," International journal of cancer, vol. 86, no. 5, pp. 603-609, 2000.

[20] J. M. Pogoda and S. Preston-Martin, "Maternal cured meat consumption during pregnancy and risk of paediatric brain tumour in offspring: potentially harmful levels of intake," Public health nutrition, vol. 4, no. 2, pp. 183-189, 2001.

[21] S. Sarasua and D. A. Savitz, "Cured and broiled meat consumption in relation to childhood cancer: Denver, Colorado (United States)," Cancer Causes & Control, vol. 5, pp. 141-148, 1994.

[22] M. McCredie, P. Maisonneuve, and P. Boyle, "Antenatal risk factors for malignant brain tumours in New South Wales children," International journal of cancer, vol. 56, no. 1, pp. 6-10, 1994.

[23] A. Shamsuddina, S. Ismailb, S. Shamc, and E. Abidind, "Nitrate in groundwater and excretion of nitrate and nitrosamines in urine: a review," Int J Sci Basic Appl Res, vol. 15, no. 2, pp. 176-91, 2014.

[24] W. Laue, M. Thiemann, E. Scheibler, and K. W. Wiegand, "Nitrates and nitrites," Ullmann's Encyclopedia of Industrial Chemistry, 2000.

[25] J. Bukowski, G. Somers, and J. Bryanton, "Agricultural contamination of groundwater as a possible risk factor for growth restriction or prematurity," Journal of occupational and environmental medicine, vol. 43, no. 4, pp. 377-383, 2001.

[26] L. A. Croen, K. Todoroff, and G. M. Shaw, "Maternal exposure to nitrate from drinking water and diet and risk for neural tube defects," American Journal of epidemiology, vol. 153, no. 4, pp. 325-331, 2001.

[27] M. I. Cedergren, A. J. Selbing, O. Löfman, and B. A. Källen, "Chlorination byproducts and nitrate in drinking water and risk for congenital cardiac defects," Environmental research, vol. 89, no. 2, pp. 124-130, 2002.

[28] S. Virtanen et al., "Nitrate and nitrite intake and the risk for type 1 diabetes in Finnish children," Diabetic Medicine, vol. 11, no. 7, pp. 656-662, 1994.

[29] S. K. Gupta et al., "Recurrent diarrhea in children living in areas with high levels of nitrate in drinking water," Archives of Environmental Health: An International Journal, vol. 56, no. 4, pp. 369-373, 2001.

[30] S. S. Nielsen, B. A. Mueller, S. Preston-Martin, F. M. Farin, E. A. Holly, and R. McKean-Cowdin, "Childhood brain tumors and maternal cured meat consumption in pregnancy: differential effect by glutathione S-transferases," Cancer epidemiology, biomarkers & prevention, vol. 20, no. 11, pp. 2413-2419, 2011.

[31] M. Xiong, Y. Zhang, X. Li, and C. Ma, "Effects of dietary Chinese cured meat on lipid metabolism in rats," Food chemistry, vol. 107, no. 1, pp. 60-67, 2008.

[32] M. McCredie, P. Maisonneuve, and P. Boyle, "Perinatal and early postnatal risk factors for malignant brain tumours in New South Wales children," International journal of cancer, vol. 56, no. 1, pp. 11-15, 1994.

[33] J. S. P.J Clemmensen, N. Brix, T. Sigsgaard, L.T.Stayner,H. A. Kolstad, and C. H. Ramlau-Hansen,, "Prenatal Exposure to Nitrate in Drinking Water and Adverse Health Outcomes in the Ofspring: a Review of Current Epidemiological Research," Current Environmental Health Reports, vol. 10:250–263, 16 July 2023.

[34] S. S. N. B.A.Mueller, S. Preston-Martin, E.A.Holly, S.Cordier, G. Filippini, ... & N.W.Choi, , " "Household water source and the risk of childhood brain tumours: results of the SEARCH International Brain Tumor Study"," International journal of epidemiology,, vol. 33(6), 1209-1216., 2004.

[35] M. H. Ward, S. D MARK, K. P. Cantor, D. D WEISENBURGER, and A. Correa-Villasenor, "Non-Hodgkin's lymphoma and nitrate in drinking water," Journal of Epidemiology & Community Health, vol. 54, no. 10, pp. 772-773, 2000.

[36] B. G. Linke, T. A. Casagrande, and L. A. Cardoso, "Food additives and their health effects: A review on preservative sodium benzoate," African Journal of Biotechnology, vol. 17, no. 10, pp. 306-310, 2018.

[37] C. Xu et al., "Investigation of benzoic acid and sorbic acid in snack foods in Jilin province, China," International journal of food properties, vol. 22, no. 1, pp. 670-677, 2019.

[38] M. Mostafavi, "In-line/on-line measuring techniques in the solution crystallization processes," 2015.

[39] M. Pongsavee, "Effect of sodium benzoate preservative on micronucleus induction, chromosome break, and Ala40Thr superoxide dismutase gene mutation in lymphocytes," BioMed research international, vol. 2015, 2015.

[40] M. Shahmohammadi, M. Javadi, and M. Nassiri-Asl, "An overview on the effects of sodium benzoate as a preservative in food products," Biotechnology and Health Sciences, vol. 3, no. 3, pp. 7-11, 2016.

[41] S. Sambu, U. Hemaram, R. Murugan, and A. A. Alsofi, "Toxicological and teratogenic effect of various food additives: An updated review," BioMed Research International, vol. 2022, 2022.

[42] W. Schaubschläger, W.-M. Becker, U. Schade, P. Zabel, and M. Schlaak, "Release of mediators from human gastric mucosa and blood in adverse reactions to benzoate," International Archives of Allergy and Immunology, vol. 96, no. 2, pp. 97-101, 1991.

[43] K.-J. Jang, C. Cha, and K.-G. Lee, "Analysis and reduction of benzene in various beverages such as vitamin drinks and cranberry juice," LWT, vol. 115, p. 108444, 2019.

[44] M. Afshar, S. Moallem, T. M. HASANZADEH, M. Shahsavan, F. Sukhtanloo, and F. Salehi, "Effect of long term consumption of sodium benzoat before and during pregnancy on growth indexes of fetal balb/c mice," 2012.

[45] N. A. Alwan, A. M. Kudayer, and E. A. Al-Masoudi, "The Toxic Effect of Oral Gavaged of Sodium Benzoate (SB) on Adult Male Rabbits," Malaysian Journal of Medicine & Health Sciences, vol. 18, 2022.

[46] D. Sohrabi, M. Rahnama, A. M. SHAMS, and F. Fakheri, "The effects of sodium benzoate (c6h5coona) on ovaries and its hormones and gonadotropins on female balb/c mice," 2007.

[47] S. Khan, K. B. Dar, S. A. Ganie, and M. N. Ali, "Toxicological impact of sodium benzoate on inflammatory cytokines, oxidative stress and biochemical markers in male Wistar rats," Drug and Chemical Toxicology, vol. 45, no. 3, pp. 1345-1354, 2022.

[48] M. Afshar, M. Taheri, S. Moallem, M. Golalipour, and M. Shahsavan, "Fetal malformations due to long term consumption of Sodium Benzoate in pregnant balb/c mice," AJPT, vol. 2, pp. 1-7, 2014.

[49] S. E. Ibekwe, A. A. Uwakwe, and M. O. Monanu, "Effect of oral intake of sodium benzoate on some haematological parameters of wistar albino rats," Sci. Res. Essays, vol. 2, pp. 006-009, 2007.

[50] S. Yılmaz, F. Ünal, and D. Yüzbaşıoğlu, "The in vitro genotoxicity of benzoic acid in human peripheral blood lymphocytes," Cytotechnology, vol. 60, pp. 55-61, 2009.

[51] M. Hu, J. Wang, J. Cai, Y. Wu, and X. Wang, "Analysis of sodium benzoate biotoxicity using atomic force microscope," Chinese Journal of Biotechnology, vol. 24, no. 8, pp. 1428-1432, 2008.

[52] S. Mamur, D. Yüzbaşıoğlu, F. Ünal, and H. Aksoy, "Genotoxicity of food preservative sodium sorbate in human lymphocytes in vitro," Cytotechnology, vol. 64, pp. 553-562, 2012.

[53] H. Vally and N. L. Misso, "Adverse reactions to the sulphite additives," Gastroenterology and hepatology from bed to bench, vol. 5, no. 1, p. 16, 2012.

[54] E. P. o. F. Additives et al., "Follow-up of the re-evaluation of sulfur dioxide (E 220), sodium sulfite (E 221), sodium bisulfite (E 222), sodium metabisulfite (E 223), potassium metabisulfite (E 224), calcium sulfite (E 226), calcium bisulfite (E 227) and potassium bisulfite (E 228)," EFSA Journal, vol. 20, no. 11, p. e07594, 2022.

[55] E. Mani-López, E. Palou, and A. López-Malo, "Preservatives: classifications and analysis," 2016.

[56] Kochen, "Sulfur dioxide, a respiratory tract irritant, even if ingested," Pediatrics, vol. 52, no. 1, pp. 145-146, 1973.

[57] S. L. Taylor, R. K. Bush, and J. A. Nordlee, "Sulfites," Food Allergy: Adverse Reactions to Foods and Food Additives, pp. 361-374, 2013.

[58] A. F. Gunnison, D. W. Jacobsen, and H. J. Schwartz, "Sulfite hypersensitivity. A critical review," CRC critical reviews in toxicology, vol. 17, no. 3, pp. 185-214, 1987.

[59] M. R. Lester, "Sulfite sensitivity: significance in human health," Journal of the American College of Nutrition, vol. 14, no. 3, pp. 229-232, 1995.

[60] D. Peroni and A. Boner, "Sulfite sensitivity," Clinical & Experimental Allergy, vol. 25, no. 8, pp. 680-681, 1995.

[61] H. Til, V. Feron, and A. De Groot, "The toxicity of sulphite. I. Long-term feeding and multigeneration studies in rats," Food and Cosmetics Toxicology, vol. 10, no. 3, pp. 291-310, 1972.

[62] F. Z. El Kadi, A. I. Bénali, M. Bénali, and S. Belbraouet, "Effect of sodium metabisulphite on blood metabolic status of wistar rats," Food and Nutrition Sciences, vol. 2014, 2014.

[63] H. A. Paula Neto, P. Ausina, L. S. Gomez, J. G. Leandro, P. Zancan, and M. Sola-Penna, "Effects of food additives on immune cells as contributors to body weight gain and immune-mediated metabolic dysregulation," Frontiers in immunology, vol. 8, p. 253755, 2017.

[64] C.-S. M. Center., ""How food preservatives may disrupt human hormones and promote obesity: Innovative stem-cell testing system demonstrates potential for evaluating health effects of chemicals used in everyday life."," ScienceDaily,, 9 August 2017.

[65] N. Halla et al., "Cosmetics preservation: a review on present strategies," Molecules, vol. 23, no. 7, p. 1571, 2018.

[66] E. Neza and M. Centini, "Microbiologically contaminated and over-preserved cosmetic products according Rapex 2008–2014," Cosmetics, vol. 3, no. 1, p. 3, 2016.

[67] E. Guzmán and A. Lucia, "Essential oils and their individual components in cosmetic products," Cosmetics, vol. 8, no. 4, p. 114, 2021.

[68] S. Papageorgiou, A. Varvaresou, E. Tsirivas, and C. Demetzos, "Abstracts: New alternatives to cosmetics preservation," International Journal of Cosmetic Science, vol. 32, no. 5, pp. 395-395, 2010.

[69] S. H. Jeong, "A Review of safety evaluations of cosmetic preservatives," Kor J Aesthet Cosmetol, vol. 11, no. 5, pp. 827-833, 2013.

[70] A. Herman, "Antimicrobial ingredients as preservative booster and components of self-preserving cosmetic products," Current microbiology, vol. 76, no. 6, pp. 744-754, 2019.

[71] S. Roy, S. Majumder, A. Deb, and L. Choudhury, "Microbial contamination of cosmetics and the pharmaceutical products, and their preservation strategies: A comprehensive review," Novel Research in Microbiology Journal, vol. 7, no. 5, pp. 2116-2137, 2023.

[72] S. Martínez and J. Carballo, "Physicochemical, sensory and nutritional properties of foods affected by processing and storage," vol. 10, ed: MDPI, 2021, p. 2970.

[73] G. Alvarez-Rivera, M. Llompart, M. Lores, and C. Garcia–Jares, "Preservatives in cosmetics: Regulatory aspects and analytical methods," in Analysis of cosmetic products: Elsevier, 2018, pp. 175-224.

[74] Yazar, S. Johnsson, M. L. Lind, A. Boman, and C. Liden, "Preservatives and fragrances in selected consumer-available cosmetics and detergents," Contact Dermatitis, vol. 64, no. 5, pp. 265-272, 2011.

[75] A. Jain, S. Soni, and K. K. Verma, "Determination of parabens in cosmetics by liquid-phase microextractions and high-performance liquid chromatography–diode array detection," Journal of Liquid Chromatography & Related Technologies, vol. 38, no. 1, pp. 82-91, 2015.

[76] Y.-f. Liu, J.-l. Zhang, X.-f. Nie, P. Zhang, X.-q. Yan, and K.-f. Fu, "Simultaneous determination of 11 preservatives in cosmetics and pharmaceuticals by matrix solid-phase dispersion coupled with gas chromatography," Acta Chromatographica, vol. 32, no. 3, pp. 203-209, 2020.

[77] A. Flyvholm, "Preservatives in registered chemical products," Contact dermatitis, vol. 53, no. 1, pp. 27-32, 2005.

[78] J. Q. Huang, C. C. Hu, and T. C. Chiu, "Determination of seven preservatives in cosmetic products by micellar electrokinetic chromatography," International journal of cosmetic science, vol. 35, no. 4, pp. 346-353, 2013.

[79] Memon, M. I. Bhanger, and M. Khuhawer, "Determination of preservatives in cosmetics and food samples by micellar liquid chromatography," Journal of separation science, vol. 28, no. 7, pp. 635-638, 2005.

[80] J. F. Schwensen, U. F. Friis, T. Menné, M.-A. Flyvholm, and J. D. Johansen, "Contact allergy to preservatives in patients with occupational contact dermatitis and exposure analysis of preservatives in registered chemical products for occupational use," International archives of occupational and environmental health, vol. 90, pp. 319-333, 2017.

[81] A. Othman, L. Norton, A. S. Finny, and S. Andreescu, "Easy-to-use and inexpensive sensors for assessing the quality and traceability of cosmetic antioxidants," Talanta, vol. 208, p. 120473, 2020.

[82] Tanaka et al., "Rapid Determination of Preservatives in Cosmetics Using a Core–Shell Column," Journal of Chromatographic Science, vol. 61, no. 7, pp. 637-643, 2023.

[83] D. Tahiraj, "Dermatoses Due to Cleaning and Cosmetic Products," ANGLISTICUM. Journal of the Association-Institute for English Language and American Studies, vol. 4, no. 6, pp. 78-83, 2015.

[84] L. Sanchez-Prado, G. Alvarez-Rivera, J. P. Lamas, M. Lores, C. Garcia-Jares, and M. Llompart, "Analysis of multi-class preservatives in leave-on and rinse-off cosmetics by matrix solid-phase dispersion," Analytical and bioanalytical chemistry, vol. 401, pp. 3293-3304, 2011.

[85] A. L. Byrd, Y. Belkaid, and J. A. Segre, "The human skin microbiome," Nature Reviews Microbiology, vol. 16, no. 3, pp. 143-155, 2018.

[86] Poddębniak and U. Kalinowska-Lis, "A Survey of Preservatives Used in Cosmetic Products," Applied Sciences, vol. 14, no. 4, p. 1581, 2024.

[87] H. Y. Sherry, A. Sood, and J. S. Taylor, "Patch testing for methylisothiazolinone and methylchloroisothiazolinone-methylisothiazolinone contact allergy," JAMA dermatology, vol. 152, no. 1, pp. 67-72, 2016.

[88] A. K. Nowak, E. Jabłońska, and W. Ratajczak-Wrona, "Controversy around parabens: Alternative strategies for preservative use in cosmetics and personal care products," Environmental research, vol. 198, p. 110488, 2021.

[89] E. M. Warshaw et al., "Importance of supplemental patch testing beyond a screening series for patients with dermatitis: the North American Contact Dermatitis group experience," JAMA dermatology, vol. 157, no. 12, pp. 1456-1465, 2021.

[90] E. M. Warshaw et al., "Contact dermatitis associated with hair care products: a retrospective analysis of the North American Contact Dermatitis Group Data, 2001–2016," Dermatitis, vol. 33, no. 1, pp. 91-102, 2022.

[91] M. J. Zirwas, "Contact dermatitis to cosmetics," Clinical Reviews in Allergy & Immunology, vol. 56, pp. 119-128, 2019.

[92] R. F. Althulthi, R. M. Moman, A. A. Ghalbun, and M. R. Alsagher, "Evaluation of Bacteriological Quality and Preservatives Efficacy of Cosmetics," Sch Acad J Biosci, vol. 12, pp. 442-451, 2023.

[93] J. Wang, Y. Liu, W. R. Kam, Y. Li, and D. A. Sullivan, "Toxicity of the cosmetic preservatives parabens, phenoxyethanol and chlorphenesin on human meibomian gland epithelial cells," Experimental eye research, vol. 196, p. 108057, 2020.

[94] X. Chen, D. A. Sullivan, A. G. Sullivan, W. R. Kam, and Y. Liu, "Toxicity of cosmetic preservatives on human ocular surface and adnexal cells," Experimental Eye Research, vol. 170, pp. 188-197, 2018.

[95] G. Song, G. Ouyang, and S. Bao, "The activation of Akt/PKB signaling pathway and cell survival," Journal of cellular and molecular medicine, vol. 9, no. 1, pp. 59-71, 2005.

[96] M. Bilal and H. M. Iqbal, "An insight into toxicity and human-health-related adverse consequences of cosmeceuticals—a review," Science of the total environment, vol. 670, pp. 555-568, 2019.

[97] A. Esrafili, Y. Yamini, M. Ghambarian, and M. Moradi, "Analysis of paraben preservatives in cosmetic samples: comparison of three different dynamic hollow fiber liquid-phase microextraction methods," Chromatographia, vol. 77, pp. 317-327, 2014.

[98] E. Jungman, "Development of a percutaneous penetration predictive model with chromatographic and spectroscopic tools," Université Paris Sud-Paris XI, 2012.

[99] M. G. Kirchhof and G. C. de Gannes, "The health controversies of parabens," Skin Therapy Lett, vol. 18, no. 2, pp. 5-7, 2013.

[100] F. A. Andersen, "Final amended report on the safety assessment of methylparaben, ethylparaben, propylparaben, isopropylparaben, butylparaben, isobutylparaben, and benzylparaben as used in cosmetic products," Int J Toxicol, vol. 27, no. Suppl 4, pp. 1-82, 2008.

[101] J. Lincho, R. C. Martins, and J. Gomes, "Paraben compounds—part I: an overview of their characteristics, detection, and impacts," Applied Sciences, vol. 11, no. 5, p. 2307, 2021.

[102] S. Siddique, C. Kubwabo, and S. A. Harris, "A review of the role of emerging environmental contaminants in the development of breast cancer in women," Emerging Contaminants, vol. 2, no. 4, pp. 204-219, 2016.

[103] D. Güzel Bayülken and B. Ayaz Tüylü, "In vitro genotoxic and cytotoxic effects of some paraben esters on human peripheral lymphocytes," Drug and Chemical Toxicology, vol. 42, no. 4, pp. 386-393, 2019.

[104] K. Shivaram, "Disproportionate chemical exposure: How the marketing and production of beauty products in the United States impose health burdens on women," Intersect: The Stanford Journal of Science, Technology, and Society, vol. 12, no. 3, 2019.

[105] L. E. Wineski and A. W. English, "Phenoxyethanol as a nontoxic preservative in the dissection laboratory," Cells Tissues Organs, vol. 136, no. 2, pp. 155-158, 1989.

[106] S. Bohn and A. Bircher, "Phenoxyethanol-induced urticaria," Allergy, vol. 56, no. 9, 2001.

[107] F. Chasset et al., "Contact dermatitis due to ultrasound gel: A case report and published work review," The Journal of Dermatology, vol. 43, no. 3, pp. 318-320, 2016.

[108] A. Panico et al., "Skin safety and health prevention: an overview of chemicals in cosmetic products," Journal of preventive medicine and hygiene, vol. 60, no. 1, p. E50, 2019.

Al-Kitab Journal for Pure Sciences (2025); 9(1):91-102.
https://doi.org/10.32441/kjps.09.01.p6

Al-Kitab Journal for Pure Sciences
ISSN: 2617-1260 (print), 2617-8141(online)

https://isnra.net/index.php/kjps

Construction of Modified Carbon Paste Electrodes for Determination of Tramadol in Very Trace Amounts

Muthana S. Ali

Department of Science, College of Basic Education, Diyala University, Diyala, Iraq.

*Corresponding Author: **basicsci18@uodiyala.edu.iq**

Citation: Ali MS. Construction of Modified Carbon Paste Electrodes for Determination of Tramadol in Very Trace Amounts. Al-Kitab J. Pure Sci. [Internet]. 2025 Jan. 11;9(1):91-102. DOI: https://doi.org/10.32441/kjps.09.01.p6.

Keywords: Tramadol, Nanosilica, Electrodes, Carbon Paste Electrodes.

Article History

Received	08 Aug.	2024
Accepted	17 Oct.	2024
Available online	11 Jan.	2025

Abstract:

This research includes estimating the drug (Tramadol Hydrochloride, TR) using the potentiometric method by constructing selective electrodes for TR drug with the active ingredient (Ammonium Reinackate, AR) using a plasticizer (Nitro benzene, NB) and adding nanomaterials (Multi wall carbon nanotube (MWCNT), Nanosilica) for carbon paste electrodes to increase selectivity and sensitivity towards the material to be estimated. The results showed that the manufactured electrodes were able to estimate tramadol hydrochloride in the pharmaceutical preparation (tramadol tablets) at very low concentrations (trace amounts**)** up to 5.0×10^{-6} M using the direct and standard methods and proved to have a wide linear range up to 1.0×10^{-8} - 1.0×10^{-2} M. The Nernstatine slope of the prepared TR-AR-NB electrodes is (58.027, 58.251, and 58.694 mV/decade) for Carbon Paste Electrodes (CPE), MCPE (MWCNTs) and MCPE (MWCNTs+ nanosilica), respectively. The lower detection limit (LDL) is 2.39×10^{-7} M for the CPE and 4.98×10^{-8} M for the MCPE (MWCNTs) and 4.7384×10^{-9} M for the electrode MCPE (MWCNTs+ nanosilica) which makes it eligible for the estimation of tramadol hydrochloride in very low concentrations. The study included measuring the selectivity of these electrodes with the presence of interferers where the values of $K_{i,j}^{pot}$ for all studied species were less than 1. The drug was identified in both urine and blood plasma, with a recovery of at least 99.309 for urine and 97.6593 for blood plasma.

Keywords: Carbon Paste Electrodes, Electrodes, Nanosilica, Tramadol.

بناء أقطاب عجينة الكربون المعدلة لتقدير الترامادول بكميات ضئيلة جداً

مثنى سعيد علي

قسم العلوم، كلية التربية الأساسية، جامعة ديالى، بعقوبة - العراق

basicsci18@uodiyala.edu.iq

الخلاصة:

يتضمن هذا البحث تقدير عقار (هيدروكلوريد الترامادول، TR) باستخدام الطريقة الجهدية من خلال بناء أقطاب انتقائية لعقار TR مع المادة الفعالة (ريناكيت الأمونيوم، AR) باستخدام مادة ملدنة (نيترو بنزين، NB) وإضافة مواد نانوية (أنابيب الكربون النانوية متعددة الجدران (MWCNT)، نانوسيليكا) لأقطاب عجينة الكربون لزيادة الانتقائية والحساسية تجاه المادة المراد تقديرها. أظهرت النتائج أن الأقطاب المصنعة كانت قادرة على تقدير الترامادول المستحضر الصيدلاني (أقراص الترامادول) عند تراكيز منخفضة للغاية (كميات ضئيلة) تصل إلى $5.0 \times 10^{-6} M$ باستخدام الطرق المباشرة والقياسية وأثبتت أن لها نطاق خطي واسع يصل إلى 1.0×10^{-2} M - 1.0×10^{-8}. إن الميل النيرنستي لأقطاب TR-AR-NB المحضرة هو (٥٨,٠٢٧ و ٥٨,٢٥١ و ٥٨,٦٩٤ ملي فولت / عقد) لأقطاب عجينة الكربون (CPE) و MCPE (MWCNTs) و MCPE (MWCNTs + نانوسيليكا) على التوالي. الحد الأدنى للكشف (LDL) هو 2.39×10^{-7} M لـ CPE و $4.98\times10^{-}$ 8M لـ MCPE (MWCNTs) و 4.7384×10^{-9}M للقطب MCPE (MWCNTs + nanosilica) مما يجعله مؤهلاً لتقدير هيدروكلوريد الترامادول في تركيزات منخفضة جدًا. تضمنت الدراسة قياس انتقائية هذه الأقطاب مع وجود متداخلات حيث كانت قيم Ki,jpot لجميع الأنواع المدروسة أقل من ١. باستخدام الطريقة المباشرة وطريقة الإضافة القياسية، تم تقدير العقار في كل من البول وبلازما الدم، مع استرداد لا يقل عن ٩٩,٣٠٩ للبول و ٩٧,٦٥٩٣ لبلازما الدم.

الكلمات المفتاحية: ترامادول، النانو سيليكا، ألاقطاب، قطب عجينة الكربون.

1. Introduction:

Tramadol (TR) is chemically (±)-*trans*-2-Dimethylaminomethyl-1-(3-methoxyphenyl) cyclohexanol hydrochloride. has a chemical structure shown in **Figure 1** **[1]**. For the temporary alleviation of acute pain, tramadol is utilized. It should only be utilized when non-opioid painkillers are either ineffective or do not assist the patient in regulating their pain **[2,3]**. This drug's content has been assessed using a variety of analytical techniques, including spectroscopy **[4-6]**, due to its medicinal relevance, HPLC **[7-9]**, voltmetery **[10]**, gas chromatography **[11]**, the colorimetric method **[12]**, LC-MS technique **[13]**, fluorometry **[14]**, A Screen-Printed Electrode **[15]** and Electrocatalytic Platform **[16]**. In the analysis procedures, the selective electrodes for ions approach is preferred over many spectrum methods because it is quick, has a broad linear range, is unaffected by the model's color, and is straightforward to set up and operate **[17]**. The goal of the current work is to create a modified electrode containing MWCNTs (MCPE), nanosilica, and unmodified electrodes (CPE) that can be used to assess TR

in pure, pharmaceutical, and biological forms with accuracy, sensitivity, and selectivity. The fundamental analytical parameters were computed and compared for each sensor. The formula for Tramadol hydrochloride is **[18]**.

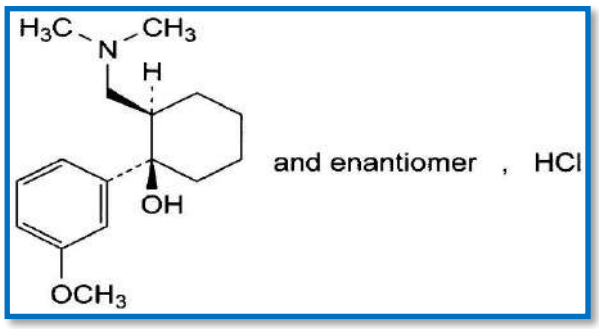

Figure 1: Chemical Structure of Tramadol

Its molecular weight is 299.8 g/mol and its formula is $C_{16}H_{25}NO_2$, HCl. It has the shape of a crystalline powder that is white or almost white. Extremely weakly soluble in acetone, yet freely soluble in water and methyl alcohol **[19].**

2. Material And Methods:

2.1 APPARATUS: Jenway 3310 pH Meter, HANNA Instruments pH Meter 211, calomel electrode Swiss source, JENWAY Hot Plate with Stirrer-Germany, C.H.N Perkin Elmer USA 2400 Series II element analyzer.

2.2 MATERIALS: The chemicals utilized were all very pure and were from Fluka, BDH, and SDI.

2.2.1 Preparation of Tramadol 100 mg/tablet solution: Ten tablets the average weight of one pill 3.941 g, made by the Dimedic Company in the UK, were crushed in an agate mortar to determine the average weight of a tablet. To obtain (1.0×10^{-2}) M, 1.1815 g of the pharmaceutical preparation was obtained and dissolved in 100 ml of deionized distilled water. Additional diluted solutions were prepared for each sample by appropriately diluting with deionized distilled water.

2.2.2 Biological fluid solutions 0.01 M AM: The lowest concentrations of the solutions were made by diluting the samples with deionized distilled water. 4.5 ml of human plasma or urine was obtained, and 0.5 ml of 0.1 M TR was added. The tube was then shaken for one minute.

2.2.3 Preparation of Interfering Solutions: Solutions of $(1.0\times10^{-3}$ M) were created by dissolving the required amounts of these compounds (NaBr, NaCl, $CaCl_2$, KCl, Na_2CO_3, Na_2SO_4, starch, glucose, fructose) in 100 ml of deionized distilled water in volumetric flasks.

2.3 Preparation of the ion-pair: The TR-AR ion-pair was prepared by mixing 10 ml of 0.1 M TR solution with 10 ml of 0.1 M AR solution to create a light red precipitate. The precipitate was then filtered, repeatedly washed with deionized water, and allowed to dry for a day at room temperature. **Table 1** displays the results of the CHN analysis of the TR-AR ion pair.

Table 1: Elemental Analysis for the TR-AR Ion Pair.

TR-AR			
Element	%C	%H	%N
Found	36.74	5.80	17.16
Calculated	36.71	5.85	17.13
Formula	$[C_{16}H_{25}NO_2Cl][C_4H_{10}CrN_7S_4].2H_2O$		

2.4 Preparation of the Electrodes

2.4.1 Construction of carbon and Modified carbon Paste Electrodes (CPE, MCPE): After conducting a number of pilot tests, the selective membrane was created by combining its constituent parts in accordance with weight ratios; the outcomes are displayed in **Table 2** The best electrode for TR-AR-NB CPE is electrode No. 2, the best electrode for CPE (MWCNTs) is electrode No. 5, and the best electrode for CPE (MWCNTs+ nanosilica) is electrode No. 8.

Table 2: Components and Characteristics of CPE and MCPE Electrodes.

CPE no.	Graphite powder (%)	NB (%)	TR-AR (%)	MWCNTs (%)	Nanosilica (%)	Slope $\frac{mV}{decade}$	Linear range $\frac{mol}{L}$	R^2
1	70	20	10	0	0	54.175	$5\times10^{-7}-1\times10^{-2}$	0.9891
2	**65**	**20**	**15**	**0**	**0**	**58.027**	$5\times10^{-7}-1\times10^{-2}$	**0.9999**
3	60	20	20	0	0	56.009	$5\times10^{-7}-1\times10^{-2}$	0.9911
4	62	20	15	3	0	57,208	$1\times10^{-7}-1\times10^{-2}$	0.9940
5	**60**	**20**	**15**	**5**	**0**	**58.251**	$1\times10^{-7}-1\times10^{-2}$	**0.9999**
6	58	20	15	7	0	57.444	$1\times10^{-7}-1\times10^{-2}$	0.9965
7	59	20	15	5	1	57.971	$1\times10^{-8}-1\times10^{-2}$	0.9980
8	**57**	**20**	**15**	**5**	**3**	**58.694**	$1\times10^{-8}-1\times10^{-2}$	**0.9999**
9	55	20	15	5	5	58.089	$1\times10^{-8}-1\times10^{-2}$	0.9975

3. Results and Discussion:

3.1. Effect of pH: It was established what pH range is ideal for maintaining a stable electrode potential. To do this, an electrode potential measurement was conducted in a TR solution (1.0×10-4) M, ranging in pH from 1 to 10. The pH was adjusted using solutions of NaOH and/or HCl. The link between the pH value of the solutions and the electrode potential for each electrode is shown in **Figure 2**. It is clear that the electrodes' pH range was wide (2–7).

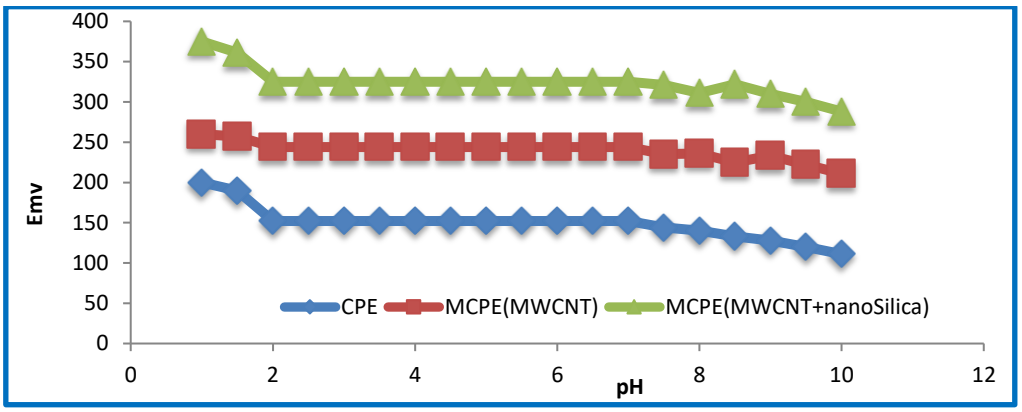

Figure 2: Effect of pH on the potential response of TR-AR-NB Electrodes

3.2. Effect of Temperature: The results in **Figure 3** showed that the ideal temperature for both CPE and MCPE (MWCNTs) electrodes is (10 – 60) °C, whereas the MCPE (MWCNTs+ nanosilica) electrode had a broader temperature range (10 – 70) °C. The results demonstrate all of the development electrodes are extremely thermally steady without noticeably changing their Nernstian slope. The potential change was observed for a concentration of (1×10^{-4}) M) TR solution by modifying the temperature of the solution compared to (5-85) oC.

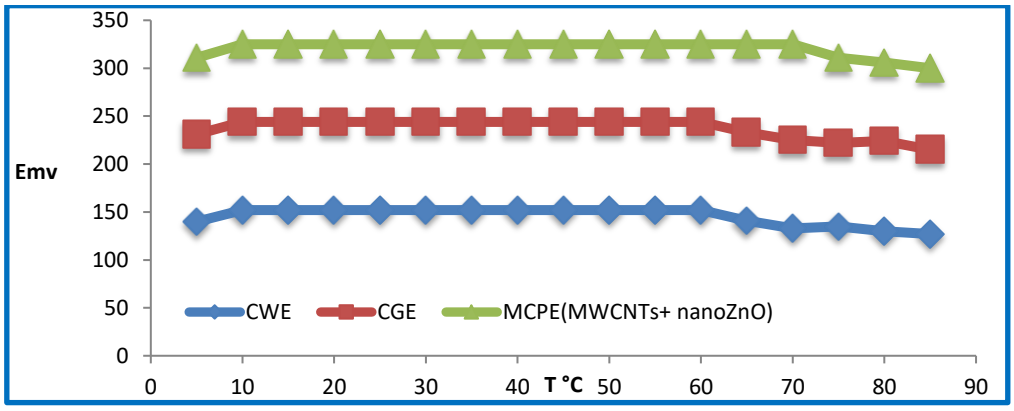

Figure 3: Effect of Temperature on the potential response of TR-AR-NB Electrodes

3.3. Calibration Curve and Detection Limit: Figure 4 displays the calibration curve that was created after several tests were conducted to determine the ideal pH and temperature. **Table 3** lists the electrode parameters. When it is evident that the electrode made with MCPE (MWCNTs+ nanosilica) is superior to the other electrodes in terms of benefits.

Table 3.: Analytical Characteristics of the Electrodes that Were Manufactured

Electrode type	Liner range M	Slope (mV decade^{-1})	Upper detection limit M (UDL)	Lower detection limit M (LDL)
MCPE (MWCNTs+ nanosilica)	1.0×10^{-8} - 1.0×10^{-2}	58.694	0.0201	4.7384×10^{-9}
MCPE (MWCNTs)	1.0×10^{-7} - 1.0×10^{-2}	58.251	0.0205	4.9827×10^{-8}
CPE	5.0×10^{-7} - 1.0×10^{-2}	58.027	0.0203	2.3920×10^{-7}

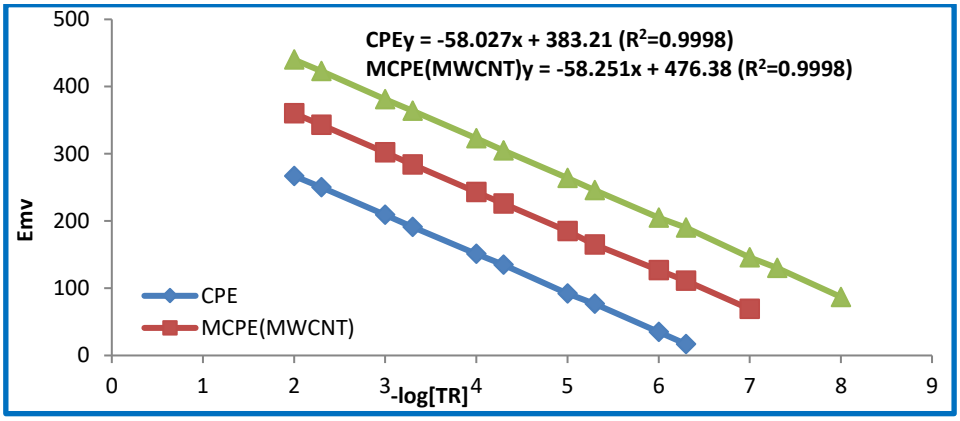

Figure 4: Calibration Curve of TR-AR-NB Electrodes.

3.4. Precision and accuracy: By measuring the potential of various drug concentrations within the linear range of the calibration curve for seven consecutive readings under ideal conditions, precision and accuracy were investigated. The results are displayed in **Table 4** and suggest that the set electrodes might be employed for determining the TR drug with precision as well as accuracy.

Table 4: Precision and accuracy of findings for TR-AR-NB electrodes.

Sample	Taken [TR] M	Found [TR] M	%Recovery	%RE
MCPE(MWCNT +nanosilica)	1×10^{-2}	9.9210×10^{-3}	**99.21**	-0.79
	1×10^{-3}	9.8026×10^{-4}	**98.02**	-1.97
	1×10^{-4}	1.0073×10^{-4}	**100.73**	-0.73
	1×10^{-5}	9.9530×10^{-6}	**99.53**	-0.46
	1×10^{-6}	9.8342×10^{-7}	**98.34**	-1.65
	1×10^{-7}	9.7169×10^{-8}	**97.16**	-2.83
	1×10^{-8}	9.6000×10^{-9}	**96.00**	-3.99
%Mean ± SD	98.4316 ± 1.5673			
N	7			
Variance	2.4564			
%RE	-1.5683			
%RSD	1.5922			
Sample	Taken [TR] M	Found [TR] M	%Recovery	%RE
MCPE (MWCNT)	1×10^{-2}	1.0048×10^{-2}	100.48	0.48
	1×10^{-3}	1.0148×10^{-3}	101.48	1.48
	1×10^{-4}	9.8524×10^{-5}	98.52	-1.47
	1×10^{-5}	9.9507×10^{-6}	99.50	-0.49
	1×10^{-6}	1.0049×10^{-6}	100.49	0.49
	1×10^{-7}	1.0150×10^{-7}	101.50	1.50
%Mean ± SD	**100.3335 ± 1.1571**			
n	**6**			
Variance	**1.3390**			
%RE	**0.3335**			
%RSD	**1.1533**			
Sample	Taken [TR] M	Found [TR] M	%Recovery	%RE
CPE	1×10^{-2}	9.9382×10^{-3}	99.38	-0.61
	1×10^{-3}	9.9489×10^{-4}	99.48	-0.51
	1×10^{-4}	9.9596×10^{-5}	99.59	-0.40
	1×10^{-5}	9.5824×10^{-6}	95.82	-4.17
	1×10^{-6}	9.9809×10^{-7}	99.80	-0.19
	5×10^{-7}	4.8862×10^{-7}	97.49	-2.50
%Mean ± SD	**98.5991 ± 1.5994**			
n	**6**			
Variance	**2.5583**			
%RE	**-1.4008**			
%RSD	**1.6222**			

3.5. Response Time: By submerging the electrode in ($1\times10^{(-6)}$-$1\times10^{(-2)}$M) drug solutions, monitoring the potential for each solution, and timing the electrode's reaction, the response time of the electrodes was examined. The response times of the created TR-AR-NB electrodes vary between 15–49 seconds, 20–53 seconds, and 23–55 seconds for MCPE(MWCNT+nanosilica), MCPE(MWCNT), and CPE electrodes, correspondingly, as can be seen from the data displayed in **Figure 5**.

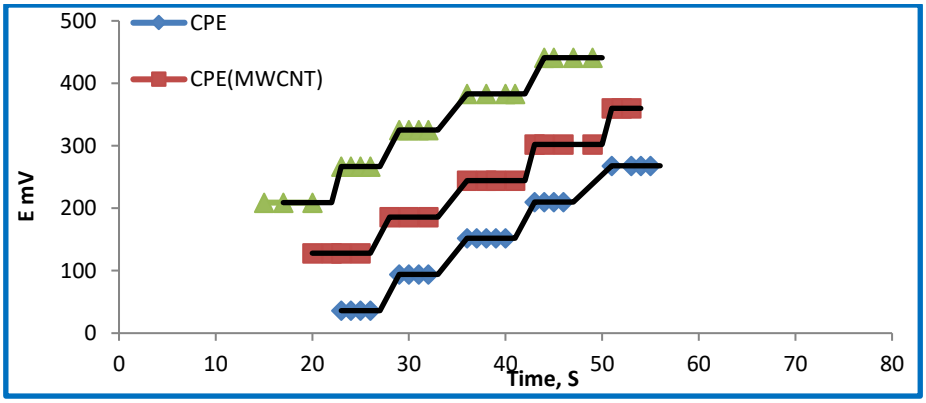

Figure 5: Response Time of TR-AR-NB Electrodes

3.6. Electrode Life Observation: By establishing the calibration curve for every single set electrode two or three times over the course of a week, the lifetime of the TR-AR-NB electrodes was estimated. For the MCPE(MWCNT+nanosilica), MCPE(MWCNT), and CPE electrodes, respectively, no aberration in the Nernstain slope was observed for 52 days, 65 days, and 70 days. The prepared electrode is kept dry between readings.

3.7. Selectivity: The method of separate solutions was used to evaluate the selectivity **[20]**. First, the drug solution's potential was checked at a concentration of 1×10^{-3} M with no interfering ion (Ei), and then the interfering ion solution's potential was observed at a concentration of 1×10^{-3} M alone (Ej). The chemicals and interfering ions used for this investigation did not appear to have any effect on the electrodes' excellent drug selectivity. According to **Table 5**, every selectivity coefficient value is lower than one.

Table 5.- Selectivity coefficient values.

the interfering ion M1 × 10^{-3}	Selectivity coefficient values $K_{i,j}^{pot}$		
	TR-AR-NB		
	CPE	MCPE(MWCNT)	MCPE(MWCNT+nanosilica)
Na^{1+}	7.15×10^{-1}	6.00×10^{-1}	5.39×10^{-1}
K^{1+}	6.11×10^{-1}	5.34×10^{-1}	4.00×10^{-1}
Ca^{2+}	8.70×10^{-2}	6.65×10^{-2}	3.79×10^{-2}
Cl^{1-}	8.59×10^{-2}	8.32×10^{-2}	7.81×10^{-2}
Br^{1-}	1.26×10^{-1}	9.75×10^{-2}	7.17×10^{-2}
CO_3^{1-}	5.98×10^{-2}	5.20×10^{-2}	5.00×10^{-2}
SO_4^{2-}	9.00×10^{-3}	3.90×10^{-2}	2.81×10^{-2}
Glucose	3.23×10^{-3}	2.22×10^{-3}	1.34×10^{-3}
Fructose	4.94×10^{-2}	4.11×10^{-2}	3.87×10^{-2}
Starch	2.90×10^{-2}	2.28×10^{-2}	1.99×10^{-2}

3.8. Ruggedness and Robustness: Using ethanol as a solvent for the making of drug solutions, the robustness of this method employing the TR-AR-NB electrodes for each kind was investigated. The reliability of such electrodes for the measurement of TR drugs can be seen in **Figure 6**. The Ruggedness of this study was conducted using another potentiometer (HANNA Instruments 211 pH Meter).

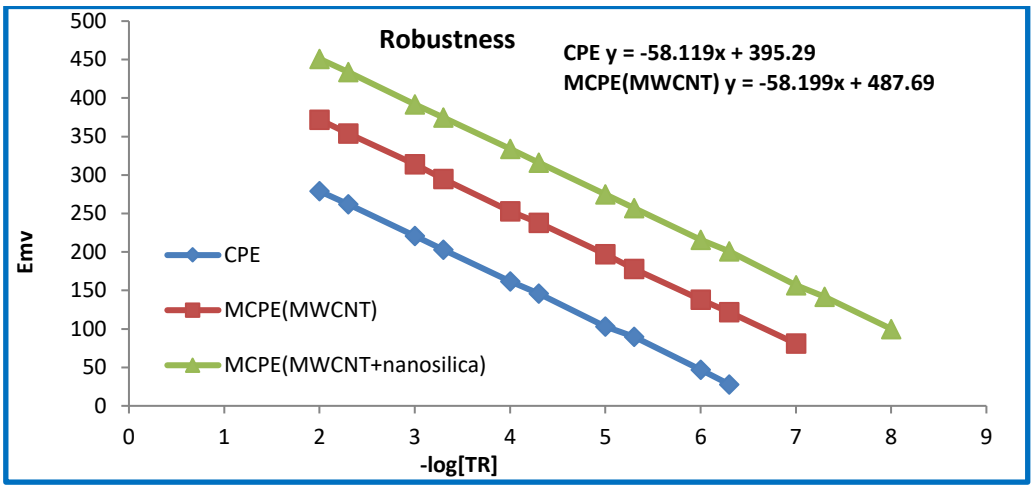

(a)

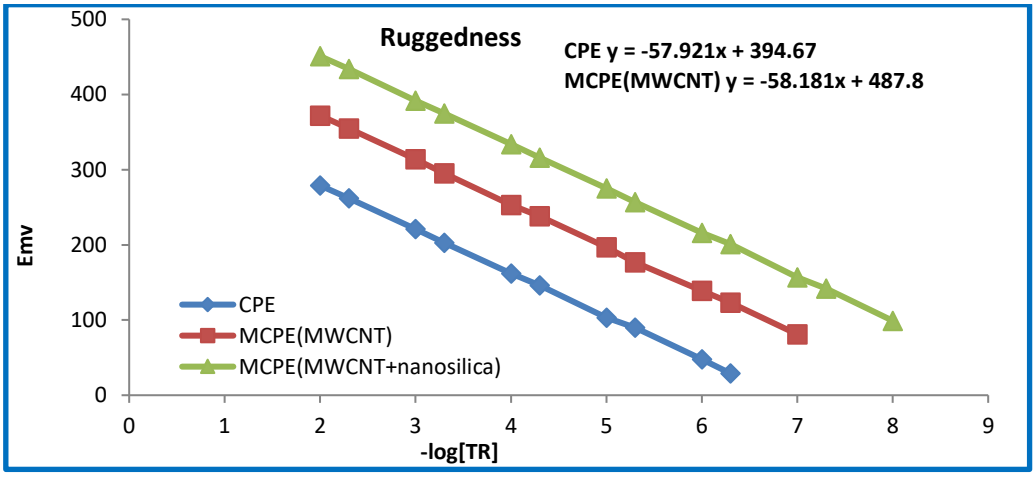

(b)

Figure 6: Robustness And Ruggedness of The TR-AR-NB Electrode-Based Analytical Technique.

3.9. Analytical Applications: Using the prepared TR-AR-NB electrodes, the TR drug was identified in the pharmaceutical composition, Tramadol tablets, and biological fluid by both direct and standard addition approaches. The results, which are displayed in **Table 6** and **Figure 7**, verify the high accuracy and precision of the assessment of AM drugs using the electrodes mentioned above.

Table 6: The direct and standard addition methods for assessing the drug.

Electrode	Taken [TR] M	Found [TR] M	%Recovery	%RSD	%RE
Direct method					
MCPE(MWCNT +nanosilica)	5×10^{-5} 5×10^{-6}	4.9715×10^{-5} 5.0095×10^{-6}	99.4314 100.1910	0.1293 0.1119	-0.56 0.19
MCPE(MWCNT)	5×10^{-5} 5×10^{-6}	5.0315×10^{-5} 5.0817×10^{-6}	100.632 101.635	0.4012 0.4979	0.63 1.63
CPE	5×10^{-5} 5×10^{-6}	5.0731×10^{-5} 4.8810×10^{-6}	101.462 97.619	0.7876 0.9933	1.462 -2.38
Standard addition method					
MCPE(MWCNT+ nanosilica)	2×10^{-4}	2.0253×10^{-4}	101.2660	1.9282	1.26
MCPE(MWCNT)	2×10^{-4}	2.0398×10^{-4}	101.9905	2.4325	1.99
CPE	2×10^{-4}	1.9843×10^{-4}	99.21558	3.8527	-0.78
Urine					
MCPE(MWCNT +nanosilica)	2×10^{-3}	1.9861×10^{-3}	99.3093	0.1371	**-0.69**
MCPE(MWCNT)	2×10^{-3}	2.0268×10^{-3}	101.3438	0.2969	1.34
CPE	2×10^{-3}	2.0322×10^{-3}	101.6125	0.3940	1.61
Plasma					
MCPE(MWCNT +nanosilica)	2×10^{-3}	2.0255×10^{-3}	101.2766	0.2094	1.27
MCPE(MWCNT)	2×10^{-3}	2.0109×10^{-3}	100.5458	0.0767	0.54
CPE	2×10^{-3}	1.9531×10^{-3}	97.6593	0.2798	-2.34

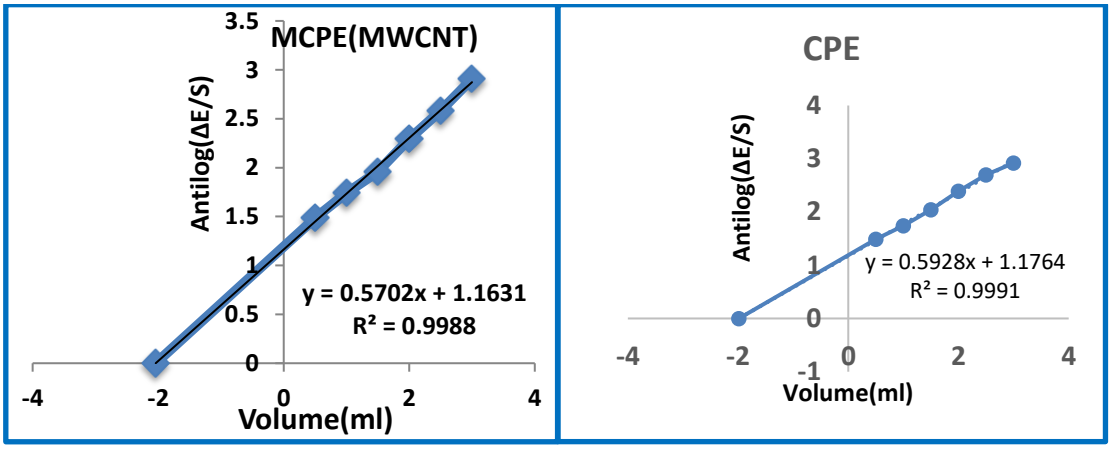

(a)

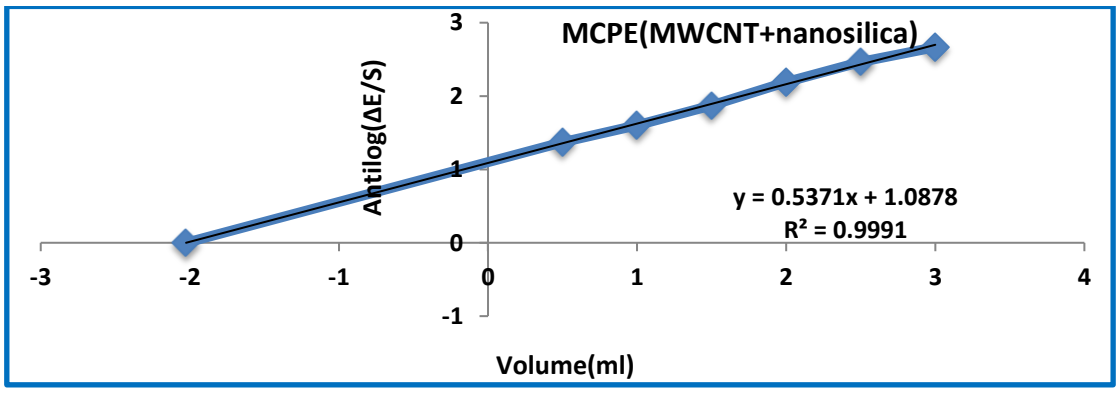

(b)

Figure 7: Standard addition curves of TR-AR-NB Electrodes.

3.10 Assessment of the net results: Using the t-test and F-test to assess the validity of employing the created electrodes to assess pharmaceutical preparations, the outcomes shown in (**Table 7** and **Table 8**) demonstrate that the developed electrodes were favorable and that there was absolutely no distinction between the recommended approach and the standard method.

Table 7: The F- And T-tests are Used to Evaluate the Results.

Electrode	%Mean ±SD	n	Calculated t-test	tabulated t-test for %95	Calculated F-test	tabulated F-test for %95
MCPE (MWCNT +nanosilica)	98.4317 ± 1.5673	7	1.7535	2.45	0.3818	4.53
MCPE(MWCNT)	100.3335 ± 1.1571	6	-1.0016	2.57	0.7005	5.19
CPE	98.5991 ±1.5994	6	1.1497	2.57	0.3666	5.19
Standard method* (HPLC)	100.85± 0.9685	5	0.00	0.00	0.00	0.00

* The HPLC technique for Wadi Al-Rafidain Pharmaceutical Industries according to the Constitution (USP41).

Table 8. Differentiation of the suggested tramadol electrodes with published electrodes.

Ref.	Slope $\frac{mV}{\text{decade}}$	Liner range M	LDL (M)
[21]	57.8	9.2×10^{-6} - 1.0×10^{-1}	6.2×10^{-6}
[22]	56.5	5.5×10^{-6} - 1.0×10^{-1}	1.8×10^{-6}
[22]	58.1	1.0×10^{-5} - 1.0×10^{-1}	1.0×10^{-5}
Present work			
CPE	58.027	5.0×10^{-7} - 1.0×10^{-2}	2.39×10^{-7}
MCPE(MWCNTs)	58.251	1.0×10^{-7} - 1.0×10^{-2}	4.98×10^{-8}
MCPE(MWCNTs+ nanosilica)	58.694	1.0×10^{-8} - 1.0×10^{-2}	4.7384×10^{-9}

4. Conclusions

When comparing the electrodes developed in this research with other previous electrodes, the modified carbon paste electrode parameters containing MWCNTs and nanosilica were superior and can be used to evaluate drugs such as tramadol in the field of forensic evidence because they have a very low detection limit of up to 4.7384×10^{-9} M. The integrated sensors have a very excellent slope, good recovery, wide pH range (2-7), very low detection limit, voltage balance, and high sensitivity. Assessing TR using the developed electrodes (CPE and MCPE) in biological fluids and pharmaceutical preparations at very low concentrations of up to 5×10^{-6} M. All the developed electrodes are suitable for application in the field of pharmacology, based on statistical analysis.

5. References

[1] Sweetman SC.Martindale: The complete drug reference (40th ed.). Pharmaceutical Press. London, 2020. p.130.

[2] Nakhaee S. et al. A review on tramadol toxicity: Mechanism of action, clinical presentation, and treatment. Forensic Toxicol. 2021;39:293–310. Available from: https:// doi. org/ 10. 1007/ s11419- 020- 00569-0.

[3] El-Ashmawy NE. et al. The plausible mechanisms of tramadol for treatment of COVID-19. Med. Hypotheses. 2021;146: Available from: https://doi. org/ 10. 1016/j. mehy. 2020. 110468.

[4] Akula G, Sapavatu SN, Jadi RK, Battineni JK & Boggula N. Analytical method development and validation for the estimation of tramadol in bulk and its formulations by UV-spectroscopy. J. Adv. Sci. Res. 2021;12:77–83.

[5] Ramadan HS, Abdel Salam RA, Hadad GM, Belal F, Salim MM. First derivative synchronous spectrofluorimetric method for the simultaneous determination of tramadol and celecoxib in their dosage forms and human plasma. Luminescence. 2024;39. Available from: https://doi.org/10.1002/bio.4774.

[6] Ramadan HS, Abdel Salam RA, Hadad GM, Belal F, Salim MM. Eco-friendly simultaneous multi-spectrophotometric estimation of the newly approved drug combination of celecoxib and tramadol hydrochloride tablets in its dosage form. Scientific Reports. 2023;13. Available from: https://doi.org/10.1038/s41598-023-38702-9.

[7] Soltani N, Habibollahi S, Salamat A. Application of oxidized multi-walled carbon nanotubes and zeolite nanoparticles for simultaneous preconcentration of codeine and tramadol in saliva prior to HPLC determination. J. of Chromatography B. 2023;1222. Available from: https://doi.org/10.1016/j.jchromb.2023.123693.

[8] YANG F, LI S, SHEN S, SU S, LI S, CHEN K, LU Z. HPLC-DAD Simultaneously Determining Tramadol, Fentanyl and Diphenoxylate in Seized Drugs. Forensic Science and Technology. 2022;47(2) :77–83. Available from: https://doi: 10.16467/j.1008-3650.2021.0138.

[9] Pereira FJ, Rodriguez-Cordero A, Lopez R, Robles LC & Aller AJ, Development and validation of an RP-HPLC-PDA method for determination of paracetamol, caffeine and tramadol hydrochloride in pharmaceutical formulations. Pharmaceuticals. 2021;14. Available from: https:// doi. org/ 10. 3390/ ph140 50466.

[10] Saichanapan J, Promsuwan K, Saisahas K, Soleh A, Chang KH, Abdullah AFL and Limbut W. Voltammetric Determination of Tramadol Using a Hierarchical Graphene Oxide Nanoplatelets Modified Electrode. *J. Electrochem. Soc.* 2021;168(11). Available from: DOI 10.1149/1945-7111/ac3529

[11] Nualdee K, Buain R, Janchawee B, Sukree W, Thammakhet-Buranachai C, Kanatharana P, Chaisiwamongkhol K, Prutipanlai S and Phonchai A. A stir bar sorptive extraction device coupled with a gas chromatography flame ionization detector for the determination of abused prescription drugs in lean cocktail samples**.j.** Analytical Methods**.** 2022;26. Available from: https://doi.org/10.1039/D2AY00603K.

[12] Thomas SP and Sankar HKN. A simple colorimetric method for estimation of tramadol hydrochloride in pure and tablet dosage forms. Indian J Pharmacol. 2016;48(5) :550–554. Available from: https://DOI: 10.4103/0253-7613.190746.

[13] Loh GOK, Wong EYL, Goh CZ, Tan YTF, Lee YL, Pang LH, Shahridzo SH, Damenthi N, Hermansyah A, Long CM, Peh KK. Simultaneous determination of tramadol and

paracetamol in human plasma using LC-MS/MS and application in bioequivalence study of -fixed-dose combination.J. Ann Med. 2023;55(2): Available from: doi: 10.1080/07853890.2023.2270502.

[14] Tolba MM & Salim MM, Inclusive study for segregation of two commonly used anticancer drugs with tramadol: Applying a green fluorimetric strategy to pharmaceutical dosage forms and human plasma. Microchem. J. 2021;162: Available from: https:// doi. org/ 10.1016/j. microc. 2020. 105859.

[15] Aflatoonian MR, Tajik S, Aflatoonian B, Beitollahi H, Zhang K, Le QV, Cha JH. Jang HW, Shokouhimehr M, Peng W. A Screen-Printed Electrode Modified With Graphene/Co_3O_4 Nanocomposite for Electrochemical Detection of Tramadol. Front. Chem. 2020;8: Available from: https://doi.org/10.3389/fchem.2020.562308.

[16] Ehirim TJ, Ozoemena OC, Mwonga PV, Haruna AB, Mofokeng TP, Wael KD and Ozoemena KI. Onion-like Carbons Provide a Favorable Electrocatalytic Platform for the Sensitive Detection of Tramadol Drug. ACS Omega. 2022;7(51) :47892–47905. Available from: https://doi.org/10.1021/acsomega.2c05722.

[17] Keresten VM, Popov AY, Mikhelson KN. Peculiarities of the potentiometric response of ISEs with membranes containing two neutral ionophores and an excess of ion-exchanger: Experiment and modeling. Sensors and Actuators B. 2024;417. Available from: https://doi.org/10.1016/j.snb.2024.136090.

[18] British pharmacopeia in CD-ROM", 9th Ed., by system simulation ltd., The stationary office, London, 2022:1827.

[19] U.S. pharmacopeia on CD-ROM", 44th Ed. NF 25, by system simulation ltd. The stationary office, America, 2021:1965.

[20] John Wiley &Sons, Ltd Florinel-Gabriel, B. Chemical Sensors and Biosensors Fundamentals and Application, United Kingdom: 2012: 165-216.

[21] Abu-Shawisha HM, Abu Ghalwab N, Zaggoutb FR, Saadehc SM, Al-Daloua AR and Abou Assid AA. Improved determination of tramadol hydrochloride in biological fluids and pharmaceutical preparations utilizing a modified carbon paste electrode., Biochemical Engineering Journal 2010;48:237–245. Available from: doi:10.1016/j.bej.2009.10.019.

[22] Ganjali MR, Razavi T, Faridbod F, Riahi S, Norouzi P, Application of a new tramadol potentiometric membrane sensor as a useful device for tramadol hydrochloride analysis in Pharmaceutical formulation and urine, Curr. Pharm. Anal. 2009;5 :28–33. Available from: https://doi.org/10.2174/157341209787314972.

Al-Kitab Journal for Pure Sciences (2025); 9(1):103-116.
https://doi.org/10.32441/kjps.09.01.p7

Al-Kitab Journal for Pure Sciences
ISSN: 2617-1260 (print), 2617-8141(online)

https://isnra.net/index.php/kjps

Isolation and Identification of Fungal Species Contaminating the Refrigerators

Hiba Hadi Taha*, Faten Noori Mula Abed, Jehaan Mowfak Al-Rawi

Department of Biology, College of Science, University of Mosul, Iraq.

*Corresponding author: hibahadi@uomosul.edu.iq

Citation: Taha HH, Abed FNM, Al-Rawi JM. Isolation and Identification of Fungal Species Contaminating the Refrigerators. Al-Kitab J. Pure Sci. [Internet]. 2025 Jan. 13 ;09(01):103-116. Doi: https://doi.org/10.32441/kjps.09.01.p7.

Keywords: Fungal Contamination, Refrigerator, Fungi, Food Spoilage, PCR.

Article History

Received	15 Jul.	2024
Accepted	31 Aug.	2024
Available online	13 Jan.	2025

Abstract:

Refrigeration is one of the most widely used methods to control the growth of microorganisms in food products. A number of isolates was 433, including 363 isolates from refrigeration and 70 isolates from freezers. The fungus *Cladosporium* sp. is the large number in both refrigeration and freezer, 187 and 28, respectively, and the lowest numbers of fungi such as *Rhizopus stolonifer*, *Rhizoctonia solani*, and *Fusarium* sp., many fungi were isolated from refrigeration, while fungal isolates from freezing were less numerous and less diverse. Molecular identification of *Cladosporium* sp. because it is the most frequent among the fungal isolated from refrigeration and freezing by using polymerase chain reaction, it has been shown that *Cladosporium sphaerospermum* strain HKA in the gene bank. The aim of the study is to recognize the fungi that contaminate the refrigerator both domestically and commercially.

Keywords: Fungal Contamination, Refrigerator, Fungi, Food Spoilage, PCR.

عزل وتشخيص أنواع الفطريات الملوثة للثلاجات

هبة هادي طه، فاتن نوري ملا عبد، جهان موفق الراوي

جامعة الموصل، كلية العلوم، قسم علوم الحياة

jehsbio88@uomosul.edu.iq fatinnuri@uomosul.edu.iq hibahadi@uomosul.edu.iq

الخلاصة:

يُعد التبريد أحد اكثر الطرق المستخدمة على نطاق واسع للتحكم في نمو الكائنات الحية الدقيقة في الأغذية . تضمنت الدراسة الحالية جمع ٢٠ عينة من الثلاجات وعزل العديد من الفطريات وكان عدد العزلات ٤٣٣ عزلة منها ٣٦٣ عزلة من التبريد و٧٠ عزلة من التجميد وظهر الفطر *Cladosporium* sp. بأعداد كبيرة في كلا التبريد والتجميد ١٨٧ و٢٨ على التوالي واقل أعداد كانت للفطريات *Rhizopus stolonifer* ، *Rhizoctonia solani* و *Fusarium* sp. وان العديد من العزلات الفطرية عزلت من التبريد بينما العزلات من التجميد اقل عدد واقل تنوعا ، كما شخصت عينة فطر *Cladosporium* جزيئيا لأنه الفطر الاكثر ترددا من بين العزلات الفطرية المعزولة من التبريد والتجميد باستخدام تفاعل البلمرة المتسلسل وتبيّن أنها *Cladosporium sphaerospermum* strain HKA والمسجلة في بنك الجينات العالمي.

الهدف من الدراسة : التعرف على الأنواع الفطرية الملوثة للثلاجات المنزلية والتجارية .

الكلمات المفتاحية: الفطريات الملوثة، الثلاجات، الفطريات، التعفن الفطري، تقنية تفاعل البلمرة المتسلسل.

1. Introduction:

People in the world are suffering from health problems related to consumption of the contaminated food every year this is one of the problems of the health of our day, many species of microorganisms can be present in food such as bacteria, fungi" yeasts, and molds" the fungi were considered important source causes of the contamination with spoilage of food, fungi damage food by different of food appearance and texture. As well as secreting mycotoxin and consequently the health of consumers for endangering [1]. Refrigeration is one of the most widely used methods to control the growth of microorganisms in food products [2]. Refrigeration is used to the control of rate some enzymes and chemical reactions and also the rate of microorganisms, growth in the food [3]. Studies have shown that food is damaged even in the temperature of the refrigerator because the microorganisms secrete enzymes and oxidation reactions, the type of container or packaging material in which the food is stored and the time of storage also the type of microbial, resulting in food poisoning and damage it while refrigerated [4]. Also, the freezing doesn't prevent the

reproduction of microorganisms [5]. In the presence of nutritious materials, humidity, and appropriate temperatures, increase the growth, leading to food-borne diseases. Microorganisms come from unclean and raw nutrients with unclean surfaces this container directly causes pollution to the other food storage and contamination of inter surface of the refrigerator, which causes indirect food pollution through preparation later [6]. Refrigerated foods can become vectors of disease through contamination with pathogens and microorganisms in markets, through storage, or in consumers' homes [7]. Different foods require different places and temperatures for storage, for example, fresh meat, fish, and poultry are stored in cold storage places, such as freezers, and in containers with ice, as they do with fish sold in markets, but fruits and vegetables are stored in cool places or m, refrigeration [8]. Fungi causes spoilage in foods more than bacteria in refrigerator when humidity and acidity are low and packaging conditions are suitable for their growth, also fungi isolated from fresh refrigerated animal products, fruits, vegetables, and prepared foods to eat [9]. Filamentous fungi produce spores that spread in refrigerators when conditions are favorable, damage food because yeast breaks sugar into Co_2 with alcohol and this causes low quality of the nutrient product [10], [11] fungal spores spread by "air, container, improper packaging, hands, and contaminated food", studies on the isolated filamentous fungi from nutrient materials such as "*Alternaria, Aspergillus, Botrytistis, Cladosporium, Fusarium, Geotrichum, Aureobasidium, Trichothecium, Mortierella, Mucor, Neurospora, Penicillium, Rhizopus, Thamnidium, Manoscus* and among the yeast genera involved *Candida, Cryptococcus, Rhodotorula, Schizosaccharomyces, Trichosporon*" ; however, this fungi is often present in (meat and poultry) but it is also found in many other nutrient products [12]. The harmful effects of fungi are not limited to the spoilage of food only, but they are also harmful to human health and animals, as they secrete toxic metabolites for example, some species of the *Aspergillus* spp. secrete aflatoxin, fungi such as *Cladosporium* cause problems for humans, as it may cause skin and toenail infections, the lung diseases including "nasal congestion, sneezing, coughing, and itchy eyes" *Cladosporium* spores cause airborne allergy and another disease of the respiratory tract, moreover, the mycotoxins which are produced by *Cladosporium* may also make volatile organic compounds (VOCs) related to smells [13].

2. Materials and methods:

Collecting the samples: 20 samples were collected from domestic and commercial refrigerators (refrigeration 4°C and freezing 0°C) from Mosul city from October to December and directly cultured on media.

Prepare medium: Potato Dextrose Agar (PDA) medium was prepared according to the supplying company, United Kingdom-Lab M. Limited, and its pH was adjusted, and then sterilized according to the optimal conditions by placing it in the autoclave (121˚C with pressure 1 atmosphere, for 20 minutes), while the antibiotic was added to the sterile medium cooled to (45-50˚C) after sterilizing it using fine membrane filters (0.22) millimicrons.

Isolation of fungi: Fungi were isolated by using sterile swabs moistened with sterile distilled water, and the PDA medium was inoculated in Petri dishes, with the antibiotic Amoxillin at 100 micrograms/ml, by streaking on the surface of the medium, and then the dishes were incubated at 25˚C for 7 days until fungal colonies appeared, [1]. The percentage of fungal frequency was calculated by the following formula:

$$\text{Frequency percentage} = \frac{\text{Number of colonies}}{\text{Total number of colonies}} \times 100$$

Diagnosis of fungi: The fungi were isolated and diagnosed by taking a part of the fungal colonies after purifying them from the edges of the colony using a method Hyphal tip technique and placing it on a slide with a drop of water in it, then putting the cover slide and it was examined with an optical microscope at 10X and 40X power, according to the shape of the mycelium and conidia, the isolated fungi were diagnosed based on the taxonomic keys of the genus [14]. To the species based on [15], [16], [17]. As well as diagnosing *Aspergillus* to different species according to the taxonomic key by [18], as the following:

1- Growth on Malt Extract Agar medium (MEA) incubated at 25 and 37°C for seven days.
2- Growth on Czapek Yeast Extract Agar medium (CYA) incubated at 25 and 37 °C for seven days.
3- Growth on Glycerol Nitrate Agar medium (G25%N at 25 and 37 °C for seven days.

Transferred discs from fungal colony with 6 mm were using a cork borer under sterile conditions, 3 replicates for each fungus, fungi were also diagnosed *Fusarium* sp. by growing it on a PDA medium according to the taxonomic key Pitt and Hocking (2009).

Molecular diagnosis (DNA extraction): The extraction equipment was used, DNA Geneaid™ according to company instructions in the United States of America. DNA bands are detected by using red safe dye, which is a safe and very sensitive dye for DNA, as an alternative to ethidium bromide dye, which is considered a strong mutagenic agent, as it gives green fluorescence when it binds to DNA [19].

Polymerase chain reaction (PCR): This method was used to detect the gene (*ITS*) Internal Transcribed Spacer, the *ITS* area is the DNA spacer between the small subunit genes of rRNA and genes rRNA with large subunits in the chromosome, it has been used to diagnose fungi and study their molecular evolution for more than twenty years **[20]**.

The Primers used in the study: Two types of specialized primers are *ITS1* the reaction primer and *ITS4* the reverse reaction primer as shown in **Table 1.**

Table 1: Gene-Specific Primers were Chosen *ITS* from (Korean Macro Gene) Company

Name and type primer	Sequence of nitrogenous bases
ITS1(Forward)	5' TCCGTAGGTGAACCTGCGG 3'
ITS4(Reverse)	5' TCCTCCGCTTATTGATATGC 3

Preparation of agarose gel: Prepare agarose gel by dissolving 2 g from agarose in 100 ml of (Tris-Borate-EDTA solution) previously prepared and warmed until boiling then left cool at 45-50°C and gel was poured gently so as to leave no air bubbles and left to cool for thirty minutes. A Comb was then gently isolated from agarose after it had been solid. Plate was fixed on the holder in the horizontal of electrophoresis and then filled the tank with TBE insulating material that covers the surface of the gel **[21]**.

Electrophoresis on agarose gel: Electrophoresis was performed to determine the size of the DNA bands, and to confirm its purity and concentration after extraction. Mix 3 µicroleter from loading solution (Intron /China) with 5 µicroleter from extracted DNA, which is bound with the loading dye, and load the mixture directly into the holes of gel and expose it to electric current at 7v/cm^2 with 1-2 hours until the DNA sample reach to the other side from gel, then gel was exposed to an UltraViolet Transilluminater source at a wavelength of 336 nanometers after placing gel in a water bath with the presence of 30 µicroleter from red safe dye and 500 ml from D.W. then the gel was photographed by using a digital camera to show the bands.

Optimal conditions for the PCR technique: The polymerase chain reaction technique according to the conditions is shown in **Table 2**.

Table 2: Optimal Conditions for Polymerase Chain Reaction Technique [22]

T	Steps	Temperature (°C)	*Duration*	Number of courses
1	Primary denaturation of DNA	95	5 minutes	One cycle
2	Secondary denaturation of DNA	95	30 seconds	35 cycles
3	Annealing process	55	1 minute	
4	First elongation process	72	1 minute	
5	Final elongation process	72	6 minutes	One cycle

Polymerase chain reaction products are sent to the Psomagene sequencing company (USA) to obtain the genetic sequence.

3. Results:

Isolation and diagnosis of fungi: Many fungi were isolated, and the number of isolates was 433, including 363 isolates from refrigeration and 70 isolates from freezers, as shown in **Table 3**.

4. Discussion

Fungi were diagnosed based on phenotypic characteristics as in **Figure 1**, and microscopic characteristics and compared with taxonomic keys, fungi within the genus *Aspergillus* it was diagnosed based on the diameter and color of the colony after growing it on three types of media, also diagnosing fungi within the genus *Fusarium* by comparing them with their taxonomic key, based on the shape of the large and small conidia and the color of the colony after growing it on medium PDA as shown in **Figure 2.**

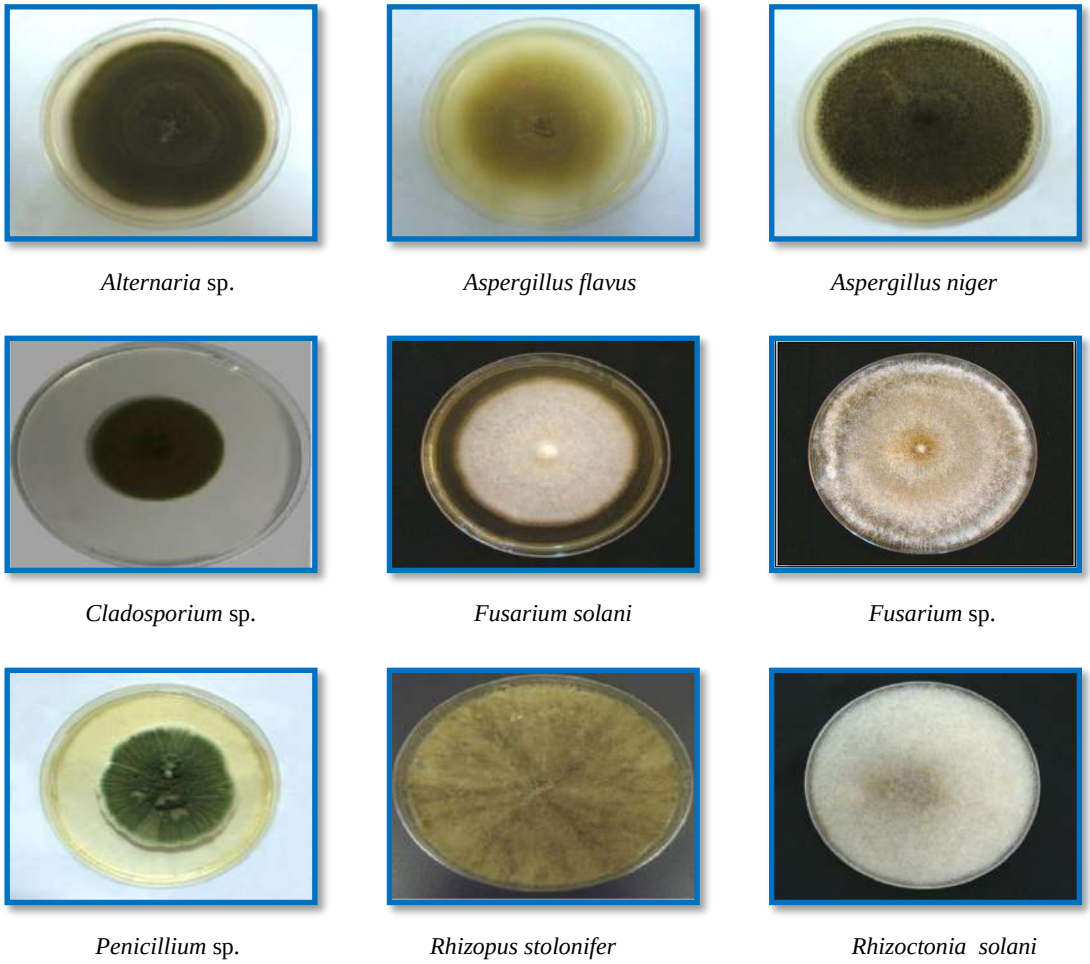

Figure 1: Phenotypic Characteristics of Fungi Isolated on PDA Medium

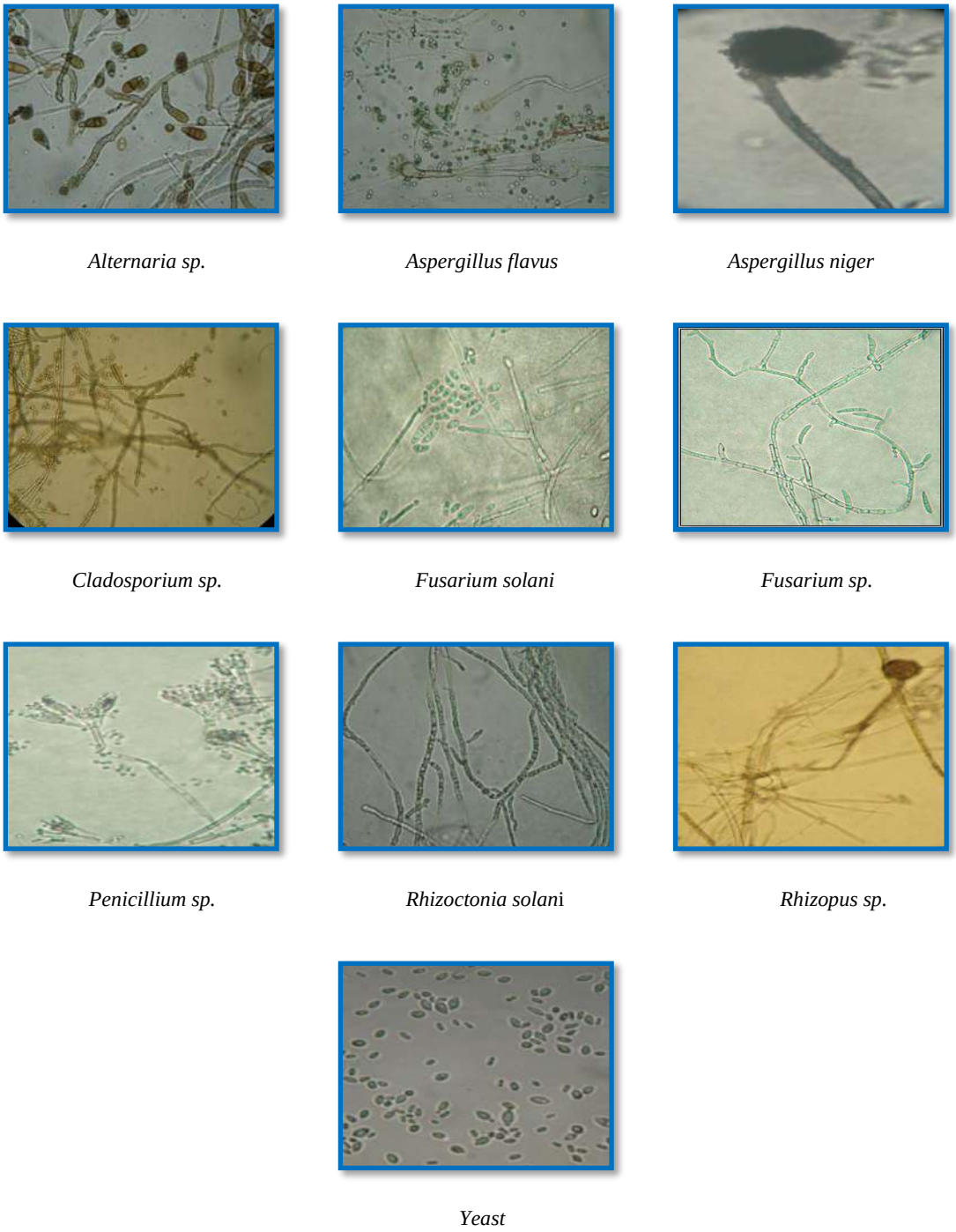

Figure (2) Microscopic diagnosis of fungi using an optical microscope at 40X

Cladosporium sp. appeared In large numbers in both refrigeration and freezers 187 and 28 respectively, followed by *Penicillium* sp. with numbers of 70 and 22, respectively, this is consistent with previous studies such as [23], [24]. The lowest numbers of fungi were *Rhizopus stolonifer*, *Rhizoctonia solani*, and *Fusarium sp*. Many fungi were isolated from refrigeration, while isolates from freezing were fewer in number and less diverse. There were fungal genera that were common in isolation from refrigeration and freezing, while there were fungal genera that appeared in

refrigeration only, such as *Aspergillus flavus*, *Alternaria* sp., *Rhizopus stolonifer*, *Rhizoctonia solani*, and *Fusarium* sp. as shown in **Table 3**.

Table 3: Number of fungi isolated from refrigeration and frozen stored food

Isolated fungi	Refrigeration	Freezing
Alternaria sp.	12	----
Aspergillus flavus	2	----
Aspergillus niger	42	14
Cladosporium sp.	187	28
Fusarium solani	4	2
Fusarium sp.	1	----
Penicillium sp.	70	22
Rhizoctonia solani	1	----
Rhizopus stolonifer	1	----
Yeast	43	4
The Total	363	70

The percentage frequency of fungi was calculated, and the highest percentage was the *Cladosporium* refrigeration, it reached 43.2% and after frozen it was about 6.5%, followed by *Penicillium* sp. which reached 16.2% and 5.1%, respectively, and the lowest percentage was for *Rhizopus stolonifer*, *Rhizoctonia* sp., and *Fusarium sp*. which reached 0.2% which was isolated from refrigeration only, as shown in **Table 4**.

Table 4: Percentage Frequency of Isolated Fungi

Isolated fungi	Refrigeration %	Freezing %
Alternaria sp.	2.8	----
Aspergillus flavus	0.5	----
Aspergillus niger	9.7	3.2
Cladosporium sp.	43.2	6.5
Fusarium solani	0.9	0.5
Fusarium sp.	0.2	----
Penicillium sp.	16.2	5.1
Rhizoctonia solani	0.2	----
Rhizopus sp.	0.2	----
Yeast	9.9	0.9
The Total	100	

The percentage frequency of all fungi in refrigeration appeared to be higher than the percentage in freezing, also there is an increase in fungal diversity in refrigeration compared with freezing, which was fewer in number and types of fungi, and thus is consistent with the study [1]. This might be due to high temperatures leading to an increase in the growth and number of microbes [25]. Food-borne diseases are caused by improper storage and unregularly cleaning the refrigerator might increase the risk of infection [26]. Fungi spread in the refrigerator from many sources such as unclean hands, unclean surfaces of the refrigerator, less cleaning of uncooked materials and some material leaks with not good packing such as meat, eggs, and milk, as well as leaving the refrigerator door open and alternative temperature, not washed vegetables and fruits. The refrigerator can contaminate other food items [6]. The current study indicates that the highest percentage of *Cladosporium* followed by *Penicillium* sp. Thus, it matches with many studies, as reports indicate that these two fungi are always found on the sides of the refrigerator and that they can live and reproduce in low temperatures [27]. These fungi produce black spots on the surface of (meat and fatty tissue) in the refrigerator, also producing mycotoxins for several reasons, such as not good packaging of food items [28]. These toxins may cause food toxicity and cancer to humans, such as aflatoxin secreted by *Aspergillus* sp., there are other toxins, such as ochratoxin and zearalenone, which have various harmful effects on the consumer, such as poor digestion, mutagenic effects, or neurological or immune damage [1]. *Cladosporium* also causes spoilage to fatty and butter and causes spoilage of many fruits with production of toxins and causes black spots on the meat [29]. One of the most important causes of contamination may be a continuous opening of the refrigerator door, consequently increasing internal temperature and allowing the entry of contaminated fungal spores, pathogens present in the refrigerator can contaminate food directly or indirectly this dangerous to the health of the consumer in terms of food poisoning even at appropriate storage temperatures [6]. This is because fungi grow well in an environment that contains food with moisture [30]. Fungal growth in refrigerated foods depends on several factors, including temperature, storage time, moisture content, and carbohydrate concentration in the food source [31].

Molecular identification of *Cladosporium* with PCR technique: After examination bands under ultraviolet source it was found that each isolate contained single band with undispersed, and this is evidence of the purity of the DNA and its high concentration. The amplification results after electrophoresis on a 2% agarose gel that the resulting bands were 600 base pairs in size, as shown in **Figure 3**.

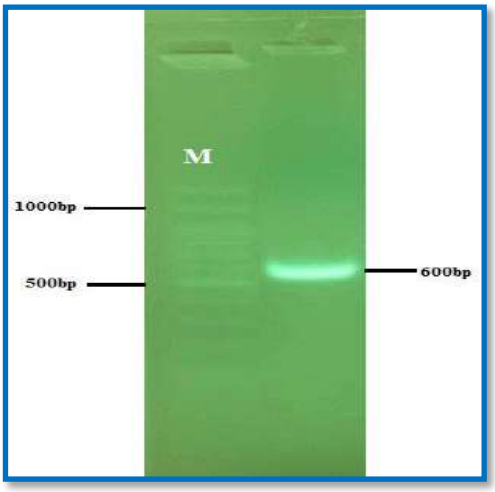

Figure 3: Electrophoresis of amplification products PCR for *Cladosporium* using 2% agarose gel at 5 V/cm^2, at an hour and using 1xTBE, the band size is 600 base pairs. **M:** DNA Ladder 1kb

Results of a study of the sequence nitrogenous bases: Polymerase chain reaction products are sent to the Psomagene sequencing company (USA) to determine and know the sequence of nitrogenous bases and compare with the gene sequence *ITS* storage within the World Gene Bank NCBI. The results showed a match rate of 99.22%, and the presence of site variation in the gene sequence in four locations, as shown in **Figure 4**. Perhaps this variation is due to point mutations that occur spontaneously in nature and include a series of changes in the sequence of nitrogenous bases in the DNA **[32]**.

Cladosporium sphaerospermum isolate 152 internal transcribed spacer 1, partial sequence; 5.8S ribosomal RNA gene and internal transcribed spacer 2, complete sequence; and 28S ribosomal RNA gene, partial sequence

Sequence ID: KP794112.1 Length: 509 Number of Matches: 2

Range 1: 4 to 509 GenBank Graphics ▼ Next Match ▲ Previous Match

Score	Expect	Identities	Gaps	Strand
917 bits(496)	0.0	502/506(99%)	0/506(0%)	Plus/Plus

```
Query  1    TCGGGCCGGGATGTTCACAACCCTTTGTTGTCCGACTCTGTTGCCTCCGGGGGCGACCCTG  60
            ||||||||||||||||||||||||||||||||||||||||||||||||||||||||||||
Sbjct  4    TCGGGCCGGGATGTTCACAACCCTTTGTTGTCCGACTCTGTTGCCTCCGGGGGCGACCCTG  63

Query  61   CCTCCGGGCGGGGGCCCCGGGTGGACATTTCAAACTCTTGCGTAACTTTGCAGTCTGAGT  120
            ||||||||||||||||||||||||||||||||||||||||||||||||||||||||||||
Sbjct  64   CCTCCGGGCGGGGGCCCCGGGTGGACATTTCAAACTCTTGCGTAACTTTGCAGTCTGAGT  123

Query  121  AAATTTAATTAATAAATTAAAACTTTCAACAACGGATCTCTTGGTTCTGGCATCGATGAA  180
            ||||||||||||||||||||||||||||||||||||||||||||||||||||||||||||
Sbjct  124  AAATTTAATTAATAAATTAAAACTTTCAACAACGGATCTCTTGGTTCTGGCATCGATGAA  183

Query  181  GAACGCAGCGAAATGCGATAAGTAATGTGAATTGCAGAATTCAGTGAATCATCGAATCTT  240
            ||||||||||||||||||||||||||||||||||||||||||||||||||||||||||||
Sbjct  184  GAACGCAGCGAAATGCGATAAGTAATGTGAATTGCAGAATTCAGTGAATCATCGAATCTT  243

Query  241  TGAACGCACATTGCGCCCCCTGGTATTCCGGGGGGCATGCCTGTTCGAGCGTCATTTCAC  300
            ||||||||||||||||||||||||||||||||||||||||||||||||||||||||||||
Sbjct  244  TGAACGCACATTGCGCCCCCTGGTATTCCGGGGGGCATGCCTGTTCGAGCGTCATTTCAC  303

Query  301  CACTCAAGCCTCGCTTGGTATTGGGCGACGCGGTCCGCCGCGCGCCTCAAATCGACCGGC  360
            ||||||||||||||||||||||||||||||||||||||||||||||||||||||||||||
Sbjct  304  CACTCAAGCCTCGCTTGGTATTGGGCGACGCGGTCCGCCGCGCGCCTCAAATCGACCGGC  363

Query  361  TGGGTCTTTCGTCCCCTCAGCGTTGTGGAAACTATTCGCTAAAGGGTGCCGCGGGAGGCC  420
            ||||||||||||||||||||||||||||||||||||||||||||||||||||||||||||
Sbjct  364  TGGGTCTTTCGTCCCCTCAGCGTTGTGGAAACTATTCGCTAAAGGGTGCCGCGGGAGGCC  423

Query  421  ACGCCGTAAAACAACCCCATTTCTAAGGTTGACCTCGGATCAGGTAGGGATACCCGCTGA  480
            ||||||||||||||||||||||||||||||||||||||||||||||||||||||||||||
Sbjct  424  ACGCCGTAAAACAACCCCATTTCTAAGGTTGACCTCGGATCAGGTAGGGATACCCGCTGA  483

Query  481  ACTTAAGCATATANANAAGGGGGGAA  506
            |||||||||||  | ||| ||||||
Sbjct  484  ACTTAAGCATATCAATAAGCGGGGAA  509
```

Figure 4: Sequence of Nitrogenous Bases of Cladosporium Sphaerospermum Strain HKA for Genes ITS1, ITS4

Figure 5: Recording the Cladosporium Sphaerospermum Strainhka in The Gene Bank

Cladosporium sp. is diagnosed because it is the most frequent among the fungi isolated from refrigeration and freezing by using polymerase chain reaction, it has been shown that it is *Cladosporium sphaerospermum* the isolate was reported in GenBank by nameHKA as shown in **Figure 5**. After examination of bands under an ultraviolet source, it was found that each isolate contained a single band undispersed, and this is evidence of the purity of the DNA and its high concentration

5. Conclusion

We conclude from the current study that the fungus *Cladosporium sphaerospermum* appeared in large numbers in both refrigeration and freezing and that fungal isolates were more numerous

and diverse from refrigeration compared with freezing, as they were less in number and diversity. and the lowest numbers of fungi such as Rhizopus stolonifer, Rhizoctonia solani and Fusarium sp. Molecular identification of Cladosporium sp. by using PCR, it has been shown that Cladosporium sphaerospermum strain HKA in the gene bank.

6. References

[1] Fazelipour M., Neisi A., Alizadehattar S., and Kiasat, N. Isolation and Identification of Psychotropic fungal contamination in food storage refrigerators in Ahvaz City Restaurants.Jun. J. Heal. Sci.2020;12(2):100866.

[2] Ye K. ,Wang J.,HanY.,Wang C., Qi C. , and Ge X. Investigation on microbial contamination in the cold storage room of domestic refrigerators .Food Con.2019; 6 (99):64-67.

[3] Scott E., Bloomfield S.F., and Barlow C.G. An investigation of microbial contamination in the home. J. of Hyg.1982; 89,279-293.

[4] Kaur G. , Sandhu P. , and Sidhu M. Microbial analysis of commonly stored food items in household refrigerators in selected containers. J. hum. Ecol.2013; 42(2): 151-155.

[5] Adebayo C.O. , Aderiye B.I., and Akpor O.B. Assessment of bacterial and fungal spoilage of some Nigeria fermented and unfermented foods. Afr. J. of Food sci. 2014; 8(3):140-147.

[6] Otu-Bassey I.B. , Ewaoche I.S., Okon B.F. , and Ibor U.A. Microbial Contamination of Household Refrigerators in Calabar Metropolis-Nigeria. Amer. J. of Epidemiol. and Inf. dis.2017;5(1): 1-7. doi:10.12691/ajeid-5-1-1.

[7] Kosa K.M. , Cates C. S., Karnes S. , Godwin S. L., and Chambers D. Consumer home refrigeration practices: Results of a web-based survey. J. of Food Protect.2007; 70: 1640-1649.

[8] Prescott L. M., Harley P. J., and Klein A. D. Microbiology. 6th edition, McGraw Hill Publishers, New York, 2005 .

[9] Lalitha C., Krishna ,V.S., and Visakhapatnam P. A. Contamination of refrigerator is a threat for infections.Int. J.of Advance Res.2019;2 (5):1514-1517.

[10] Barth M.,Hankinson T.R., Zhuang H.,and Breidt F. Microbiological spoilage of fruitsand vegetables. Compendium of the microbiological spoilage of foods and beverages. Spr.2009; p. 135–83.

[11] Oluwaseun O.J., Oluwatosin O.L., and Oluwasoga F.A . Microbial Analysis of Processed Foods Stored in Domestic Refrigerators of Selected Eateries in Ile-Ife, Osun State, Nigeria .Amer. J. of Biosci. and Bioeng.2018;6(3): 21-26.doi: 10.11648/j.bio.20180603.11.

[12]Maila S.,Richard H.O., Olabode K.,and Osanupin R. Isolation and identification of fungi associated with spoilt fruits vended in Gwagwalada market, Abuja, Nigeria. Vet. World .2017;10(4):393.

[13] Samuel O. Ifeanyi O. ,and Ugochukwu O. Filamentous fungi associated with the spoilage of post-harvest sweet orange fruits (Citrussinensis) sold in Awka major markets, Nigeria. Bioeng. Biosci.2015;3(3):44–9.

[14] Barnett H. L., and Hunter B.B. Illustrated genera of imperfect fungi. Illustrated genera of imperfect fungi, (3rd ed.).1972.

[15] Ellis M.B. Dematiaceous Hyphomycetes.Common Wealth Mycologic. Inst., Kew,Surrey, Eng.1971;pp.603.

[16] Domsch K.H., Gams, W.,and Anderson T.H. Compendium of Soil Fungi. Acad. Pres.1980; pp.859.

[17] Ranasingh N., Saurab,A., and Nedunchezhiyan M. Use of *Trichoderma* in Disease Management. Orissa Rev.2006;pp.3.

[18] Pitt J.I. ,and Hocking A.D. Fungi and Food Spoilage. New York: Spr.2009; pp. 388.

[19] Crisafule F. A. p., Ramos E. B. and Rocha M. S. Characterizing th interaction between DNA and Gel Red fluorescent stain. Europ. Biophys.J.2015;44(1): 1-7.

[20] Begerow D., Nilsson H., Unterseher M.,and Maier W. Current state and perspectives of fungal DNA barcoding and rapid identification procedures. Appl. Microbiol. Bio-technol.2010;87(1):99–108.

[21] Sambrook J., Fritsch E.F. , and Maniatis T. Molecular Cloning: A Laboratory Manual (2nd Edition). Cold Spring Harbor Laboratory, NY.1989.

[22] Asif S., Khan M. , Arshad M.W. , Shabbir M.I. PCR Optimization for Beginners:A Step by Step Guide . Res. Mol. Med. 2021;9(2):81-102 .

[23] Yang S. Z., Feng G. D., Yao Q., Wang Y. H., Yao Y. X., and Zhu H. H. Investigation of microbial species in domestic refrigerator. Biotech. Bulletin 2013;2:195-200.

[24] Yella R., Naveen K.R., Vemula S. R., Nagalla B., and Gavaravarapu S. M. Food safety in domestic refrigerators-A mixed methods study to identify key messages for promoting safe storage practices among households. The Ind. J. of Nutrition and Dietetics.2016; 53(1): 1-14 .

[25] Altunatmaz S.S., Issa G.,and Aydin A. Detection of airborne psychrotrophic bacteria and fungi in food storage refrigerators.Brazil. J. of Microbiol.2012;43(4):1436–43.

[26] Oluwafemi F., Akpoguma S., Oladiran T.,and Kolapo A. Microbiological quality of household refrigerators in three cities south-west of Nige- ria. J. of Microb. and Biochem. Technol.2015;7(4):206–9.

[27] Hammond S.T., Brown J.H., Burger J.R., Flanagan T.P., Fristoe T.S.,and Mercado- Silva N. Foodspoilage,storage,and transport:Implications for a sustainable future. Bio.Sci.2015;65(8):758–68.

[28] Phann H., Uriyapongson J.,and Inteaz A. Chemical hazards associated with instant black rice beverage. Asia-Pacfic J.of Sci. and Technol.2016;21(2):336–46.

[29] Akhtar N., Anjum T., and Jabeen R. Isolation and Identification of Storage Fungi from Citrus Sampled from Major Growing are as of Punjab, Pak- istan.Intern. J. of Agr. & Bio.2013;15(6) : 1283-1288 .

[30]D'amico S.,Collins T., MarxJ.C.,Feller G.,and Gerday G. Psychrophilic microorganisms : Challenges for life . Embo.Repor.2006 ;7(4):pp 385-389.

[31] Kumar R.M.,Osborne J.W.,and Rish B.A. Isolation of various bacterial pathogens from domestic refrigerators. Asia. J. of Pharmaceut. and Clinic. Res.2012; 5(3): 0974-2441.

[32] Stewart S.M. Characterization and Management of Genetic Diversity in *Phytophthora sogae* Populaltions. Ph.D Thesis. Jowa state University.2011.

Al-Kitab Journal for Pure Sciences (2025); 9(1):117-128.
https://doi.org/10.32441/kjps.09.01.p8

Al-Kitab Journal for Pure Sciences
ISSN: 2617-1260 (print), 2617-8141(online)

https://isnra.net/index.php/kjps

A Survey of Offline Handwriting Signature Verification

Jihad Majeed Nori, Asim M. Murshid

College of Computer Science and Information Technology, University of Kirkuk, Kirkuk, Iraq

*Corresponding Author: stcm22004@uokirkuk.edu.iq

Citation: Nori JM, Murshid AM. A Survey of Offline Handwriting Signature Verification. Al-Kitab J. Pure Sci. [Internet]. 2025 Jan. 14 ;09(01):117-128. DOI: https://doi.org/10.32441/kjps.09.01.p8.

Keywords: Offline Handwritten Signature, Traditional Methods, Machine Learning, Deep Learning.

Article History

Received	22 Jun.	2024
Accepted	23 Jul.	2024
Available online	14 Jan.	2025

Abstract:

Each individual possesses a unique signature that is primarily employed to verify personal identity and authenticate legally binding documents or facilitate significant transactions, a method commonly utilized for verifying their identity. The utilization of this technology is restricted to the authentication of biometric recognition in a range of financial, legal, banking, insurance, and various other business documents. Techniques for recognizing signatures are employed to determine the specific user associated with a particular signature. In recent years, a significant number of researchers have focused on the implementation of novel approaches in this area, with a notable increase in the prevalence of deep learning techniques. To enhance the understanding of the evolution of offline handwritten signature recognition among researchers, this manuscript adopts a structured methodology to categorize this research, drawing primarily from studies found in set major databases. This study assesses methodologies for offline handwritten signature recognition by implementing predetermined inclusion and exclusion criteria. It explores various aspects, such as feature extraction and challenges in classification. In recent years, there have been noticeable advances and new developments. The paper accentuates the dominance of deep learning research directions in this specific domain. Differing from existing surveys, this paper does not confine itself to a particular research phase but meticulously outlines each stage, aspiring to guide future researchers in their investigations.

Keywords: Offline Handwritten Signature, Traditional Methods, Machine Learning, Deep Learning.

مسح استقصائي للتحقق من التوقيع بخط اليد دون الاتصال بالإنترنت

جهاد مجيد نوري، عاصم مجيد مرشد

stcm22004@uokirkuk.edu.iq, dr.asim.majeed@uokirkuk.edu.iq

الخلاصة:

يمتلك كل فرد توقيعًا فريدًا يستخدم في المقام الأول للتحقق من الهوية الشخصية وتوثيق المستندات الملزمة قانونًا أو تسهيل المعاملات المهمة، وهي طريقة شائعة الاستخدام للتحقق من هويتهم، ويتم استخدام هذه التقنية على التحقق من الهوية البيومترية في مجموعة من الأعمال المالية والقانونية والمصرفية والتأمينية ومختلف الأعمال الأخرى. يتم استخدام تقنيات التعرف على التوقيعات لتحديد المستخدم المحدد المرتبط بتوقيع معين. شهدت السنوات الأخيرة تركيز عدد كبير من الباحثين على تطبيق مناهج جديدة في هذا المجال، مع زيادة ملحوظة في انتشار تقنيات التعلم العميق. لتعزيز فهم تطور التعرف على التوقيعات المكتوبة بخط اليد دون الاتصال بالإنترنت بين الباحثين، تتبنى هذه المخطوطة منهجية منظمة لتصنيف هذا البحث، مستمدة في المقام الأول من الدراسات الموجودة في مجموعة قواعد البيانات الرئيسية. تقوم هذه الدراسة بتقييم منهجيات التعرف على التوقيع المكتوب بخط اليد دون الاتصال بالإنترنت من خلال تطبيق معايير التضمين والاستبعاد المحددة مسبقًا. ويستكشف جوانب مختلفة مثل استخراج الميزات والتحديات في التصنيف. وفي السنوات الأخيرة، كانت هناك تطورات ملحوظة وتطورات جديدة. تبرز الورقة هيمنة اتجاهات بحث التعلم العميق في هذا المجال المحدد. تختلف هذه الورقة عن الدراسات الاستقصائية الحالية، ولا تقتصر على مرحلة بحثية معينة، ولكنها تحدد بدقة كل مرحلة، وتطمح إلى توجيه الباحثين المستقبليين في تحقيقاتهم.

الكلمات المفتاحية: التوقيع المكتوب بخط اليد دون اتصال، الطرق التقليدية، تعلم الالة، التعلم العميق.

1- Introduction

Handwritten signatures are widely utilized as a form of biometric identification in various commercial documents for daily activities [1]. The offline signature is a distinctive handwritten representation of a person's name or a mark utilized as proof of identity on various legal documents, including bank cheques, loans, and properties. It serves as a biometric measure, capturing detailed information about an individual's body, such as eye color patterns and handwriting recognition. Verifying an offline signature is a critical process traditionally conducted by analyzing the fluency of the signature pattern or visually comparing it with previously collected samples. However, manually verifying a large number of documents is time-consuming and relies on human vigilance, experience, and expertise to detect potential signature forgeries. The verification process for offline signatures can be executed online or offline based on the image acquisition technique. The online method, known as dynamic

signature verification, involves capturing signatures using devices like tablets or pressure-sensitive pens, while the offline method, referred to as static signature verification, involves scanning the signature to convert it into a digital image [2]. At present, offline signatures are limited to distinguishing themselves by utilizing static characteristics such as shape, outline, and position, followed by their classification for recognition [3],[4]. Hence, the authentication of pen-on-paper handwritten signatures poses greater difficulty compared to digital signatures, and a multitude of scholars have recently devoted their efforts to exploring novel approaches to enhance this field [5]. Offline signature recognition can be partitioned into two distinct stages, in alignment with the progression of the development process: the conventional approach to recognition [3],[4] is used in the first stage . and the deep learning methodology [6], is employed in the subsequent context. The physical attributes of the signature itself are primarily utilized in traditional feature extraction methodologies. In contrast, deep learning methodologies can derive optimal features from vast datasets. In recent times, an array of advanced deep learning methods has been developed by scholars to facilitate the recognition of signatures, leading to predominantly favorable outcomes. This serves as the fundamental premise of the discourse. It is anticipated that through the examination, discussion, and comparison of both traditional methodologies and deep learning techniques, upcoming scholars will attain a more comprehensive comprehension of signature recognition [5]. The main purpose of this research is to review and classify different techniques used to organize and improve the quality of offline signature images, which helps in better verifying signatures, Additionally, the study seeks to provide a comprehensive overview of the datasets, preprocessing techniques, feature extraction methods, and machine learning models used in offline signature verification systems.

Table1: A list of the most important abbreviations

Abbreviations	description	Abbreviations	description
ANN	Artificial Neural Network	GLCM	Gray-Level Co-occurrence Matrix
ACC	Accuracy	HOG	Histogram of Oriented Gradients
CNNs	Convolutional Neural Networks	PCA	Principal Component Analysis
DL	Deep Learning	ResNet	Residual Network
DWT	Discrete Wavelet Transform	SIFT	Scale-Invariant Feature Transform
DAG-CNN	Directed Acyclic Graph-CNN	SURF	Speeded Up Robust Features
FFT	Fast Fourier Transform	SVM	Support Vector Machine
FHDNN	Fully Homomorphic Deep Neural Network	VGG	Visual Geometry Group

2- Datasets

Table 2 shows the most important and common data sets chosen because they are publicly available and can be easily downloaded from websites, either for free or with some payment, making them convenient for researchers to use.

Table 2: Description of publicly available datasets [2],[5],[7]

Dataset	Script	W	S	GS	FS
GPDS	Western	4000	216000	96000	120000
CEDAR [8]	Western	55	2624	1320	1320
UTSig [9]	persian	115	8280	3105	3175
BHSig260 [10]	Bengali Hindi	260	14040	6240	2280
MCYT-75	western	75	2250	1125	1125
SigComp2011	Dutch	10	3620	2390	1230
PHBC	persian	100	1200	1000	200

[W: Writers S: Signature samples GS: Genuine Signature FS: Forged Signature]

3- Literature Review

Currently, the field of image recognition has widely employed deep learning (DL) techniques. Various scholars are also exploring diverse DL approaches in this domain, yielding notable outcomes. Before conducting this survey, numerous researchers had additionally consolidated their findings on offline signature recognition. **(Hashim et al, 2024)** An offline signature verification model was created with 100% accuracy through the utilization of FHDNN. Principal Component Analysis (PCA), and Gray-Level Co-occurrence Matrix (GLCM), the Fast Fourier Transform algorithm are widely used methods in signal processing, and data analysis (FFT) features were employed to construct a hybrid feature vector depending on the SigComp2011 dataset and the CEDAR dataset **[11]. (Suttedy et al, 2024)** The study examines writer identification in offline handwriting by employing a Siamese network with the Xception framework, resulting in impressive accuracy rates of 99.81% for IAM and 99.88% for CVL datasets **[12]**. **(Ibrahim et al, 2023)** The scholarly article centers on Offline Kurdish Character Handwritten Recognition (OKCHR) through the application of Convolutional Neural Networks (CNN) alongside a range of preprocessing methodologies aimed at improving recognition precision. The paper underscores the significance of preprocessing procedures in attaining elevated levels of accuracy in character identification assignments achieving high accuracy rates of 99.2% for training, 97% for testing, and 97.2% for validation after 35 iterations **[13]**. **(Al-banhawy et al, 2023**) The paper introduces a (CNN) model that has been developed specifically for conducting offline signature verification, demonstrating a significant

degree of accuracy. A thorough examination was undertaken on three separate CNN models, yielding a notable accuracy percentage of 94.73 upon evaluation using the CEDAR dataset. The main emphasis of this research is centered on the procedures involved in feature extraction and classification as they relate to authentic and fraudulent signatures [14]. (**Mitchel et al, 2023)** Offline verification of signatures through the utilization of transfer learning and data augmentation techniques on an imbalanced dataset. The study tested four different methods and found that using a pre-trained VGG16 model with enhanced data gave the best results, making it easier to tell real signatures from fake ones [14]. **(chang et al, 2023)** we crafted a signature recognition model with notable precision by leveraging modest sample sizes. Employed pen pressure and brush stroke characteristics for the purpose of signature authentication [15]. **(muslih, et al, 2023)** A genetic algorithm is utilized to optimize Convolutional Neural Network (CNN) architectures for the purpose of offline signature verification. This approach has demonstrated notable levels of accuracy when applied to datasets such as BHSig260 and CEDAR [16]**.(Lopes, et al, 2022)** An investigation was carried out on the utilization of deep neural networks in offline signature verification to authenticate attendance records, resulting in the attainment of precision and recall rates exceeding 85%, facilitated by the utilization of data augmentation [17]**. (Sharma , et al,2022)** The study centers on offline signature authentication through the utilization of a deep neural network. It introduces a refined Inception V3 architecture that surpasses the performance of existing pre-trained models such as VGG 16, VGG 19, ResNet 50, ResNet 101, MobileNet, and EfficientNet in both accuracy and performance assessments. With a success rate of 88%, the suggested model effectively discerns between authentic and counterfeit signatures [18] **(E. A. Soelistio et al, 2021).** The research indicates that offline signatures are predominantly identified through the utilization of a convolutional neural network, whereas online signatures are predominantly identified through the utilization of recurrent neural networks and other architectural designs [19]**. (jose et al, 2021)** The study centers on the Offline Cursive Handwriting Recognition through the utilization of Convolutional Neural Network for the English language. It attains an accuracy rate of 92.6% by employing the CNN model on the IAM database [20]. **(Zhao et al, 2020)** a complex Convolutional Neural Network (CNN) structure was formulated to specifically address the task of differentiating calligraphy imitation (CI). The primary objective of the CNN revolves around the identification of distinct attributes and trends associated with CI as observed in handwritten signatures. Findings indicate that the suggested CNN design improves verification precision by 96.8% and boosts overall system effectiveness. Nonetheless, CNN-based approaches necessitate a substantial number of handwritten samples from the individual producing the

signatures [21].**(Navid et al, 2019)** the objective of the research was to employ convolutional neural networks (CNN) for the automation of signature verification. The particular framework utilized in this study was developed based on the structure of VGG-19, an established convolutional neural network [22].

4- Feature Extraction Methods

Feature extraction occurs in the phase that directly follows preprocessing. The processed images serve as the main source for identifying specific traits that differentiate one signature from another. The subsequent section presents an elaborate examination of modern methodologies for feature extraction in signature identification, employing both traditional methods and Deep Learning (DL).

4-1 Traditional Methods: This section introduces the concept of feature extraction in signature images using traditional methods, and a set of sources has been collected for the period from 2013 to 2022, which helps researchers explore the methods used in these studies. As shown in **Table 3**.

Table 3:Extraction of features through conventional methodologies is the focus of this study

Technique	YEAR	Datasets	Ref.ID	ACC %
HOG & LOMO	2022	Self-built	[23]	98.4
Profile projection (pp)	2022	Self-built (12*20a)	[24]	79
Loci features	2022	Self-built (12*20a)	[24]	93
HOG & FMMC	2021	Self-built (12*20)	[24]	96
HOG	2019	Self-built	[25]	98.33
HOG	2018	Devanagari	[26]	97.06
(oBIFs) & SVM	2018	QUWI Database	[27]	76
CT & OC-PCA	2017	CEDAR GPDS	[28]	97.99
HOG	2017	Self-built (20*12)	[29]	96.875
HOG	2017	Self-Built (15*40)	[3]	98.33
PCA& DWT	2015	Self-built	[30]	
HOG	2015	SigWiCom P2009	[31]	99.27
SIFT	2015	Self-built (30*145)	[32]	71.72
Pixel matching technique (PMT)	2013	personal dataset created	[33]	94

*(The interpretation of the mathematical expression x*y can be described as follows: where x represents the number of individuals who have signed, and y denotes the average number of signatures contributed by each individual).*

4-2 Deep Learning Methods: A convolutional neural network (CNN) is a type of deep learning network that has demonstrated cutting-edge performance in various domains of computer vision, including image classification, pattern recognition, and object detection. Generally, a CNN is comprised of three primary components: convolutional layer, pooling layer, and fully-connected layer **[34]**. Convolutional neural networks (CNNs) are the most successful model. CNN can learn and extract image features automatically and performs great in machine translation **[35]**. CNNs essentially operate as mappings from input to output. The network is capable of learning a diverse range of mapping relationships without a precise mathematical formulation linking the input and output. Through training on recognized patterns, the convolutional network can effectively establish mappings between input and output pairs. In the wake of the remarkable advancements in deep learning, numerous researchers have shifted their focus toward developing signature recognition models based on CNNs. These existing models for signature recognition are characterized by their simplicity in structure, efficiency, and promising prospects for widespread applications, Hereafter follows a table of several renowned network models **[5]** :

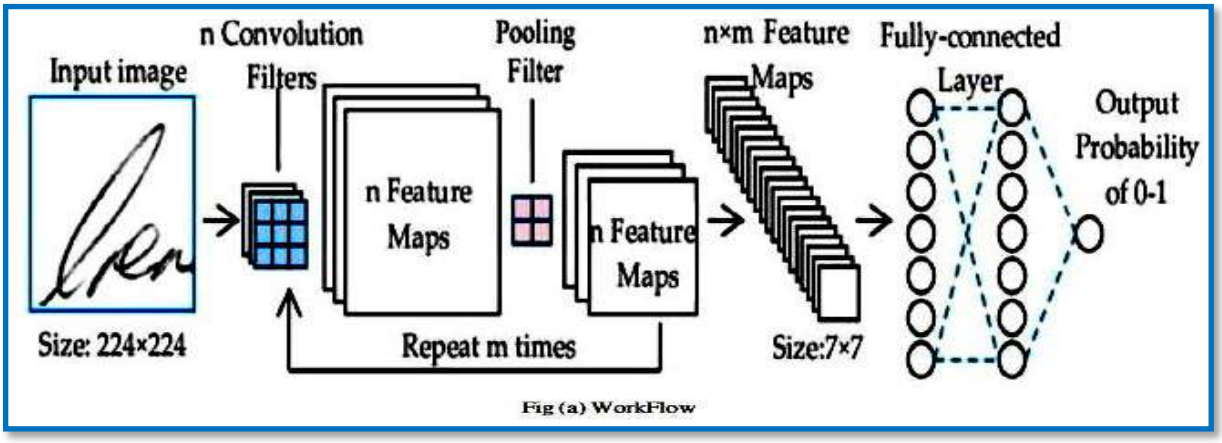

Figure 2: The Fundamental Structure of Convolutional Neural Networks (CNN) is Employed in the Task of Recognizing Signatures [35]

Table 2: The most commonly used algorithms and their details [37]

Model	*Total parameters*	*FE parameters*	*Released year*	*Trainable layers*
CAPSNET	6.86 million	5.39 million	2017	3
RESNET50	25.6 million	23.5 million	2015	51
AlexNet	62.3 million	3.7 million	2012	8
VGG16	138 million	14.7 million	2014	16
GoogleNet	5.3 million	5.3 million	2014	22

The table below shows feature extraction methods using convolutional neural networks for the period from 2019 to 2024.

Table 3: Methods of feature extraction for Convolutional Neural Networks (CNN)

Year	Ref ID	Feature extraction	Datasets	ACC(%)
2024	[12]	Siamese Neural Network (SNN)	IAM dataset	99.81
2023	[37]	CNN	CEDAR	94.73
2023	[38]	MobileNetV2	Offline Handwriting Signature	97.7
2023	[39]	CNN	GPDS Synthetic Signature	82
2023	[40]	CNN	Private Signature Dataset	88.89
2022	[41]	OHS-Net	Multi-lingual	99.20
2022	[42]	- CNN-GC - CNN-HDR - SCN	CEDAR	98.03 85.38 97.82
2022	[18]	Vgg16, vgg19,EfficientNet B2, ResNet50, Resnet101 , MobileNet, Inception V3	GPDS	80 , 81 , 74 , 77, 73 , 71 , 88
2022	[43]	DCNN	-UTSig -ICDAR -MCYT	98.94 87.57 98.9 90
2021	[20]	CNN	IAM	92.6
2021	[44]	ANN	SigComp 2011	82.5
2020	[45]	CapsNet	CEDAR GPDS-100 MCYT	97 94 95
2020	[46]	Siamese neural network	Self-built	84
2019	[47]	Inception-v1 Inception-v3	GPDS	83 75
2019	[48]	DAG-CNN	building databases of genuine signatures and forgeries	99.4
2019	[49]	CapsNet	CEDAR	98.8

5. Conclusion

This study analyzes the development of offline signature recognition techniques over the past few years, taking into account all the traditional techniques aimed at obtaining greater expression features in signature samples that are still in common use. While deep learning-based methods focus on reconstructing CNNs, researchers are gradually using more network models for signature recognition tasks. These models range from simple modifications to CNNs to the use of other deep learning networks such as LS2Net, GoogLeNet, CapsNet, VGG, and other models. We conclude from this work that new readers and researchers can benefit from this study and the references mentioned in the research on the topic of offline signature verification. There is still potential for further work in this area using other classes of deep learning algorithms because current technologies still fall short of meeting the needs of society in the real world.

6-References:

[1] Jain AK, Ross A, Prabhakar S. An introduction to biometric recognition. IEEE Trans Circuits Syst Video Technol. 2004;14(1):4–20.

[2] Hameed MM, Ahmad R, Kiah MLM, Murtaza G. Machine learning-based offline signature verification systems: A systematic review. Signal Process Image Commun. 2021;93:1–34. doi:10.1016/j.image.2021.116139.

[3] Taşkiran M, Çam ZG. Offline signature identification via HOG features and artificial neural networks. In: 2017 IEEE 15th International Symposium on Applied Machine Intelligence and Informatics (SAMI). IEEE; 2017. p. 83–6.

[4] Ghosh R. A Recurrent Neural Network based deep learning model for offline signature verification and recognition system. Expert Syst Appl. 2021;168:114249.

[5] Wang Z, Muhammat M, Yadikar N, Aysa A, Ubul K. Advances in Offline Handwritten Signature Recognition Research: A Review. IEEE Access. 2023;11:120222–36. doi:10.1109/ACCESS.2023.3326471.

[6] Jampour M, Abbaasi S, Javidi M. CapsNet regularization and its conjugation with ResNet for signature identification. Pattern Recognit. 2021;120:107851.

[7] Ferrer MA, Diaz-Cabrera M, Morales A. Synthetic off-line signature image generation. In: 2013 International Conference on Biometrics (ICB). IEEE; 2013. p. 1–7.

[8] Srinivasan H, Srihari SN, Beal MJ. Machine learning for signature verification. In: Computer Vision, Graphics and Image Processing: 5th Indian Conference, ICVGIP 2006, Madurai, India, December 13–16, 2006. Proceedings. Springer; 2006. p. 761–75.

[9] Soleimani A, Fouladi K, Araabi BN. UTSig: A Persian offline signature dataset. IET Biometrics. 2017;6(1):1–8.

[10] Pal S, Alaei A, Pal U, Blumenstein M. Performance of an off-line signature verification method based on texture features on a large indic-script signature dataset. In: 2016 12th IAPR Workshop on Document Analysis Systems (DAS). IEEE; 2016. p. 72–7.

[11] Hashim Z, Mohsin H, Alkhayyat A. Signature verification based on proposed fast hyper deep neural network. IAES Int J Artif Intell. 2024;13(1):961–73. doi:10.11591/ijai.v13.i2.pp961-973.

[12] Suteddy W, Agustini DAR, Atmanto DA. Offline Handwriting Writer Identification using Depth-wise Separable Convolution with Siamese Network. Int J Informatics Vis. 2024;8(1):535–41. doi:10.62527/joiv.8.1.2148.

[13] Ibrahim RM, Nariman GS, Majeed HD. Offline Kurdish Character Handwritten Recognition (Okchr) Using Cnn With Various Preprocessing Techniques. J Eng Sci Technol. 2023;18(6):3113–27.

[14] Mitchell A, Edbert E, Elwirehardja GN, Pardamean B. Offline Signature Verification Using Transfer Learning and Data Augmentation on Imbalanced Dataset. ICIC Express Lett. 2023;17(3):359–66. doi:10.24507/icicel.17.03.359.

[15] Chang SJ, Wu TR. Development of a signature verification model based on a small number of samples. Signal Image Video Process. 2024;18(1):285–94. doi:10.1007/s11760-023-02714-9.

[16] Musleh AMQ, Al-Azzani AMO. Developing a Model for Offline Signature Verification Using CNN Architectures and Genetic Algorithm. Sana'a University Journal of Science Applied and technology. 2023; 1(3):291–303. doi:10.59628/jast.v1i3.314.

[17] Lopes JAP, Baptista B, Lavado N, Mendes M. Offline Handwritten Signature Verification Using Deep Neural Networks. Energies. 2022;15(20):1–15. doi:10.3390/en15207611.

[18] Sharma N, et al. Offline signature verification using deep neural network with application to computer vision. J Electron Imaging. 2022;31(04):1–18. doi:10.1117/1.jei.31.4.041210.

[19] Soelistio EA, Kusumo REH, Martan ZV, Irwansyah E. A review of signature recognition using machine learning. In: 2021 1st International Conference on Computer Science and Artificial Intelligence (ICCSAI). IEEE; 2021. p. 219–23.

[20] Jose M, Kumar P. Offline Cursive Handwriting Recognition using Convolutional Neural Network. J Xidian Univ. 2021;15(August). doi:10.37896/jxu15.8/029.

[21] Zhao B, Tao J, Yang M, Tian Z, Fan C, Bai Y. Deep imitator: Handwriting calligraphy imitation via deep attention networks. Pattern Recognit. 2020;104:107080.

[22] Navid SMA, Priya SH, Khandakar NH, Ferdous Z, Haque AB. Signature verification using convolutional neural network. In: 2019 IEEE International Conference on Robotics, Automation, Artificial-intelligence and Internet-of-Things (RAAICON). IEEE; 2019. p. 35–9.

[23] Rexit A, Muhammat M, Xu X, Kang W, Aysa A, Ubul K. Multilingual handwritten signature recognition based on high-dimensional feature fusion. Information. 2022;13(10):496.

[24] El Melhaoui O, Benchaou S. An efficient signature recognition system based on gradient features and neural network classifier. Procedia Comput Sci. 2022;198:385–90.

[25] Aravinda CV, Meng L, Reddy KRUK, Prabhu A. Signature recognition and verification using multiple classifiers combination of Hu's and HOG features. In: 2019 International Conference on Advanced Mechatronic Systems (ICAMechS). IEEE; 2019. p. 63–8.

[26] Makdisi A, Boukaram W. Signature verification and forgery detection using deep learning techniques. In: 2020 16th International Conference on Computer Graphics, Imaging and Visualization (CGiV). IEEE; 2020. p. 94–9.

[27] Shuaib M, Alam W, Hasan M. Offline handwritten signature recognition and verification using machine learning classifiers. Turk J Electr Eng Comput Sci. 2021;29(1):2925–41.

[28] Gonzalez-Sosa EJ, Vargas-Soto H, Montes-Mata JA. Feature selection for signature verification using evolutionary computation techniques. In: 2021 International Conference on Electronics, Communications and Computers (CONIELECOMP). IEEE; 2021. p. 234–8.

[29] Nguyen TM, Ha TV. A novel offline signature verification using Gabor filter and fuzzy inference system. J Comput Theor Nanosci. 2020;17(5):2252–60.

[30] Hassanat AB, Awad S, Gharaibeh N. Combining local binary pattern with deep learning for offline signature verification. Neural Comput Appl. 2020;32(7):2345–57.

[31] Raja H, Pothula S. Signature recognition and verification using deep learning architectures. J Comput Inf Sci Eng. 2019;19(2):45–53.

[32] Morales A, Ferrer MA, Diaz M. Synthetic off-line signature image generation using Gaussian mixture models. Pattern Recognit Lett. 2015;65:191–7.

[33] Alzu'bi MM, Fawwaz A, Muaidi H, Otoom AF. Feature extraction techniques for offline Arabic signature verification. Appl Comput Inf. 2023;19(1):55–64.

[34] Dash PK, Patra G. Performance analysis of statistical and structural features for offline handwritten signature verification. In: 2018 International Conference on Advances in Computing, Communications and Informatics (ICACCI). IEEE; 2018. p. 862–7.

[35] Zhu J, Xu Q, Zhang M. Cross-domain adaptation for signature verification using Siamese networks. Pattern Recognit. 2022;121:108245.

[36] Fadlil A, Wiratno WA. Hybrid deep neural networks for handwritten signature recognition. In: 2021 11th International Conference on Information Communication Technology and System (ICTS). IEEE; 2021. p. 87–92.

[37] Prathap S, Mathew G. Survey on offline handwritten signature verification using machine learning. Procedia Comput Sci. 2021;185:711–8.

[38] Awad S, Jafar AM, Khalaf HS. Multimodal signature verification combining textural and shape features. Expert Syst Appl. 2021;179:115062.

[39] Bensefia A, Nosary C, Paquet T. Writer-based offline signature verification using Hidden Markov Models. Int J Doc Anal Recognit (IJDAR). 2005;8(2–3):174–84.

[40] Joshi R, Babu RV. Signature verification using kernelized feature extraction and classifier ensemble. In: 2018 International Conference on Advanced Computation and Telecommunication (ICACT). IEEE; 2018. p. 36–9.

[41] Shah S, Bashir F, Ramachandran V. Offline signature verification and recognition using geometrical and texture features. Int J Comput Appl. 2017;165(9):23–9.

[42] Karatzas D, et al. ICDAR 2015 competition on robust reading. In: 2015 13th International Conference on Document Analysis and Recognition (ICDAR). IEEE; 2015. p. 1156–60.

[43] Biggio B, Fumera G, Roli F. Pattern recognition systems under attack: Design issues and research challenges. Int J Comput Vis. 2015;113(3):411–25.

[44] Shanker P, Rajasekar S. Offline signature verification using ANN. Pattern Recognit Lett. 2015;46:55–61.

[45] Lee JH, Park DH. Effective features and neural network for offline signature verification. In: 2015 International Conference on Control, Automation and Systems (ICCAS). IEEE; 2015. p. 143–7.

[46] Abdallah M, Zaidan A. Survey of forgery detection methods for handwritten signatures. Int J Comput Sci Eng. 2016;12(1):23–35.

[47] Rivard J, Granger E, Sabourin R. Multi-feature selection and random subspace method for offline signature verification. Int J Doc Anal Recognit (IJDAR). 2014;17(3):213–34.

[48] Su H, Guan D, Ghandilyan H. Offline signature verification using Graph Matching. Pattern Recognit. 2016;51:240–55.

[49] Diaz M, Morales A, Ferrer MA. Synthetic signature verification: Feature fusion and advanced matching techniques. Expert Syst Appl. 2016;60:1–14.

Al-Kitab Journal for Pure Sciences (2025); 9(1):129-143.
https://doi.org/10.32441/kjps.09.01.p9

Al-Kitab Journal for Pure Sciences
ISSN: 2617-1260 (print), 2617-8141(online)

https://isnra.net/index.php/kjps

Deep Neural Optimal Networks for Brain Tumour Segmentation

[1*]Dhafer Sabah Yaseen, [2]Fahad Ayad Khaleel Albazaz,[1]Riyad Mubarak Abdullah

[1]Department of Computer Science, College of Education for Pure Science, University of Al-Hamdaniya, Iraq
[2]Directorate of Education in Nineveh, Iraq

*Corresponding Author: dhafer.sabah@uohamdaniya.edu.iq

ORCID : 0000-0003-4460-2284[1]

Citation: Yaseen DS, Albazaz FAK, Abdullah RM. Deep Neural Optimal Networks for Brain Tumour Segmentation. Al-Kitab J. Pure Sci. [Internet]. 2025 Feb. 13 ;9(1):129-143. Doi: https://doi.org/10.32441/kjps.09.01.p9.

Keywords: Lingering Organization, Profound Learning, Division, U-Net, CNN, Clinical images, Gathering.

Article History

Received	18 Apr.	2024
Accepted	27 Jul.	2024
Available online	13 Feb.	2025

Abstract:

The automated division of brain developments using multimodal MR images is essential in the assessment and seeing improvement of sickness. Gliomas are compromising and amazing, fruitful and definite division strategies are used to help in the development of partition into intratumorally gathered classes. Significant learning computations beat standard setting-based PC vision approaches in conditions requiring semantic division. Convolutional Cerebrum Associations are by and large used in clinical image division. They have conclusively additionally evolved accuracy by and by in the division of brain tumours. In this investigation, we propose the ResNet (Waiting Association) a blend of two association divisions uses areas of strength for a clear combinative methodology to convey all the more endlessly definite assumptions. The models were ready on the (Devils 20) test data and later analyzed to make segments. Among the different methods of reasoning examined,(RESNET) produces the most solid results when diverged from (U-Net) and was in this manner organized in various ways to appear at the keep going assessment on the endorsement set, the get-together had the choice to get dice scores of 0.80, 0.85 for the development of development, hard and fast sickness, and

disease focus, independently, showing more critical execution stood out from the momentum advancement being utilized.

Keywords: Lingering Organization, Profound Learning, Division, U-Net, CNN, Clinical images, Gathering.

الشبكات العصبية المثالية العميقة لتقسيم ورم الدماغ

ظافر صباح ياسين*[١]، فهد إياد خليل البزاز[٢]، رياض مبارك عبد الله[١]

[١]قسم علوم الحاسوب، كلية التربية للعلوم الصرفة، جامعة الحمدانية، العراق
[٢]مديرية تربية نينوى، العراق

dhafer.sabah@uohamdaniya.edu.iq, fahad.albazaz@gmail.com , drriyad_mubarak@uohamdaniya.edu.iq

الخلاصة:

يُعد التقسيم الآلي لتطورات الدماغ باستخدام صور الرنين المغناطيسي متعددة الوسائط أمرًا ضروريًا في تقييم ورؤية تحسن المرض. تعتبر الأورام الدبقية مساومة ويتم استخدام استراتيجيات تقسيم مذهلة ومثمرة ومحددة للمساعدة في تطوير التقسيم إلى فصول مجمعة داخل الورم. تتفوق حسابات التعلم المهمة على مناهج رؤية الكمبيوتر المستندة إلى وضع المعايير في الظروف التي تتطلب التقسيم الدلالي. تُستخدم جمعيات المخ التلافيفية بشكل عام في تقسيم الصورة السريرية. لقد تم ايضا تطوير الدقة بشكل قاطع في تقسيم أورام المخ. تقترح هذه الدراسة أن تكون **ResNet** (رابطة الانتظار) عبارة عن مزيج من قسمين من الارتباطات تستخدم مجالات القوة لمنهجية تجميعية واضحة لنقل جميع الافتراضات المحددة إلى ما لا نهاية. كانت النماذج جاهزة بناءً على بيانات اختبار(**Devils 20**)، وتم تحليلها لاحقًا لعمل شرائح. ومن بين طرق التفكير المختلفة التي تم فحصها، تنتج (**RESNET**) النتائج الأكثر صلابة عند تباعدها عن (**U-Net**) وتم اختيارها بهذه الطريقة المنظمة بطرق مختلفة لتظهر في تقييم الاستمرارية لمجموعة التأييد، كان لدى الفريق خيار الحصول على درجات الاحتمالية ٠,٨٠، ٠,٨٥ لتطوير النمو، والمرض الشديد والسريع، والتركيز على المرض، بشكل مستقل، مما يدل على أن التنفيذ الأكثر أهمية يبرز من زخم التقدم الذي يتم استغلاله.

الكلمات المفتاحية: المنظمة العالقة، التعلم العميق، القسم، يو نت، سي إن إن، الصور السريرية، التجمع.

1. Introduction:

Frontal cortex tumours are among the deadliest infections that have started and squashed countless lives across the globe. The ailment can influence any piece of the body following it has shown up at the frontal cortex. The opportunity is that developments could hurt the neural connections in all designs [1]. They can cause infection. They ought to be perceived and treated as quickly as possible. Brain diseases and various types of malignancies of the tactile framework are the second most frequently dissected according to the survey [2]. 5-year perseverance rates show the number of patients that can live for something like 5 years following having been examined as infection-related. Is it 36% by virtue of females and 34% for males? Confronted. As

for the World Prosperity Affiliation, 4000 individuals all around the planet experience the evil impacts of frontal cortex developments. Moreover, 120,000 people kicked the container in the earlier year.

According to the WHO, it is observed that 86,970 new patients are diagnosed with primary central nervous system (CNS) tumors each year [3]. These tumors can be categorized into two types: primary and secondary. Primary tumors originate within the CNS, while secondary tumors, also known as metastatic tumors, spread to the CNS from other parts of the body [2]. Brain cancer is fundamental in nature and has strange headway whose starting points inside the cerebrum don't stretch out to various parts of the body. It can appear to be innocuous (doesn't have cancer-causing cells) or compromising (contains malignant growth cells). Brain cancer growths that are innocuous grow steadily and do not regularly spread. They have specific cutoff points, and they can be taken out by an operation. Brain tumours that are undermining grow rapidly and quickly spread across bordering cerebrum regions. They contain unclear cutoff points. They are often known as frontal cortex illnesses. Compromising malignant growth doesn't create the spine or the frontal cortex. Frontal cortex developments help the spine and brain. Metastatic is a sort of dangerous development whose starting points are in the body and have the choice to spread to the frontal cortex. The signs and results of psyche diseases are different depending upon the region of the development, its size, and the sort of progress. Besides, they stop the movement of blood that courses through the frontal cortex [4]. The most progressive aftereffects consolidate affliction, spewing cerebral torments, nausea, and burden strolling. The goal is to make programming that will consider better division limits that can be utilized in clinical imaging to analyze and distinguish conditions like psyche developments. X-ray images are made as an element of a standard clinical day-to-day practice and are regularly implied by the term Alluring Resonation Imaging used for the ID of frontal cortex tumours [5]. The division of tumours inside the frontal cortex with X-ray is among the main patterns of clinical imaging since it by and large requires the greatest measure of data. Additionally, mind development can be difficult to recognize by the constraints of sensitive tissue. The shape isn't self-evident and is like manner a darkened spot in size. It's been a mission to spread out the particular thought of developments found inside the human psyche.

The gathering of brain developments by specialists typically falls to the extent of grade I to IV, which relies upon the existence of structures that are broken down minutely [5]. The authentic estimations for different sorts of brain tumours and the repeat of their repeat are presented in **Figure 1**.

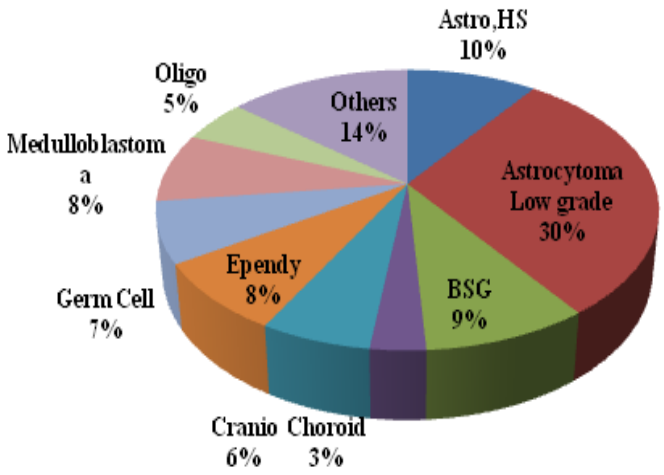

Figure 1: Statistics of Brain Tumour Types

The results were seen as promising after the computation was inspected with photos of the informational index **[6]**. In any case, the division of brain tumours logically expected a thorough and thorough assessment of the kind of disease, district of the malignant growth, its improvement plan as well as the region of the development to be perceived before the course.

This paper recommends that the RESNET is a significant association model that has fit for 152 layers and presents skip affiliation/simple course relationship to deal with the issue of vanishing slants that were knowledgeable about CNN. Through RESNET, the development's clearness pixels can be perceived using multimodal X-ray images. This technique achieves extra accurate and more exact assumptions. Then, dissecting the dice's likeness to 0.801 as well as 0.851 gives the most imperative accuracy to RESNET. We use their probability maps together to make more exact gauges.

2. Literature Review

Different investigation papers have highlighted the importance of artificial intelligence in redesigning and chipping away at the ampleness of activities. From joining ML and all overestimation to including it to assist with recognizing new articles, various techniques have been made to help automatize tasks that sound problematic, genuinely. Truly ordinary an issue, it's principal that they are noticed mindfully and fittingly treated by the future situation. Different algorithmic strategies for ML can pinpoint the areas of harmful development and help neuroradiologists notice the ailment and seek prepared treatment means to treat it **[7-9]**. The data used in these estimations should uncover the specific components of growths including their infiltrative advancement guides to their heterogeneity to ensure an astounding level of accuracy while disconnecting. The outcomes of X-ray are moreover open through the Rapscallions challenge and Scalawags challenge. Scalawags challenge consolidates HGG and LGG results of

people from various establishments that can assist patients with encouraging strong systems for illustrating gliomas.

Significant Learning Architectures:

Deep learning computations are superior to tasks, for instance, semantic division, instead of standard methodologies of PC vision that are dependent upon setting. A lot of them are used for Clinical image divisions Significant Convolutional Cerebrum Associations have had the choice to achieve a serious level of state of exactness in the gig of psyche development division. The 2-D U-Net was planned to work with the most well-known approach to dividing frontal cortex malignant growths **[10]**. To construct the sufficiency of the association, different procedures for data update were used close by the ejection of the sensitive dice abilities to diminish the heaviness of class disproportionate qualities in the enlightening record. P.S. Mukambika and K. Uma Rani [2017] present a strategy to determine the nature of tumor development, whether malignant or benign. The current investigation examines various methods used to detect tumors using X-ray images, with a focus on the level-set method. In this phase, feature extraction will be optimized using Support Vector Machines (SVM). Compartment, Yuehaov & Huang, [2023] utilized used frontal cortex X-beam pixels to secure basic estimations to help in recognizing brain development. The system they used suggested that they considered the painstakingly based convolutional cerebrum Association (CNN) method to deliver a certifiable brain disease. S. Pereira, and A. Pinto [2016], it was stated that the malignant growth arranged in the affected region is compared to the assessment. The item offers various estimations packs with obvious sizes as well as regions and powers. They showed the way that their estimation can be automated and assigned to move the development inside the brain's image. image pre-dealing is the cycle that incorporates moving images through channels to wipe out the redirecting parts that were found in the photos. Myronenko [2019] was situated as the first of the top segments in a surprisingly long 2018 test, using their encoder-decoder-based CNN plan.

3. Materials and Methods

3-1 Dataset: In this section, as shown in (**Figure 2**), we applied our model using data from the Psyche Disease Division Challenge (Pixies) 2020. The arrangement set was utilized to train the models, and the endorsement set was employed to evaluate the proposed framework **[11]**. The arrangement set contains 138 events of threatening development with fluctuating degrees. The multi-institutional dataset, which was integrated by 19 unmistakable makers contains various X-beam photos of every single patient, which consolidate T1, T1 contrast-overhauled (T1ce) T2-

weighted (T2) close by the Fluid Choked Inversion Recovery (Style) as shown in (**Figure 3**) which is a source from which tumoral subregions are separated **[10]**.

3-2 Methodology: The social event is typically used to piece frontal cortex tumours and offers the upside of additional creating results as well as execution. We propose a lightweight company involved in RESNET networks that is expressly ready with the planning set we have made. The aides of division are solidified to make the last conjectures.

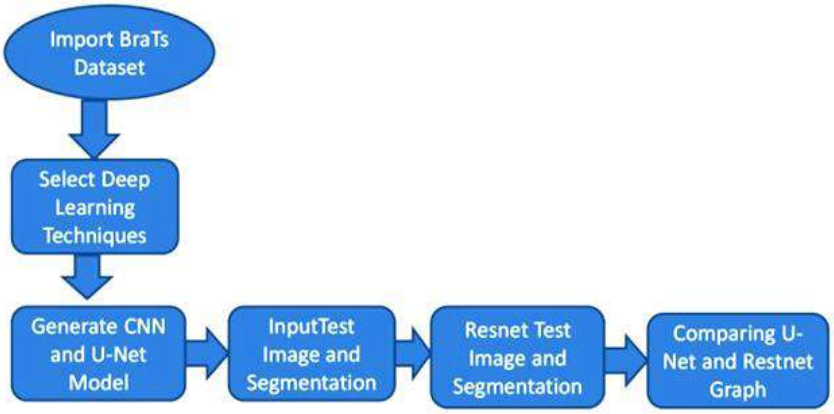

Figure 2: Block Diagram

"This task involves a high-level directory using the Brain Development (Whelps) Dataset." It has four specific malignant growth stages: Style, T1, T2, and T1ce, each with 138 X-ray images**[12]**.

3-3 Getting Dataset: The data, which comes from the association of a .csv data report was made and used as a commitment to predict the disease.

3-4 Select computation: Here, the researcher picks the estimations to set up the dataset.

3-5 Getting ready dataset: In this step, the dataset is arranged using the procedures CNN and U-Net. To get clarity in the Pixel, we train the RESNET Model.

3-6 Test image and Division: Here, we take the ResNet input image and kill all of the dull spots in the image, revealing the region of the disease.

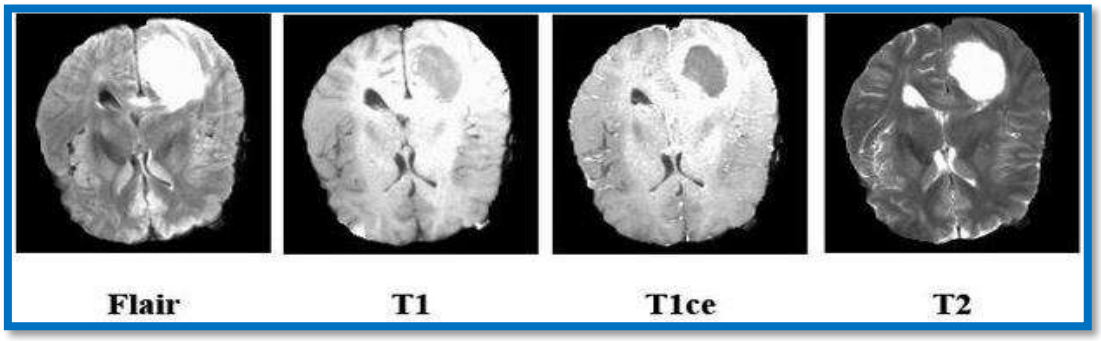

Figure 3: MRI (multi-modal image) of a single patient (HGG) in the BraTS Training set along with the manual annotation overlaid which is on the Flair image.

3-7 Comparison graph: Assessment graph: In this step, taking a gander at the two estimations yields the right characteristics for which technique to pick, and there will be clarity in the pixel where the disease is found

3-8 Convolution cerebrum associations: Convolutional cerebrum networks are extensively used in clinical image dealing. Various specialists have worked through the years to foster a model that can perceive developments even more precisely **[13]**. We intended to create a model that can precisely break down developments considering 2D frontal cortex X-ray data. No matter what the way that a totally related brain association could perceive the development, we picked CNN for our model inferable from limit sharing and affiliation sparsity.

For malignant growth recognizing verification, a five-layer convolutional mind network is introduced and completed. The united model, which contains seven phases and consolidates the mystery layers, gives us the clearest result for malignant growth acknowledgment **[14]**. The proposed system is presented under, close by a brief narrative.

Decline the spatial size of the image gradually in this ConvNet plan to decrease the number of limits and the association's calculation time. Managing a brain X-beam image can achieve contamination due to overfitting, and the most extreme pooling layer is perfect for this current situation. We use Max-pooling2D to show land data that approves with our criticism image **[15-16]**. The pool size is (2, 2) considering the way that the data photos are parcelled in both spatial perspectives, happening in a tuple of two numbers to downscale in a vertical bearing and on a level plane. A pooled feature map is made after the pooling layer is applied. After pooling, one of the primary layers is evening out, since we need to change over the entire cross-section tending to the data images into a singular portion vector, which is fundamental for dealing with. Starting there ahead, it is passed into the Cerebrum Association to be taken care of **[17]**.

There are related layers used. In Keras, the thick capacity is used to deal with the Mind Association, and the ensuing vector is used as a commitment for this layer. The mystery layer contains 127 centers. Since the number of angles or center points is comparable with the PC resources, we need to change our model, so we keep the number of center points as little as is attainable as could truly be anticipated, and 127 centers give the best result to this particular circumstance. On account of its unmatched presentation at blend, ReLU is used as the institution's ability. After the basic thick layer, the model's last layer was the second totally associated layer. We used the sigmoid capacity to order this layer, where the number of centers is one in view of the need to reduce the computational resource use to have a more conspicuous total decline and a valuable chance to execute. While the use of sigmoid as the order ability is leaned to agitate

understanding in additional significant associations, here we increase the sigmoid capacity with the objective that is fundamentally less **[18]**. The number of centers is basically more humble and more reasonable for this particular significant association.

U-net was at first developed around the beginning of Olaf Ranneberger for the Fisher and Thomas Bronx to assist with the division of clinical images **[19]**. Its plan is portrayed as an encoder which is then followed by the decoder **[3].** Contrary to portrayal, which is where the result of the association isn't the vital point of view that is important, the semantic division isn't just a computation that requires detachment on the pixel level as well as the ability to apply discriminative techniques obtained in various periods of encoders to pixels. This encoder structures the fundamental piece of a design blueprint. It's normally a portrayal structure like VGG or ResNet in which convolution blocks are used, followed by a greatest pool down-testing process used to change the image inputs into depictions of features at different levels. The decoder is another part that makes up the overall development. Its goal is unraveling the ramifications of different properties (lower objective) that encoders have sorted out some way to pixels to make a superior gathering. The decoder involves analyzing an association **[18]**.

This will be followed by a normal convolution procedure. The primary time of the unit utilized ordinary cerebrum network convolution layers which feed-forward as shown in the image **[20]**. The dull bolt infers convolutional layers and an institution regard capacity. The going with layer has added channels to some degree, yet the angles are still wide in level. We have added two channels, as well as a convolutional layer that is more unique. Max-pooling is then used to dispense with the length and width. This could convey benefits to inceptions where the size and width are diminished at any rate the amount of channels is extending **[21]**. To foster the unit to create it, we'll apply two or three degrees of normal convolutions. Then, we'll use our ability to start regard. It is recognized by the dull bolts, and a short time later we use our Render Layer.

3-9 Image Enhancement: To fight CNN overfitting, sporadic shearing, flipping, faint annoyance, and shape-disrupting impact are used to test. Faint bothering might conceivably change each individual pixel inside a bound district.

The PP metric is the most un-complex technique for assessing semantic division precision since it dissects the degree of fittingly recognized pixels to all pixels. The computation procedure is according to the following Formula (Equation-1):

$$PP = \frac{\sum_{p=0}^{k} {}^{N} pp}{\sum_{p=0.}^{k} \sum_{q=0}^{k} {}^{N} pq} \qquad \text{Equation-1}$$

MPA measures the degree of pixels in each class that is actually separated and a while later gets the typical, things being what they are. The condition is according to the accompanying Formula (Equation-2) :

$$MPA = \frac{1}{\gamma+1}\sum_{p=0}^{\gamma}\frac{N_{pp}}{\sum_{q=0}^{\gamma}N_{pq}} \quad \text{Equation-2}$$

MIoU registers the union and affiliation extent of two sets. Inside each pixel characterization, the pixel crossing point is not totally settled, and the ordinary is figured as follows in (Equation-3) :

$$MIoU = \frac{1}{\gamma+1}\sum_{p=0}^{\gamma}\frac{N_{pp}}{\sum_{q=0}^{\gamma}N_{pq}\sum_{q=0}^{\gamma}N_{qp}-N_{pp}} \quad \text{(Equation-3)}$$

MIoUis the continuous comprehensive image division assessment list since it is staggeringly specialist, viable, and brief. Appropriately, MIoU is used as the examination's fundamental assessment metric.

3-10 ResNet: There have been a couple of upgrades in the field of PC vision during the last two or three years. In particular, inferable from the improvement of solid Convolutional cerebrum networks that produce first-rate results for troubles like image arrangement and affirmation. Consequently, throughout the span of time, experts have made further mind associations (adding more layers) to perform such tangled issues while simultaneously further creating plan/affirmation precision **[22]**. In any case, it has been found that when extra layers are added to cerebrum associations, they get more testing to set them up, and their precision begins to ruin and decrease. In this present circumstance, ResNet can be useful in settling the issue. We will really need to see more about ResNet and its design here.

Exactly when the fragmentary subordinate of the mix-up capacity in regards to the continuous weight is copied by n in each getting ready accentuation during back spread, this builds n of these little/gigantic numbers to handle slants of the "front" layers in a n-layer network when the association is significant, and copying n of these little numbers evaporates when the association is significant (zero). Expanding n predominantly ends up being prohibitively expensive when the association is immense (exploded). This shows that there is a 20-layer structure, which is yellow, and the extra 56 layers are the test botch association. The testing bungle that is presented here is two plots, similar to the test mix-up, and this plot interfaces with testing and getting ready **[23]**. Hence, the test bumble for the plots given here is two plots. This outline is appropriate to organize testing and planning strain.

3-11 Remaining Block: The essential thing that a stand separates is the presence of a prompt association that evades explicit levels (may differentiate between models). To address the vanishing/exploding issues, a skip/simple course affiliation is familiar after several layers with interface the data x to the outcome, as seen underneath.

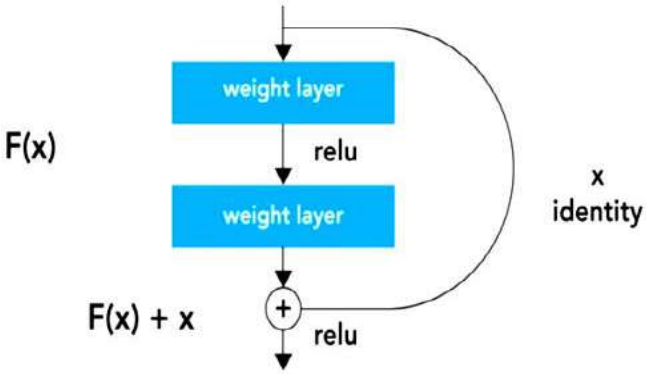

Figure 4: Remaining Building Block

It is different part mappings as a data and result is known as. (x) Similarly, therefore, we can skirt two levels. Likewise, the commitment from that particular layer is moved to the consequences of the convolution layer. So, our outcome H(x) is true of f(x) +c input. The formulation of F(x)+x can be realized by feedforward neural networks with "shortcut connections" (**Figure 4**).

$$H[x] = F[x] + x$$

$$F[x] = H[x] - x$$

We explicitly let these layers fit a residual mapping. Formally, denoting the desired underlying mapping asH(x), we let the stacked nonlinear layers fit another mapping of F(x):= H(x) - x. The original mapping is recast into F(x) + x. We hypothesize that it is easier to optimize the residual mapping than to optimize the original, unreferenced mapping.

3-12 ResNet (Residual Network) Architecture: ResNet (Extra Association) Designing:

The image net of RESNET has 152 layers that are 8X more important than VGG's nets and has fewer limits. VGG-19 is the most cutting-edge advancement that was presented at ILSVRC 2014. The clear 34-layer association (focus) was acknowledged to be the VGG-19's more significant association, having a further evolved convolution layer **[24]**. The major layer 34-layer RENET (Extra Association) with the thought of a simple course affiliation or skip interface.

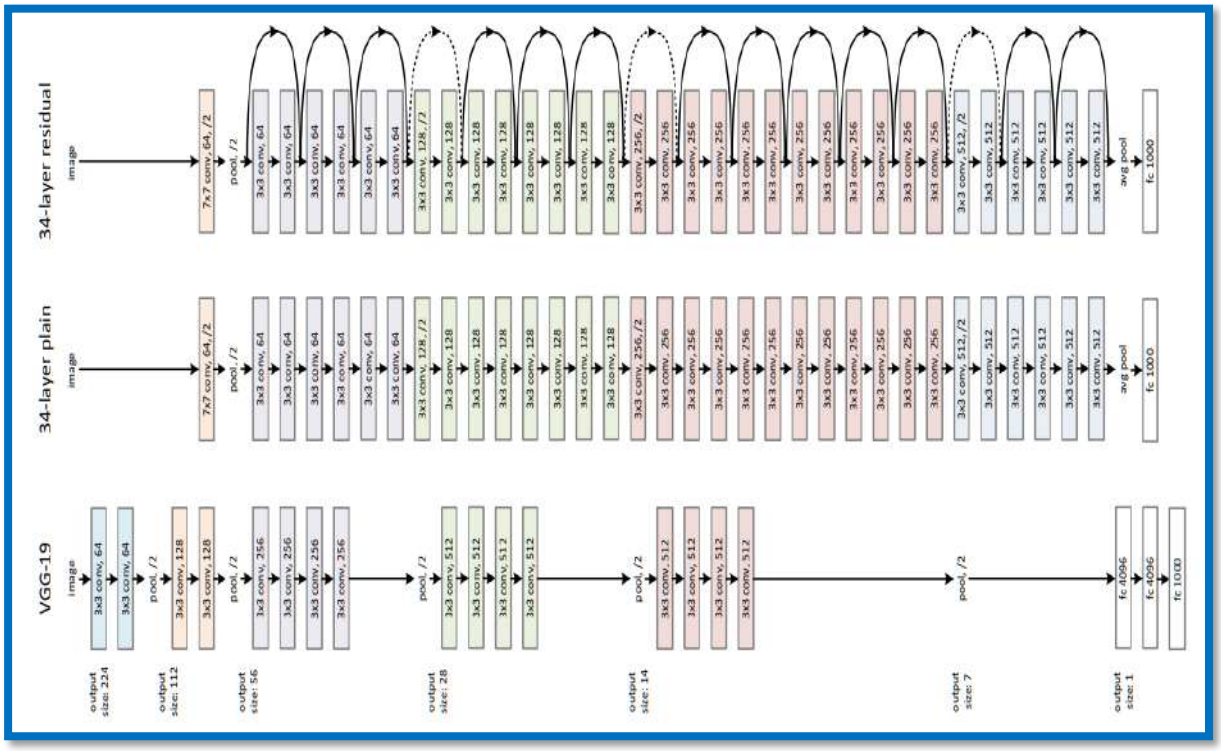

Figure 5: Proposed Architecture

4. Results and Discussion

The methodology used to parcel frontal cortex diseases has been supported by appraisal estimations, which are by and large utilized in a grouping of definite imaging applications. Evaluation estimations are relevant to the sub-locales referred to. The suitability of division is assessed by differentiating it and the division of the ground truth of a comparative image made by a gathering of radiologists. The Dice Equivalence Coefficient is generally used to choose the degree of resemblance between two photographs. Expressness, responsiveness, and exactness assessments are used to review the closeness of images, too. The DSC concludes the level of consideration that is accessible between the frontal cortex tumors-segmented images and the genuine image. The TP (certified positive) is the amount of development pixels that can be unequivocally perceived. The FPS (false certain) is the number of pixels that can be gainfully perceived from non-development-related ones **[17, 23]**. The deceptive negative (false negative) is how many non-development related pixels that are not true form apparent and. The signs of responsiveness show and expressness, study the reasonability of the proposed development division system. The precision of the activity is in relationship with the expressness and mindfulness measures. The maxim "positive expected regard" (PPV) is a proportion of the rate from the total of both FP and the TP.

Table 1: Performance Comparison of Proposed Methodologies

	Dice Score			Specificity			Accuracy			Precision		
	Core	En	Whole	Core	En	Whole	Core	En	Whole	Core	En	Whole
CNN (Pereira, 2016)	0.89	0.93	0.85	0.832	0.83	0.83	0.81	0.83	0.80	0.95	0.95	0.91
U-Net (Ronneberger, 2015)	0.86	0.87	0.85	0.80	0.83	0.82	0.78	0.879	0.80	0.90	0.90	0.91
Unet-res (Kermi, 2019)	0.91	0.94	0.86	0.82	0.87	0.88	0.82	0.85	0.83	0.90	0.93	0.921
ResNet (2020)	0.92	0.95	0.85	0.82	0.90	0.90	0.83	0.89	0.85	0.96	0.97	0.91

In this section, we applied our model on the use of the "Psyche Disease Division Challenge (Pixies) 2020," to arrange mind developments considering X-ray analyses. We overviewed our model by standing out it from the proposed model by using three particular division procedures: CNN (U-Net) and U-Net with waiting blocks (Unet-Res). In the above table, we compare the performance of different neural network models (CNN, U-Net, Unet-res, and ResNet) on segmentation tasks. The performance is evaluated using four metrics: Dice Score, Specificity, Accuracy, and Precision across three different segmentation targets (Core, En, and Whole). ResNet (2020) shows the best overall performance, particularly excelling in Dice Score, Specificity, and Precision for En and Core segments. Unet-res (Kermi, 2019) also demonstrates strong performance, especially in Dice Score and Precision. CNN (Pereira, 2016) and U-Net (Ronneberger, 2015) perform well but generally fall short compared to the more recent models, particularly in Specificity and Accuracy.

Table 2: Calculating Average Computation Time

Technique	Computation Time
U-NET	344 min
Unet-res	277 min
CNN	151 min
ResNet	63 min

In this above table we compared the average computation time required by various neural network models (U-NET, Unet-res, CNN, and ResNet) for processing:

Summary of Computation Time:

- U-NET
  - Computation Time: 344 minutes
  - Insight: U-NET takes the longest time to compute among the listed models.
- Unet-res
  - Computation Time: 277 minutes

- Insight: Unet-res is faster than U-NET but still requires significant computation time.

➢ CNN

- Computation Time: 151 minutes
- Insight: CNN is considerably faster than both U-NET and Unet-res.

➢ ResNet

- Computation Time: 63 minutes
- Insight: ResNet is the fastest model, taking the least amount of time to compute.

➢ Results

- ResNet demonstrates the best computational efficiency with the shortest computation time.
- CNN is also relatively efficient, taking less than half the time of Unet-res.
- Unet-res and U-NET require more computation time, with U-NET being the most time-consuming.

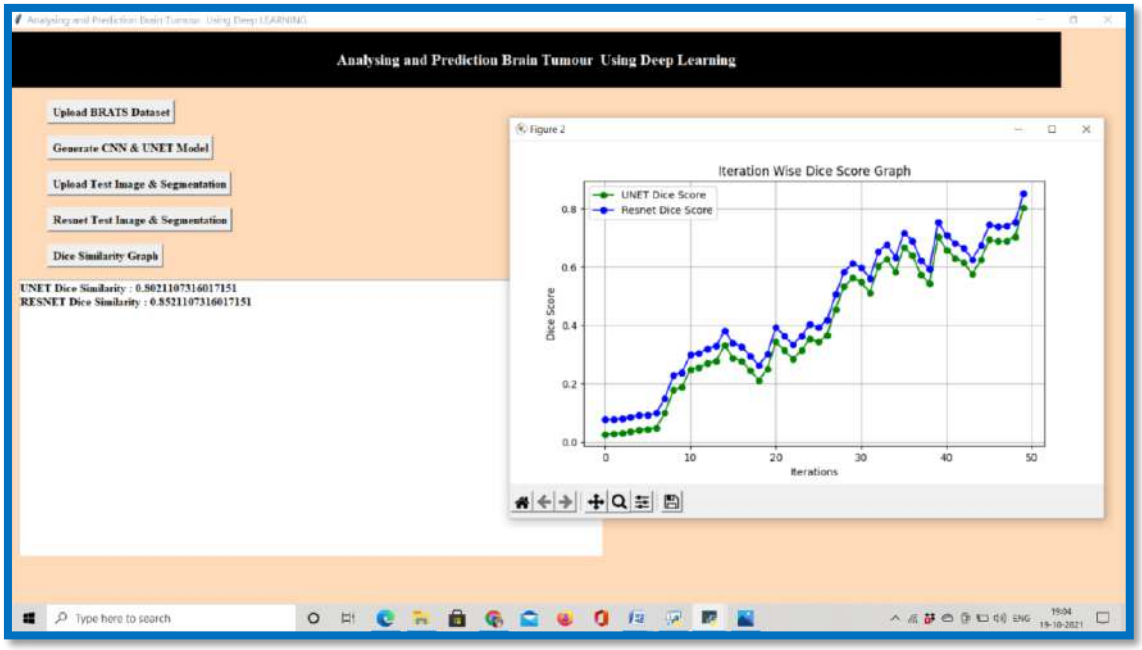

Figure 6: Dice Similarity Graph

In the chart over the x-center tends to the number of cycles used in the planning of the two models at each rising age, it is evident that the equivalence of the two models among expected and remarkable images extended, yet ResNet gained resemblance to the first and expected images, so its score is higher appeared differently in relation to UNET. The graph shows that the green line tends to be the UNET score while the blue line is the score for RESNET.

5. Conclusion

Development division is a key part of the treatment of malignancies in any construction. Significant Mind Associations are convincing division procedures. Regardless, they've gone up against obscuring incline gives that arise during the time spent learning. This investigation proposes a response known as" the Extra Association to beat this issue. It is a"character simple course organization" in ResNet that permits the slant to be multiplied back to the layers going before it. To the extent of accuracy and handling time, the procedure defeats existing CNN, FCN (U-Net), and Un-Res techniques. When appears differently in relation to substitute ways, the strategy is prepared for achieving an immaterial estimation time running off (on various occasions more useful). The proposed technique might be utilized to recognize Low-quality GLIOMAS. The component extraction strategy for LGG frontal cortex developments incorporates alterations to the model plan or structure settings to give higher division results. This will extend the exactness, accuracy, and trustworthiness of X-ray based development division.

6. References

[1] Saouli R, Akil M, Kachouri RJCm, biomedicine pi. Fully automatic brain tumor segmentation using end-to-end incremental deep neural networks in MRI images. 2018;166:39-49.

[2] Goetz M, Weber C, Binczyk F, Polanska J, Tarnawski R, Bobek-Billewicz B, et al. DALSA: Domain adaptation for supervised learning from sparsely annotated MR images. 2015;35(1):184-96.

[3] Louis DN, Perry A, Reifenberger G, Von Deimling A, Figarella-Branger D, Cavenee WK, et al. The 2016 World Health Organization classification of tumors of the central nervous system: a summary. 2016;131:803-20.

[4] Farahani K, Menze B, Reyes MJUhwbo. Brats 2014 Challenge Manuscripts (2014). 2014.

[5] Bengio Y, Courville A, Vincent PJItopa, intelligence m. Representation learning: A review and new perspectives. 2013;35(8):1798-828.

[6] Hinton GE, Osindero S, Teh Y-WJNc. A fast learning algorithm for deep belief nets. 2006;18(7):1527-54.

[7] Bengio Y, Lamblin P, Popovici D, Larochelle HJAinips. Greedy layer-wise training of deep networks. 2006;19.

[8] Lee H, Ekanadham C, Ng AJAinips. Sparse deep belief net model for visual area V2. 2007;20.

[9] Srivastava RK, Greff K, Schmidhuber JJAinips. Training very deep networks. 2015;28.

[10] Wang G, Li W, Ourselin S, Vercauteren TJFicn. Automatic brain tumor segmentation based on cascaded convolutional neural networks with uncertainty estimation. 2019;13:56.

[11] Wang J, Yang Y, Mao J, Huang Z, Huang C, Xu W, editors. Cnn-rnn: A unified framework for multi-label image classification. Proceedings of the IEEE conference on computer vision and pattern recognition; 2016.

[12] Mukherjee P, Mukherjee A. Advanced processing techniques and secure architecture for sensor networks in ubiquitous healthcare systems. Sensors for health monitoring: Elsevier; 2019. p. 3-29.

[13] Menze BH, Jakab A, Bauer S, Kalpathy-Cramer J, Farahani K, Kirby J, et al. The multimodal brain tumor image segmentation benchmark (BRATS). 2014;34(10):1993-2024.

[14] Bauer S, Wiest R, Nolte L-P, Reyes MJPiM, Biology. A survey of MRI-based medical image analysis for brain tumor studies. 2013;58(13):R97.

[15] Leece R, Xu J, Ostrom QT, Chen Y, Kruchko C, Barnholtz-Sloan JSJN-o. Global incidence of malignant brain and other central nervous system tumors by histology, 2003–2007. 2017;19(11):1553-64.

[16] Dolecek TA, Propp JM, Stroup NE, Kruchko CJN-o. CBTRUS statistical report: primary brain and central nervous system tumors diagnosed in the United States in 2005–2009. 2012;14(suppl_5):v1-v49.

[17] Mukambika P, Uma Rani KJIRJET. Segmentation and classification of MRI brain tumor. 2017;4(07):683-8.

[18] Stupp R, Hegi ME, Mason WP, Van Den Bent MJ, Taphoorn MJ, Janzer RC, et al. Effects of radiotherapy with concomitant and adjuvant temozolomide versus radiotherapy alone on survival in glioblastoma in a randomised phase III study: 5-year analysis of the EORTC-NCIC trial. 2009;10(5):459-66.

[19] Pereira S, Pinto A, Alves V, Silva CAJItomi. Brain tumor segmentation using convolutional neural networks in MRI images. 2016;35(5):1240-51.

[20] Bakas S, Reyes M, Jakab A, Bauer S, Rempfler M, Crimi A, et al. Identifying the best machine learning algorithms for brain tumor segmentation, progression assessment, and overall survival prediction in the BRATS challenge. 2018.

[21] Menze BH, Van Leemput K, Lashkari D, Weber M-A, Ayache N, Golland P, editors. A generative model for brain tumor segmentation in multi-modal images. Medical Image Computing and Computer-Assisted Intervention–MICCAI 2010: 13th International Conference, Beijing, China, September 20-24, 2010, Proceedings, Part II 13; 2010: Springer.

[22] Bakas S, Akbari H, Sotiras A, Bilello M, Rozycki M, Kirby JS, et al. Advancing the cancer genome atlas glioma MRI collections with expert segmentation labels and radiomic features. 2017;4(1):1-13.

[23] Spyridon B, Hamed A, Aristeidis S, Michel B, Martin R, Justin K, et al. Segmentation labels and radiomic features for the pre-operative scans of the TCGA-LGG collection. 2017.

[24] Simonyan KJapa. Very deep convolutional networks for large-scale image recognition. 2014.

Al-Kitab Journal for Pure Sciences (2025); 9(1):144-163.
https://doi.org/10.32441/kjps.09.01.p10

Al-Kitab Journal for Pure Sciences
ISSN: 2617-1260 (print), 2617-8141(online)
https://isnra.net/index.php/kjps

Azo Compounds and their Potential Applications: Article Review

Zainab Radhi Al-Majdi[1], Wedad Hamad Al-Dahhan[1,2], Mehdi Salih Shihab[1], Mehdi Honarvar Nazari[3]

[1]Department of Chemistry, College of Science, Al-Nahrain University, Jadriah, Baghdad, Iraq.
[2]Higher Institute of Forensic Sciences, Al-Nahrain University, Baghdad, Iraq
[3]Laboratory of Corrosion Science & Electrochemical Engineering (CSEE), Department of Civil & Environmental Engineering, Washington State University, USA.

*Corresponding Author: **zainab.mchs22@nahrainuniv.edu.iq**

Citation: Al-Majdi ZR, Al-Dahhan WH, Shihab MS, Nazari MH. Azo Compounds and their Potential Applications: Article Review. Al-Kitab J. Pure Sci. [Internet]. 2025 Feb. 14;9(1):144-163. DOI: https://doi.org/10.32441/kjps.09.01.p10.

Keywords: Azo Dyes, Diazo Coupling Reactions, Anti-Bacterial, Anti-Cancer, Anti-Tuberculosis, Anti-Viral, Material Science.

Article History
Received 19 Jun. 2024
Accepted 23 Jul. 2024
Available online 14 Feb. 2025

Abstract:

A review of the existing body of literature about azo compounds and their practical applications. Azo compounds, which include a (-N=N-) group, serve as the fundamental structure for several produced compounds in different fields of chemistry, particularly coordination chemistry. These compounds are extensively utilized as coloring agents, as they account for around fifty percent of synthetic colors. Azo compounds are a significant class of chemicals with different applications in various fields of life. Due to the wide variety of their applications, it is essential to possess different synthesis techniques in order to get new azo derivatives with high yields. The main viable techniques for synthesizing azo compounds are diazotization and azo coupling reactions. Azo compounds have diverse uses in areas including anticancer, antifungal, antioxidant, anti-inflammatory, and anti-bacterial activities. In addition, it has several additional uses such as coloring fiber, printing systems, photo-electronics, polymer additives, and storage, and providing resistance to solvents, water, light, and weather.

Keywords: Azo Dyes, Diazo Coupling Reactions, Anti-Bacterial, Anti-Cancer, Anti-Tuberculosis, Anti-Viral, Material Science.

مركبات الآزو وتطبيقاتها المحتملة: مقالة مراجعة

زينب راضي المجدي[1]، وداد حمد الدهان[1,2]، مهدي صالح شهاب[1]، مهدي هونارفر نزاري[3]

[1]قسم الكيمياء، كلية العلوم، جامعة النهرين، الجادرية، بغداد، العراق.
[2]المعهد العالي للعلوم العدلية، جامعة النهرين، بغداد، العراق
[3]مختبر علوم التآكل والهندسة الكهروكيميائية، قسم الهندسة المدنية والبيئية، جامعة ولاية واشنطن، الولايات المتحدة الأمريكية

zainab.mchs22@nahrainuniv.edu.iq, wedad.aldahhan@nahrainuniv.edu.iq, mahdi.shihab@nahrainuniv.edu.iq, m.honarvarnazari@wsu.edu

الخلاصة:

تتضمن هذهِ المقالة مراجعة للأدبيات الموجودة حول مركبات الآزو واستخداماتها العملية. تعمل مركبات الآزو، والتي تتضمن مجموعة *(-N=N-)*، بمثابة البنية الأساسية للعديد من المركبات المنتجة في مجالات مختلفة من الكيمياء، وخاصة الكيمياء التناسقية. وتستخدم هذه المركبات على نطاق واسع كعوامل تلوين، حيث إنها تمثل حوالي خمسين بالمائة من الألوان الاصطناعية. مركبات الآزو هي فئة مهمة من المواد الكيميائية ذات تطبيقات مختلفة في مختلف مجالات الحياة. ونظرًا للتنوع الكبير في التطبيقات، فمن الضروري امتلاك تقنيات تركيبية مختلفة للحصول على مشتقات آزو جديدة ذات إنتاجية عالية. التقنيات الرئيسية القابلة للتطبيق لتصنيع مركبات الآزو هي تفاعلات اقتران الآزو. تتمتع مركبات الآزو باستخدامات متنوعة في مجالات تشمل الأنشطة المضادة للسرطان والفطريات ومضادات الأكسدة والمضادة للالتهابات والمضادة للبكتريا بالإضافة إلى ذلك، له عدة استخدامات إضافية مثل تلوين الألياف، وأنظمة الطباعة، والإلكترونيات الضوئية، وإضافات البوليمر، والتخزين، وتوفير مقاومة للمذيبات، والماء والضوء والطقس.

الكلمات المفتاحية: أصباغ الآزو، تفاعلات اقتران داي ازو، مضاد للبكتيريا، مضاد للسرطان، مضاد للسل، مضاد للفيروسات، علم المواد.

1. Introduction:

Azo compounds exhibit distinct color features because they have a chromophore group (-N=N-) attached to aromatic or heterocyclic systems. [1]. Azo days contain at least one nitrogen-nitrogen double bond, and they can exist in various structural forms [2]. Azo dyes, being widely used in numerous industries, are the oldest and broadest category of industrially manufactured organic dyes [3]. Their applications in coloring fabrics, leather, paper, food, and cosmetic items [4], [5], as well as their applications in biomedical research as well as studies [6]. Furthermore, it found use in the most advanced fields including laser technology photodynamic treatment [7], and dye-sensitized solar cells [8]. Diazotization and coupling reactions are two easy methods for producing these dyes. To increase the dispersibility of the dye, several approaches and modifications are utilized to achieve the required color properties, income, and particle dimensions [9]. Azo dyes are the most prevalent category of dyes, comprising almost 60% of the overall dye composition [10]. Azo dyes constitute nearly 70 percent of the dyes used in the industrial sector [11]. The azo group, represented by the chemical

formula N=N-, is a chromophore group that gives color to azo dyes. Azo dyes can include a single or several auxochromic groups, which are functional groups [12]. Azo dyes could exhibit an enormous variety of colors, including yellow, orange, red, blue, and green. The two nitrogen atoms have a double bond that allows light in the visible spectrum to be absorbed, which is what gives the color, namely wavelengths ranging from 400 to 750 nm [13].

2- Material and Methods:

2.1 General Properties of Azo Compounds: The presence of the -N=N- functional group is indicative of the presence of azo compounds [14]:

- The structures of aromatic azo compounds are more stable than those of compounds with alkyl groups because the R groups in these compounds are arene rings.
- This occurs because the arene groups and the (-N=N-) group form an extended delocalized system.
- The aromatic azo groups are typically employed as dyes due to their high color intensity.
- A diazonium salt and a coupling agent undergo a coupling reaction to produce aromatic azo compounds.

2.2 Types of Azo Compounds: Azo chromophores are a distinct category of organic substances that function as colorants. Their basic structural framework is characterized by the absence of azo groups. The presence of two azo groups is referred to (bis-azo). Compound 2, specifically known as 6-hydroxy-1,4-dimethyl-2-oxo-5-((4 (phenyldiazenyl) phenyl) diazenyl)-1,2-dihydropyridine-3-carbonitrile, has two fundamental azo structures. Occasionally, there might be three groups (tris-azo), four groups (tetrakis-azo), or even more (poly-azo) under certain circumstances, but this occurrence is rare. See (**Figure 1**) [15].

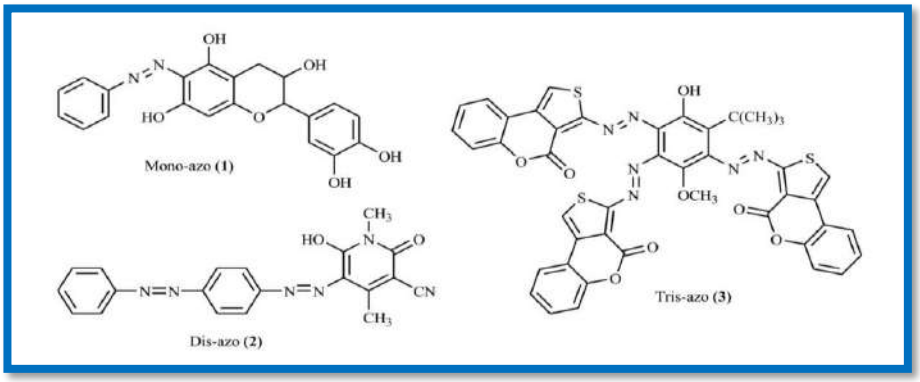

Figure 1: Chemical structures of azo dyes with different numbers of azo groups [15]

2.3 Diazo Coupling Reactions:

- In a diazo coupling reaction, the doazonium salt reacts with an additional arene to form a coupling agent.
- The coupling agent's benzene ring undergoes a reaction with the diazonium salt, which functions as an electrophile.

- When a frigid solution of diazonium salt is added to a solution containing the coupling agent, a colored precipitate of an azo compound is generated; several of these compounds are used as dyes.
- Usually, the coupling agent works in one of the Benzene Ring's two or four locations (the functional group is located in position four).
- The color of the chemical produced is contingent upon the coupling agent that is being reacted with the diazonium salt, **Scheme1 [16]**.

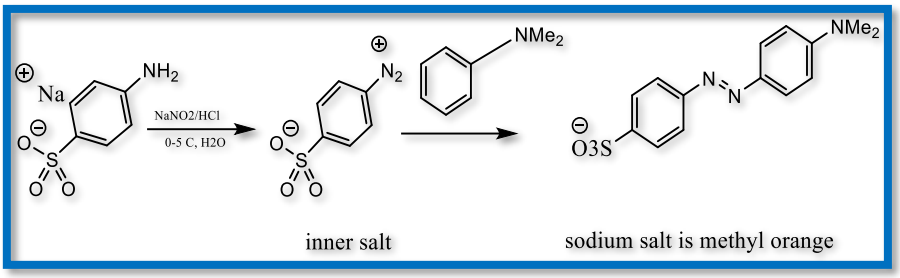

Scheme 1: Diazo coupling reaction

2.4: Applications for Azo Dyes: Azo dyes are commonly utilized in several sectors like textile, fiber, cosmetics, leather, paint, and printing. Azo compounds have been shown to possess antibacterial, antiviral, anti-fungal, and cytotoxic properties, in addition to their involvement in coloring (**Figure 2**) **[17]**.

Figure 2: Applications of azo dyes [17]

They possess the ability to act as drug carriers **[18]**. (**Figure 3**) may function as a carrier that captures therapeutic substances or can use a prodrug approach. The administration of the medication is triggered by either internal or external stimuli specifically inside the area of interest, as shown in colon-targeted drug delivery. Furthermore, certain azo dyes are used in cellular staining to examine cellular components and metabolic processes, in addition to their drug-like qualities and the ability to act as drug carriers (**Figure 4**) **[19]**.

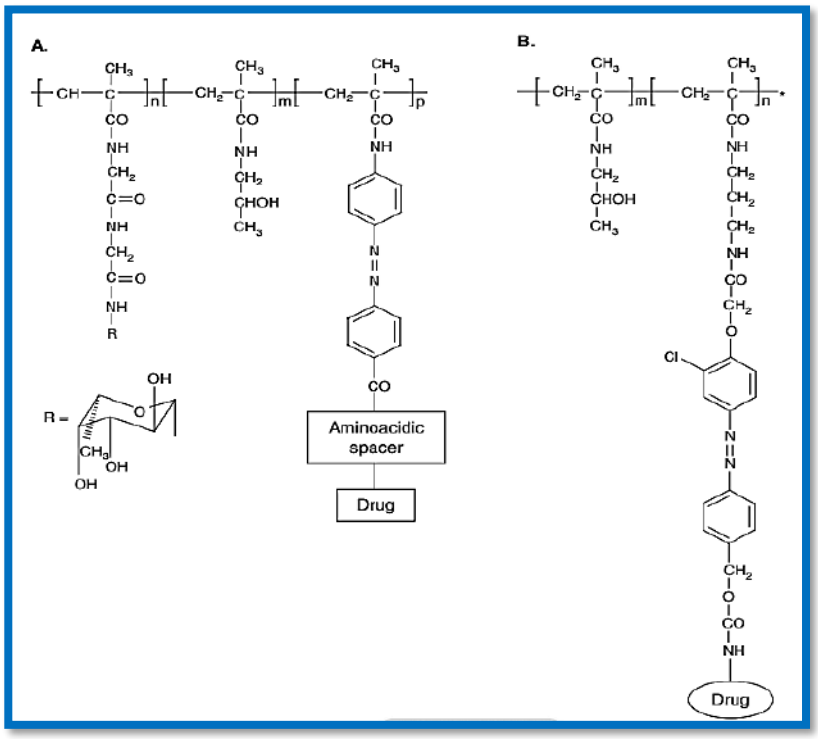

Figure 3: Structures Of Bioadhesive, Colon-Specifi C Hydroxypropyl Ethacrylamide Copolymers Containing: A.An Aminoacid Spacer, And B.A Self-Eliminating Group [18]

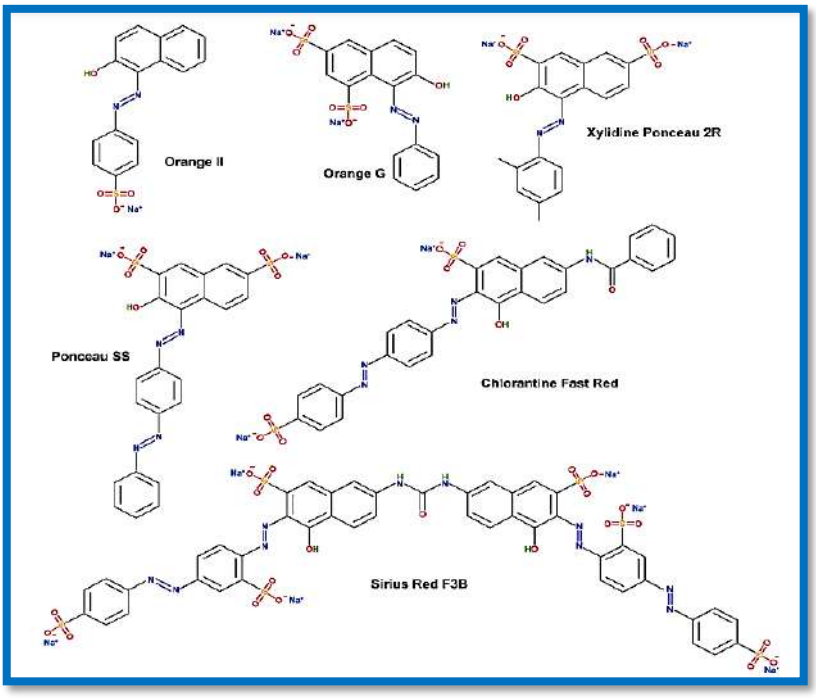

Figure 4: Examples Of Sulfonated Azo Dyes That Are Frequently Used to Stain Proteins [19]

Nevertheless, the biological role of azo compounds, specifically in the field of chemotherapy for cancer, is still in its early stage of development. These findings may be linked to the first discovery that revealed azo compounds as possible factors in the development of cancer and mutagenesis. Presently, scientists are investigating aromatic azo compounds to evaluate their

potential in the realm of biomedicine, namely for the purposes of cancer diagnostics and treatment [20]. Generally, due to the extensive potential of heterocycle-containing azo dye bk derivatives in pharmaceutical and drug research, there is still a lack of sufficient information on their usage [21]. Currently, there is a significant focus on the generation of azo dyes and their derived compounds that include heterocycles. The reason for this is that these compounds have shown potent biological activity, like chemosensing properties, analgesic properties, antibacterial, antifungal, antiviral, anticonvulsant, anti-diabetic, anti-inflammatory, anti-tubercular, and anticancer DNA binding properties. Herein, we show an overview of the production of several azo dyes and their by-products including heterocycles. Additionally, we discuss their potential medicinal characteristics (Figure 5) [22].

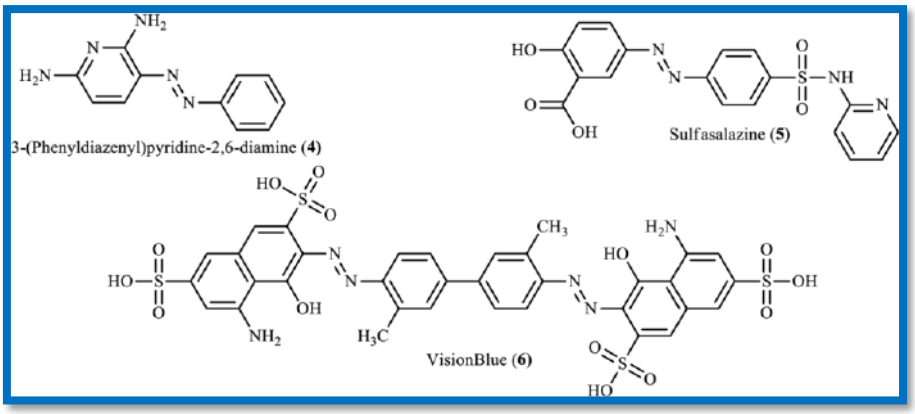

Figure 5: Chemical structures of azo-based drugs [22]

2.5 Food Industries: Azo dyes provide around seventy percent of all organic dyes produced worldwide, making them the biggest class of synthetic food colors [23, 24]. Furthermore, it has been shown that the yellow dyes (tartrazine and sunset yellow) and red dyes (azorubine, ponceau, amaranth, and Allura red) are the most widely used azo dyes in the food business. They are often added to jams, candies, confections, ice cream, jellies, alcoholic beverages, soft drinks, and other goods of a similar kind to provide color. Although widely used, several investigations have identified specific adverse effects on human health. There is sufficient evidence indicating that the decomposition of azo dyes produces toxic and carcinogenic compounds, such as aromatic amines. The relationships between azo dyes, hemoglobin, and human serum albumin have been verified by recent studies [25, 26]. According to some studies, youngsters who use artificial food coloring may become more stimulated and active, particularly if they use it often. Moreover, they could have the potential to lead to the development of asthma and allergy conditions. Therefore, it is crucial to regulate the levels of azo compounds in food products (Figure 6) [27].

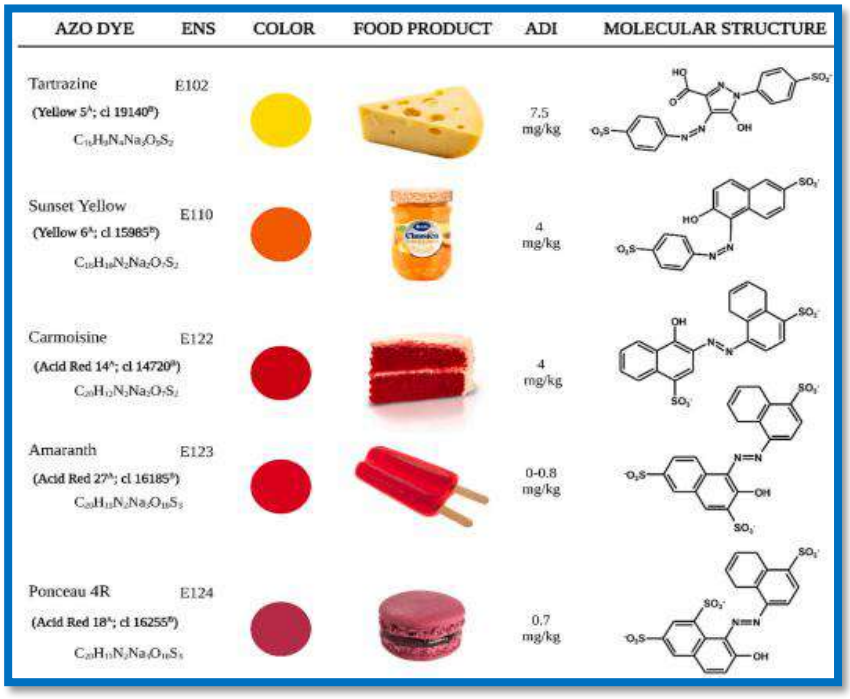

Figure 6: Features Of the Azo Compounds Most Utilized in The Food Industrial [27]

2.6 Textile of Azo Dyes: Approximately four decades ago, the pigment known as indigo was discovered under the wrappings of mummified bodies within Egyptian tombs, marking the first occurrence of an organic colorant. Every year, the globe produces more than 7,107 tons of dyestuff, and there are over 100,000 dyes that are available for purchase. Among the many uses for these dyes, the textile sector accounts for the lion's share, followed by the food and cosmetics industries, and paper printing **[28]**. Synthetic organic dyes, including processing dyes, reactive dyes, and direct dyes, are now the mainstay of the textile industry. The term "natural dye" encompasses any colorant derived from elements found in nature, including but not limited to plants, animals, and minerals. In order to apply non-substantive natural dyes to textiles, it is necessary to utilize mordants, which are usually metallic salts. These mordants exhibit a strong attraction to both the dye and the fiber **[29]**. The textile processing industries are the primary users of synthetic dyes, which are widely employed in other sectors. (**Figure 7**) **[30]**.

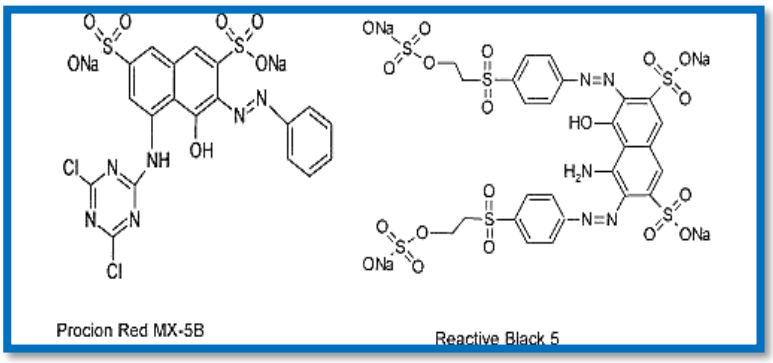

Figure 7: Azo Dyes in Textile Industry [30]

Perkin was a trailblazer in the production of synthetic organic dye, namely mauve, as far back as 1856. In 1871, Wolfe created the first synthetic organic dye by using nitric acid to process the natural color indigo, resulting in the production of picric acid. Since then, a plethora of other chemical dyes have been included in the ever-growing collection of dyes **[31]**. The textile sector utilizes around 70 percent of all dyestuffs. When dying or printing on cotton, you must use reactive dyes, vat dyes, or azo dyes. At approximately 21% of the total, disperse dyes make up the biggest category in the industry. There is a 16 percent share for direct dyes and an 11 percent share for reactive dyes in the market. One common way to categorize textile dyes is by the chemicals they contain, but another is by the many purposes they have in the textile industry (**Figure 8**) **[32]**.

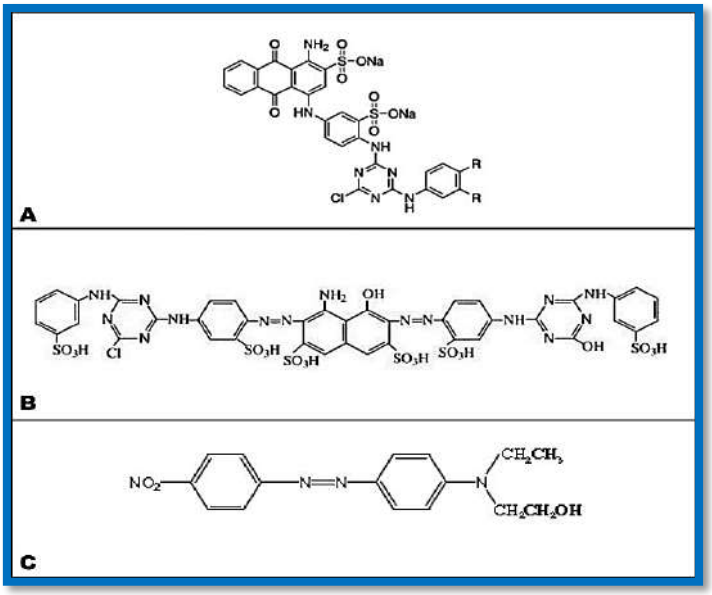

Figure 8: The chemical compositions of the textile dyes that were investigated are as follows: (A) reactive blue 2 (anthraquinone dye); (B) reactive green 19 (azo dye); (C) diffuse red 1 (azo dye) [32]

2.7 Azo Dyes in Material Science: Azo dyes possess high photosensitivity and demonstrate both linear and nonlinear optical characteristics. These properties are utilized in the development of optical storage devices, semiconductors, photovoltaic cells **[33]**, holographic recording using azo dye-doped polymers **[34]**, optical computing **[35]**, and dye-sensitized solar cells **[36]**. Researchers Asif et al, conducted a study on five azo dyes, namely Direct Red 111, Acid Orange 5, Food Yellow 6, Metanil Yellow, and Acid Orange 61. Their electrical and nonlinear optical characteristics were determined using DFT. They exhibited three clearly differentiated categories of azo dye: two with an acidic nature and one with an alkaline nature. The introduction of a proton to the dye greatly amplifies the nonlinear optical response. It is crucial that optical characteristics not be linear for optical data processing devices, modulators, ultra-fast optical switches, sensors, and high-density optical storage systems **[37]**. The great

optical and thermal properties, together with the excellent photosensitivity and photo-isomerization capabilities, of azo dyes have led to their usage in recording devices and high-density optical storage [38]. Azo dyes possess desirable optical, thermal, and electrical characteristics, making them appealing for use in dye-sensitized solar cells (DSSCs). Additionally, they exhibit robust chemical stability. Azo DSSCs have higher priority over standard semiconductor photovoltaic cells because they are more cost-effective, readily accessible, and exhibit greater efficiency. When an azo dye molecule is excited, it undergoes oxidation, which increases its conductivity by bringing one electron into the conduction band. The electrolyte's iodide content makes it easier for electrons to get through, which oxidizes the dye molecule. The oxidized dye molecule is then restored to its initial form by reduction by triiodide [39]. Louis et al, have examined C.I. Disperse Yellow 56 (DA, DB, DC), a commercially available dye, and two mono azo dyes derived from 1-nitroso-2- and 2-nitroso-1-naphthol (**Figure 9**). The optical properties, energy band gaps, and charge transfer electron excitation of these dyes were the primary areas of investigation in the research. According to the findings, the excited state of the dyes resides above TiO_2's conduction band and has the potential to swiftly introduce electrons into the semiconductor. To get the best possible photocurrent response, the chosen molecules must have high light-harvesting efficiency (LHE). The best result (0.7308 for dye DC) is shown by acetone. The results of this study, the dyes exhibit favorable characteristics and might potentially be used as photosensitizers in DSSC [40]. In DSSC devices, azo dyes have shown very high conversion efficiencies. Because of their high molar extinction coefficient, ease of synthesis, and lack of environmental effect, these dyes have various benefits over other photosensitive compounds. They also include an azo (-N = N-) chromophore [40].

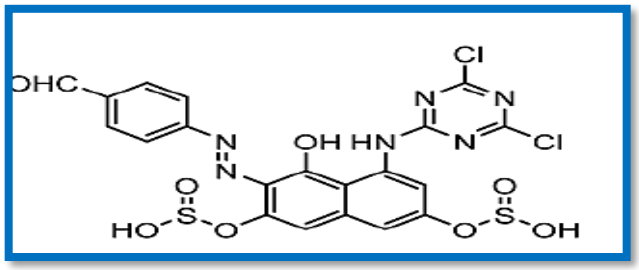

Figure 9: Azonitrobenzaldehyde Derivatives [40]

2.8 Antibacterial Azo Dyes: Antimicrobial efficacy, which involves combating microorganisms and inhibiting their growth, depends entirely on the presence of chemicals that accomplish this discreetly and without causing substantial harm to surrounding tissues. Antimicrobial compounds may be classified as either bactericidal or bacteriostatic, based on whether they have the ability to kill bacteria or only inhibit their growth. The increasing

resistance of germs to antibacterial treatments is causing significant health consequences. This problem motivates research aimed at identifying new chemicals that can efficiently inhibit bacterial growth. Azo dyes exhibit strong antibacterial efficacy and can either kill or prevent the growth of microorganisms, making them bactericidal or bacteriostatic, respectively, through their specific mechanisms of action **[41]**. Studying the in-vitro antibacterial properties of oxazolone azo dyes against certain gram-negative and gram-positive bacteria, Fawzia et al, examined Streptococcus pneumoniae, Bacillus subtilis, Pseudomonas aeruginosa, and Escherichia coli. As standards, Ampicillin and Gentamicin were used in the agar diffusion technique to determine various amounts. When contrasted with the reference medications, the findings demonstrated that the dyes showed encouraging promise. The investigation revealed that the oxazolone azo chromophore derivatives were effective against both gram-positive and gram-negative bacteria, with moderate to high efficiency against Streptococcus pneumonia and Bacillus subtilis, respectively. On the other hand, gram-negative bacteria, such as Pseudomonas aeruginosa, were not effectively combatted by them **[42]**. These creative azo dyes, namely 3-[(E)-(4-hydroxyquinolin-5-yl) diazenyl], were developed by Shoukat et al. Its molecular formula is 4-[(E)-(4-hydroxyquinolin-5-yl) diazenyl]-4-methylbenzoic acid-(a).6-Methoxybenzoic acid-(b) is the name of the chemical. Diazenyl, 4-[(E)-(4-hydroxyquinolin-5-yl)] \ Trimethylbenzoic acid-(c),5-[(E)-(4-hydroxyquinolin-5-yl) diazenyl is the chemical name of the substance. A combination of amino-methylbenzoic acid and 8-hydroxy quinoline is used to create 2-methylbenzoic acid-(d). Using the disk diffusion technique and Amoxycillin as the reference medication, the antibacterial activity of the azo dyes is next evaluated against Pseudomonas Aureus and Streptococcus Aureus. Furthermore, their ability to inhibit the growth of Fusareum Oxyporum is assessed by means of the cup plate technique, with fluconazole serving as the reference antifungal medication. The outstanding antimicrobial capabilities and accessible availability of azo dyes make them a preferred ingredient in compounds with antibacterial and antifungal properties. On top of that, they are inexpensive and easy to prepare (**Figure 10**) **[43]**.

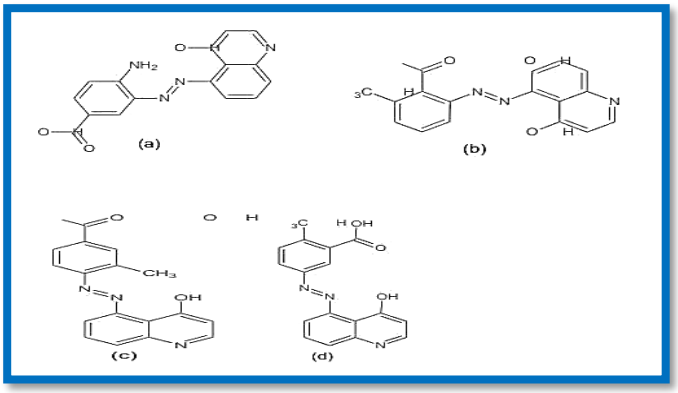

Figure 10: Amino-Methyl Benzoic Acid Derived Azo Dyes [43]

2.9 Antiviral Azo Dyes: The development of antiviral treatment is challenging due to the fact that viruses are intracellular parasites that depend on their hosts for energy, machinery for macromolecular synthesis, and workstations for genome replication and particle assembly **[44]**. There are two main methods for developing antiviral drugs: one is to focus on the elements of the host cell, while the other is to directly target the viruses. Antiviral drugs that specifically target viruses include uncoating inhibitors, polymerase inhibitors, protease inhibitors, nucleoside and nucleotide reverse transcriptase inhibitors, and integrase inhibitors. A plethora of therapies have been devised to counteract herpes viruses, and influenza, as well as innovative antiviral drugs for the control of hepatitis C infection and HIV. Experimental research has shown that azo dye has promise as a prospective antiviral treatment. Its mechanism of action involves the suppression of pathogen proliferation, interference with protein production, and prevention of viral attachment to host cells (**Figure 11**) **[45]**.

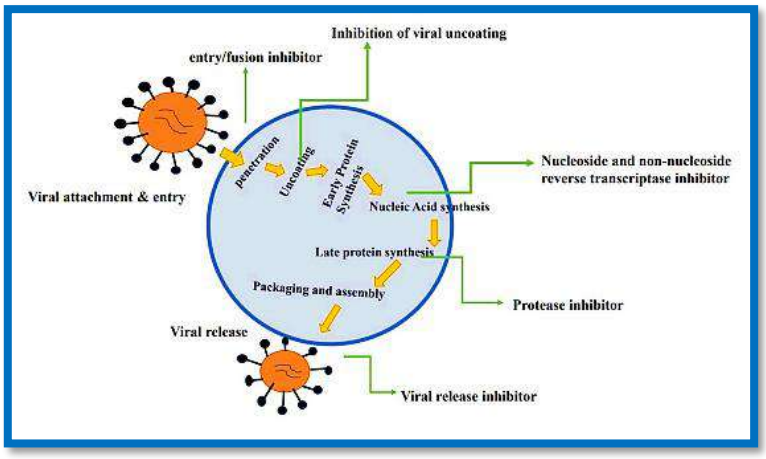

Figure 11: General Antiviral Action of Mechanism [45]

Research on human enteroviruses, including EV71, CVA16, and CVA6, was carried out by Meng et al. The primary focus of the research was to determine whether or not brilliant black bn, a sulfonated food azo dye, might limit the infection of these viruses in both laboratory and in vivo conditions. Among children in particular, these human viruses are very contagious and cause hand, foot, and mouth illness. Scientists have discovered that several sulfonated azo dyes, which are often added to food, have potent antiviral properties when tested against human enteroviruses. The capacity to efficiently inhibit all tested strains of CVA16, CVA6, and EV71 was proven by brilliant black BN (E151) and others. E151 and other azo dyes used in food prevented the virus from entering. The release of related viruses was dose-dependent, and dye E151 reduced the binding of EV71. An essential component of the virus's uncoating process, E151 blocked the interaction between EV71 and cyclophilin A. Animal studies shown that AG129 mice were protected against EV71 isolates 10 times the fatal dose when given E151 at

a dosage of 200 mg/kg body weight daily during the first four days of the trial. Taken as a whole, these findings suggest that E151 may effectively combat EV71 infections. The study focused on the synthesis compounds of the azo series (**Scheme 2**) **[46]**.

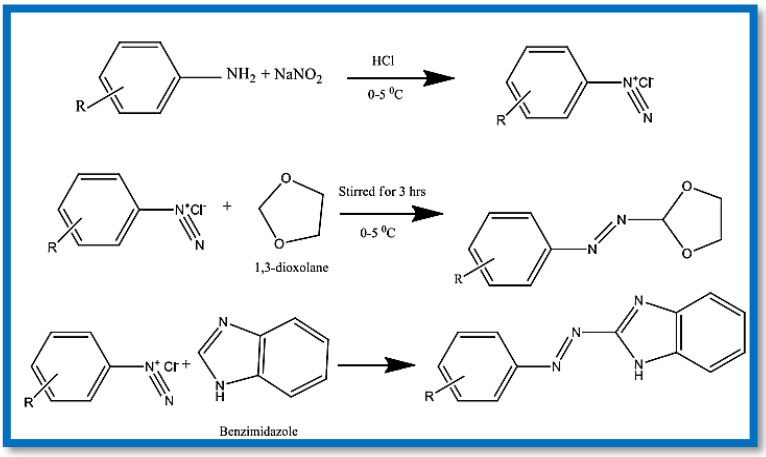

Scheme 2. Synthesis scheme of azo compounds A1-A5

Diazonium salt solutions were coupled with active methylene compounds (1,3-dioxolane and benzimidazole) to produce the compounds listed in the title. This reaction resulted in the formation of [(E)-1-(1,3-dioxolan-2-yl)-2-phenyldiazene] (A1), [(E)-1-(1,3-dioxolan-2-yl)-2-(4-methyl-phenyl)diazene](A2), 2-[(E)-phenyldiazenyl]-1H-benzimidazole](A3), [(E)-1-(1,3-dioxolan-2-yl)-2-(4-ethylphenyl) diazene](A4), and [(E)-1-(1,3-dioxolan-2-yl)-2-(2 methylphenyl)diazene] (A5). Utilizing spectroscopic methods, particularly electron ionization mass spectrometry (EI-MS) and Fourier transform infrared spectroscopy (FT-IR), the molecular structures of the recently produced substances were ascertained. In vivo techniques were used to test compounds against the H9N2 strain of avian influenza and the Lasota strain of Newcastle disease. At a concentration of 0.1 mg/100 µL, the assessment results showed that azo dyes A5 had the strongest anti-NDV and anti-AIV action. Alternatively, when tested at the same doses, the other azo compounds showed reduced activity **[47]**.

2.10 Antitumoral and Anticancer Azo Dyes: Cancer and tumors arise due to abnormal proliferation of cells. Chemotherapy, a commonly used cancer therapy, is cytotoxic and works by inhibiting the growth of cancer cells. Azo dyes have been shown to exhibit cytotoxicity and possess anticancer effects. In vitro, assays are performed to evaluate the antitumoral properties of azo dyes and determine their effectiveness and potential in suppressing tumor growth. This is achieved by reducing the synthesis of DNA, RNA, and proteins inside the cells **[48]**. Conventional procedures were used to synthesize a set of novel azo dye derivatives (**Scheme 3**) using pyrano-quinolinone as the initial substance. The synthesized compounds underwent spectral analysis to determine their chemical properties and were then tested for their anticancer

effects on many human tumor cell lines, examples of cancer cell lines are HepG2 for liver cancer, HCT-116 for colon carcinoma, and MCF-7 for breast cancer. 5-fluorouracil served as a reference medication. The in vitro cytotoxicity screening findings showed that all of the substances tested had significant action against MCF-7 cells. Compounds 6a and 6b have shown exceptional efficacy against three different types of human tumor cell lines **[49]**.

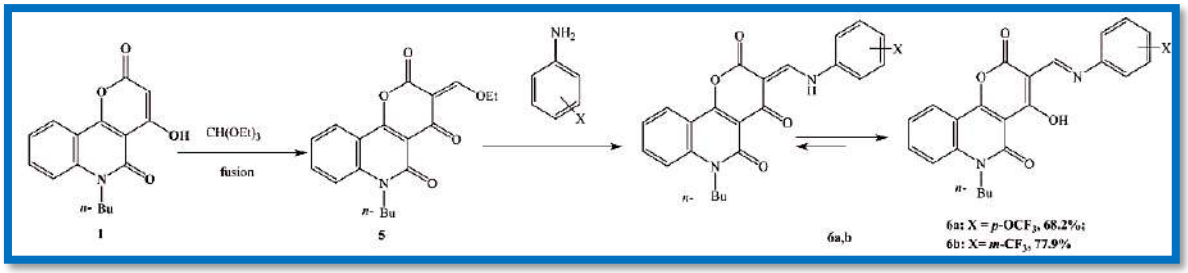

Scheme 3: Synthesis of Compounds 6a, b

The diazo coupling of diazonium salts of 3-substituted-2-amino-4,5,6,7-tetrahydrobenzo[b]thiophenes 1a-c with 3-methyl-1H pyrazol-5(4H)-one, 3-methyl-1-phenyl-1H-pyrazol-5(4H)-one, or 3-amino-1H-pyrazol-5(4H)-one, respectively, was used to synthesize a series of thiophenes 5a-f and 6a-c that incorporate pyrazolone moieties. The color measurements and fastness qualities of recently synthesized dyes were evaluated when applied as dispersion dyes on polyester fabric. When compared to aniline-based azo dyes, they have a high extinction coefficient and a color shift from red to blue. The synthesized colors were tested for their anticancer effects. Compounds 5c and 5d exhibited a moderate degree of activity, whereas the bulk of them showed good activity, according to the data. (**Scheme 4**) **[50]**.

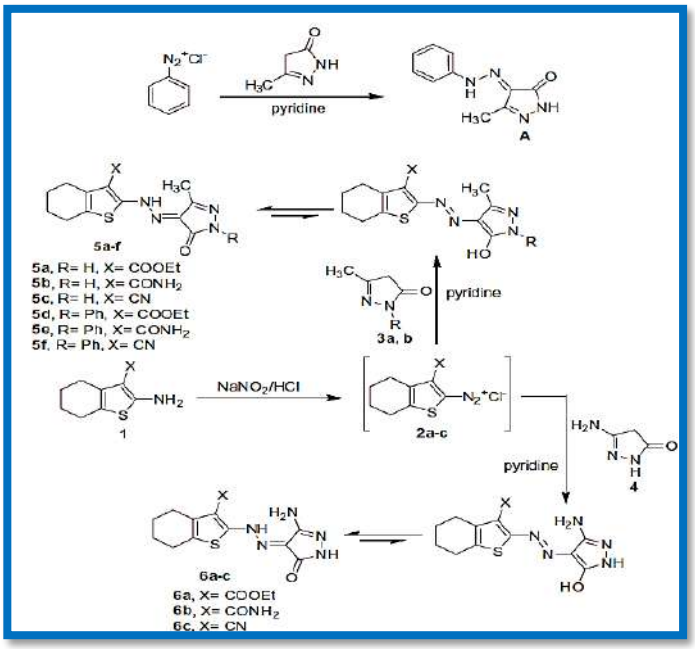

Scheme 4: Preparation of substituted-4- {2- [(or 3-phenyl-)4,5,6,7-tetrahydrobenzo[b]thiophen-2-yl] hydrazono} Derivatives 5 and 6 of -1H-pyrazol-5(4H)-one

Abdalla et al, achieved research on the biological activity of new chelates made from sulfamerazine-resorcinol azo-dye. These chelates were either mono- or homo-bi-nuclear in structure. The chelates were produced by the reaction between sulfamerazine diazonium salt and resorcinol. The investigation revealed that these compounds had potent antibacterial and antitumoral properties, particularly when they formed complexes with anticancer drugs. Out of all the produced complexes, the Ni (II) molecule showed notable promise in suppressing the development of human liver cancer, as assessed in the study **[51]**. By using $NaNO_2$/HCl, a diazotization procedure was carried out on a series of 4-(1-azolyl) aniline derivatives that included azole groups such as benzimidazole, 3-methylpyrazole,4-methylpyrazole, pyrazole, and imidazole. A series of aromatic molecules, including N, N-dimethylaniline, 2-naphthol, 8-hydroxyquinoline, and phenol, were further reacted with the diazonium salts to get the related azo compounds. Some of the items were tested for their antibacterial activity against both Gram-positive (Staphylococcus aureus, ATCC 25923) and Gram-negative (Escherichia coli, ATCC 25922) bacteria. Additionally, they exhibited anticancer characteristics against MCF7 breast cancer cells in laboratory tests performed on a variety of items (**Scheme 5**) **[52]**.

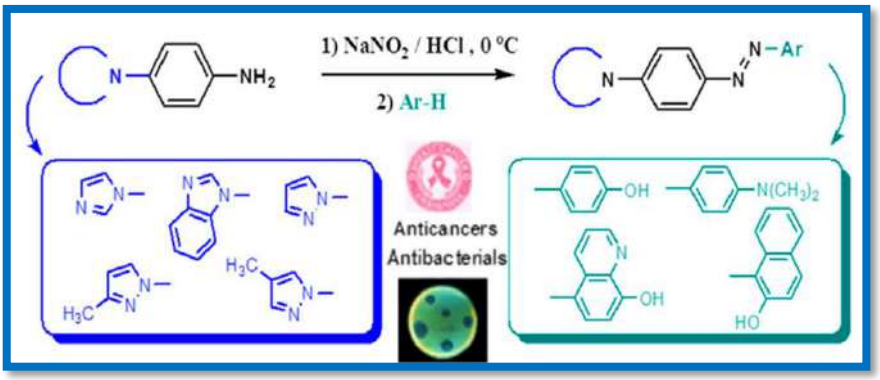

Scheme 5: Steps For Preparation of Azo Derivatives

2.11 Antituberculosis Azo Dye: Tuberculosis is an extremely perilous illness that presents a significant global challenge. Thus, in order to identify a potent medication, the process of synthesizing hydrazone ligands and forming metal complexes with Co (II), Ni (II), Cu (II), and Zn (II) were conducted. These compounds were extensively examined utilizing a variety of spectroscopic and analytical methods. The confirmation of the geometry octahedral of the complexes was achieved via spectrum analysis. In addition, the compounds (1-10) were tested for their effectiveness in controlling tuberculosis (TB) formation in a laboratory setting. The results showed that complexes (6), (9), and (10) had the highest potency, with a MIC value ranging from 0.0028 ± 0.0013 to 0.0063 ± 0.0013 µmol/mL. Among these complexes, the Zn(II) complex (10) was particularly effective, with a MIC value of 0.0028 ± 0.0013 µmol/mL.

In fact, it was nearly four times more effective in suppressing TB disease compared to streptomycin, which had a MIC value of 0.0107 ± 0.0011 µmol/mL. The antibacterial and anti-inflammatory evaluations demonstrated that the complex (10) exhibited higher activity, as shown by its lowest MIC (0.0057–0.0114 µmol/mL) and IC50 (7.14 ± 0.05 µM) values, which are equivalent to those of the standard medicines (**Scheme 6**) **[53]**.

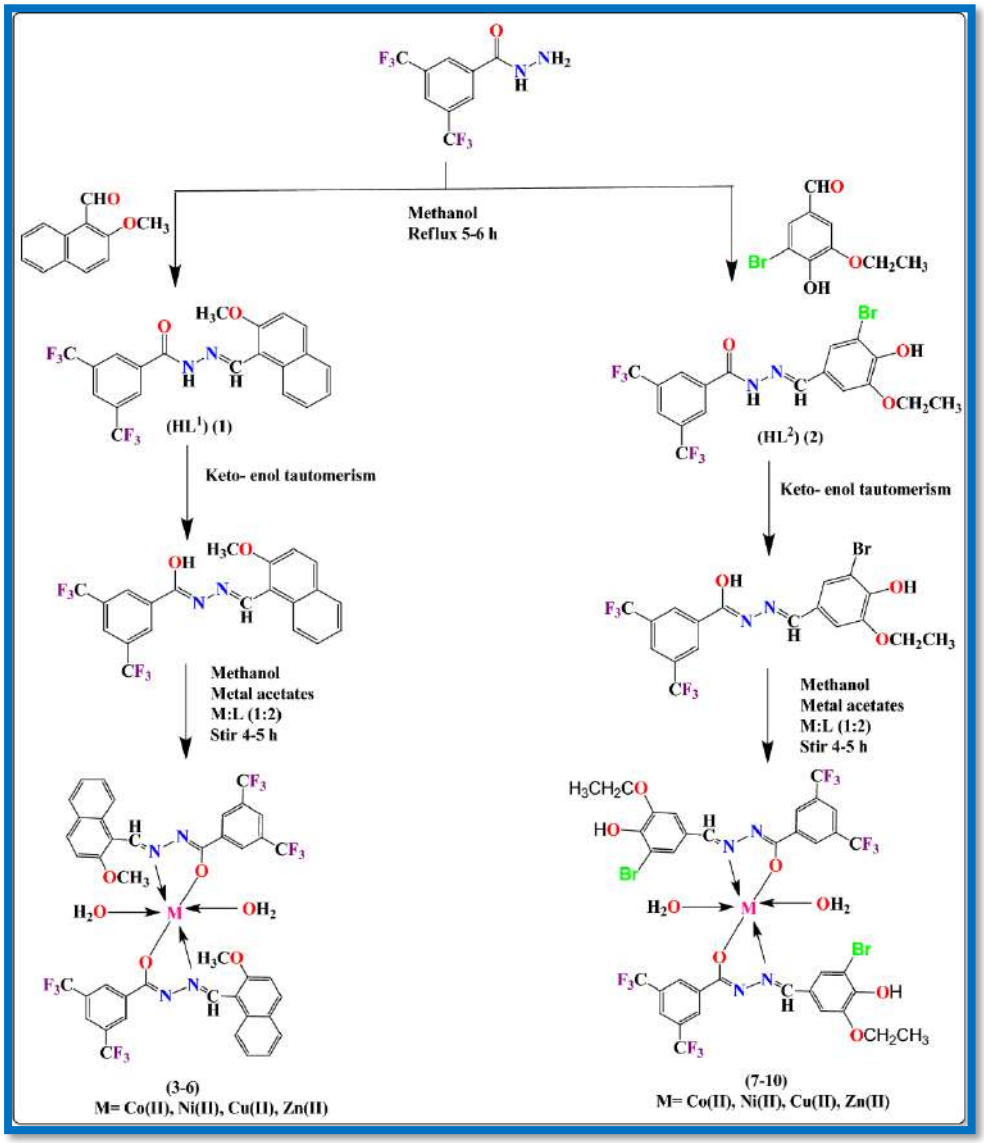

Scheme 6: Synthesis of (HL^1–HL^2) hydrazone ligands (1–2) and their transition metal complexes (3–10)

A study was done to evaluate the connections among the structure and activity of several triclosan azo-adducts against both Mycobacterium TB and non-tuberculous mycobacteria. The most potent molecule in the series had activity that was fourfold higher than triclosan and sixteenfold higher than rifabutin against drug-resistant Mycobacterium abscessus. Furthermore, this chemical exhibited lower toxicity towards human macrophages compared to triclosan on the first day. Furthermore, one of the azo-adducts demonstrated a twofold increase in potency

against M. tuberculosis in comparison to triclosan, and a twofold increase in efficiency against Mycobacterium marinum in comparison to isoniazid. Furthermore, the synthesized azo-adducts have shown comparable efficacy against M. abscessus strains that exhibit overexpression of InhA. This implies that these chemicals operate via a distinct mechanism, as shown in **Scheme 7 [54]**.

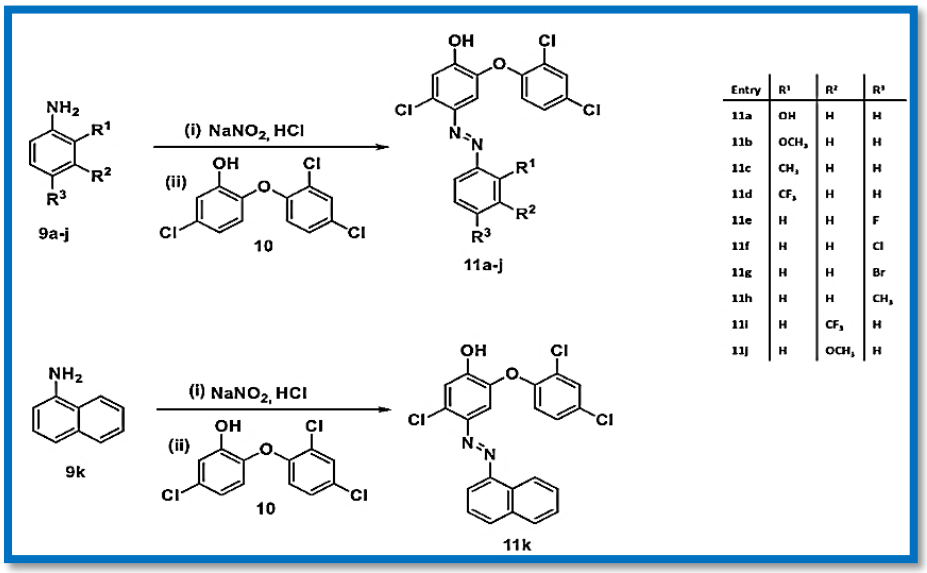

Scheme 7: Synthesis of TCS azo-adducts 11a-k

The pharmacological activity of a set of azo dyes (C1-C5) generated from benzothiazole was evaluated against Mycobacterium TB. The efficacy of colors (C1-C5) against Mycobacterium TB (H37 RV strain) was assessed using the microplate Alamar Blue Assay (MABA) technique. The findings were compared to those obtained with the conventional therapy of streptomycin. The results of the anti-TB activity tests show that compounds C1, C2, C3, and C5 showed comparable sensitivity to the standard streptomycin (MIC = 6.24 g/mL) and also showed significant sensitivity (MIC = 1.6 g/mL). Compound C4, a chemically synthesized dye, stands out due to the presence of an ethoxy group at the 6th position of the benzothiazole molecule. The minimal inhibitory concentration (MIC) is 3.2 grams per milliliter (g/mL) (**Figure 12**) **[55]**.

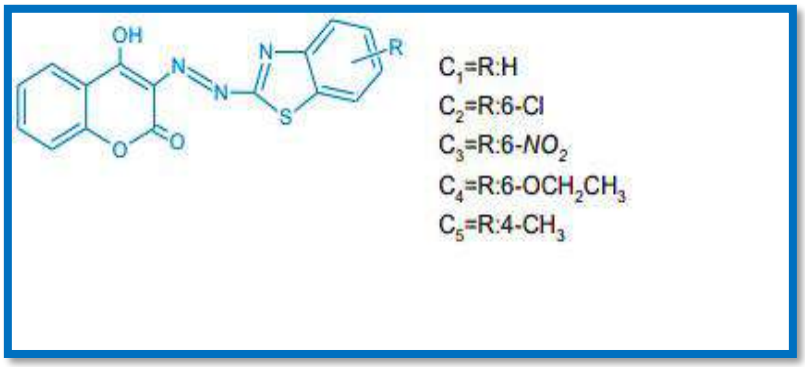

Figure 12: Coumarin-Benzothiazole Based Azo Dyes [55]

3. Conclusions

Azo dyes are now the most produced dye chemistry, and they may become much more significant in the future. Azo dyes are often employed in a wide range of industries, such as the textile, leather, food, pharmaceutical, paper, and cosmetics sectors. They make up around half of all synthetic dyes. Additionally, azo dyes have found the widest use, as seen by the findings in this research, since they are simple to synthesize via the reaction of an azo coupling component that contains atom-active hydrogen bonded to a carbon atom. This reaction is explained by the electron-rich electrophilic aromatic substitution mechanism. About 60% of the synthetic hues created are produced using this method. Azo dyes are substances with intense colors that result from the azo coupling reaction of aromatic amines, phenols, or naphthols with diazonium ions.

4. References

[1] Ferreira I, et al. Seawater as an alternative to dye cotton fiber with reactive dyes. Textile Research Journal, 2020; 91, (9-10): 1184–1193.

[2] Helal T, Abbas J, Mohammed F. Synthesis and Identification of new 4-Amino phenazone derivatives containing azo group. Chemistry, 2014; 2(7).

[3] Mohamed S, Soumaya B, et al. Synthesis, characterization and antimicrobial activity of some new azo dyes derived from 4-hydroxy-6-methyl-2H-pyran-2-one and its dihydro derivative. Dyes and Pigments, 2021; 188: 109073.

[4] Zhi-gang Y, et al. Monoazo dyes based on 5, 10-dihydrophenophosphazine, Part 2: Azo acid dyes. Dyes and Pigments, 2009; (81)2: 137-143.

[5] Zhi-gang, Y, et al. Monoazo dyes based on 5, 10-dihydrophenophosphazine, Part 2: Azo acid dyes. Dyes and Pigments, 2009; (81)2: 137-143.

[6] Chung K. Azo dyes and human health: A review. Journal of Environmental Science and Health, Part C, 2016; (34)4: 233-261.

[7] Piao W, et al. Development of an azo-based photosensitizer activated under mild hypoxia for photodynamic therapy. Journal of the American Chemical Society, 2017; (139)39: 13713-13719.

[8] EL mekkawi D. Abdel-mottaleb M. The interaction and photostability of some xanthenes and selected azo sensitizing dyes with TiO2 nanoparticles. International Journal of Photoenergy, 2005; (7)2: 95-101.

[9] Shankarling G, Deshmukh P, Joglekar A. Process intensification in azo dyes. Journal of environmental chemical engineering, 2017; (5)4: 3302-3308.

[10] Gürses A, et al. Classification of dye and pigments. Dyes and pigments, 2016; 31-45.

[11] Berradi M, et al. Textile finishing dyes and their impact on aquatic environs. Heliyon, 2019; 5(11).

[12] Alsantali R, et al. Miscellaneous azo dyes: a comprehensive review on recent advancements in biological and industrial applications. Dyes and pigments, 2022; 199: 110050.

[13] Fei Na, Sauter B, Gillingham D. The pK a of Brønsted acids controls their reactivity with diazo compounds. Chemical Communications, 2016; 52(47): 7501-7504.

[14] Aljamali N, Rahi D. New Formazan Compounds (Synthesis, Identification, Physical Properties). Journal of Chemical and Pharmaceutical Sciences, 2017; (10)3: 1461-1472.

[15] Benkhaya S, M'rabet S, EL harfi A. Classifications, properties, recent synthesis and applications of azo dyes. Heliyon, 2020; (6)1.

[16] Aljamali, N. Review in azo compounds and its biological activity. Biochem Anal Biochem, 2015; (4)2: 1-4.

[17] Aljamali N. Review in azo compounds and its biological activity. Biochem Anal Biochem, 2015; (4)2: 1-4.

[18] Roldo M, et al. Azo compounds in colon-specific drug delivery. Expert opinion on drug delivery, 2007; (4)5: 547-560.

[19] Mello M, Dos anjos E, De campos B. Usefulness of sulfonated azo dyes to evaluate macromolecularly oriented protein substrates. Acta Histochemica, 2024; (126)3: 152154.

[20] Udoikono A, et al. Reactive azo compounds as a potential chemotherapy drugs in the treatment of malignant glioblastoma (GBM): Experimental and theoretical studies. Journal of Photochemistry and Photobiology, 2022; 10: 100116.

[21] Benkhaya S, M'rabet S, EL harfi A. Classifications, properties, recent synthesis and applications of azo dyes. Heliyon, 2020; (6)1.

[22] Singh K, et al. Insights into the structure activity relationship of nitrogen-containing heterocyclics for the development of antidepressant compounds: An updated review. Journal of Molecular Structure, 2021; 1237: 130369.

[23] Popli S., Patel U. Destruction of azo dyes by anaerobic–aerobic sequential biological treatment: a review. International Journal of Environmental Science and Technology, 2015; (12): 405-420.

[24] Singh P, Singh R. Bio-removal of azo dyes: a review. International Journal of Applied Sciences and Biotechnology, 2017; (5)2: 108-126.

[25] Lipskikh O, et al. Sensors for voltammetric determination of food azo dyes-A critical review. Electrochimica Acta, 2018; 260: 974-985.

[26] Puvaneswari N, Muthukrishnan J, Gunasekaran P. Toxicity assessment and microbial degradation of azo dyes. 2006.

[27] Barciela P, Perez-vazquez A, Prieto M. Azo dyes in the food industry: Features, classification, toxicity, alternatives, and regulation. Food and Chemical Toxicology, 2023; 178: 113935.

[28] Silveira E, et al. Selection of Pseudomonas for industrial textile dyes decolourization. International Biodeterioration & Biodegradation, 2009; (63)2: 230-235.

[29] Samanta A, Agarwal P. Application of natural dyes on textiles. 2009.

[30] Benkhaya S, M'rabet S, EL harfi A. Classifications, properties, recent synthesis and applications of azo dyes. Heliyon, 2020; (6)1.

[31] Mathur N, Bhatnagar P, Bakre P. Assessing mutagenicity of textile dyes from Pali(Rajasthan) using Ames bioassay. Applied ecology and environmental research, 2006; (4)1: 111-118.

[32] Leme D, et al. Genotoxicity assessment of reactive and disperse textile dyes using human dermal equivalent (3D cell culture system). Journal of Toxicology and Environmental Health, Part A, 2015; 7(8)7: 466-480.

[33] Aljamali N, Hassen H. Review on azo-compounds and their applications. Journal of Catalyst & Catalysis, 2021; (8)2: 8-16.

[34] Rahmouni A, et al. Photoassisted holography in azo dye doped polymer films. The Journal of Physical Chemistry B, 2016; (120)43: 11317-11322.

[35] Guru prasad L. Azo dye doped polymer films for nonlinear optical applications. Chinese Journal of Polymer Science, 2014; 32: 650-657.

[36] Derkowska-zielinska B, et al. Photovoltaic cells with various azo dyes as components of the active layer. Solar Energy, 2020; 203: 19-24.

[37] Asif M, et al. Shedding light on the second order nonlinear optical responses of commercially available acidic azo dyes for laser applications. Dyes and Pigments, 2022; 202: 110284.

[38] Madiahlagan E, et al. Synthesis, liquid crystalline properties and photo switching properties of coumarin-azo bearing aliphatic chains: Application in optical storage devices. Journal of Molecular Liquids, 2019; 292: 111328.

[39] Behera A, Sen A. Pyrrole–Best additional spacers for azo based dye sensitized solar cells: A computational study. Journal of Photochemistry and Photobiology A: Chemistry, 2022; 433: 114146.

[40] Odey J, et al. Experimental and theoretical studies of the electrochemical properties of mono azo dyes derived from 2-nitroso-1-naphthol, 1-nitroso-2-naphthol, and CI disperse yellow 56 commercial dye in dye-sensitized solar cell. Journal of Molecular Structure, 2021; 1241: 130615.

[41] Singh K, et al. Antiviral and antimicrobial potentiality of nano drugs. In: Applications of targeted nano drugs and delivery systems. Elsevier, 2019; 343-356.

[42] Albelwi F, et al. Novel oxazolones incorporated azo dye: Design, synthesis photophysical-DFT aspects and antimicrobial assessments with In-silico and In-vitro surveys. Journal of Photochemistry and Photobiology, 2021; 7: 100032.

[43] Prashantha A, Ali R, Keshavayya J. Synthesis, spectral characterization, DFT studies and antimicrobial activities of amino-methylbenzoic acid based azo dyes. Inorganic Chemistry Communications, 2021; 127: 108392.

[44] Khanum R, et al. Recent review on Synthesis, spectral Studies, versatile applications of azo dyes and its metal complexes. Results in Chemistry, 2023; 5: 100890.

[45] Meng T, et al. In vitro and in vivo inhibition of the infectivity of human enterovirus 71 by a sulfonated food azo dye, brilliant black BN. Journal of Virology, 2019; (93)17: 10.1128/jvi. 00061-19.

[46] Meng T, et al. In vitro and in vivo inhibition of the infectivity of human enterovirus 71 by a sulfonated food azo dye, brilliant black BN. Journal of Virology, 2019; (93)17: 10.1128/jvi. 00061-19.

[47] Tahir T, et al. Antiviral evaluation of bioactive azo derivatives to treat endemic poultry viruses. The Thai Journal of Veterinary Medicine, 2020; (50)3: 435-443.

[48] Mbeunkui F, Johann D. Cancer and the tumor microenvironment: a review of an essential relationship. Cancer chemotherapy and pharmacology, 2009; 63: 571-582.

[49] Saeed A, Alneyadi S, Abdou I. Anticancer activity of novel Schiff bases and azo dyes derived from 3-amino-4-hydroxy-2H-pyrano [3, 2-c] quinoline-2, 5 (6H)-dione. Heterocyclic Communications, 2020; (26)1: 192-205.

[50] Gouda M, et al. Synthesis and antitumor evaluation of thiophene based azo dyes incorporating pyrazolone moiety. Journal of Saudi Chemical Society, 2016; (20)2: 151-157.

[51] Khedr A, Gouda A, El-ghamry H. Nano-synthesis approach, elaborated spectral, biological activity and in silico assessment of novel nano-metal complexes based on sulfamerazine azo dye. Journal of Molecular Liquids, 2022; 352: 118737.

[52] GHASEMI, Zarrin, et al. Synthesis of azo dyes possessing N-heterocycles and evaluation of their anticancer and antibacterial properties. *Monatshefte für Chemie-Chemical Monthly*, 2018, 149: 149-157.

[53] Kumar B, et al. Investigation of antituberculosis, antimicrobial, anti-inflammatory efficacies of newly synthesized transition metal (II) complexes of hydrazone ligands: structural elucidation and theoretical studies. Scientific Reports, 2023; (13)1: 15906.

[54] Alcaraz M, et al. Tailoring selective triclosan azo-adducts: Design, synthesis, and anti-mycobacterial evaluation. Heliyon, 2023; (9)11.

[55] Manjunatha B, et al. Coumarin-benzothiazole based azo dyes: synthesis, characterization, computational, photophysical and biological studies. Journal of Molecular Structure, 2021; 1246: 131170.

Al-Kitab Journal for Pure Sciences (2025); 9(1):164-171.
https://doi.org/10.32441/kjps.09.01.p11

Al-Kitab Journal for Pure Sciences
ISSN: 2617-1260 (print), 2617-8141(online)

https://isnra.net/index.php/kjps

Ring Classification of Ideal-Based Zero Divisor Graph with Vertices 9

Husam Q. Mohammad[1], Sahbaa A.Younus[2], Wafa Y. Yahya[2*]

[1] Department of Mathematics, College of Computer Science and Mathematics, University of Mosul, Iraq.

[2] Department of Mathematics, College of Education for Pure Sciences, University of Al-Hamdaniya, Iraq.

[*]Corresponding Author: rwafa1993@uohamdaniya.edu.iq

Citation: Mohammad HQ, Younus SA, Yahya WY. Ring Classification of Ideal-Based Zero Divisor Graph with Vertices 9. Al-Kitab J. Pure Sci. [Internet]. 2025 Mar. 10;9(1):164-171. DOI: https://doi.org/10.32441/kjps.09.01.p11

Keywords: Zero Divisor Graph, Ideal-Based Zero Divisor Graph, Direct Product, Finite Ring, Local Ring.

Article History

Received	14 Apr.	2024
Accepted	30 Jul.	2024
Available online	10 Mar.	2025

Abstract:

Let R be a finite commutative ring with a non-zero unit, and L be an ideal of R. focuses on expanding the notation of the Zero Divisor Graph to create what is known as the Ideal-Based Zero Divisor Graph. The main goal is to classify rings using the ideal-based Zero divisor graph that consists of 9 vertices and symbolizes ($\Gamma_L(R)$) by using the properties $|V(\Gamma_L(R))|=|L|.|V((\Gamma(R/L))|$, $|L|\geq 2$.

Keywords: Zero Divisor Graph, Ideal-Based Zero Divisor Graph, Direct Product, Finite Ring, Local Ring.

(Immediately after the abstract, provide 5-7 keywords and arrange them alphabetically, using American spelling and avoiding general and plural terms and multiple concepts (avoid, for example, 'and', 'of'). Be sparing with abbreviations: only abbreviations firmly established in the field may be eligible. These keywords will be used for indexing purposes).

تصنيف الحلقات ببيان قاسم الصفر أساسه المثالي بتسعة رؤوس

حسام قاسم محمد[1]، صهباء عبد الستار يونس[2]، وفاء يونس يحيى[2*]

[1]قسم الرياضيات كلية علوم الحاسوب والرياضيات، جامعة الموصل، العراق
[2]قسم الرياضيات، كلية التربية، جامعة الحمدانية، العراق
husamqm@uomosul.edu.iq, sahbaa1977@uohamdaniya.edu.iq, rwafa1993@uohamdaniya.edu.iq

الخلاصة:

لتكن G حلقة ابدالية منتهية بعنصر محايد ليس صفريا، وليكن L مثالي في الحلقة R، تمركز هذا البحث على تعميم وتوسيع مصطلح بيان قاسم الصفر الى بيان قاسم الصفر الذي أساسه المثالي والذي يرمز له $(\Gamma_L(R))$. في هذا البحث قمنا بتصنيف جميع الحلقات التي لها بيان قاسم الصفر الذي أساسه المثالي وعدد رؤوسه 9. بالاعتماد على الخاصية $|L|\geq 2$, $|V(\Gamma_L(R))|=|L|.|V((\Gamma(R/L))|$.

الكلمات المفتاحية: بيان قاسم الصفر، بيان قاسم الصفر أساسه المثالي، الضرب المباشر، الحلقة المنتهية، الحلقة المحلية.

1. Introduction:

Let R be a commutative ring with identity and Z(R) the collection of all zero divisor elements in R. The polynomial ring R[X] is defined to be the set of all formal sums $a_0+ a_1 X+\ldots+a_nX_n+ a_{n+1}X_{n+1} +\ldots= \Sigma\, a_iX_i$, where the coefficients $a_i \in R$ for i=0, 1, 2, …n, n+1, … When working with polynomial rings, say R[X]/L, we will let X denote the coset X+L. It is well-known that any finite ring R is a direct product of local rings R_i for i=1, 2, …, n.

In 2003, SP. Redmond [1]introduced a new definition called an ideal-based zero-divisor graph, denoted by $\Gamma_L(R)$, which is defined as a statement in which the vertices, $r_1, r_2 \in R - L$ are adjacent if, $r_1.r_2 \in L$, where L is an ideal of R. This definition generalizes the zero-divisor graph proposed by D. F. Anderson and P. S. Livingston [2], which has the vertices, $r_1, r_2 \in Z(R)^*$. adjacent if and only if $r_1.r_2 = 0$, which is denoted by Γ(R). If L = 0 then $\Gamma_L(R) = \Gamma(R)$ and $\Gamma_L(R) = \emptyset$ if and only if L is a prime ideal of R, additionally, $\Gamma_L(R)$ is a connected graph. **[3]** The study of algebraic graphs, which is considered a modern and important topic linking the theory of rings in abstract algebra and graph theory, has received wide attention from researchers, for example, **[4,5,6]**.

Clearly, every ring has $\Gamma_L(R)$ graph, and if $R_1 \cong R_2$, then $\Gamma_L(R_1) \cong \Gamma_L(R_2)$, but the convers is not true in general as well as there are $\Gamma_L(R_1) \cong \Gamma_L(R_2)$,but $R_1 \ncong R_2$. Redmond proved the following relationship: $|V(\Gamma_L(R)| = |L| \cdot |V(\Gamma(R/L))|$ and $|L| \geq 2$. Using this mathematical expression, researchers in **[7,8]** were able to find all rings corresponding to the ideal L with the number of vertices n, where $1\leq n\leq 7$ or n is a prime number. In this work, we used this

relationship to classify a ring when an ideal-based zero divisor graph with vertices 9. In [2] it is provided that Γ(R) is connected, if R is an integral domain, then Γ(R) is empty, Γ(R) has - finitely many vertices if, either R is finite or an integral domain, diam (Γ (R)) ≤ 3 [9,10] Gan and Yang presented the Zero-divisor graphs of MV-algebras

2. Ring | V(Γ_L(R))| =9

In this section, we give all possible rings with |V(Γ_L(R))| =9.

2.1 Remark: We consider when a non-trivial Γ_L(R) is the graph on 9 vertices since | V(Γ_L(R)|=|V(Γ(R /L) |.| L | and | L | ≥ 2 we get two possibilities :-

1- | L | = 9 and |V (Γ (R /L)| =1.

2- | L | = 3 and |V (Γ (R /L)| =3.

2.2 Proposition: When R is a ring with | Γ_L(R) | = 9 , then R is nonlocal ring

Proof: We impose R to be a local ring with | Γ_L(R) | = 9, therefore by remark 2.1 there are two cases:

Case 1: If |L|=9 and | V (Γ (R /L) | =1, then by [11,12] , R/L ≅ Z_4 or $Z_2[A] / (A^2)$ and so |(R/L) | =4 which implies that |R| =9.4=36, but R local which is a contradiction.

Case 2: If |L|=3 and | V(Γ(R/L) | =3, then by [4,12] R /L≅ Z_8, $Z_2[A]/(A^3)$, $Z_2[A,B]/(A,B)^2$, $Z_4[A]/(A^2,2A)$, $Z_4[A]/(A^2 - 2,2A)$ or $F_4[A]/(A^2)$. If R/ L ≅ Z_8, $Z_2[A]/(A^3)$, $Z_2[A,B]/(A,B)^2$, $Z_4[A]/(A^2,2A)$ or $Z_4[A]/(A^2- 2,2A)$ then | (R /L) | =8 therefore| R |=24, but R local which is a contradiction. When R/ L ≅ $F_4[A]/(A^2)$, the order | R/ L| = 16, therefore | R |=48, but R local which is a contradiction. So R is not local.

2.3 Theorem: let R be isomorphic with $R_1 \times R_2$, when R_1, R_2 will be local rings and |V(Γ_L(R)) |=9, therefore R isomorphic to one of 12 rings with corresponding ideal L from **Table 1**.

Table 1: R isomorphic with $R_1 \times R_2$

Ring	Ideal	Figure
$Z_9 \times Z_4$	$Z_9 \times (0)$	K_9
$Z_9 \times Z_2[A]/ (A^2)$	$Z_9 \times (0)$	K_9
$Z_3 [A]/(A^2) \times Z_4$	$Z_3 [A]/(A^2) \times (0)$	K_9
$Z_3 [A]/(A^2) \times Z_2[A]/(A^2)$	$Z_3 [A]/(A^2) \times (0)$	K_9
$Z_9 \times Z_2$	(3) × (0)	1
$Z_3 [A]/(A^2) \times Z_2$	(A) × (0)	1
$Z_8 \times Z_3$	(0) × Z_3	K_9
$Z_4[A]/(2A, A^2) \times Z_3$	(0) × Z_3	K_9
$Z_2 [A]/(A^3) \times Z_3$	(0) × Z_3	2
$Z_2 [A,B]/(A,B)^2 \times Z_3$	(0) × Z_3	K_9
$Z_4[A]/(2A, A^2 -2) \times Z_3$	(0) × Z_3	K_9
$F_4 [A] / (A^2) \times Z_3$	(0) × Z_3	K_9

Proof: If $|L| = 9$ and $|V(\Gamma(R/L)| = 1$, then $(R/L) \cong Z_4$ or $Z_2[A]/(A^2)$ so that $|R| = 36$, then $|R_1| = 9$ and $|R_2| = 4$ so $R_1 \cong Z_9$ or $Z_3[A]/(A^2)$ and $R_2 \cong Z_4$, or $Z_2[A]/(A^2)$, then R isomorphic one of 4 rings with corresponding ideal L from **Table 2**.

Table 2: $|R| = 36$

Ring	Ideal
$Z_9 \times Z_4$	$Z_9 \times (0)$
$Z_9 \times Z_2[A]/(A^2)$	$Z_9 \times (0)$
$Z_3[A]/(A^2) \times Z_4$	$Z_3[A]/(A^2) \times (0)$
$Z_3[A]/(A^2) \times Z_2[A]/(A^2)$	$Z_3[A]/(A^2) \times (0)$

If $|L| = 3$ and $|V(\Gamma(R/L)| = 3$, then by **[4,5]** $R/L \cong Z_6, Z_8, Z_2[A]/(A^3), Z_2[A,B]/(A,B)^2$, $Z_4[A]/(A^2,2A)$, $Z_4[A]/(A^2 - 2,2A)$ or $F_4[A]/(A^2)$.

If $(R/L) \cong Z_6$, then $|R| = 18$, $|R_1| = 9$, and $|R_2| = 2$ then $R_1 \cong Z_9$ or $Z_3[A]/(A^2)$ and $R_2 \cong Z_2$. Hence R isomorphic one of 2 rings with depending on the ideal L from **Table 3**.

Table 3: $|R| = 18$

Ring	Ideal
$Z_9 \times Z_2$	$(3) \times (0)$
$Z_3[A]/(A^2) \times Z_2$	$(A) \times (0)$

Now, when $R/L \cong Z_8$, $Z_2[A]/(A^3)$, $Z_2[A,B]/(A,B)^2$, $Z_4[A]/(A^2,2A)$, or $Z_4[A]/(A^2 - 2,2A)$, then $|R| = 24$, and we get $|R_1| = 8$, $|R_2| = 3$, then R will be one of 5 rings with corresponding ideal L from **Table 4**.

Table 4: $|R| = 24$

Ring	Ideal
$Z_2[A]/(A^3) \times Z_3$	$(A) \times (0)$
$Z_8 \times Z_3$	$(0) \times Z_3$
$Z_4[A]/(2A,A^2) \times Z_3$	$(_0) \times Z_3$
$Z_2[A]/(A^3) \times Z_3$	$(_0) \times Z_3$
$Z_2[A,B]/(A,B)^2 \times Z_3$	$(0) \times Z_3$

When $R/L \cong F_4[A]/(A^2)$, we have $|R/L| = 16$, so $|R| = 48$ where $|R_1| = 16$, then R_1 isomorphism of one 18 rings from **Table 5** and $|R_2| = 3$, $R_2 \cong Z_3$, there is only one ring of order 16 it is $F_4[A]/(A^2)$, $R \cong F_4[A]/(A^2) \times Z_3$, with $I = (0) \times Z_3$.

Table 5: | R | = 16

Ring
$F_2[A]/(A^4)$
$Z_4[A]/(A^2-2)$
$Z_4[A]/(A^2–2A-2)$
$Z_4[A]/(A^2-2A)$
$Z_4[A]/(A^3–2,2A)$
$F_2[A,B]/(A^3,AB,B^2)$
$F_2[A,B]/(AB,A^2-B^2)$
$F_2[A,B]/(A^2,B^2)$
$Z_{p^2}[A,B]/(A^2,AB-2,B^2)$
$Z_4[A]/(A^2)$
$Z_4[A,B]/(A^2-2,AB,B^2,2A)$
$Z_4[A]/(A^3,2A)$
$Z_8[A]/(A^2-4,2A)$
$Z_8[A]/(A^2,2A)$
$Z_4[A,B]/(A,B,2)^2$
$F_2[A,B,C]/(A,B,C)^2$
$Z_4[A,B]/(A^2–2,AB,B^2-2,2A)$
Z_{16}

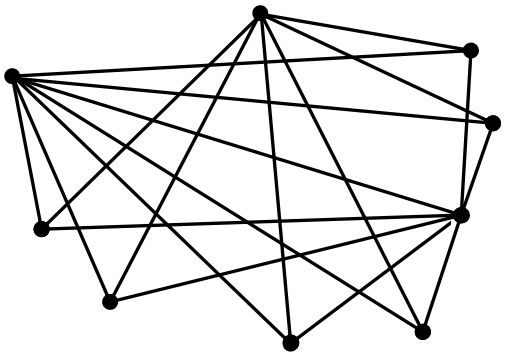

Figure 1

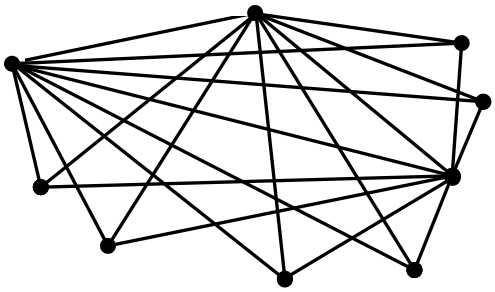

Figure 2

Figures 1 & 2: Ideal-Based Zero Divisor Graph with Vertices 9

2.4 Theorem:

When $R \cong R_1 \times R_2 \times R_3$, where R_i local ring $i \in \{1,2,3\}$ as well as $|V(\Gamma_L(R))|=9$; therefore, R isomorphic to one of 3 rings with depending on ideal L from **Table 6**.

Table 6: | R | = 36

Ring	Ideal	Figure
$Z_3 \times Z_3 \times Z_2$	$Z_3 \times Z_3 \times (0)$	K_9
$Z_3 \times Z_3 \times Z_2\ [A]/(A^2)$	$Z_3 \times Z_3 \times (0)$	K_9
$Z_3 \times Z_3 \times Z_2$	$Z_3 \times (0) \times (0)$	1

Proof:

1- Suppose $|L| = 9$ and $|V(\Gamma(R/L)| = 1$, we note $(R/L) \cong Z_4$ or $Z_2[A]/(A^2)$ so that $|R| = 36$, which implies that $R \cong R_1 \times R_2 \times R_3$, where $|R_1| = |R_2| = 3$ and $|R_3| = 4$, so that R_1 and $R_2 \cong Z_3$,& $R_3 \cong Z_4$ or $Z_2[A]/(A^2)$, then $R \cong Z_3 \times Z_3 \times Z_4$ or $Z_3 \times Z_3 \times Z_2[A]/(A^2)$ with $L = Z_3 \times Z_3 \times (0)$.

2- When $|L| = 3$ and $|V(\Gamma(R/L)| = 3$, we see $R/L \cong Z_6$ or Z_8 or $Z_2[A]/(A^3)$, $Z_2[A,B]/(A,B)^2$, $Z_4[A]/(A^2,2A)$, $Z_4[A]/(A^2 - 2,2A)$ or $F_4[A]/(A^2)$.

If $R/L \cong Z_6$, then $|R| = 18$, we have $R \cong R_1 \times R_2 \times R_3$, we see $|R_1| = |R_2| = 3$ & $|R_3| = 2$. Then R is isomorphic $Z_3 \times Z_3 \times Z_2$, with $L = Z_3 \times (0) \times (0)$.

But if $R/L \cong Z_8$, $Z_2[A]/(A^3)$, $Z_2[A,B]/(A,B)^2$, $Z_4[A]/(A^2,2A)$ or $Z_4[A]/(A^2 - 2,2A)$ then $|R| = 24$, we have $R \cong R_1 \times R_2 \times R_3$, such that $|R_1| = 2$, $|R_2| = 3$ and $|R_3| = 4$. Then $R \cong Z_2 \times Z_3 \times Z_4$ or $Z_3 \times Z_2 \times Z_2[A]/(A^2)$, with $L = (0) \times Z_3 \times (0)$. But $R/L \ncong Z_8$, $Z_2[A]/(A^3)$, $Z_2[A,B]/(A,B)^2$, $Z_4[A]/(A^2,2A)$ or $Z_4[A]/(A^2 - 2,2A)$ we get contradiction.

If $G/L \cong F_4[A]/(A^2)$, then $|(R/L)| = 16$, so $|R| = 48$ where $|R_1| = |R_2| = 4$ and $|R_3| = 3$. Then $R \cong Z_4 \times Z_4 \times Z_3$, $Z_2[A]/(A^2) \times Z_2[A]/(A^2) \times Z_3$ or $Z_4 \times Z_2[A]/(A^2) \times Z_3$, with $L = (0) \times (0) \times Z_3$. But $G/L \ncong F_4[A]/(A^2)$ we get a contradiction.

2.5 Theorem:

If R is isomorphic with $R_1 \times R_2 \times R_3 \times \ldots \times R_n$, where $n \geq 4$, and R_i local rings for all $i = 1,\ldots,n$ with $|V(\Gamma_L(R))| = 9$, we get G no isomorphic with any ring

Proof: If $n \geq 5$, then by same method in proof theorem 1.4, then we get contradiction. Let $n = 4$, then by remark 1.1, we have two cases:

Case 1: If $|L| = 9$ and $|V(\Gamma(R/L)| = 1$, then $(R/L) \cong Z_4$ or $Z_2[A]/(A^2)$ so that $|R| = 36$, which implies that $R \cong R_1 \times R_2 \times R_3 \times R_4$, such that $|R_1| = |R_2| = 3$ & $|R_3| = |R_4| = 2$, so that R_1 & $R_2 \cong Z_3$ but $R_3 \cong Z_2$, then $R \cong Z_3 \times Z_3 \times Z_2 \times Z_2$ with $L = Z_3 \times Z_3 \times (0) \times (0)$. But $R/L \ncong Z_4$ or $Z_2[A]/(A^2)$, we get a contradiction.

Case 2: If $|L| = 3$ and $|V(\Gamma(R/L)| = 3$, then $R/L \cong Z_6$, Z_8, $Z_2[A]/(A^3)$, $Z_2[A,B]/(A,B)^2$, $Z_4[A]/(A^2,2A)$, $Z_4[A]/(A^2 - 2,2A)$ or $F_4[A]/(A^2)$. If $R/L \cong Z_6$, then $|R| = 18$ there is no existence R of order 18, $\therefore$ R is isomorphic $R_1 \times R_2 \times R_3 \times R_4$, we get contradicts. If $R/L \cong Z_8$,

$Z_2[A]/(A^3)$, $Z_2[A,B]/(A,B)^2$, $Z_4[A]/(A^2,2A)$ or $Z_4[A]/(A^2 - 2,2A)$, then | R | = 24 and $R \cong Z_2 \times Z_2 \times Z_2 \times Z_3$ with L = (0) ✕ (0) ✕(0)✕Z_3, but $R/L \ncong Z_8$ or $Z_2[A]/(A^3)$, $Z_2[A,B]/(A,B)^2$, $Z_4[A]/(A^2,2A)$, $Z_4[A]/(A^2 - 2,2A)$, we have a contradiction. If $R/L \cong F_4[A]/(A^2)$, then | R | =48. So that $R \cong Z_2 \times Z_2 \times Z_3 \times Z_4$ with L = (0) ✕ (0) ✕ Z_3 ✕ (0). But $R/L \ncong F_4[A]/(A^2)$ contradiction.

3. Results

Ring| $V(\Gamma_L(R))$| =9 shown in **Tables [1-6]**

4. Discussion

If R commutative non local ring with identity, I an ideal of R and $\Gamma_I(R)$ zero divisor graph with ideal based I and $V(\Gamma_I(R)) = 9$, then there are three graphs (Fig 1, Fig 2, K_9) realized ring R with respect ideal I. Additionally, if R direct product n local rings, where $n \geq 4$, then no graph realized R.

5. Conclusions

Finally, we expand the notation of the Zero divisor graph to create what is known as the Ideal-Based Zero Divisor Graph, in our research we find and classify all rings using the ideal-based Zero divisor graph that consists of 9 vertices as shown in **Tables (1-6)** and find the graph of Ring | $V(\Gamma_L(R))$| =9 as shown in figures **(1,2)**.

6. References

[1] Redmond SP. An Ideal-Based Zero-Divisor Graph of a Commutative Ring. Journal of Communications in Algebras. 2003; 31, 4425–4443.

[2] Anderson DF, Livingston PS. The Zero-Divisor Graph of a Commutative Rings. Journal of Algebra. 1999; 217, 434-447.

[3] S.D,M.Richard," Abstract Algebra. Prentice Hall Inc.U.S.A. 1991.

[4] Atani SE. The Zero-Divisor Graph with Respect to Ideals of a Commutative Semiring, Glasnik Matematicki Journal, Serija III. 2008; 43(63), 309–320.

[5] ESSA SS, Mohammad HQ. On The Structure of a k-Annihilating Ideal Hypergraph of Commutative Rings, Journal of Communications of the Korean Mathematical Society. 2023; 38, no.1, pp55-67.

[6] Maimani HR, Pournaki MR, Yassemi S. Zero-Divisor Graph with Respect to an Ideal. Journal of Communications in Algebras. 2006; 34(3), 923-929. 2

[7] Smith JG. Properties of Ideal-Based Zero-Divisor Graphs of Commutative Rings. PhD diss. University of Tennessee, Knoxville. 2014.

[8] Smith JG. When Ideal-Based Zero-Divisor Graphs are Complemented or Uniquely Complemented. International Electronic Journal of Algebra. 2017; 21, 198-204. 2

[9] Gan AP, Yang BC. Annihilator Graphs of MV-algebras. Journal of Algebra and its Applications. 2021; 20, 2150188.

[10] Gan AP, Yang BC. Zero-Divisor Graphs of MV-algebras. Journal of Soft Computing. 2020; 24, 6059-6068.

[11] Corbas B, Williams GD. Rings of Order p^5 Part I. Nonlocal rings. Journal of Algebra. 2000; 231 (2), 677-690.

[12] Corbas B, Williams GD. Rings of Order p^5 Part II. Local rings. Journal of Algebra. 2000; 231 (2), 691-704.

Al-Kitab Journal for Pure Sciences (2025); 9(1):172-182.
https://doi.org/10.32441/kjps.09.01.p12

Al-Kitab Journal for Pure Sciences
ISSN: 2617-1260 (print), 2617-8141(online)

https://isnra.net/index.php/kjps

Isolation and Diagnosis of Antibiotic-Resistant *Escherichia Coli* Bacteria from Urinary Tract Infection Patients in Mosul

Zainab Baqir Abbas*, Hasan Faisal Hussein

***Department of Biology, College of Education for Pure Sciences, University of Mosul, Mosul, Iraq**

*Corresponding Author: email: Zainab.22esp15@student.uomosul.edu.iq

Citation: Abbas ZB & Hussein HF. Isolation and diagnosis of antibiotic-resistant *Escherichia coli* bacteria from urinary tract infection patients in Mosul. Al-Kitab J. Pure Sci. [Internet]. 2025 Mar. 11;9(1):172-182. DOI: https://doi.org/10.32441/kjps.09.01.p12.

Keywords: Urinary Tract Infection, *Escherichia Coli*, Antibiotic Resistantce.

Article History

Received	28 Jun.	2024
Accepted	29 Aug.	2024
Available online	11 Mar.	2025

Abstract:

In this study, 15 isolates of *Escherichia coli* were isolated from patients with urinary tract infections from Al-Khansa'a Teaching Hospital Nineveh/Iraq from May 2023 to July 2023. The isolates were studied and diagnosed biochemically. The result of microscopic tests showed isolates that are short Gram-negative bacilli, and the result of biochemical tests was that the isolates were positive for catalase, triple sugar iron, indole, methyl red, coagulation enzyme, fermentation of the following sugars maltose, sucrose, galactose and glucose, while *Escherichia coli* isolates showed negative results for urease, Voges-Proskauer, and citrate tests. The isolates also showed resistance to all antibiotics used, with high resistance to both ampicillin 100%, erythromycin 100% and cephalothin 100%. 60% for nalidixic, 53.33% for azithromycin and 53.33% levofloxacin and the lowest resistance rate shown by the isolates to gentamicin was 46.7%.

Keywords*:* Urinary Tract Infection, *Escherichia Coli*, Antibiotic Resistantce.

عزل وتشخيص بكتريا *Escherichia coli* المقاومة للمضادات الحيوية من مرضى التهابات المسالك البولية في مدينة الموصل

زينب باقر عباس*، حسن فيصل حسين

قسم علوم الحياة، كلية التربية للعلوم الصرفة، جامعة الموصل، الموصل، العراق

zainab.22esp15@student.uomosul.edu.iq, dr.hasankahya@uomosul.edu.iq

الخلاصة:

تم في هذه الدراسة عزل ١٥ عزلة من بكتريا الأشريكية القولونية *Escherichia coli* من مرضى التهابات المسالك البولية من مستشفى الخنساء التعليمي نينوى / العراق من أيار ٢٠٢٣ الى يوليو ٢٠٢٣. درست العزلات وشخصت كيموحيويا. أظهرت نتائج الاختبارات المجهرية أن العزلات عصيات قصيرة سلبية لصبغة كرام، كما أنها إيجابية لكل من اختبار الكتاليز Catalase، السكريات الثلاثية والحديد Triple Sugar Iron، الأندول Indol، المثيل الأحمر methyl Red، أنزيم تجلط الدم Coagulase وتخمر كل من السكريات الآتية مالتوز Maltose ، سكروز Sucrose ، كالاكتوز Galactose، كلوكوز Glucose، في حين أظهرت عزلات الأشريكية القولونية نتائج سلبية لاختبار اليوريز urease، فوكس-برسكاور Voges-Proskauer وسيتريت Citrate. وكذلك أظهرت العزلات مقاومة لجميع المضادات المستخدمة حيث وجد مقاومة عالية لكل من الأمبسلين ampicillin 100%,الأيرثرومايسين Erythromycin100% والسيفالوثين Cephalothin 100%. ٦٠٪ للنالدكسيك، 53.33% ازيثروميسين Azithromycin وبلغت مقاومة العزلات لليفلوفلوكساسين levofloxacin 53.33% واقل نسبة مقاومة أظهرتها العزلات للجنتامايسين Gentamycin بلغت 46.7%.

الكلمات المفتاحية: التهاب المسالك البولية، بكتريا الأشريكية القولونية، مقاومة المضادات.

1. Introduction:

Urinary tract infections (UTIs) are one of the most common infections in humans across all age groups, from newborns to the elderly [1]. An estimated 150 million infections occur annually worldwide [2]. It is the second most common bacterial infection in humans after respiratory infections. The infection occurs in the urinary tract, whether in the urethra (urethritis), bladder (cystitis) or kidneys (pyelonephritis). Upper urinary tract infections can be fatal if bacteria from an infected kidney travels into the bloodstream, a condition known as sepsis [3]. *Escherichia coli* is one of the most important members of the intestinal family and grows as a normal house in the gastrointestinal tract, and it is also considered an opportunistic pathogenic bacterium as it causes watery diarrhea as well as three diseases outside its natural

habitat such as meningitis in newborns, septicemia and urinary tract infections, as it causes about 90% of urinary tract infections. It causes about 90% of urinary tract infections and can be easily transmitted from the anal area to the urinary tract and bladder and is about 14 times more common in females than males due to the shorter urethra in females **[4]**. Some studies have shown that *Escherichia coli* resistance is not limited to a specific group of antibiotics such as Beta-lactam but may extend to several types of antibiotics (quinolones, aminoglycosides, sulfa compounds, macrolides, tetracyclines, and vancomycin). The characteristic of multiple resistance to antibiotics is an indicator of the seriousness of infection with these bacteria, when the infection occurs, the pathogenic bacteria acquire high resistance and sometimes it is silent **[5]**. *Escherichia coli* has multidrug resistance due to its ability to accumulate resistance genes mostly through horizontal gene transfer, such as the acquisition of genes encoding Beta-lactam enzymes conferring resistance to cephalosporins, carbapenemases conferring resistance to carbapenems, 16SrRNA methylase conferring resistance to aminoglycosides, and quinolone resistance genes by(PMQR) plasmid conferring resistance to quinolones **[6]**. The main objective of this study was to isolate and diagnose *Escherichia coli* bacteria from UTI patients attending Al-Khansa'a Teaching Hospital and to determine the sensivity and resistanance isolates to a group of selected antibiotics and compare them with previous studies Furthermore, it encourages the use of antibiotics that combat microorganisms and implement preventive measures to minimize the emergence of resistance to these microorganisms

2. Material and methods:

2.1 Bacterial sample collection: *Escherichia coli* isolates were collected from the urine of patients with urinary tract infections at Al-Khansa'a Teaching Hospital in Nineveh/Iraq from 1/8/2023 to 1/10/2023. Sterile collection containers were used to collect urine samples early in the morning. Then 100 microliters of urine were taken and cultured on blood agar and MacConkey agar and incubated at 37°C for 18-24 hours.

2.2 Culture diagnostics: The phenotypic characteristics of isolated bacterial colonies were studied after cultivation and purification of bacterial isolates on different culture media, such as MacConkey agar, Eosin methylene blue, and blood agar (India, Himedia). The study included aspects such as shape, size, texture, color, edges, and heights of isolated bacterial colonies **[7]**.

2.3 Microscopic diagnosis: Swabs of bacterial isolates previously grown on MacConkey agar for 18-24 hours were prepared by Gram technique and then examined under a compound light microscope using a 100x oil immersion lens **[4]**.

2.4 Biochemical test of *Escherichia coli* isolates: Biochemical tests were performed on bacterial isolates isolated from patients with urinary tract infections and included the following tests: Catalase [8], methyl red [9], Voges-Proskaur, citrate utilization [10], urease [11], Coagulation enzyme, Indole [12], triple sugar iron [13] and fermentation of various sugars [14].

2.4 Antibiotic Disk Susceptibility Test: Antibiotic susceptibility test was performed for ampicillin 25µg, azithromycin 15µg, cephalothin 30µg, erythromycin 10µg, gentamicin 10µg, levofloxacin 5µg, and nalidixic acid 5µg (Turkey, Bioanalyse). Using the Kirby-Bauer disk diffusion method according to Clinical and Laboratory Standards [15]. Pure single colony isolates were selected using a sterile inoculation loop and inoculated into a 5ml tube of sterile water, and then the turbidity of the bacterial suspension was matched with the turbidity standard (McFarland's 0.5 standard). A sterile cotton swab was dipped into the bacterial suspension to thoroughly culture the plates containing Muller-Hinton agar (India, Himedia). Using sterile forceps, place the tablets on the surface. The plates were then incubated for 24 hours at 35°C. The susceptibility pattern was then determined by measuring the zones of inhibition in millimeters [16].

3. Results:

3.1 Phenotype diagnostics: The bacterial isolates were diagnosed based on their morphological characteristics observed after cultivation in different media. The results revealed that Escherichia coli is capable of fermenting lactose, as it formed smooth, shiny, pink colonies on MacConkey agar, indicating its ability to ferment lactose and produce acids. The isolates also produced metallic green colonies on Eosin Methylene Blue (EMB) agar, which is a characteristic feature of this bacterium. On blood agar, the colonies appeared round, shiny, and transparent, reflecting the typical growth characteristics of E. coli on this medium. These morphological features serve as an important basis for the preliminary diagnosis of these bacterial isolates in the laboratory **Figure 1**.

3.2 Microscopic diagnostics: After a swab was taken from a single colony on an 18-24 hour old MacConkey agre and stained with gram dye, the bacteria appeared as short bacilli negative for Gram dye and non-spore-forming **Figure 2**, these results agree with the results of the researcher [4].

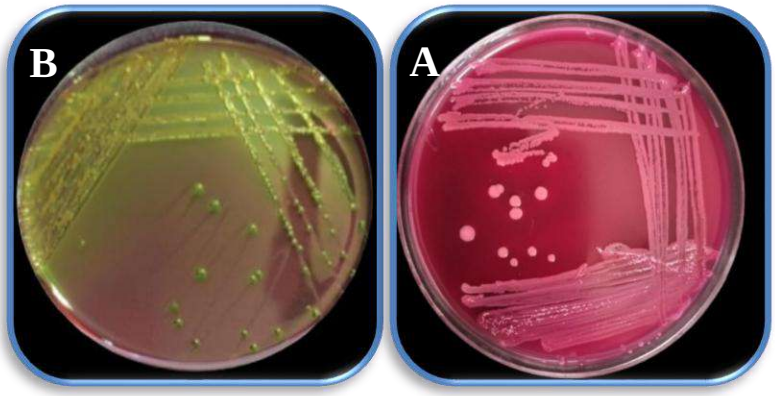

Figure 1: *Escherichia coli* colonies (Phenotypic diagnosis)
A: Colonies of pink *Escherichia coli* bacteria on MacConkey agar
B: Green *Escherichia coli* colonies with a metallic luster on Eosin methylene blue aga

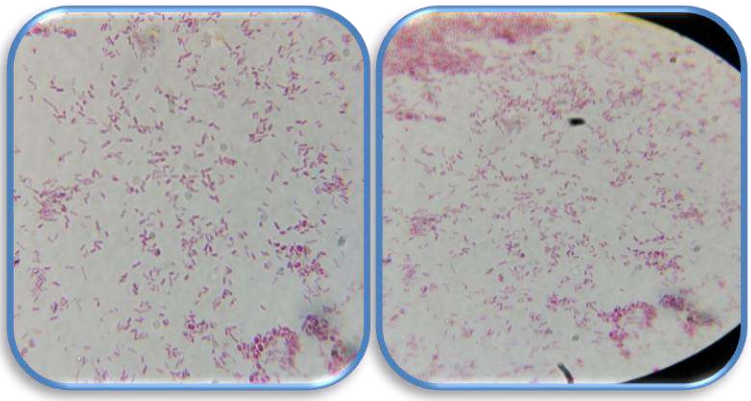

Figure 2: Microscope image for *Escherichia coli* bacteria stained with Gram stain

3.3 Biochemical diagnostics: Biochemical tests were performed on all bacterial isolates and the results are shown in Table 1 and Figure 3 It was found that all isolates were positive for the catalase test, it was negative for the urease test as there was no change in the color of the medium, isolates gave a positive result for the fermentation test of sugars such as sucrose, galactose, maltose and glucose and positive for the triple sugar iron test.

Table1: Biochemical Teasts Diagnosis of *Escherichia coli*

Results	Teasts
Catalase	+
Urease	-
Sucrose	+
Galactose	+
Maltose	+
Glucose	+
Triple sugar iron	+
Indole	+
Methyl red	+
Voges-Proskauer	-
Citrate	-
Coagulase enzyme	+

As for the results of the tests of the IMVIC group, the bacteria were positive for both the indole test. A positive result for the methyl red test, where it was observed that the color turned red,. As for the vogs- Perskauer test, the isolates gave a negative result where the medium appeared yellow and brown. For the citrate test, the medium did not turn blue-green, the isolates gave a negative. The isolates were positive for the coagulation enzyme test as a result of a clump appearing on the plasma droplet placed on a sterile glass slide within 10 seconds when a pure colony of bacteria was placed on It.

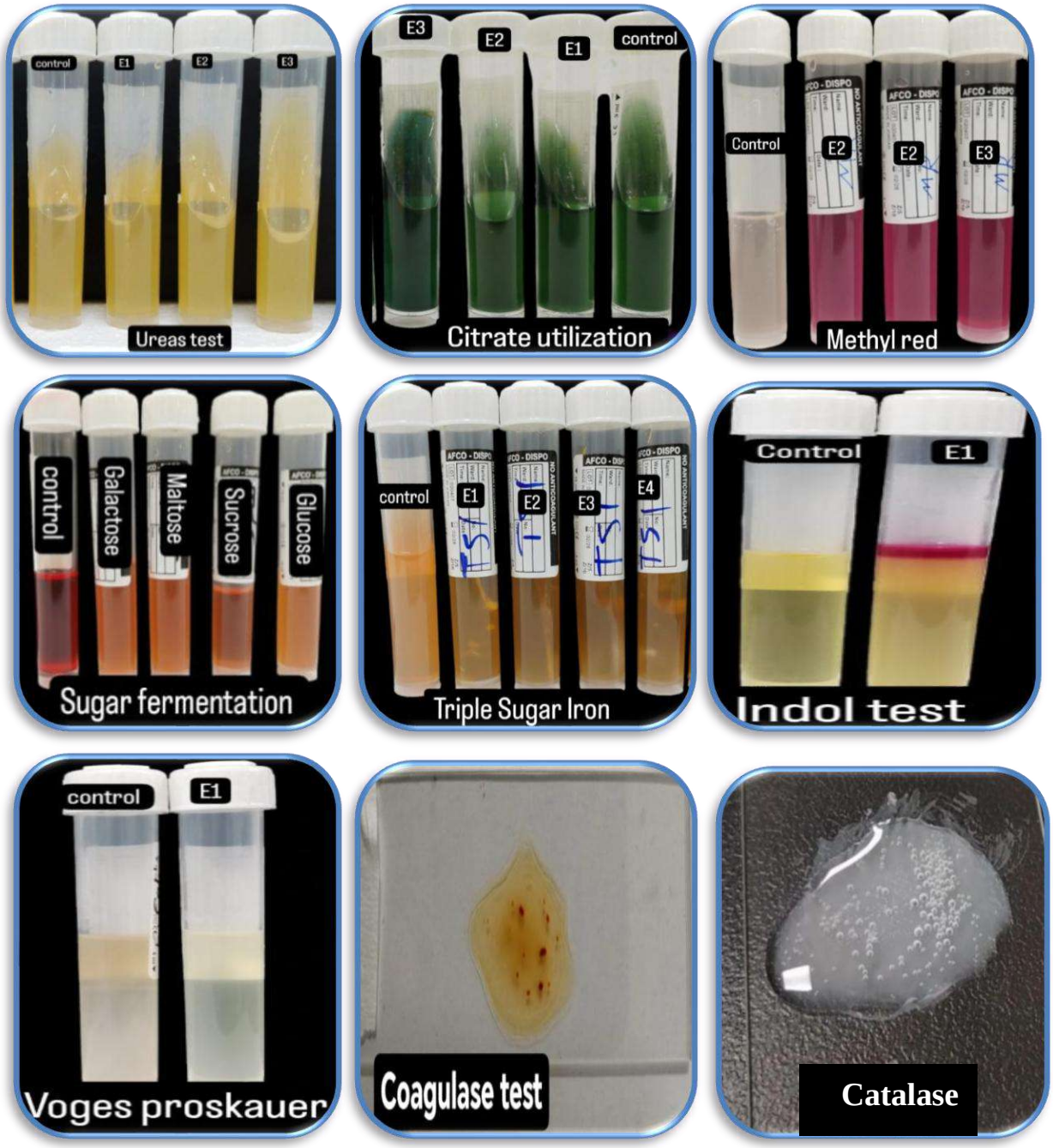

Figure 3: Biochemical tests for *E. coli* bacterial isolates

3.4 Antibiotic Disk Susceptibility Test: The results of the antibiotic susceptibility testing of bacterial isolates, interpreted according to the Clinical and Laboratory Standards Institute (CLSI) 2024 guidelines **[15]**, showed that all *Escherichia coli* isolates exhibited multi-drug resistance. The findings revealed that 15 isolates (100%) were resistant to the antibiotic Ampicillin, and 15 isolates (100%) were resistant to the antibiotic Cephalothin. Additionally, 15 isolates (100%) were resistant to the antibiotic Erythromycin, and 9 isolates (60%) were resistant to Nalidixic Acid. Twenty-one isolates were resistant to the antibiotic Azithromycin, while 8 isolates(53.33%) were resistant to Levofloxacin. The lowest resistance rate was observed for the antibiotic Gentamicin, with a resistance rate of 7(46.7%), **Table 2** and **Figure 4**.

Table 2: Antibiotic sensitivity pattern of *Escherichia coli* isolates.

Antibiotic	Code	concentration	Resistant n(%)	Intermediate n(%)	Sensitivity n(%)
Ampicillin	AM	25	15(100%)	0	0
Azithromycin	AZM	15	8(53.33%)	0	7(46.67%)
Cephalothin	KF	30	15(100%)	0	0
Erythromycine	E	10	15(100%)	0	0
Gentamycin	CN	10	7(46. 7%)	2(13.3%)	6(40%)
Levofloxacin	LEV	5	8(53.33%)	2(13.3%)	5(33.33%)
Nalidixic acide	NA	30	9(60%)	4(26.7%)	2(13.3%)

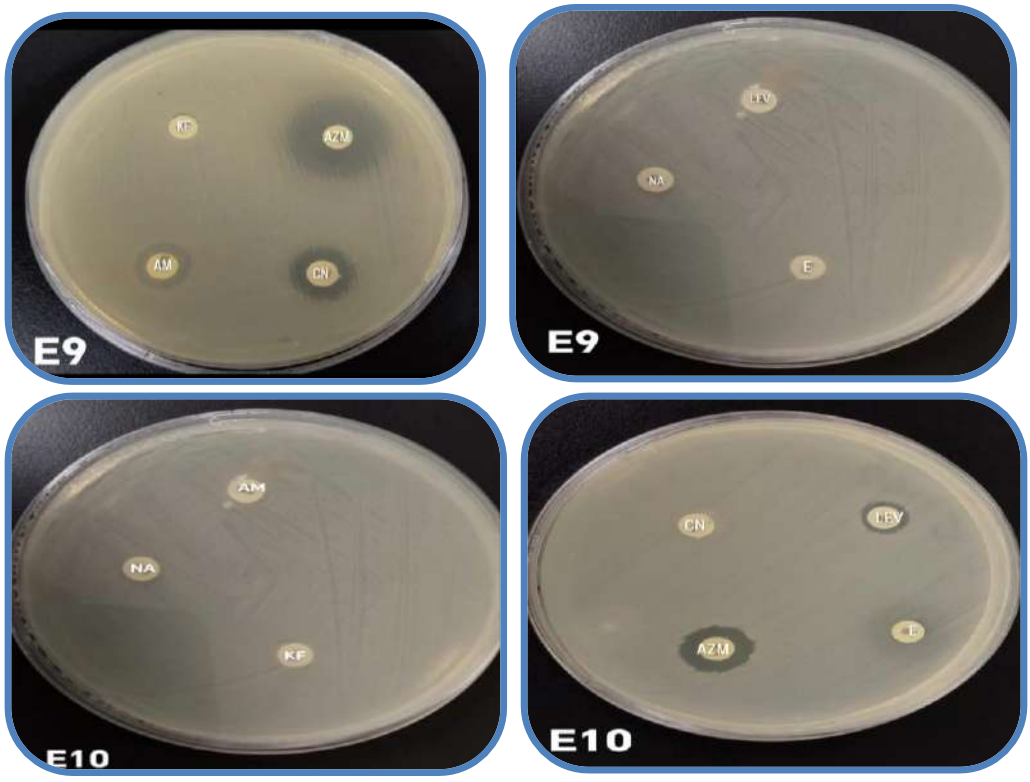

Figure 4: Testing the sensitivity of *E. coli* isolates to antibiotics.

4. Discussion

Escherichia coli bacteria are capable of fermenting lactose, leading to the formation of pink colonies on MacConkey agar, which contains bile salts and crystal violet dye. This composition allows the growth of Gram-negative bacteria, such as members of the Enterobacteriaceae family, while inhibiting the growth of Gram-positive bacteria **[17]**. On the other hand, the shiny green colonies on Eosin-Methylene Blue agar result from the presence of eosin and methylene blue dyes that precipitate in the acidic medium after binding with certain substances. This reaction gives the colonies a metallic green sheen, indicating that the bacteria have produced organic acids as a result of fermenting lactose and sucrose **[12]**. Garding the biochemical tests, all isolates were positive for the catalase test, indicating their ability to break down hydrogen peroxide into water. As for the urea test, the results were negative, as the isolates were unable to utilize urea due to the absence of the urease enzyme. The isolates were also positive for the test of the Triple sugar iron, glucose, maltose, galactose, and sucrose, as they demonstrated the ability to ferment these sugars. Regarding the tests of the enteric group, which distinguish *E. coli* from other genera of the Enterobacteriaceae family, the results were positive for the indole test, where a red ring appeared on the surface of the medium in the alcohol layer isoamyl, due to the breakdown of the amino acid tryptophan by the enzyme tryptophane. The results were also positive for the methyl red test, where the color changed to red due to the bacteria's fermentation of glucose. On the other hand, the result was negative for the Voges-Proskauer test, indicating that the isolates could not convert glucose into acetyl methyl carbonyl. Additionally, the result was negative for the citrate test, as the isolates did not use citrate as a sole carbon source, and therefore, the color of the medium did not turn bluish-green due to the absence of the citrate permease enzyme **[10,11,12]**.

As resistance to ampicillin Beta -lactam antibiotics reached 100%, consistent with the results of the researcher Al-Saadi which reported 100% resistance of isolates to ampicillin, Several studies have shown that 90% of *E. coli* are resistant to beta-lactam antibiotics due to the secretion of Beta-lactamase **[18]**. The bacterial isolates showed high resistance to the Cephalothin (100%) and were close to the results obtained by the researcher Ait-Mimoune *et. al,*. where the percentage of resistance of isolates to the antibiotic Cephalothin amounted to (85%) while there are high levels of resistance to ampicillin, tetracycline and cephalothin among *E. coli* and this may be related to the high rate of prescribing these antibiotics in the treatment of urinary tract infections and the excessive and inappropriate use of broad-spectrum antibiotics by patients is the main reason for the emergence of resistance caused by bacterial mutations **[19]**. While the results of the current study differed with the results of study

Hashemian *et.al,*. in Iran where the highest percentage of antibiotic resistance of isolates was for cephalothin (77.1%) and ampicillin (78.8%) **[20]**.

Gentamicin resistance in this study amounted to 46.7%. The result was close to the previous study Ismael *et. al,*. where the percentage of resistance of isolates in his study was 40% **[21]**. while it differed from the results obtained by searcher Ramirez-Castillo *et. al,*. who indicated that 28.2% of isolates are resistant to gentamicin and that the mechanisms of resistance to aminoglycosides are mutation Enzymatic site and ribosome site modification and the accumulation of decreasing intracellular antibiotic accumulation by altering the permeability of the outer membrane **[22]**. The isolates showed resistance to nalidixic and levofloxacin in our study 60%, 53.33% and was close to the study results Ghotaslou *et. al,*. (73%, 58%) **[23]**. Zaman *et. al,*. showed that *Escherichia coli* inhibits DNA synthesis through inhibition of the DNA gyrase enzyme or as a result of genetic mutations in it, which leads to resistance to antibiotics belonging to the quinolines group **[24]**. The isolates showed high resistance to erythromycin, reaching 100%, and agreed with the results of the Al-Saadi who found that 98% of the isolates were resistant to this antibiotic, and the resistance of the isolates to azithromycin amounted to 53.33, and differed from what Salhy found, as he indicated that 30.3% of the isolates were resistant to azithromycin **[17, 25]**. Zaman *et. al,*. pointed out that some of the reasons for the resistance of *Escherichia coli* isolates to macrolides are hydrolysis, which results in the degradation of the antibiotic and inhibition of its effectiveness, the production of glogsylation and phosphorylation enzymes that inhibit the action of the antibiotic and the acquisition of flow systems as well as a change in the targeting locations **[24]**.

5. Conclusions

In recent years, antibiotic resistance has become a global threat to health systems around the world, and E. coli poses the greatest threat to human health due to its increasing resistance to antibiotics, and all isolates in our study showed multiple resistance to the antibiotics used Ampicillin, Erythromycin, Cephalothin, Azithromycin. Gentamicin, levofloxacin and Nalidixic acid, as a result of the diverse resistance mechanisms exhibited by *E. coli* as a result of the overuse and misuse of antibiotics. and misuse, which may lead to serious health effects.

Acknowledgements:

This study is supported by the Department of Biology, College of Education for Pure Science, University of Mosul. Many thanks to all participants and patients. A great thankful to Central Laboratories/ Nenawa Health Office including doctors and nurses who were supportive to accomplish this study.

6. References

[1] Walker MM, Roberts JA, Rogers BA, Harris PNA, Sime FB. Current and emerging treatment options for multidrug-resistant *Escherichia coli* urosepsis: A Review. Antibiotics (Basel). 2022;11(5):456

[2] Zagaglia C, Ammendolia MG, Maurizi L, Nicoletti M, Longhi C. Urinary tract infections caused by uropathogenic *Escherichia coli* strains—new strategies for an old pathogen. Microorganisms. 2022;10(7),1425.

[3] Lin W-H, Wang M-C, Liu P-Y, Chen P-S, Wen L-L, Teng C-H, et al. *Escherichia coli* urinary tract infections: host age-related differences in bacterial virulence factors and antimicrobial susceptibility. J Microbiol Immunol Infect. 2022;55:249–56.

[4] Levinson W. Review of Medical Microbiology and Immunology. 14th ed. New York: McGraw-Hill Education; 2016. p. 821.

[5] Khawcharoenporn T, Vasoo S, Singh K. Urinary Tract Infections due to Multidrug-Resistant Enterobacteriaceae: Prevalence and Risk Factors in a Chicago Emergency department. *Emergency medicine international*, 2013(1),158517

[6] Poirel L, Madec JY, Lupo A, Schink AK, Kieffer N, Nordmann P, Schwarz S. Antimicrobial Resistance in *Escherichia coli*. Microbiol Spectr. 2018 Jul;6(4).

[7] Wanger A, Chavez V, Huang R, Wahed A, Dasgupta A, Actor JK. Microbiology and molecular diagnosis in pathology: a comprehensive review for board preparation, certification and clinical practice. 1st edition, 2017.

[8] Procop GW, Church DL, Hall GS, Janda WM. Koneman's color atlas and textbook of diagnostic microbiology. Jones & Bartlett Learning; 2020.

[9] Hemraj V, Diksha S, Avneet G. A review on com monly used biochemical test for bacteria. IJLS. 2013;1(1):1-7.

[10] Brown AE, Smith HR. Benson's Microbiological Applications Laboratory Manual in General Microbiology. 14th ed. New York: McGraw-Hill Higher Education; 2017. 438 p.

[11] Tille PM. Baily and Scott's Diagnostic Microbiology. 14th ed. China: Elsevier Inc.; 2017. 1115 p.

[12] Forbes BA, Saham DF, Weissfeld AS. Baily and Scott’s Diagnostic Microbiology. 12th ed. Mosby Inc., an affiliate of Elsevier Inc.; 2007. 1031 p.

[13] Harley JP, Prescott LM. Laboratory Exercises in Microbiology. 4th ed. McGraw-Hill Education, Inc.; 2002. 466 p.

[14] Mahon CR, Lehman DC, Manuselis G. Textbook of Diagnostic Microbiology. 4th ed. Philadelphia: W.B. Saunders Co.; 2011.

[15] Clinical and Laboratory Standards Institute (CLSI). Performance standards for antimicrobial susceptibility testing; twenty fifth informational supplement. CLSI Document M100-S31. 2021.

[16] Abdal Jabar RM, Hassoon AH. Study of acrA efflux pump gene in local isolates of Klebsiella pneumoniae exposed to different types of antibiotics. M.Sc. thesis. College Of education for pure sciences/ Ibn Al-Haitham, Department of Biology. Baghdad University, Baghdad, Iraq; 2018.

[17] Basavaraju, M., & Gunashree, B. S. (2022). Escherichia coli: An overview of main characteristics. *Escherichia Coli-Old and New Insights*. https://www.intechopen.com/chapters/84764

[18] Al-Saadi ZA. Phenotypic and molecular detection of *Escherichia coli* efflux pumps from UTI patients. Master Thesis, Education for Pure Sciences, University of Baghdad, Baghdad, Iraq; 2019.

[19] Ait-Mimoune N, Hassaine H, Boulanoir M. Bacteriological profile of urinary tract infections and antibiotic susceptibility of *Escherichia coli* in Algeria. Iran J Microbiol. 2022;14(2):156-160.

[20] Hashemian H, Saleh ZV, Afzalipoor M, Jafari A. Antibiotic resistance patterns of uropathogenic causes of urinary tract infections in <3-year-old children: a single-center cross-sectional study. Arch Pediatr Infect Dis. 2023;11(3).

[21] Ismael NM, Azzam M, Abdelmoteleb M, El-Shibiny A. Phage vB_Ec_ZCEC14 to treat antibiotic-resistant *Escherichia coli* isolated from urinary tract infections. Virol J. 2024;21(1):44.

[22] Ramirez-Castillo FY, Moreno-Flores AC, Avelar-González FJ, Márquez-Díaz F, Harel J, Guerrero-Barrera AL. An evaluation of multidrug-resistant *Escherichia coli* isolates in urinary tract infections from Aguascalientes, Mexico: cross-sectional study. Ann Clin Microbiol Antimicrob. 2018;17:1-13.

[23] Ghotaslou R, Baghbani S, Ghotaslou P, Mirmahdavi S, Leylabadlo HE. Molecular epidemiology of antibiotic-resistant *Escherichia coli* among clinical samples isolated in Azerbaijan, Iran. Iran J Microbiol. 2023;15(3):383.

[24] Zaman SB, Hussain MA, Nye R, Mehta V, Mamun KT, Hossain N. A review on antibiotic resistance: alarm bells are ringing. Cureus. 2017;9(6):1-9.

[25] Salehi A, Davari K, Karimoddini M, Sanani MGP. Evaluating the macrolide resistance of *Escherichia coli* isolated from urinary infection and determining the phylogeny using the ERIC-PCR method. Eur J Mol Clin Med. 2021;8(1):2113.

Al-Kitab Journal for Pure Sciences (2025); 9(1):183-201.
https://doi.org/10.32441/kjps.09.01.p13

Al-Kitab Journal for Pure Sciences
ISSN: 2617-1260 (print), 2617-8141(online)

https://isnra.net/index.php/kjps

The Impact of Two Selected Doses of Gabapentin on the Kidney and Brain of Adult White Male Rats: A Histological, Biochemical, and Immunohistochemical Study

Sura Salim Mahmood, Baidaa Abdulaziz Mohamed Salah*

Department of Biology, College of Education for Pure Science, University of Mosul, Mosul, Iraq.

*Corresponding Author: email :baidaamohmmed@uomosul.edu.iq

Citation: Mahmood SS, Salah BAM. The Impact of Two Selected Doses of Gabapentin on the Kidney and Brain of Adult White Male Rats: A Histological, Biochemical, and Immunohistochemical Study. Al-Kitab J. Pure Sci. [Internet]. 2025 Mar. 17 ;9(1):183-201. DOI: https://doi.org/10.32441/kjps.09.01.p13.

Keywords: Apoptosis, Cholinesterase, Histopathology, Brain, Kidney, Gabapentin.

Article History

Received	12 Jul.	2024
Accepted	18 Aug.	2024
Available online	17 Mar.	2025

Abstract:

Gabapentin is a medication commonly used in the treatment of epilepsy and sciatic neuropathy. Histology, biochemistry, immunohistochemical changes, body, kidneys, and brain weights were investigated in this study, where 15 male albino rats were used. The animals were split into 3 sets: A, B, and C (5 rats/set). Set A was administrated in distilled water (control set). Gabapentin was administrated orally to both B and C sets at doses 21.8 and 43.6 mg/kg, respectively. The dosing period was 30 days. The findings showed glomerular atrophy and changes in renal tissue in the B and C sets. Brain sections of B and C sets showed necrotic and degenerative changes. The findings showed insignificant body and brain weight increases in B and C sets, while set B significantly decreased kidney weight. Biochemical analysis showed an insignificant increase in the urea and creatinine in both experimental sets. Both B and C sets showed insignificant increases in the cholinesterase enzyme activity in the brain. Immunohistochemical assessment of the kidney tissue showed positive and strong positive immunoreactivity of both caspases 3 and 8. Both B and C sets showed weakly positive and positive Glial Fibrillary Acidic Protein (GAFP) immunoreactivity in the brain. It was obvious that gabapentin caused the induction of apoptosis in the kidney through the overexpression of caspases 3&8. The medication also induced various lesions in the brain, especially in the axons

of the neurons. The severity of its effect depended on the given dose and duration of treatment.

Keywords: Apoptosis, Brain, Cholinesterase, Gabapentin, Histopathology, Kidney.

تأثير اثنتين من الجرعات المختارة من عقار الكابابنتين على كلية ودماغ الجرذان البيض البالغة: دراسة نسجيه، كيموحيوية، وكيميائية مناعية نسجيه

سرى سالم محمود، بيداء عبد العزيز محمد صالح*

قسم علوم الحياة، كلية التربية للعلوم الصرفة، جامعة الموصل، الموصل، العراق

sura.22esp16@student.uomosul.edu.iq , baidaamohmmed@uomosul.edu.iq

الخلاصة:

يعد الكابابنتين عقار شائع لعلاج الصرع والتهاب العصب الوركي . في الدراسة الحالية ، استخدم ٣٠ جرذ ابيض ذكر. قسمت الحيوانات الى ثلاث مجاميع *A,B* و*C* (5جرذان/مجموعة). مجموعة *A* جرعت بالماء المقطر(مجموعة سيطرة). جرعت المجموعتين *B* و*C* فمويا بعقار الكابابنتين وعند التركيزين ٢١,٨ و٤٣,٦ ملغم /كغم من وزن الجسم .كانت مدة التجريع ٣٠ يوم. تم التحري عن التغيرات النسجيه، الكيموحيوي، الكيميائية الحيوية ،والكيميائية المناعية النسجيه ، فضلا عن التغيرات في وزن الجسم ،الكلية والدماغ .أظهرت النتائج ضمور الكبيبة وتغيرات مرضية أخرى في النسيج الكلوي للمجموعتين *B* و*C* . وأظهرت مقاطع الدماغ للمجموعتين *B* و*C* تغيرات تنكسية وتنخريه . وأظهرت النتائج زيادة غير معنوية في وزن الجسم والدماغ ، في حين كان هناك انخفاض معنوي في وزن الكلية . بينت نتائج التحليل الكيموحيوي زيادة غير معنوية في اليوريا والكيراتين في كلتا المجموعتين التجريبيتين *B* و *C*. وأظهرت المجموعتين *B* و *C* زيادة غير معنوية في فعالية أنزيم الكولين ستيريز. اظهر التحليل الكيميائي المناعي النسجي لنسيج الكلية استجابة موجبة وموجبة قوية لبروتيني *caspases 3*و٨ في كلتا المجموعتين التجريبيتن *B* و *C*. كلتا المجموعتين التجريبيتن *B* و*C* أظهرت استجابة موجبة ضعيفة وموجبة لبروتين *GAFP* في نسيج الدماغ .كان واضحاً أن عقار الكابابنتين سبب حث مسارات الموت المبرمج من خلال التعبير الجيني المفرط لبروتيني *caspases 3* و٨ . حث العقار ظهور أفات مختلفة في نسيج الدماغ وخاصة في محاور الخلايا العصبية . وكانت شدة التأثير معتمدة على الجرعة والفترة الزمنية للمعاملة.

الكلمات المفتاحية: موت الخلايا المبرمج، علم الأمراض النسيجي، الدماغ، الكلية، جابابنتين.

1. Introduction:

Anticonvulsant medications are mostly used for managing epilepsy, although they are additionally employed to treat migraines, bipolar mood disorder, neuropathy, and inflammation of the nerves **[1].** One of the most prominent anticonvulsant drugs is gabapentin (gamma-aminobutyric acid), which is used to treat electrical brain disorders and pain resulting from damage to the nerves, especially the cranial nerve. The drug is also used to treat nerve damage caused by diabetes, which is known as diabetes mellitus neuropathy. It is also used to treat nerve pain after infection with the herpes virus. The drug also treats dysesthesia **[2].**

The drug was discovered in 1970 through a campaign conducted to discover drugs to treat neurological disorders **[3].** Following the United States FDA's confirmation, the medication was initially made available to Americans in 1993. It is functionally related to another drug, pregabalin, and the drug works to inhibit the release of irritating neurotransmitters, thus helping

in its use against pathological neurotransmission **[4].** Despite its benefits, this medication produces negative effects, such as drowsiness and loss of balance. The drug's use raises the possibility of allergy responses, breathing difficulties, and depression **[5].**

The toxic role of the drug is evident from its interaction with some other anticonvulsants **[6].** The drug falls under category C. The drug causes apoptosis at certain doses and tissue damage to the kidneys in rats **[7].** The drug is well absorbed orally and exists in plasma in an unbound form. The medication affects calcium channels that are voltage-gated in neurons in the cortex at the accessory nerve units. Thus, the concentration of GABA increases at the synapse area, and the drug reduces the monoamine transporters **[8].** The liver and kidneys are the organs concerned with getting rid of most drugs, and therefore any defect affects them and makes them unable to perform their functions properly. This causes the deposition of drugs, especially anticonvulsant. Liver and kidney dysfunction causes a prolongation of the period allocated for the elimination or excretion of the medication or from the toxic metabolic compound, leading to clinical toxicity that can impact the attaching, distribution of cellular proteins, and the metabolism process. For example, protein binding is significantly reduced for acidic, negatively charged drugs, such as phenytoin and valproate in patients with kidney failure **[9].**

Case study reports stated that gabapentin causes liver damage, but without causing symptoms. The drug caused liver cirrhosis in a 90-year-old patient when he took 900 mg/kg for two weeks **[10, 11].** When the drug is used for 5 weeks in the case of treating neuropathic pain, the drug causes neutropenic fever. Long-term use of the drug impacts the healing or recovery process of bones, especially bone fractures, through its effect on some biochemical parameters and histological composition in rats **[12].** The drug has a significant effect on the gene expression of some cancer genes **[13].** Gabapentin impacts the male and female reproductive systems in rats, as it causes a decrease in testosterone levels and the process of sperm production while in females, it inhibits the steroids of the pineal gland, stimulates gonad hormones, and increases the atretic follicles. The drug also affects the period of pregnancy, especially affecting the development of the skull **[14].** The current research aimed to identify the toxic effects of the drug gabapentin at doses 21.8 and 43.6 mg/kg on some biochemical, histopathological, and immunohistochemical variables in the liver and brain of male albino rats.

2. Material and methods:

2.1. Ethical Approve: According to The Institutional Animal Care and Use Committee (IACUC) ethical approval number UM.VET.2023.046 dated 2/10/2023, the study was carried out in an animal's housing at the Faculty of Veterinary Medicine at the University of Mosul, Iraq.

2.2. Obtaining and raising animals: 15 male rats were used in the current study. The average weight was 195±5 grams. The entire experiment was carried out in a facility of animals at the Faculty of Veterinary Medicine, University of Mosul, Mosul, Iraq after the animals were transported there from Cihan University in Erbil. The animals were kept in typical cages in normal circumstances. The animals were cared for by specialists in the animal house. The animals were fed pellets and given water daily during the experiment period for all groups.

2.3.Medication dosing and supplementation: Gabapentin was obtained from a local pharmacy in Nineveh Governorate. The drug is manufactured by JENERIS Pharmaceutica, S.A., Rua Jaoa de Deus,19. 2700-487 Amadora, Portugal. The research doses were calculated based on the oral LD50 rate, which is 5000 mg/kg **[15].** The doses chosen in the current research are 21.8 and 43.6 mg per 1 kg. Each concentration was diluted in six ml of filtered water and then the relevant dose was withdrawn depending on the weight of the animal **[16].** The medication was administered orally by gavage needle to the male rats **[17].** The selected doses were dissolved in distilled water. The medicine was given for only one month.

2.4. Study design: A, B, and C were the three sets of fifteen mature male rats. Every set has five animals in it. A set was considered a control group. B&C sets were given gabapentin orally (21.8 and 43.3 mg/kg) body weight [b.w.] by a special dosing needle for 30 consecutive days. Weekly weigh-ins were conducted on the animals.

2.5. Histopathological preparation: The kidney and brain were obtained after dissection and placed in a 10% neutral buffered formalin to fix the tissues for 3 consecutive days. The weight of the previous organs was recorded. The tissue samples were washed with running water for 1 hour to remove traces of the fixative **[18].** The histological slides were prepared routinely. The paraffin blocks were sectioned by typical microtome. The histological sections were between 4-5 micrometers in thickness. Harri's Hematoxylin and Eosin were used to stain histological sections **[19].** DPX was used for mounting the slides. It was cleaned, prepared, and mounted with D.P.X. as a suitable medium **[20].** The microscopic assessment and photography were done using a compound microscope attached to a digital single-lens reflex camera (type MDCE-6A, Japan) **[21].**

2.6. Detection of the kidney Urea, and creatinine: After a full month of dosing with gabapentin, the rats were euthanized, and blood samples (1.5-2 ml) were collected from the eye's corner using capillary tubes. The taken blood was stored in small containers with anticoagulants, and samples of it went through a centrifuge (3000 rpm) for over 10 minutes to produce serum for biochemical evaluation. Before use, the serum had been kept in a freezer at -20 C. **[20].** Biosystems S.A.UREA/ BUN color, Costa Brava30,08030, Barcelona, Spain kit

was used.

2.7. Detection of cholinesterase enzyme in the brain tissue: The brain was ground and homogenized using a homogenizer Electroporation for 30 seconds at a speed of 400 r/min to the brain and it was a tube. The homogenizer was immersed in ice during the homogenization process as the brain was triturated in a Phosphate buffer solution with a pH of 8.1 after adding three ml/100 mg of tissue weight **[21].** The samples were stored in test tubes immersed in crushed ice until cholinesterase tests were performed immediately after the previous process was done.

2.8. Immunohistochemical assessment: The avidin-biotin immunoperoxidase method was employed to conduct immunohistochemistry. CASP1, CASP3, and CASP8 (Elabscience, USA, catalog No. E-AB-70300, Catalog No. E-AB-70388, Catalog No. E-AB-19664, respectively were investigated in the kidney. GFAP (Elabscience, USA, catalog No. E-AB- 650669) was investigated in the brains. A quantitative cell scoring method was used to detect the immunoreactive bodies in cells. A four-point score based on the IHC staining intensity of the cells was employed for negative (-), weak positive (+), positive (++), and strong positivity (+++).

2.9. Data analysis: The criteria chosen to be measured in the current research were statistically analyzed, including variations in body weight and specific body parts, criteria for measuring kidney and brain function, and changes in the cholinesterase enzyme using Graph Pad Prism 5.0 (San Diego, USA) software. All previous parameters were described as an average ± standard deviation (SD). The P-value was estimated as; significant ($P<0.05$), and very significant ($P<0.01$), respectively.

3. Results:

The light microscopic assessment of the kidney belongs to A set (control set) showed the normal histological structure of the kidneys **Figure 1**.

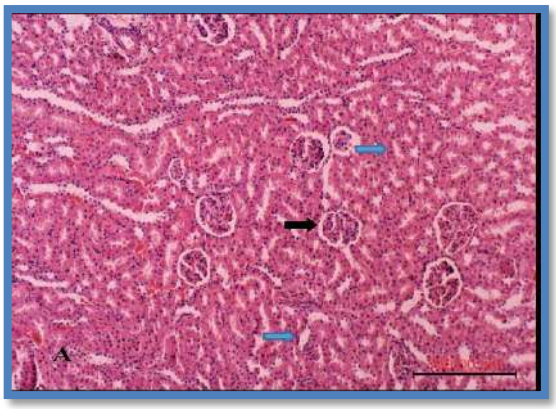

Figure 1: The histological section of the cortical part of the rat kidney of set A (control group) shows the normal histological structure of the glomeruli (black arrow) and surrounding tubules (blue arrow). (200µm H&E).

It is represented by Malpighian corpuscles (glomeruli) and renal tubules. Sections of set B (21.8 mg/kg) demonstrated the presence of significant and evident glomerular atrophy, oedema, Bowman's gap expansion, and alterations, including partial cell death, in the urine tubules **Figure 2**.

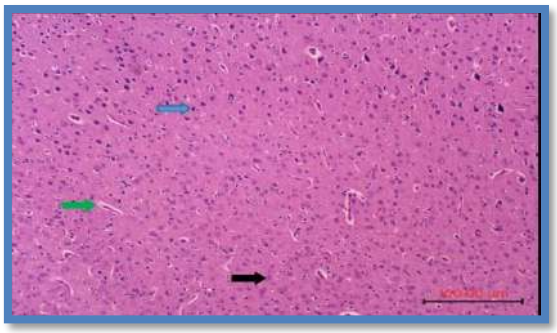

Figure 2: The histological section of the cortical part of the rat kidney of set B shows the presence of atrophy in the glomeruli, effects of oedema, widening of Bowman's space (black arrows), and changes in the urinary tubules, including partial destruction of cells (blue arrows) and congestion in the blood vessels (green arrow) (100µm H&E).

Sections from set C (43.6 mg/kg) showed the presence of severe atrophy of the Malpighian corpuscles, effects of oedema, damage to the tiny, filtering blood vessels, widening of Bowman's space, and destruction of most of the urinary tubules, including the destruction of cells **Figure 3**.

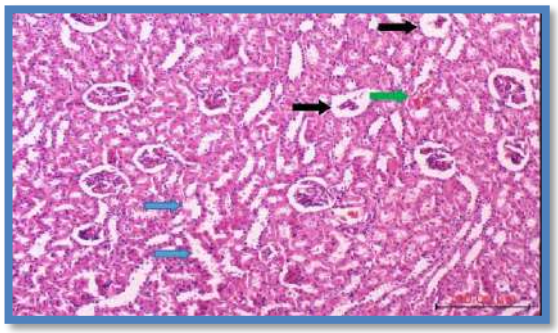

Figure 3: The histological section of the cortical part of the rat kidney of set C shows severe atrophy of the glomerulus, expansion of Bowman's space (black arrows), and destruction of the renal tubules (blue arrows) (100µm, H&E).

The light microscopic assessment of the brain belongs to the A set (control set) and shows normal histology of the brain that is represented by neurons, glial cells, and normal blood vessels that exist in the cortical part of the brain **Figure 4**.

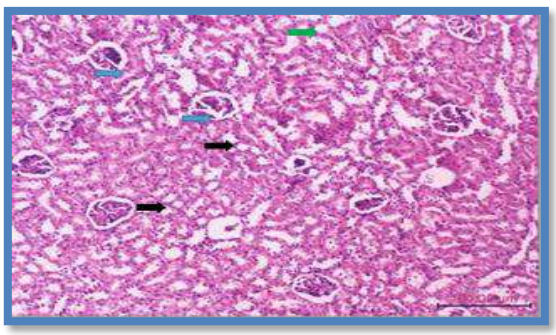

Figure 4: The histological section of the brain belongs to the A set (control set) showing normal neurons (black arrow), glial cells (blue arrow), and blood vessels (green arrow) in the brain cortex (100µm H&E).

Brain sections of set B revealed neuronal necrosis, degenerative changes, and blood vessel congestion **Figure 5**.

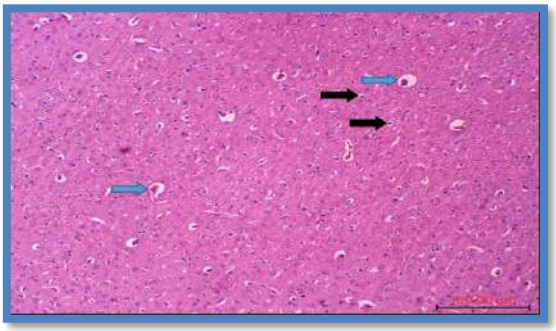

Figure 5: The histological section of the brain belonging to the B set shows cell death (necrosis) of nervous cells (black arrow), vacuolation of the neuronal cytoplasm (green arrow), and blood vessel congestion (blue arrow). (100µm, H&E)

while sections of set C revealed severe necrotic and degenerative changes in nervous tissue as well as congestion **Figure 6**.

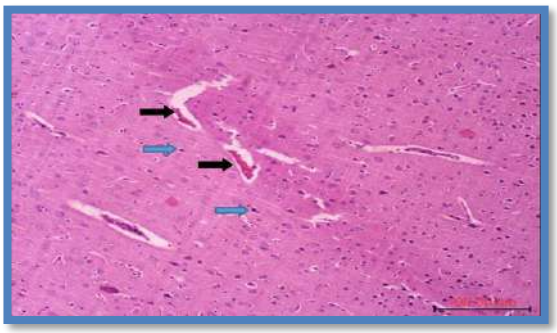

Figure 6: The histological section of the brain belonging to the C set shows severe necrotic (black arrows) and degenerative changes (blue arrows). (100µm, H&E).

3.1. Effect of gabapentin on body, kidney, and brain weights: The findings revealed an insignificant increase in the body weight for both experimental groups (21.8, 43.6 mg /kg) compared to set A **Figure 7.**

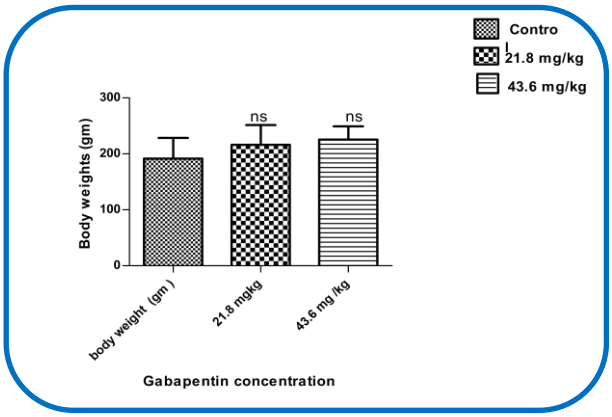

Figure 7: The effect of gabapentin at the doses 21.8 and 43.6 mg/kg (sets B and C) on the body weight. The medication was given for 30 consecutive days (1 month). P< 0.01 is considered highly significant, and n = not significant in comparison to set A. By comparing the average of each concentration in the two test sets to the means of set A, Dunnett's test was utilized to demonstrate the discrepancies.**

Brain weight showed an insignificant increase for both previous sets **Figure 8**.

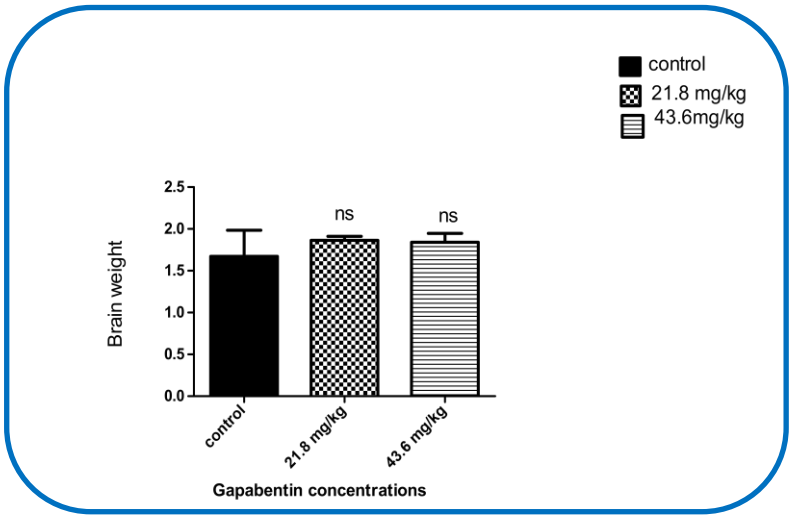

Figure 8: The effect of gabapentin at the doses 21.8 mg /kg (sets B and C) on the brain weight. The medication was given for 30 constitutive days (1 month), n = not significant in comparison to set A. By comparing the average of each concentration in the two test sets to the means of set A, Dunnett's test was utilized to demonstrate the discrepancies.

In addition, kidney weight revealed a highly meaningful (P > 0.01) abate at the concentration of 21.8 mg/kg and an insignificant decrease in weight at the dose of 43.6 mg/kg in comparison with the set A **Figure 9**. When comparing the results of the two experimental sets, we note that the kidneys of the third set (43.6 mg /kg) showed a non-significant increase compared to the second set (21.8 mg /kg).

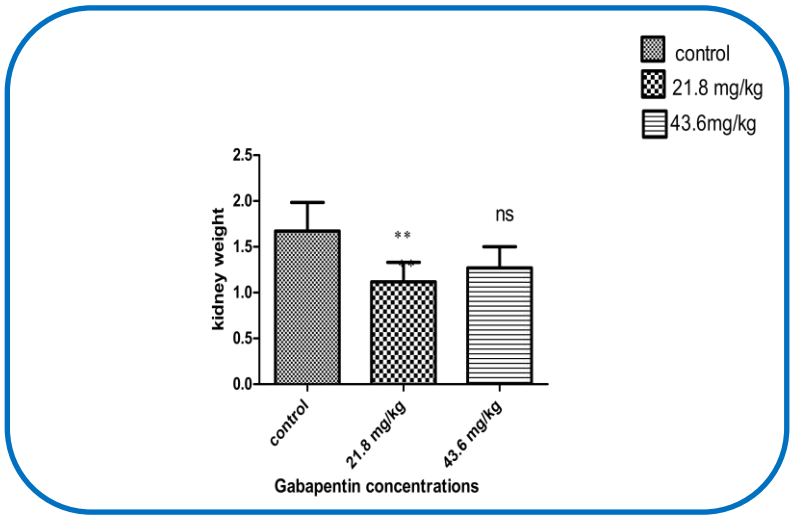

Figure 9: The effect of gabapentin at the doses 21.8 and 43.6 mg/kg (Sets B and C) on the kidney's weight. The medication was given for 30 consecutive days (1 month). P>0.01 is considered highly significant, and n = not significant in comparison to set A. By comparing the average of each concentration in the two test sets to the means of set A, Dunnett's test was utilized to demonstrate the discrepancies.**

3.2. Effect of Gabapentin on the level of Urea and creatinine: The findings showed a significant (P> 0.05) and insignificant increase in the urea level of both sets B and C, respectively, in comparison to set A **Figure 10**. Creatinine levels showed an insignificant increase at the two selected doses **Figure 11**.

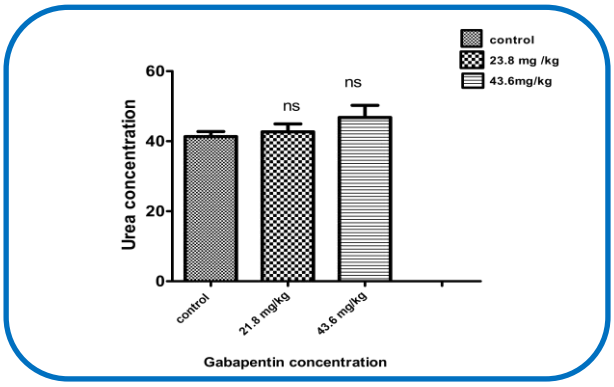

Figure 10: The effect of Gabapentin medication on the Urea level at the concentration 21.8 (set B) and 43.6 (set C) mg/kg. The medication was given for 30 consecutive days (1 month). * Considered as significant at P<0.05, and ns = not meaningful in comparison to set A. By comparing the average of each concentration in the two test sets to the means of set A, Dunnett's test was utilized to demonstrate the discrepancies

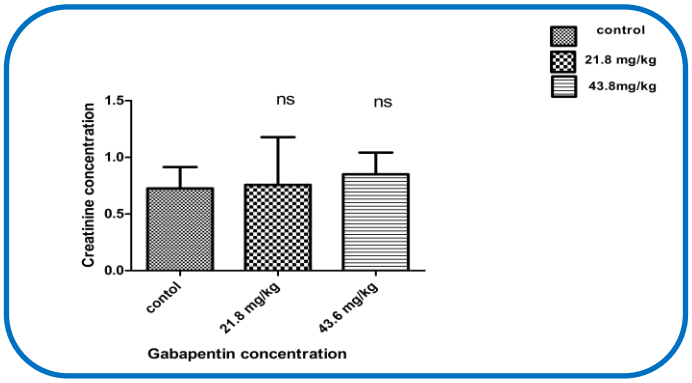

Figure 11: The effect of Gabapentin medication on the Creatinine level at the doses 21.8 (set B) and 43.6 (set C) mg/kg. The medication was given for 30 consecutive days (1 month). ns = not significant in comparison to set A. By comparing the average of each concentration in the two test sets to the means of set A, Dunnett's test was utilized to demonstrate the discrepancies

3.3. Effect of Gabapentin on the cholinesterase level in the brain: The findings revealed that there is an insignificant change in the brain cholinesterase activity in set B and insignificant increase in its activity in the set C in comparison with set A **Figure 12**.

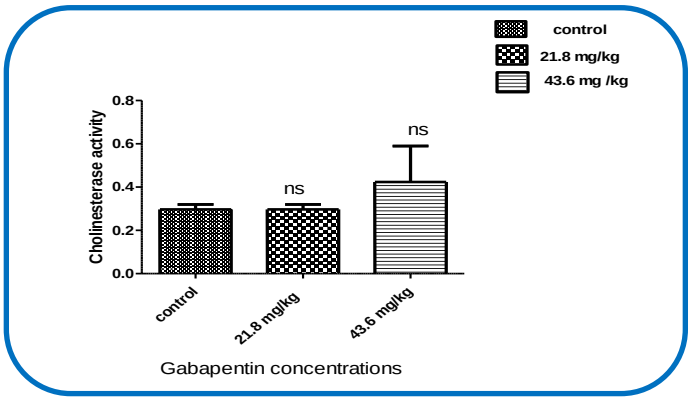

Figure 12: The effect of Gabapentin medication on the cholinesterase activity at the doses 21.8 and 46.6 mg/kg . The medication was given for 30 constitutive days (1 month). ns = not meaningful in comparison to control. By comparing the average of each concentration in the two test sets to the means of set A, Dunnett's test was utilized to demonstrate the discrepancies

3.4. Effect of Gabapentin on the expression of CASP3 and CASP8 in the kidney: To determine the impact of 21.8 and 43.6 mg/kg of gabapentin in the enhancement programmed cell death in the kidney of a male rat, the positivity of caspase-3 and caspase-8 was examined.

The microscopical assessment of renal tissue of set A showed negative immunoreactivity of CASP3 (-) **Figure 13**. A positive and a strong positive (+++) of CASP3 expression in the renal epithelial cytoplasm were detected in sets B **Figure 14** .

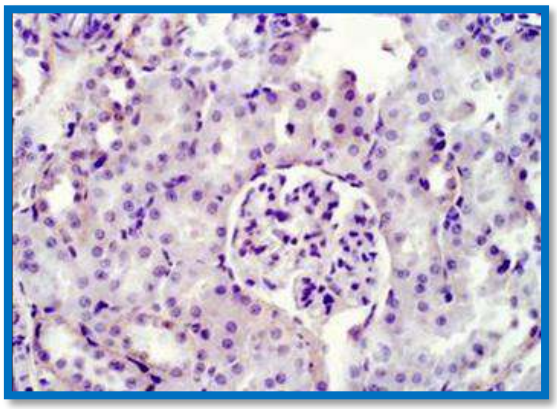

Figure 13: A photomicrograph of the kidney cortex of set A showing revealed negative (-) caspase-3 immunoreactivity in the renal tubule's epithelia. Immunohistochemical stain, 400 x

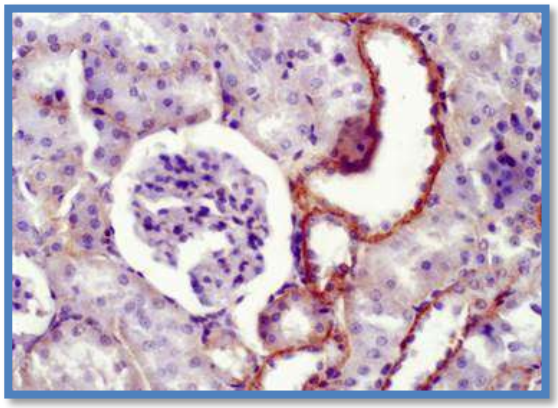

Figure 14: A photomicrograph of the kidney cortex of set B shows a positive (++) immunoreactivity (black arrow) of caspase-3 in set B in the renal tubule epithelia. Immunohistochemical stain, 400 x

In set C there was a similar response to set B compared to set A **Figure 15**.

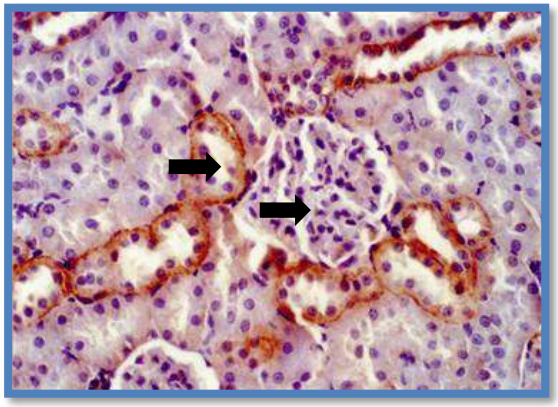

Figure 15: A photomicrograph of the kidney cortex showing a strong positive (+++) caspase-3 immunoreactivity (black arrow) in set C in the renal tubule's epithelia. Immunohistochemical stain, 400 x

As for investigating the immunoreactivity of caspase- 8 in the renal tissue, the microscopical examination revealed a weak positive reaction (+) which appears as golden-brown granules in epithelial cells lining renal tubules in set A **Figure 16** .

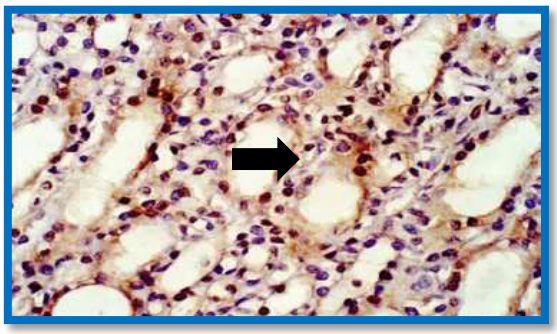

Figure 16: A photomicrograph of the kidney cortex shows weak caspase-8 immunoreactivity (-) in the renal epithelial cells: immunohistochemical stain, 400 x.

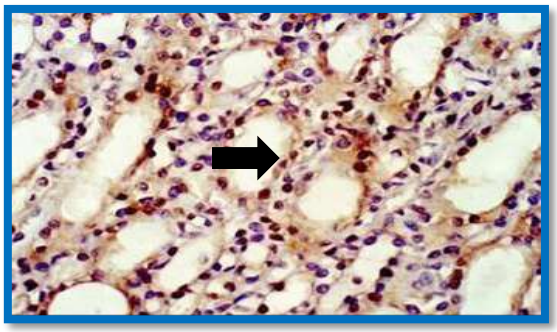

Figure 17: A photomicrograph of the kidney cortex of set B shows positive (++) immunoreactivity) in the renal epithelial cells. Immunohistochemical stain, 400 x.

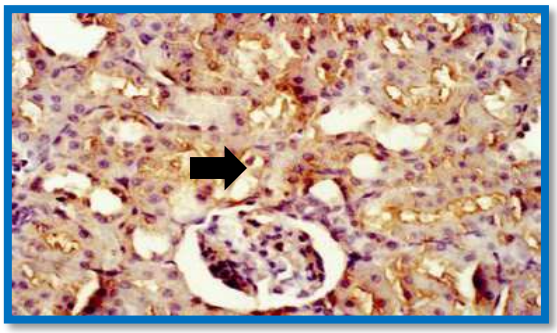

Figure 18: A photomicrograph of the kidney cortex of C shows revealed a highly (strong) positive (+++) immunreactivity (black arrow). Immunohistochemical stain, 400 x.

3.5. Effect of Gabapentin on the expression of GFAP in the brain: The positivity of the intermediate filament-III protein (GFAP) was investigated in the brain tissue of adult male rats at doses 21.8 and 42.6 mg/kg. The microscopical assessment of the brain tissue sections of set A revealed negative (-) immunoreactivity of GFAP expression as golden-brown fibers neurons **Figure 19**.

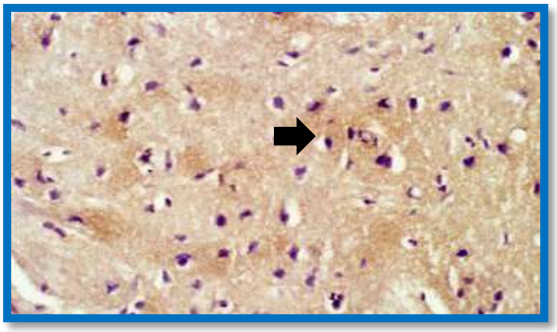

Figure 19: A photomicrograph of GFAP expression in the brain of set A revealed a negative (-) response (black arrow). Immunohistochemical stain, 400 x.

A weak positive (+) response was detected in set B **Figure 20**

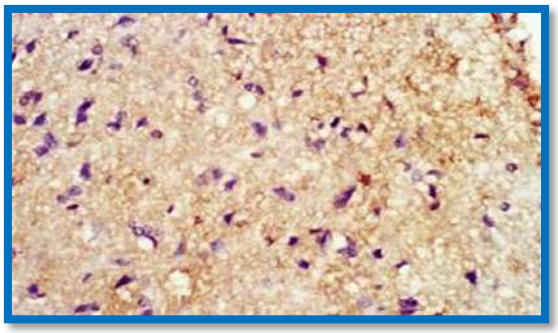

Figure 20: A photomicrograph of GFAP expression in the brain of set B weak positive (+) response (black arrow). Immunohistochemical stain, 400 x

and positive (++) immunoreactivity was detected in set C **Figure 21**, compared to set A as golden-brown fibers in neurons.

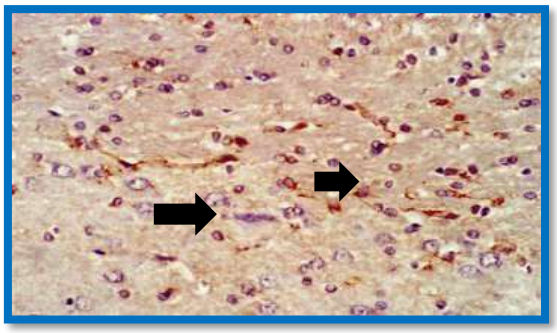

Figure 21: A photomicrograph of GFAP expression in the brain of set C revealed a positive (++) response (black arrow). Immunohistochemical stain, 400 x.

4. Discussion

Gabapentin's historic outlook emphasizes its anticonvulsant and antiepileptic actions. Gabapentin was first investigated in clinical trials at modest dosages and demonstrated to be beneficial as an additional medication. Despite the therapeutic benefits, it had and still has side effects that vary in severity depending on the doses **[22].** This is what the current study investigated and the results showed several lesions in the kidney at both studied doses like Malpighian corpuscles atrophy oedema and destruction of most urinary tubules the severity of histological changes was dose-dependent manner. The present findings were identical to the findings of **[23],** who discovered that treating male rats with gabapentin at high doses causes a lot of kidney lesions like vacuole degeneration and haemorrhage. The outcomes also were comparable to the outcomes of **[24],** who indicated that the selected drug could cause renal cell destruction.

The current findings were not consistent with the findings of **[25, 26].** The previous lesions' occurrence may be due to the that gabapentin affects the sympathetic nervous system, which controls the regulation of blood vessel functions and blood flow to the kidneys. This effect

could cause a change in blood pressure and its distribution in the renal blood vessels, which affects their functions **[27].** or perhaps because the studied drug causes an increase in the level of oxidative stress in the renal cells, which caused the above lesions (7). The medication alters the balance of calcium and ions inside the renal cells by acting as a blocking agent of calcium-transport pathways in the brain and spinal cord, which impacts the function of ion channels in the kidney **[28].**

The painkiller gab can occasionally generate DRESS disorder (drug response with eosinophilia and systemic signs). This is a severe allergic response that might damage essential tissues **[29].** The current outcome revealed some lesions in the brain at both doses such as necrosis and degenerative changes, and the severity of these lesions increases with increasing the concentration of the drug administered to the animals and that may be due to the that the drug easily passes through the selective semi-permeable membrane of the brain and affects the cortex layer, hippocampus, and spinal cord by affecting the calcium channels which may cause tissue lesions **[30].** The current outcomes were not consistent with the findings of **[31],** who found that the damage in the central nervous tissue may be due to the lack of Ache, and this condition is linked to memory and cognition deficits. The findings revealed that in significant increase in the body weight of both sets B and C those outcomes were not partially consistent with the findings of **[32],** who indicated a meaningful increase in the rat body weight after the administration of 300mg/kg for 40 days orally to albino rats.

The slight increase in the body mass in the present research could be explained by that the long-term GBP use may be linked to body mass gain because it may alter the activity of voltage-gated calcium channels in pancreatic β-cells that regulate the release of insulin. This depends on GBP's structure and mechanism of action, which is supposed to modulate neuron signaling by supplying the voltage-dependent calcium channels particular subunit **[33].** The findings were opposite to the results of **[14, 34 , 35].** The current findings showed a meaningful decrease at the dose of 21.8 mg/kg and an insignificant reduction at the dose of 43.6. mg/kg in the kidney weight. The results of the present study were corroborated by research, which claimed that excessive use of gabapentin may result in kidney damage **[32].**

The concentration levels of urea and creatinine in both doses revealed a non-meaningful change. The current outcomes were incomparable to the outcomes of **[36],** who found that gabapentin affects the regulation and flow of blood, in addition to its effect on the filtering and secretion process in the kidney, which causes an elevation in the urea and creatinine concentrations. The current results may be due to the drug concentration and dosing period. the

findings showed insignificant change in the level of cholinesterase of set B but there was an insignificant increase in the same enzyme level of set C. The present outcomes findings were comparable with the findings of **[31].** The slight increase in enzyme level maybe It may be because the drug affects the electrical channels in the brain, as it works too. modify the activity of these channels in the nerve cells, which affects the reception of nerve signals and thus the secretion of neurotransmitters **[37] and** affects the interaction of these transmitters with the nerve cells and their signalling **[38].** in addition to its effect on the secretion of the hormone's aldosterone and renin, which changes the balance of minerals and fluids in the body **[39].**

It is generally accepted that apoptosis triggers tissue dysfunction and that caspase -8 and apopain (caspase -3) are key factors in its development **[40].** The immunohistochemical assessment of the current study in kidneys showed positive and strong positive caspase 3 and caspase-8 at both selected doses, respectively in the basement membrane of the renal tubules. The current outcomes were comparable to those **[23, 41],** who found in contrast to Bcl-2, which had a much lower expression in the brains of gabapentin fetuses, Caspase 3 expression was significantly higher. Researchers found that gabapentin inhibits the levels of caspase-3 in the retinal cells of diabetic rodents **[42, 43].** which is opposite to the present results. The previous findings' appearance may be due to the destruction of the rough endoplasmic reticulum and mitochondria resulted in the release of Cyt c, which then activated caspase-3 and oxidative phosphorylation of caspase-8, initiating an irreversible stage of apoptosis. The over-expression in the caspase- 8 may be due to specific functions for reactive oxygen species in the external apoptotic process that have been discovered and identified. These functions involve facilitating apoptotic activation and death receptor activation via ROS-induced receptor aggregation and forming signalling pathways produced by rafts of lipids **[44].**

The results showed a weak positive and a positive immunoexpression of GAFP in the neuronal axons of damaged neurons in both selected doses respectively. The current findings consisted partially with the findings of **[45],** who found pregabalin reduced spinal GFAP activation and the medication did not lower spinal Iba1 expression. The current results are consistent with the findings of **[46].** The current findings are not consistent with the findings of **[47].** A rise in astrocyte activity corresponds to the removal of the overabundance of dopamine. It is well known that this neurotransmitter can be actively and specifically removed from outside of cells by astrocytes as well as neurons via dopamine transporters. It is then either transported into vesicles or degraded by the chemicals (enzymes) found in glial and nerve cells, namely monoamine oxidase B and catechol-O-methyl transferase **[48].** The increase in the GAFP

expression in the current study may be due to the Excessive dopamine that might promote the process of auto-to ortho-quinone resulting in damage from oxidation **[49].**

5. Conclusions

Gabapentin is a drug used to treat epilepsy and nerve pain. Through the results of the current research, we conclude that using double doses for one month caused pathological lesions in the kidneys and brain. It was observed that the drug induces programmed cell death in the kidney by activating gene expression of caspase proteins in the kidney. The immunohistochemical responses in the treated groups were moderate to severe compared to the control group. Positive responses appeared as a golden brown staining of the cytoplasm of kidney cells. In the brain, the axons of the nerve cells were stained with the same color, indicating excessive production of GAFP protein. This indicates that the drug causes an increase in the gene expression of a GAFP protein. Therefore, you must be careful when taking this drug, and you must adhere to the therapeutic doses specified by the doctor.

Acknowledgment: The researchers extend their sincere thanks to the College of Education for Pure Sciences / University of Mosul / Mosul /Iraq for the facilities they provided to carry out the experiments of this research.

6. References

[1] Wiebe S, Téllez-Zenteno J F,Shapiro M. An evidence-based approach to the first seizure. Epilepsia 2008; 49(1):50-57. https://doi.org/10.1111/j.1528-1167.2008.01451.x.

[2] Attal N, Cruccu G, Baron RA, Haanpää M, Hansson P, Jensen TS, Nurmikko T. EFNS guidelines on the pharmacological treatment of neuropathic pain: 2010 revision. European journal of neurology. 2010 Sep;17(9):1113-e88. https://doi.org/10.1111/j.14681331.2010.02999.x.

[3] Lumsden DE, Crowe B, Basu A, Amin S, Devlin A, DeAlwis Y, Kumar R, Lodh R, Lundy CT, Mordekar SR, Smith M, Cadwgan J. Pharmacological management of abnormal tone and movement in cerebral palsy. Arch Dis Child. 2019; 104(8):775-780. https://doi.org/10.1136/archdischild-2018-316309.

[4] Chincholkar M. Gabapentinoids: pharmacokinetics, pharmacodynamics and considerations for clinical practice. Br J Pain. 2020 May; 14(2):104-114. https://doi.org/10.1177/2049463720912496.

[5] Risher C and Eroglu C. Emerging roles for α2δ subunits in calcium channel function and synaptic connectivity. Curr Opin Neurobiol. 2020; 63:162-169. https://doi.org/10.1016/j.conb.2020.04.007.

[6] Tanabe T, Notomi M, Mitsugi S, Shinya A, Kuramochi E. Fast bistable all-optical switch and memory on a silicon photonic crystal on-chip. Optics Letters. 2005; 30(19): 2575-2577. https://doi.org/10.1364/OL.30.002575.

[7] Welson N N, Rofaeil RR , Ahmed SM, Gaber SS, Batiha GE , Shahataa MG. gabapentin-induced chronic hepatic and renal damage associated with the inhibition of

apoptosis and tissue injury in rats. Life Sciences.2021; 267:118940. https://doi.org/10.1016/j.lfs.2020.118940.

[8] Patel R, Dickenson A H. Mechanisms of the gabapentinoids and α2δ-1 calcium channel subunit in neuropathic pain. PRP. 2016; 4(2):e00205. https://doi.org/10.1002/prp2.205

[9] Attal N, Cruccu G, Baron RA, Haanpää M, Hansson P, Jensen TS, Nurmikko T. EFNS guidelines on the pharmacological treatment of neuropathic pain: 2010 revision. European journal of neurology. 2010 Sep;17(9):1113-e88. https://doi.org/10.1016/B978-0-7020-4086-3.00027-8.

[10] Lasso-de-la-Vega MC, Zapater P, Such J, Pérez-Mateo M, Horga JF. Gabapentin-associated hepatotoxicity. Official journal of the American College of Gastroenterology| ACG. 2001 Dec 1;96(12):3460-2. https://doi.org/10.1111/j.1572-0241.2001.05357.x.

[11] Jackson CD, Clanahan MJ, Joglekar K, Decha-Umphai ST. Hold the Gaba: A Case of Gabapentin-induced hepatotoxicity. Cureus. 2018; .10(3):e2269. https://doi.org/10.7759/cureus.2269.

[12] Sofu H, Kockara N, Aydin BK, Suleyman B, Tayfur M, Malkoc I. Should orthopedic surgeons consider the effects of gabapentin administration on bone healing while treating a long bone fracture: experimental study in a rat model. SICOT-J. 2016 Nov 1;2:36. https://doi.org/10.1051/sicotj/2016028.

[13] Dethloff L, Barr B, Bestervelt L, Bulera S, Sigler R, LaGattuta M, De la Iglesia F. Gabapentin-induced mitogenic activity in rat pancreatic acinar cells. Toxicological sciences. 2000 May 1;55(1):52-9. https://doi.org/10.1093/toxsci/55.1.52.

[14] Shokry DA, El Nabrawy N, Yassa HD, Gaber SS, Batiha GE, Welson NN. Pregabalin induced reproductive toxicity and body weight changes by affecting caspase3 and leptin expression: protective role of wheat germ oil. Life Sciences. 2020 Nov 1;260:118344. https://doi.org/10.1016/j.lfs.2020.118344.

[15] Anderson NG. Practical process research and development: a guide for organic chemists. Academic Press; 2012 May 23.

[16] Al-Zahid JM, Sharba IR, Ghani JM, Alshemkh M. Effects of Gabapentin Drug on Hematological Parameters and Histological Structures in Female Mice. Systematic Reviews in Pharmacy. 2020 Dec 1;11(12):695-700. https://doi.org/10.31838/srp.2020.12.109.

[17] Salah BA. Histopathological effect of fluoxetine drug on the brain of pregnant mice and their embryos. Iraqi J Vet Sci. 2020 Apr 28;34(1):71-6.

[18] Al-Hajj A. Optical laboratory preparation. 1st ed. Amman: Dar Al-Massera; 2010: 40-44.

[19] Al-Haaik AG. A gross anatomical and histological study of pancreas in adult Kestrel (Falco tinnunculus). IJVS. 2019;33(2):175-180. https://doi.org/10.33899/ijvs.2019.162960.

[20] Luna LG. Manual of histologic staining methods of the Armed Forces Institute of Pathology. InManual of histologic staining methods of the Armed Forces Institute of Pathology 1968 (pp. xii-258).

[21] Salah BA, Sadoon HS. Histopathological and some biochemical effects of platinum drug on the liver and kidney of pregnant mice Mus musculus and their embryos. 2021; 35(2): 291-300. https://doi.org/10.33899/ijvs.2020.126706.1364.

[22] Al-Badrany YM, Mohammad FK. Effects of acute and repeated oral exposure to the organophosphate insecticide chlorpyrifos on open-field activity in chicks. Toxicology Letters. 2007 Nov 1;174(1-3):110-6. https://doi.org/10.1016/j.toxlet.2007.09.001

[23] Fajrin FA, Junaidi Khotib N, Susilo I. Effect of Gabapentin and Baclofen on Histology Study in Neuropathic Pain. Indonesian Journal of Clinical Pharmacy. 2015;4(4):250-6. https://doi.org/10.15416/ijcp.2015.4.4.250.

[24] Badawy GM. Ginger ameliorates the nephrotoxicity induced by gabapentin in rat fetuses (Doctoral dissertation, Menoufiya University, Egypt).

[25] Ma Y, Su Q, Yue C, Zou H, Zhu J, Zhao H, Song R, Liu Z. The effect of oxidative stress-induced autophagy by cadmium exposure in kidney, liver, and bone damage, and neurotoxicity. International Journal of Molecular Sciences. 2022 Nov 4;23(21):13491. https://doi.org/10.3390/ijms232113491.

[26] Latief M, Bhat MI, Wani ML, Sharfi O, Goud LN, Abbas F, Wani M. Gabapentin Toxicity and Role of Dialysis; Case Series and Literature Review, JRENHEP .2022; 6(1):7–9. https://doi.org/10.15586/jrenhep.v6i1.104.

[27] Burch J. Anatomy and physiology of the urinary tract and associated disease processes. InStoma care specialist nursing: A guide for clinical practice 2023 Mar 2 (pp. 101-116). Cham: Springer International Publishing.

[28] Wulf MJ, Tom VJ. Consequences of spinal cord injury on the sympathetic nervous system', Frontiers in Cellular Neuroscience. 2023, 17: 999253. https://doi.org/10.3389/fncel.2023.999253.

[29] Rubio C, Gatica F, Uribe E, Ochoa E, Campos V, Rubio-Osornio M. Molecular and genetic mechanisms of neurotoxicity during anti-seizure medications use. Revista de investigación clínica. 2023 Feb;75(1):1-2. https://doi.org/10.24875/RIC.22000260.

[30] Torregrosa-de Juan E, Olagüe-Díaz P, Royo-Maicas P, Fernández-Nájera E, García-Maset R. Acute renal failure due to gabapentin. A case report and literature review. Nefrología (English Edition). 2012 Jan 1;32(1):130-1. https://doi.org/10.3265/Nefrologia.pre2011.Nov.11087.

[31] Mansfield AS, Qian Q. 71–year–old man with chronic kidney failure and sudden change of mental status.Mayo Proc. 2009;48(11):5-1. https://doi.org/10.1016/S0025-6196(11)60673-3.

[32] Cammalleri M, Amato R, Olivieri M, Pezzino S, Bagnoli P, Dal Monte M, Rusciano D. Effects of topical gabapentin on ocular pain and tear secretion. Frontiers in Pharmacology. 2021 Jun 7;12:671238. https://doi.org/10.3389/fphar.2021.671238.

[33] El-Kattan M, Khattab MA, Abdel Maksoud FA, Emad Eldein M, Abdel-raof N, Awad W, Elshatory A. Nephrotoxicity after sub chronic misuse of gabapentin and the protective role of alpha-tocopherol, an experimental study. Zagazig Journal of Forensic Medicine and Toxicology. 2024 Jan 1;22(1):33-54. https://doi.org/10.21608/zjfm.2023.218877.1154

[34] Tuluc P, Theiner T, Jacobo-Piqueras N, Geisler SM. Role of high voltage-gated Ca2+ channel subunits in pancreatic β-cell insulin release. From structure to function. Cells. 2021 Aug 6;10(8):2004. https://doi.org/10.3390/cells10082004.

[35] Elsukary AE, Helaly AM, El Bakary AA, Moustafa ME, El-Kattan MA. Comparative study of the neurotoxic effects of pregabalin versus tramadol in rats. Neurotoxicity Research. 2022 Oct;40(5):1427-39. https://doi.org/10.1007/s12640-022-00557-9.

[36] Elgazzar FM, Elseady WS, Hafez AS. RETRACTED: Neurotoxic effects of pregabalin dependence on the brain frontal cortex in adult male albino rats. 2021; 83 , 146-155. https://doi.org/10.1016/j.neuro.2021.01.004.

[37] Smith DI. Uremic neuropathy', in pathogenesis of neuropathic pain: diagnosis and treatment. 2022; 189–211.

[38] Kelkar S, Nailwal N, Bhatia NY, Doshi G, Sathaye S, Godad AP. An update on proficiency of voltage-gated ion channel blockers in the treatment of inflammation-associated diseases. Current Drug Targets. 2022 Oct 1;23(14):1290-303. https://doi.org/10.2174/1389450123666220819141827.

[39] Russo M, Graham B, Santarelli DM. Gabapentin—Friend or foe?. Pain Practice. 2023 Jan;23(1):63-9. https://doi.org/10.1111/papr.13165.

[40] Prachayawarakorn J, Kansanthia P. Characterization and properties of singly and dually modified hydrogen peroxide oxidized and glutaraldehyde crosslinked biodegradable starch films. International Journal of Biological Macromolecules. 2022 Jan 1;194:331-7. https://doi.org/10.1016/j.ijbiomac.2021.11.150.

[41] Tijani AS, Farombi EO, Olaleye SB. Mechanisms underlying the healing potentials of the methanol extract of chasmanthera dependens stem on indomethacin-induced gastric ulcer. Egypt J Basic Appl Sci. 2021;8(1):17–31. https://doi.org/10.1080/2314808X.2021.1881746.

[42] Ismail OI, Shaltout ES, Abdellah NZ, Hetta DF, Abd El-Ghani WM, Abdelzaher LA, Mahmoud AM, Hasan AM, Rashed NA, Ebrahem NE. The teratogenic effect of pregabalin on heart, liver and kidney in rats: a light microscopic, electron microscopic and immunohistochemical study. BMC Pharmacology and Toxicology. 2022 Dec;23:1-9. https://doi.org/10.1186/s40360-021-00546-2.

[43] Abdelnaser M, Alaaeldin R, Attya ME, Fathy M. Modulating Nrf-2/HO-1, apoptosis and oxidative stress signaling pathways by gabapentin ameliorates sepsis-induced acute kidney injury. Naunyn-schmiedeberg's Archives of Pharmacology. 2024 Feb;397(2):947-58. https://doi.org/10.1007/s00210-023-02650-y.

[44] Ola MS, Alhomida AS, LaNoue KF. Gabapentin attenuates oxidative stress and apoptosis in the diabetic rat retina. Neurotoxicity Research. 2019 Jul 15;36(1):81-90. https://doi.org/10.1007/s12640-019-00018-w.

[45] Ceran EU, Inan N, Kucuk A, Ozer A, Dursun AD, Tosun M, Arslan M. Effects of Pregabalin on Kidney Tissue in Spinal Cord Ischemia Reperfusion Injured Rats. Gazi Medical Journal. 2021 Oct 1;32(4). http://dx.doi.org/10.12996/gmj.2021.115.

[46] Dong L, Crosby ND, Winkelstein BA. Gabapentin alleviates facet-mediated pain in the rat through reduced neuronal hyperexcitability and astrocytic activation in the spinal cord. The Journal of Pain. 2013 Dec 1;14(12):1564-72. http://dx.doi.org/10.1016/j.jpain.2013.07.016.

[47] Rossi A R, Angelo M F, Villarreal A, Lukin J, Ramos AJ. Gabapentin administration reduces reactive gliosis and neurodegeneration after pilocarpine-induced status epilepticus. PLoS One. 2013; 8(11): e78516. http://dx.doi.org/10.1371/journal.pone.0078516.

[48] Amaral AI, Tavares JM, Sonnewald U, Kotter MR. Oligodendrocytes: development, physiology and glucose metabolism. The Glutamate/GABA-Glutamine Cycle: Amino

Acid Neurotransmitter Homeostasis. 2016:275-94. http://dx.doi.org/10.1007/978-3-319-45096-4_10

[49] Karakaya S, Kipp M, Beyer C. Oestrogen regulates the expression and function of dopamine transporters in astrocytes of the nigrostriatal system. Journal of neuroendocrinology. 2007 Sep;19(9):682-90. http://dx.doi.org/10.1111/j.1365-2826.2007.01575.x.